The physiological and functional characterisation of the subpallial dopaminergic neurons in larval zebrafish

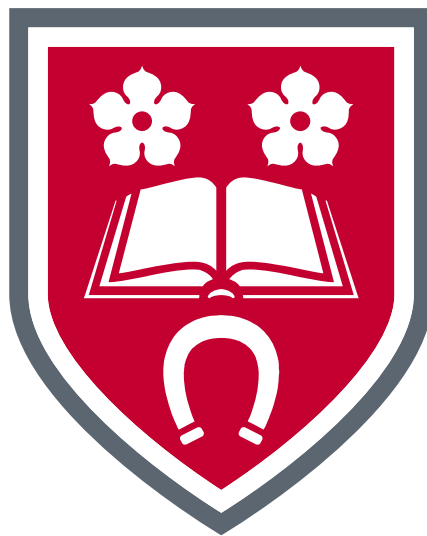Thesis submitted for the degree of

Doctor of Philosophy

at the University of Leicester

by

Neal Rimmer

BSc Honours (The University of Sheffield)

Neuroscience, Psychology and Behaviour

University of Leicester

2019

The physiological and functional characterisation of the subpallial dopaminergic neurons in larval zebrafish

Thesis submitted for the degree of

Doctor of Philosophy

Neal Rimmer

Supervisors: Dr Jonathan McDearmid, Dr William Norton & Dr Jaime McCutcheon

Department of Neuroscience, Psychology and Behaviour

University of Leicester

Abstract

The physiological and functional characterisation of the subpallial dopaminergic neurons in larval zebrafish

Neal Rimmer

Dopamine is a highly conserved neurotransmitter, and it is known to be involved reward, locomotion, cognition and motivation. Moreover, dysfunction or loss of dopamine neurons has been implicated in diseases such as addiction and Parkinson's disease, respectively. Dopamine neurons develop early in life, and zebrafish possess a complete compliment of dopaminergic neurons by 5 days post fertilisation. Previous anatomical and genetic studies have suggested the dopaminergic interneurons of the zebrafish subpallium are equivalent to mammalian midbrain DAergic neurons. In this thesis the physiology and functional role of the cluster of dopamine neurons found in the zebrafish subpallium have been examined.

In the first results chapter, the anatomical, morphological and physiological development of subpallial dopaminergic neurons has been examined. This revealed that by 5 dpf, subpallial dopaminergic neurons innervate the telencephalon, thalamus and hypothalamus whilst receiving input from across the brain. Additionally, subpallial dopaminergic neurons receive excitatory and inhibitory synaptic input, are intrinsically excitable and exhibit endogenous firing. Together, these findings suggest the subpallial dopaminergic neurons are functionally integrated into the brain during early development.

In the second and third results chapters, the functional role of subpallial dopaminergic neurons was investigated. To delineate their function, these neurons were targeted for laser ablation. These investigation demonstrated loss of subpallial dopaminergic neurons was sufficient to perturb foraging and startle behaviours in free-swimming fish without affecting locomotion. Physiological recordings revealed these neurons are active when zebrafish are exposed to attractive and aversive stimuli. In sum, these investigations provide insights into the role of dopamine signalling in modulating decision-making, approach, and avoidance behaviours.

Acknowledgements

Firstly, I would like to thank my supervisor, Jonathan McDearmid, for his guidance, expert insight and support throughout the course of my PhD. Jonathan has been an excellent and patient supervisor, and if it was not for his expertise and support, I would not have accomplished nearly as much as, especially with patch clamping. I will always be indebted to Joe for giving me the opportunity to join his lab. I would also like to thank Jaime for supporting me throughout my PhD, training and letting me borrow his FSCV equipment. It has been a privilege to work with them both, their passion for science is truly infectious, and I aspire to follow in their footsteps.

To all the members of the lab, both past and present, I would like to thank them for their help and support throughout my time in Leicester. Mai Tai say thank you to my family and friends for their support, understanding and most importantly for enduring my rants. A special mention to Luke Martinson, Barbara Ottolini, Mark Openshaw and Diviya Gorsia for those recommended trips to Cank street. I'd also like to thank all my friends at the University of Leicester, our weekly cake and coffee events made my life that bit easier.

Finally, I would like to thank NC3Rs for their funding, enabling me to pursue this PhD and providing training to develop a career in research.

Contents

Table of tables

Table of Figures

Abbreviations

AADC	aromatic L-amino acid decarboxylase
AC	adenylyl cyclase
ADH	aldehyde dehydrogenase
AHP	After hyperpolarisation
AO	anterior octaval nucleus
AOS	accessory olfactory system
AP	Area Postrema
ASPA	Animals (Scientific Procedures) Act 1986
ASR	Acoustic startle reflex
ATP	Adenosine triphosphate
AuC	Auditory cortex
AVI	audio video interleave
BK	Large-conductance calcium-activated potassium channel
BLA	Basolateral amygdala
BMA	Basomedial amygdala
BNST	Bed nucleus of stria terminaris
CaCl2	Calcium chloride
CaL	L-type calcium channel
CaN	N-type calcium channel
CaP/Q	P/Q-type calcium channel
CaT	T-type calcium channel

Cb	Cerebellum
CeA	Central amygdaloid nuclei
CiD	Circumferential Descending
CNS	Central nervous system
CoA	Cortical amygdala
CoLo	Commissural local
COMT	catechol-O-methyl transferase
CRNs	cochlear root neurons
CsCl	Cesium chloride
CsOH	Cesium hydroxide
Ctrax	California Institute of Technology Fly Tracker
DA	Dopamine
DAergic	Dopaminergic
DAT	Dopamine transporter
DC	Diencephalon cluster
DDN	Diencephalon dopaminergic neurons
dH20	distilled water
DON	descending octaval nucleus
DOPAC	3,4-dihydroxyphenylacetic acid
DOPAL	3,4-dihydroxyphenylacetaldehyde
dpf	days post fertilisation
DRG	Dorsal root ganglion
DβH	dopamine-β-hydroxylase
ERK	extracellular signal-regulated kinase

FPS	frames per second
FSCV	fast scan cyclic voltammetry
GABA	GAMMA -Aminobutyric acid
GC	griseum centrale
GFP	green fluorescent protein
GIRK	G-protein-coupled inwardly rectifying potassium
GPCR	G protein-coupled metabotropic receptors
GPe	Globus pallidum externus
Gpi	Globus pallidum internus
GUI	graphical user interface
H	Hypothalamus
Hb	Habenula
HB	Hindbrain
HCN	hyperpolarisation-activated cyclic nucleotide-gated
hpf	hours post fertilisation
HVA	homovanilic acid
IAs	slowly inactivating A-type K+ channel
Ih	hyperpolarisation-activated inward current
IHC	immunohistochemistry
INaP	TTX-sensitive persistent sodium current
INa-TTX	voltage-dependent sodium current
ISI	interspike interval
JAABA	Janelia Automatic Animal Behavior Annotator
KCl	Potassium chloride

KOH	Potassium hydroxide
Kv2	voltage-gated potassium channel
KYN	Kynurenic acid
LA	Lateral amygdala
LC	locus coeruleus
L-DOPA	L-3,4-dihydroxyphenylalanine
LGE	lateral ganglionic eminence
LGN	lateral geniculate nucleus
LLC	Long latency C start
M-cell	Mauthner cells
MeA	Medial amygdaloid nuclei
MgCl2	magnesium chloride
MGE	medial ganglionic eminence
MLR	mesencephalic locomotor region
MO	Medulla Oblongata
MOA	Monoamine oxidase
MOS	Medial olfactory system
mPFC	medial prefrontal cortex
MPP+	1-methyl-4-phenylpyridinium
mPSCs	miniature post synaptic currents
MPTP	1-methyl-4-phenyl-1,2,3,6-tetrahydropyridine
MS-222	ethyl 3-aminobenzoate methanesulfonate
MSNs	Medium spiny neurons
MTN	midline thalamic nuclei

NA	Noradrenaline
Na2ATP	Adenosine triphosphate sodium salt
NA2GTP	Guanosine triphosphate sodium salt
NAc	Nucleus accumbens
NaCl	sodium chloride
NAergic	Noradrenergic
NaOH	Sodium hydroxide
NMDA	N-Methyl-D-aspartic acid
NMDG	N-Methyl-D-glucamine
nMLF	nucleus of the medial longitudinal fasciculus
NTP	Nucleus of the tuberculum posterior
OB	Olfactory Bulb
OKR	Optokinetic response
OMR	Optomotor response
P	pallium
PAG	Periaqueductal gray
PB	Parabrachial nucleus
PBS	phosphate buffer solution
pERK	phosphorylated ERK
PFA	paraformaldehyde
PG	Preglomerular
PHPcol	passive hyperpolarizing potential collateral
PHPcom	passive hyperpolarizing potential commissural
PIC	picrotoxin

PMN	Primary motor neuron
PnC	nucleus reticularis pontis caudalis
PNMT	phenylethanolamine N-methyltransferase
PO	Preoptic region
PPI	Prepulse inhibition
PPTg	pedunculopontine tegmental nucleus
PSp	parvocellular superficial pretectal nucleus
PSTH	Peri-stimulus time histogram
PT	Pretectum
PTc	Posterior tuberculum
RA	Raphe nucleus
RGC	Retinal ganglion cells
RPE	reward-prediction errors
RRF	retrorubral field
SC	Superior colliculus
Sdd	dorsal subdivision of dorsal subpallium
Sdv	Ventral subdivision of dorsal subpallium
SEM	standard error of the mean
SFNs	spiral fiber neurons
SK	small- conductance calcium-activated potassium channel
SLC	Short latency C start
SMNs	secondary motor neurons
SNc	Substantia nigra pars compacta
SNr	substantia nigra pars reticulata

SOP	secondary octaval population
SP	Subpallium
STN	Subthalamic nucleus
Sv	ventral division of subpallium
T	Thalamus
Tel	Telencephalon
TH	Tyrosine hydroxylase
TIDA	tuberoinfundibular dopamine
TRH	thyrotropin releasing hormone
TSc	central nucleus of the torus semicircularis
TTX	Tetrodotoxin
ufmf	micro fly movie format
V1	Primary visual cortex
Vc	Central zone of the ventral telencephalon
Vd	Dorsal zone of the ventral telencephalon
Vl	Lateral zone of the ventral telencephalon
Vmat2	vesicular monoamine transporter2
Vp	Postcommissural region of the ventral telencephalon
VP	Ventral pallidum
Vs	Supracommissural region of the ventral telencephalon
VTA	Ventral tegmental area
Vv	Ventral zone of the ventral telencephalon

CHAPTER 1

Introduction

Dopamine (DA) is a highly conserved catecholamine neurotransmitter within the central nervous system (CNS), where it is known to play a modulatory role in several behavioural processes such as reward, locomotion, cognition and motivation (Missale et al., 1998, Schultz, 1998, Koob, 1992, Graybiel, 1990). Dysfunction or degeneration of dopaminergic (DAergic) neurons can lead to perturbed DA signalling and is associated with a range of motor deficits including bradykinesia, rigidity and tremors, as well as cognitive deficits in diseases such as schizophrenia, addiction, depression and Parkinson's disease (Chen et al., 2017, Keiflin and Janak, 2015, Matsumoto, 2015, Chung et al., 2016, Grace, 2016). Therefore, DA plays a key role in a range of behavioural processes in normal physiological and pathophysiological states.

1.1 Dopamine synthesis, storage and degradation

DA is synthesised from L-tyrosine by a two-step biochemical reaction. Initially, the enzyme tyrosine hydroxylase (TH) converts L-tyrosine into L-3, 4-dihydroxyphenylalanine (L-DOPA). Next, aromatic L-amino acid decarboxylase (AADC) converts L-DOPA to DA (Figure 1:1). TH is the rate-limiting enzyme in the synthesis of DA (Daubner et al., 2011, Elsworth and Roth, 1997). In noradrenergic (NAergic) neurons, DA is converted to noradrenaline (NA) by dopamine-β-hydroxylase (DβH; Figure 1:1). NA can be further converted to synthesise adrenaline when NA is exposed to phenylethanolamine N-methyltransferase (PNMT) (Sauter et al., 1977). Once synthesised, DA is transported into synaptic vesicles by vesicular monoamine transporter 2 (VMAT2), a protein that facilitates the movement of monoamines such as DA, NA, histamine and serotonin into the synaptic vesicles (Eiden and Weihe, 2011, Guillot and Miller, 2009). There is no singular molecular marker for identifying DAergic neurons as TH is expressed in DAergic, NAergic and some non-aminergic neurons (Kumer and Vrana, 1996).

During neurotransmission, vesicles containing DA are exocytosed into the synaptic cleft where it binds to pre and postsynaptic DA receptors. DA transmission is terminated by presynaptic reuptake mediated by the dopamine transporter (DAT) protein (McHugh and Buckley, 2015) or metabolised for

degradation. DA can be metabolised via one of two pathways. Monoamine oxidase (MAO) can convert DA into the reactive species 3,4-dihydroxyphenylacetaldehyde (DOPAL), which is then oxidised into the unreactive metabolite 3,4-dihydroxyphenylacetic acid (DOPAC) by the enzyme aldehyde dehydrogenase (ADH) (Meiser et al., 2013). Alternately, catechol-O-methyl transferase (COMT) converts DA to 3-methoxytyramine which is then further converted into homovanilic acid (HVA) by MAO (Meiser et al., 2013).

L-Tyrosine

L-DOPA

TH

Dopamine

AADC

Noradrenaline

DβH

Adrenaline

PNMT

3
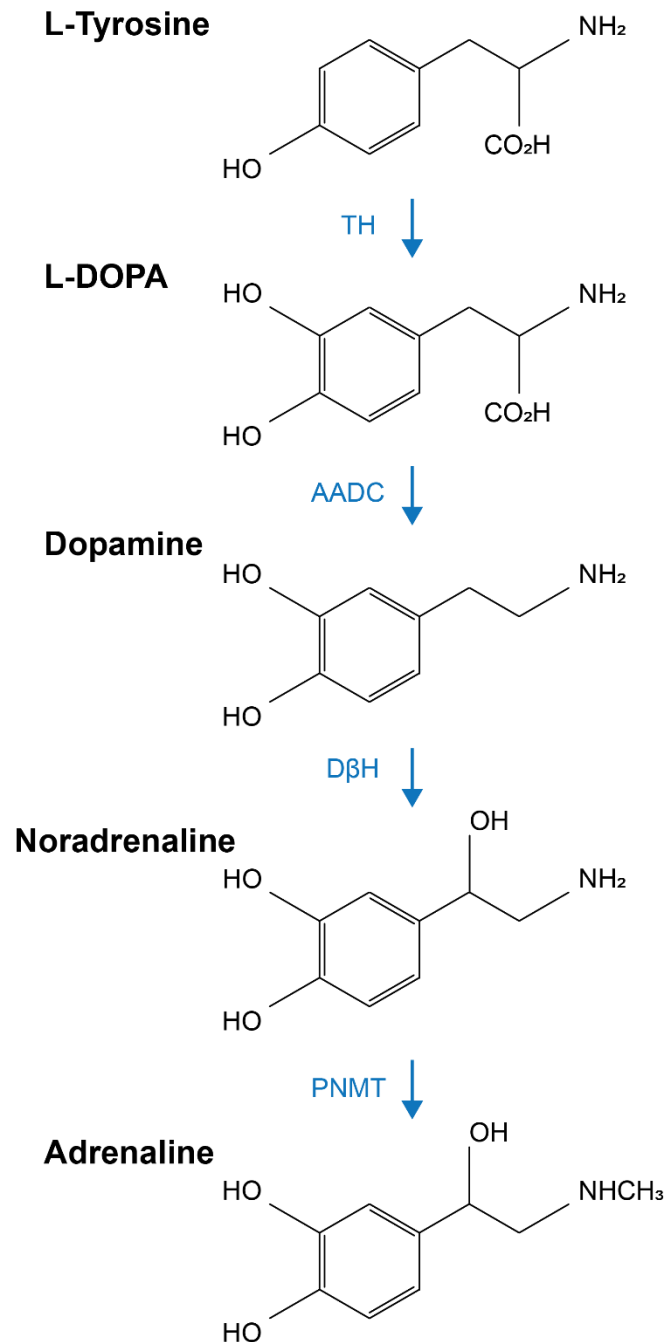
Figure 1:1 Biosynthesis of catecholamines. Catecholamines are synthesised from L-tyrosine by multiple steps. Tyrosine hydroxylase (TH) converts L-Tyrosine to L-DOPA. Aromatic L-amino acid decarboxylase (AADC) converts L-DOPA to dopamine. NAergic neurons express dopamine-β-hydroxylase which converts dopamine to noradrenaline. Noradrenaline is converted to adrenaline by phenylethanolamine N-methyltransferase (PNMT).

1.2 Dopamine receptors

DA receptors are 7-transmembrane domain G protein-coupled metabotropic receptors (GPCRs). In mammals, there are five DA receptors which are segregated into two families: D_1-like and D_2-like (Sidhu and Niznik, 2000). These receptors are classified on the basis of their ability to regulate adenylyl cyclase (AC) (Spano et al., 1978, Kebabian and Calne, 1979). The D_1-like receptors, which comprise D_1 and D_5 receptors, are bound to the $G\alpha_s$ G-protein which activates AC, resulting in an increase in cAMP production (Jaber et al., 1996, Missale et al., 1998). The D_2-like receptor family comprises D_2, D_3 and D_4 receptors that are linked to the $G\alpha_i$ G-protein which decreases AC activity and thus cAMP synthesis (Jaber et al., 1996, Missale et al., 1998). There are two splice variants of D_2 receptors, short and long isoforms that differ in the third intracellular loop (Missale et al., 1998). The D_{2S} and D_{2L} isoforms have similar pharmacological profiles (Missale et al., 1998, Rani and Kanungo, 2006).

All DA receptors subtypes are expressed post-synaptically whilst D_2 and D_3 receptors can also be found presynaptically (Elsworth and Roth, 1997, McGinnis et al., 2016). Here, they act as autoreceptors that inhibit DA release (Stagkourakis et al., 2016, Fasano et al., 2010), ensuring that DA does not reach pathological concentrations (Mercuri et al., 1997). The autoreceptor function of D_2 receptors is primarily achieved by the activation of the inwardly rectifying potassium channel, GIRK2, and the activation of GIRK2 causes the hyperpolarisation of the neuron (Ford, 2014). Thus, presynaptically expressed D_2 and D_3 receptors functions as a negative feedback loop to modulate DA transmission.

1.3   Mammalian dopaminergic system

In the mammalian brain, DAergic neurons are localised into ten clusters, designated A8 – A17 (Bjorklund and Dunnett, 2007, Fu et al., 2012) (Figure 1:2). The DAergic clusters are primarily located in the midbrain (Parker et al., 2013) and give rise to four major ascending DAergic axon tracts: the mesostriatal, mesolimbic, mesocortical and tuberoinfundibular pathways (Fu et al., 2012). In addition, the A11 cluster sends descending projections into the spinal cord (Luo and Huang, 2016, Ryczko et al., 2016b).

The mesostriatal pathway terminates in the dorsal striatum and originates from the A9 DAergic cell group, which forms the substantia nigra pars compacta (SNc) (Strange, 1990). This pathway is involved in voluntary motor behaviours and in Parkinson's disease, loss of these neurons results in motor perturbation (Grealish et al., 2010). The mesolimbic pathway is composed of the A10 cell group which forms the ventral tegmental area (VTA) (Reynolds et al., 2001). These neurons project to multiple areas of the CNS, including the nucleus accumbens (NAc), amygdala and olfactory tubercle (Beier et al., 2015). The mesolimbic pathway modulates both reward-seeking (via the NAc) and aversive behaviours (via the amygdala) (Adinoff, 2004, Brooks and Berns, 2013).

The mesocortical pathway also originates from the VTA, but these neurons send projections to the frontal cortex (Goldman-Rakic, 1992), where they influence cognition (Miller et al., 2002). The final ascending pathway originates from the tuberoinfundibular group located in A12 (arcuate nucleus) and A14 (periventricular nucleus) of the hypothalamus (Lerant et al., 1996). This pathway innervates the pituitary gland and modulates the neuroendocrine release (Renaud, 1981, Ben-Jonathan and Hnasko, 2001).

The sole descending DAergic pathways of the mammalian brain originates from the A11 population and is the only source of DA innervation to the spinal cord (Koblinger et al., 2014a). Interestingly, A11 neurons do not express the DA reuptake transporter DAT (Koblinger et al., 2014a) or D_2 autoreceptors (Pappas et al., 2008). Therefore, A11 neurons lack the negative feedback loop to control neurotransmission.
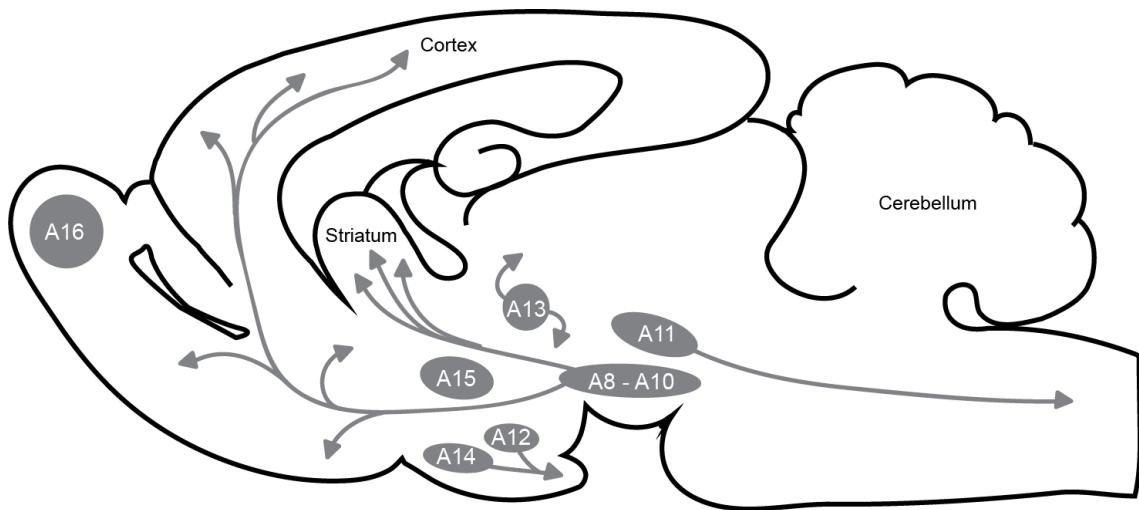
Figure 1:2 Distribution of DAergic cell populations in rodent brain.
Schematic illustration of the adult rat brain, displaying the distribution of DAergic cell populations, A8 – A16. Redrawn from Bjorklund and Dunnet, (2007).

1.4 Expression of the dopamine receptors in the mammalian nervous system

The expression and distribution of D_1 and D_2 receptors are highly conserved between mammalian species, including rat, monkey and human (Levey et al., 1993). D_1 receptors are expressed throughout the brain but are particularly enriched in the striatum, NAc and frontal cortex, regions where mesostriatal, mesolimbic and mesocortical DA neurons terminate (Stagkourakis et al., 2016, Cadet et al., 2010). D_2 receptors have been found in abundance in the core of NAc (Rani and Kanungo, 2006), SNc, VTA, hippocampus and hypothalamus (de Jong et al., 2015, Chaiseha et al., 2003, Hitzemann et al., 2003). The striatum expresses all five DA receptors, however, D_1 and D_2 receptors are the most abundant (Gerfen and Surmeier, 2011). The expression of D_1 and D_2 receptors is highly segregated across the dorsal and ventral striatum (Surmeier et al., 2007, Robertson et al., 2015, Le Moine and Bloch, 1995, Sillivan and Konradi, 2011), with the exception of a small number of cells (Gagnon et al., 2017). The striatum is primarily composed of GABAergic medium spiny striatal neurons (MSNs), which can divided into two populations based which receptor they express, either D_1 or D_2 receptors (Ren et al., 2017). They are known as D1 or D2-MSNs, and

their associated projections constitute two pathways of the striatum, known as the direct and indirect striatal pathways (Gerfen and Surmeier, 2011) (see section 4.1.1.2).

D_3 receptors are part of the D_2-like receptor family and have been found in many regions including the NAc, olfactory tubercle, SNc, VTA, striatum and hippocampus (Gobert et al., 1995, Gurevich and Joyce, 1999). In the striatum, the D_3 receptors are expressed in the MSNs, however, the distribution of the receptors varies: the dorsal striatum expresses a lower density of D_3 receptors compared to the shell of the NAc (Nicola et al., 2000, Fiorentini et al., 2015). D_3 receptors are expressed presynaptically and possess similar autoreceptor function to D_2 receptors (De Mei et al., 2009). D_4 receptors are less abundant but have been found in the frontal cortex, amygdala, hypothalamus, SNc and basal ganglia (Missale et al., 1998, Jaber et al., 1996). The expression of D_5 receptors is low in comparison to other DA receptors and can be found in the cortex, striatum and SNc (Missale et al., 1998).

1.5 Zebrafish development

Zebrafish embryo development is rapid and well documented (Kimmel et al., 1995). When incubated at 28.5ºC, a newly fertilized egg (1 cell stage) undergoes rapid division until it reaches the 128-cell stage or blastula period at 2.25 hours post fertilisation (hpf) (Figure 1:3). The blastula period lasts until 5.25 hpf when the embryo begins to undergo gastrulation (Figure 1:3). During gastrulation the primary germ layers form, along with the embryonic axis. After gastrulation completes (10 hpf), the embryo enters the segmentation period in which somites develop sequentially along the trunk (Kimmel et al., 1995). During this period, 26 bilateral pairs of somites develop until the zebrafish reach the age of 24 hpf (Figure 1:3). By this stage, the body plan of the zebrafish has been established.
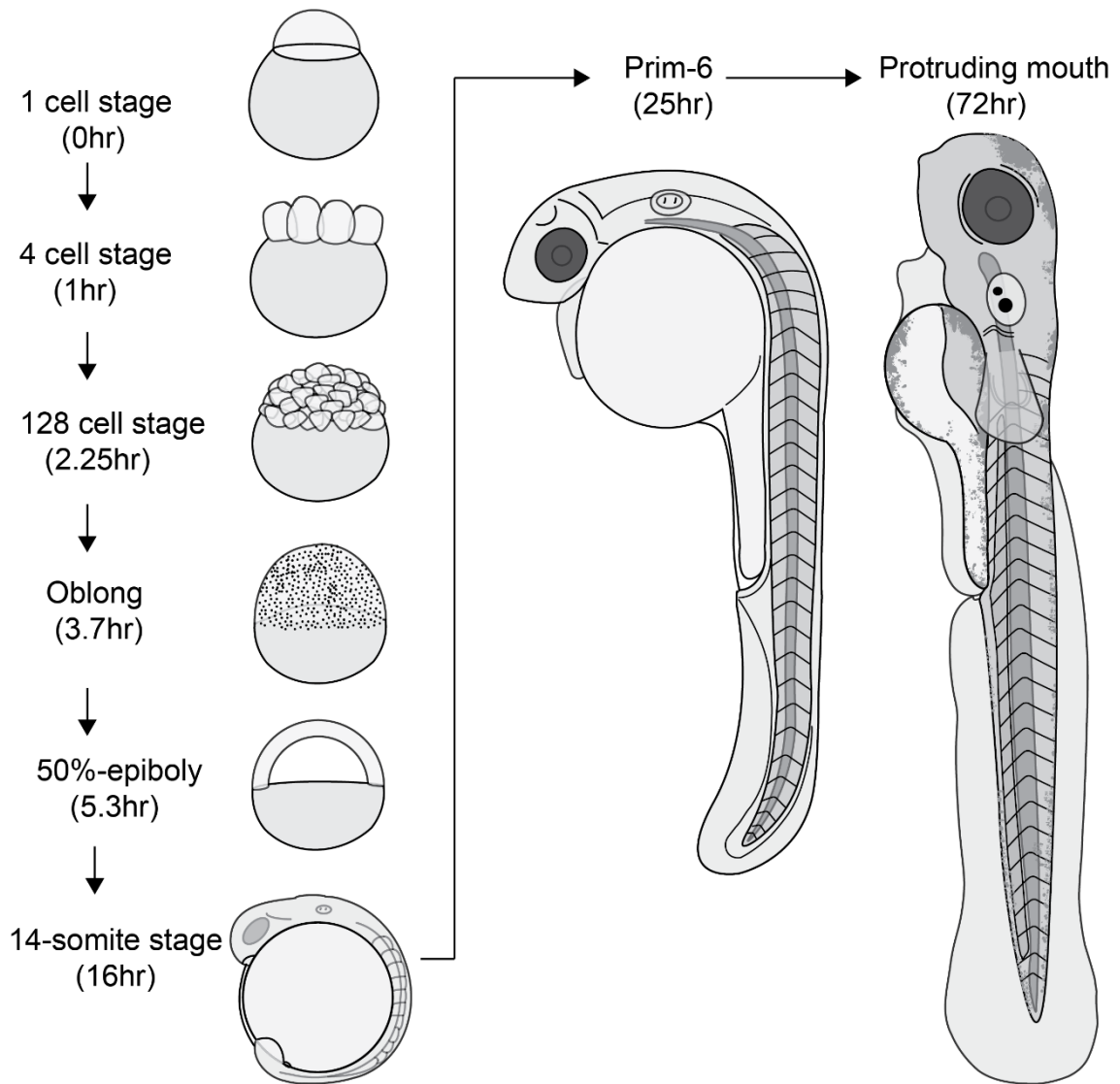
Figure 1:3 Early Zebrafish development. Illustration of the rapid development zebrafish embryo until larval stage at 3 dpf. Data derived from Kimmel et al., (1995).

After the first 24 hpf, zebrafish development enters the pharyngular period, which lasts until 48 hpf. During this stage the embryo develops the median fin fold, and the retina and skin develops pigment. During this stage, the embryo develops the touch evoked escape response (Kimmel et al., 1995). From 48 hpf onwards, the pectoral fins continue to develop, and jaw morphogenesis begins, triggering the movement of the mouth anteriorly (Kimmel et al., 1995). By 72 hpf, the mouth protrudes beyond the eyes and the yolk sac is significantly reduced (Figure 1:3). At this stage melanophores, melanin containing pigment cells, can be observed over the swim bladder (Kimmel et al., 1995). After the first 72 hrs, zebrafish reach their larval state, when morphogenesis is mostly completed and they have

hatched (Kimmel et al., 1995). At this stage they continue to grow, and inflation of the swim bladder occurs at 4 days post fertilisation (dpf) (Kimmel et al., 1995). During the early larval stage zebrafish begin to exhibit several innate behaviours including beat-glide swimming, acoustic startle response and foraging. However, they are not able to feed and are dependent on nourishment from the yolk sac until after 5 dpf, when their mouth opens, they become protected by the Animals (Scientific Procedures) Act 1986 (ASPA).

1.6 Zebrafish as a model to study dopaminergic systems

Zebrafish have several properties that make them a suitable model for investigating vertebrate nervous systems. Their genome has been sequenced, and genetic analysis reveals that approximately 71% of their genes are orthologues to those found in the human genome (Howe et al., 2013). Additionally, a range of genetic tools, including CRISPR/cas/9, have been adapted for use in zebrafish (Cornet et al., 2018). Zebrafish eggs are laid and fertilised externally, which allows the development of zebrafish to be studied from the single-cell stage. Furthermore, embryonic and larval zebrafish are transparent which makes them ideal for *in vivo* imaging and electrophysiology. Finally, by 5 dpf, larval zebrafish exhibit a range of complex behaviours, including locomotion, thigmotaxis, place preference, foraging and startle response (Kalueff et al., 2013).

The zebrafish DAergic systems has been studied by multiple laboratories including Driever, Panula/Sallinen and Wullimann (Schweitzer et al., 2012, Kaslin and Panula, 2001, Panula et al., 2010). Each laboratory employs their own naming system to identify DAergic clusters in the zebrafish brain. The nomenclature used by Sallinen and colleagues, refers to catecholamine (CA) groups including DAergic and NAergic clusters (1-17) according to their location on the rosto-caudal axis (Schweitzer et al., 2012, Kaslin and Panula, 2001, Panula et al., 2010). Alternatively, the nomenclature used by Wullimann, refers to the CA groups based on their anatomical location; however, the diencephalon groups were assigned numbers (1-7). This is based on morphology and rostro-caudal axis (Rink and Wullimann, 2002b). The subpallial DAergic neuron cluster

currently do not have a corresponding cluster in mammals. The terminology used by Sallinen and colleagues to describe these neurons designates these neurons with the olfactory bulb (A16). Therefore, the neuroanatomical terminology of DAergic cell populations used within this thesis is derived from the nomenclature first described by Rink and Wullimann (2002) to specify the difference between the two telencephalic DAergic populations.

Zebrafish possess eleven DA neuron clusters that form early during development (Schweitzer et al., 2012). In contrast to mammals, where the majority of DAergic are found in the mesencephalon, the zebrafish DAergic clusters are located in the forebrain (Parker et al., 2013). This has limited direct comparison of DAergic clusters across species. Several hodological and genetic studies have suggested homologous groups between zebrafish and mammals (Table 1.1). However, corresponding mammalian midbrain DAergic groups (A8 – A10) have not identified in zebrafish. Conversely, the zebrafish DAergic groups in the pretectum and subpallium do not correspond any mammalian DAergic cluster (Schweitzer and Driever, 2009, Parker et al., 2013).

Table 1.1 Comparison of DA groups in mammals and zebrafish

Mammalian	Zebrafish	Region
Mesencephalon (A8-A10)	**(*)**	Midbrain
(**)	Pretectum	Forebrain
Diencephalon (A11, A13)	DC1/2/3/4 and DC6	
Hypothalamic (A12, A14)	DC5, 7	
Preoptic (A15)	Preoptic group	
(***)	Subpallial DAergic neurons	
Olfactory bulb (A16)	Olfactory bulb	
Retinal group (A17)	Retinal amacrine DA clusters	Retina

Data derived from Schweitzer and Driever, (2009) and Parker et al., (2013). (*) No midbrain DAergic neurons in zebrafish. (**) No equivalent pretectal DAergic neurons found in mammals. (***) No corresponding DAergic neurons located in the mammalian striatum/amygdala.

1.7 The zebrafish telencephalon

Understanding functional roles of telostean subregions is limited due to the lack of comparative anatomical structures. Like other teleosts, the zebrafish telencephalon develops via eversion. This contrasts with the telencephalon of other vertebrates which develops by invagination (Rink and Wullimann, 2002a, Wullimann and Mueller, 2004). During eversion, the dorsal aspect of the telencephalon expands to fold over the subpallium, exposing the ventricular surface as an external structure (Folgueira et al., 2012). This contrasts with invagination, whereby the telencephalon expands, and the roof plate and floor plate fold inwards to the centre of the neural tube (Figure 1:4). In the invagination model of development, the ventricular surface remains an internal surface. Therefore, the eversion and invagination models generate markedly different topographies which in turn results in limited comparable anatomical structures.
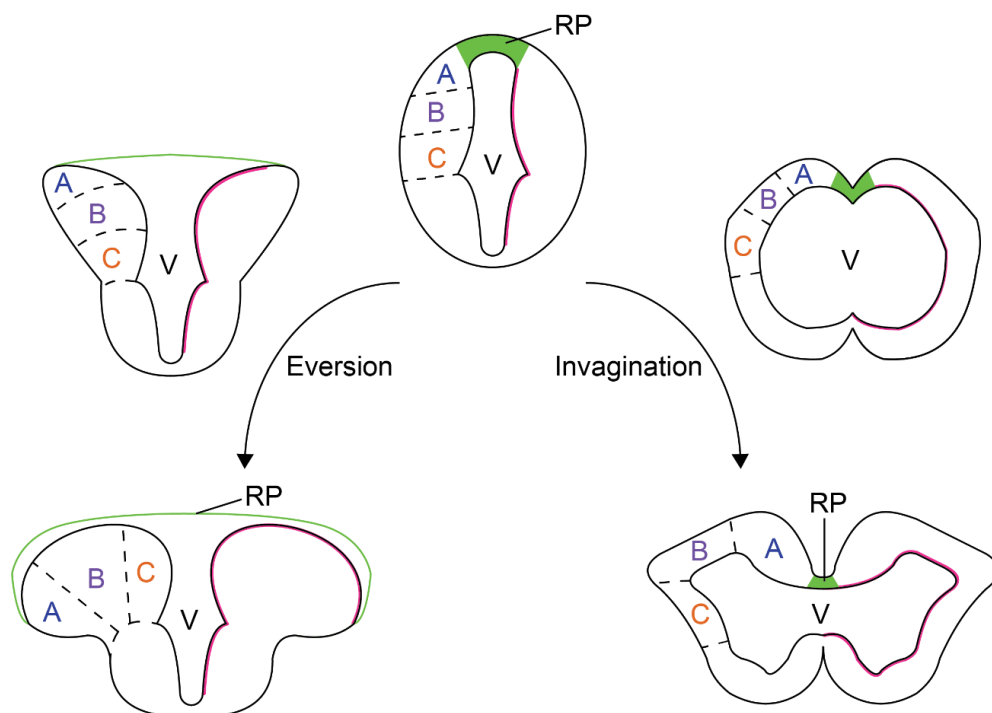
Figure 1:4 Schematic illustration of eversion of teleost forebrain. Illustration showing the development of the telencephalon via eversion (left) and invagination (right). During eversion, the dorsal structure of the neural tube expands laterally, with the ventricular wall (magenta) an exposed surface. During invagination, the roof plate (green) and floor plate of the tube invaginate, and the walls of the neural

tube expands laterally, whilst the ventricle remains encapsulated. Abbreviation: V; ventricle, RP; roof plate. Redrawn from Folgueira et al., (2012).

1.7.1 Zebrafish subpallium

The zebrafish telencephalon can be divided into two regions, the pallium (dorsal region) and subpallium (ventral region). These regions are anatomically and also genetically distinct. The pallium expresses various transcription factors including Ascl1a, Emoesa, Emx1, Emx2, Emx3 and Prox1 (Ganz et al., 2015). By contrast, the subpallium expresses the genes Lhx6, Lhx7, Dlx2a, and GAD67 as well as the pallial gene Tbr2 (Figure 1:5A) (Mueller et al., 2008, Ganz et al., 2012, Ganz et al., 2015). The subpallium can be divided into regions based on this gene expression, including the striatum, pallidum and septum-like regions (Mueller et al., 2008) (Figure 1:5A). Genetic analysis of the zebrafish telencephalon has shown homology with that of other vertebrates including mouse (Figure 1:5A) (Mueller et al., 2008, Osorio et al., 2010, Wullimann, 2009). Based on the spatial gene expression profiles, studies have suggested the ventral aspect of the zebrafish telencephalon is homologous to the mammalian striatum, pallidum and septum (Wullimann and Mueller, 2004, Wullimann and Rink, 2002) (Figure 1:5B).
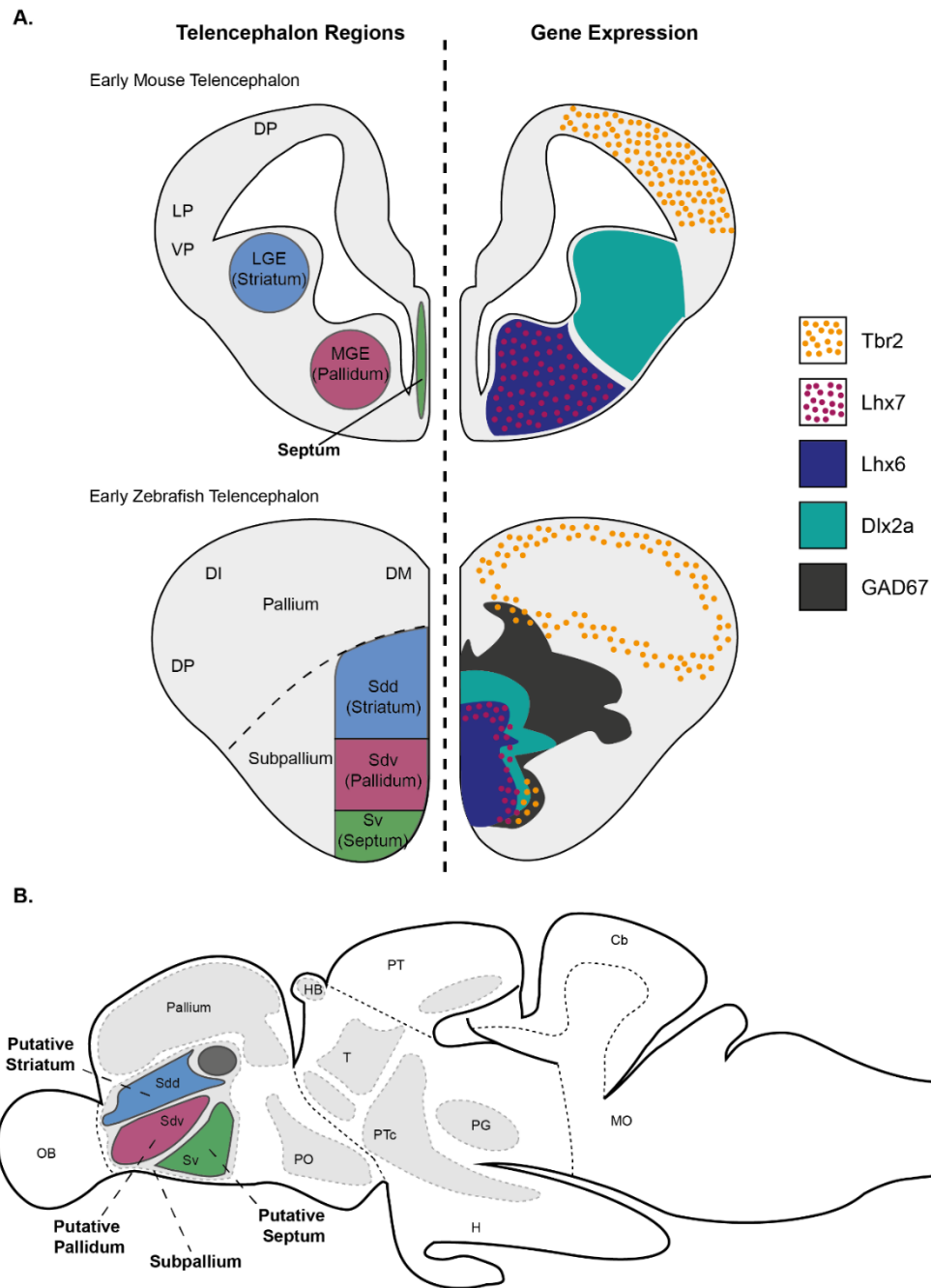
Figure 1:5 Schematic illustration of the gene expression and regions of the zebrafish and rodent forebrain. A: Illustration showing the early telencephalon of mouse (upper panel) and zebrafish (lower panel), specifying the regions that develop into the striatum, pallidum and septum (left) and the gene expression across the telencephalon that is the marker for those regions (right). **B:** Lateral view of adult telencephalon specifying the subpallium and the regions of the putative striatum, pallidum and septum. Abbreviation: Hb; habenular, Cb; Cerebellum, MO; Medulla, H; Hypothalamus, T; Thalamus, Tel; telencephalon, PO; preoptic region, PTc; posterior tuberculum, PT; pretectum, PG; preglomerular, OB; olfactory bulb. Sdd; dorsal subdivision of dorsal subpallium, Sdv; ventral subdivision of dorsal subpallium, Sv; ventral subpallium. Adapted

from Mueller et al., (2008), Wullimann and Mueller, (2004) and Wullimann and Rink, (2002).

1.8 Zebrafish catecholaminergic systems

Many studies have used genetic and immunohistochemical approaches to characterise catecholamine systems within the larval zebrafish (Rink and Wullimann, 2002b, Schweitzer et al., 2012, Tay et al., 2011). These show the presence of a full complement of DAergic cell groups by 72 hours post fertilisation (Mahler et al., 2010, Schweitzer et al., 2012). The DAergic system of zebrafish is restricted to the forebrain (Schweitzer et al., 2012, Rink and Wullimann, 2001, Tay et al., 2011), which contrasts with mammals where they are predominately found in the midbrain.

There are eleven DAergic clusters within the zebrafish brain (Figure 1:6A) (Schweitzer et al., 2012). The telencephalon contains DAergic clusters localised to the olfactory bulb and subpallium (Figure 1:6B) (Schweitzer et al., 2012). The remaining nine clusters are located in the diencephalon, which comprises preoptic and pretectal clusters and seven clusters that collectively make up the posterior tuberculum group known as diencephalon cluster (DC) 1 to DC7 (Figure 1:6B) (Mahler et al., 2010, Rink and Wullimann, 2002b). The DA clusters DC1 to DC7 are also known as the diencephalic DAergic neurons or DDNs (Figure 1:6C). The DDNs form a horse-shoe shaped chain of cells that extend from posterior tuberculum to the hypothalamus (Tay et al., 2011, Schweitzer et al., 2012). Anatomical studies have shown that DC1 neurons project to the pretectum, tectum and hypothalamus as well as the hindbrain (Tay et al., 2011). Previous investigations of DC2 and DC4 have shown these neurons possess descending projections and innervate the spinal cord (Jay et al., 2015, Lambert et al., 2012). It has also been shown that DC2/4 neurons possess ascending projections to the subpallium, in which it was suggested these neurons could be equivalent to the mammalian midbrain DAergic neurons, however, more recent studies have suggested these neurons are homologous to the A11 group (Schweitzer et al., 2012, Rink and Wullimann, 2001, Tay et al., 2011). A study revealed DC3 and DC7 clusters exhibit short range projections, innervating the hypothalamus (Tay et al., 2011). Additionally, this study also found that the DC5 cluster which are

located in the hypothalamus, have similar projectome to that of the DC2/4 cluster, innervating the hypothalamus as well as the tectum and hindbrain (Tay et al., 2011). Furthermore, examination of the DC6 cluster has revealed these neurons innervate the hypothalamus locally as well as the anterior hindbrain (Mahler et al., 2010, Tay et al., 2011, McLean and Fetcho, 2004a).
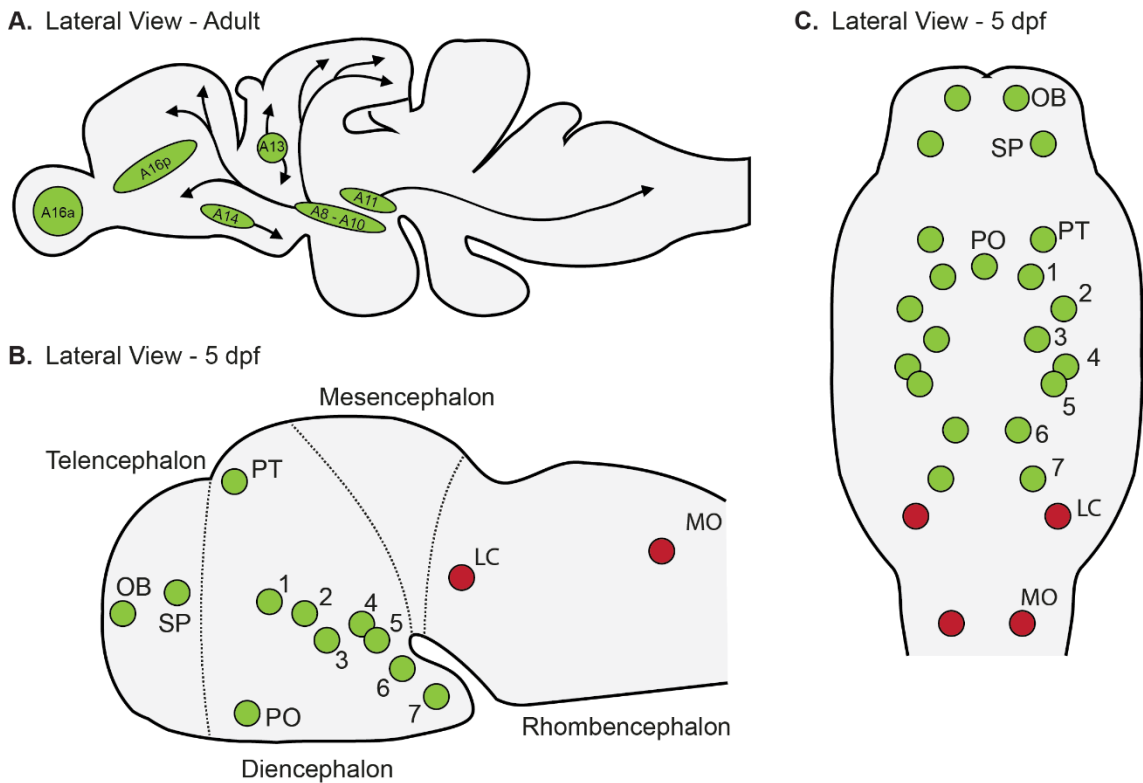
Figure 1:6 Distribution of the catecholaminergic system. A-C: Schematic illustration of the zebrafish brain and the distribution of the catecholaminergic neurons of larvae and adult zebrafish brains. **A:** Lateral view of the adult brain illustrating the DAergic populations and projection pathways. **B:** Lateral view of a 5 dpf brain, illustrating the DAergic and NAergic clusters as well as the dorsal view **C:** Abbreviations: MO, Medulla oblongata; Lc, Locus coeruleus; OB, Olfactory bulb; PO, Preoptic; PT, Pretectum; SP, subpallium. Schematics are derived from Mahler et al., (2010), Schweitzer et al., (2012), and Parker et al., (2013).

The development of the catecholaminergic system has been investigated by multiple methods (Holzschuh et al., 2001, McLean and Fetcho, 2004a, Mahler et al., 2010). Investigations using EdU-based birth dating techniques have revealed that catecholaminergic clusters begin to appear from 8 hpf (Figure 1:7) and their differentiation is complete by 3 dpf (Mahler et al., 2010). The first neurons to

appear are located in DC1, 2, 3, 4, 5, 6. The pioneer neurons of the olfactory bulb and subpallium appear at 12 hpf, and the remaining clusters including preoptic, pretectum and DC7 appear at 16 hpf. Examination of the TH expression in the catecholaminergic clusters showed DC2/4 are the earliest DAergic clusters to express TH (Figure 1:7) (Mahler et al., 2010). The remaining CAergic clusters (olfactory bulb, subpallium, DC5, DC6) except for DC7 and pretectum clusters in which the expression of TH is observed from 48 hpf. TH is expressed in DC7 and pretectum clusters from 60 hpf (Mahler et al., 2010).
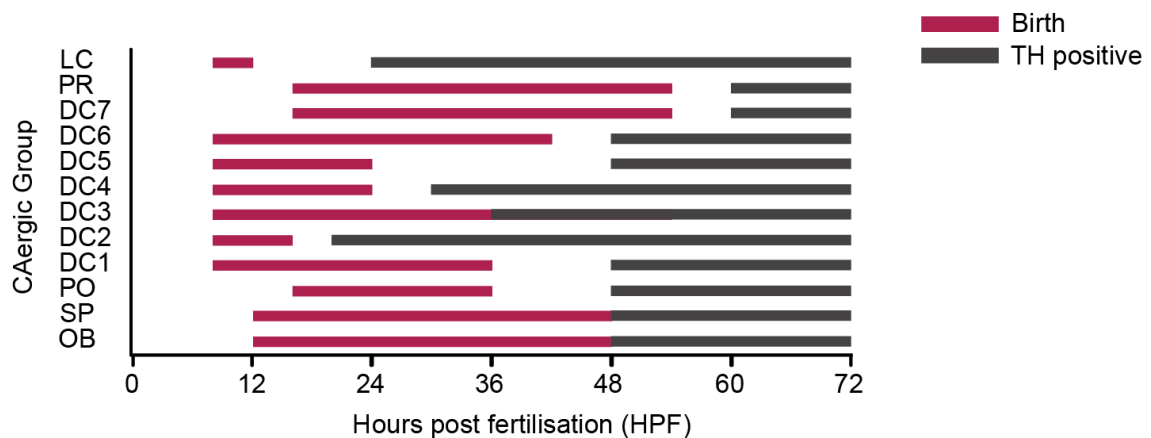
Figure 1:7 Ontogeny of the catecholaminergic system during zebrafish development. The development of the catecholaminergic system, revealed by EdU-based birth dating. Red lines illustrate the time frame of proliferation. Black lines represent the time point at which each catecholaminergic population expresses TH. Data derived from Mahler et al., (2010).

Many studies have focused on the development and projectome of the DAergic systems in zebrafish (Mahler et al., 2010, Tay et al., 2011, McLean and Fetcho, 2004a); however, relatively few studies have examined expression of DA receptors across the brain. Examination of the zebrafish D_1 receptor gene (*drd1*) sequence revealed a high degree of conservation with other species (Liu et al., 2007). *drd1* is found in the diencephalon from 30 hpf and by 5 dpf also localises to rhombomeres of the hindbrain (Liu et al., 2007). Boehmler and colleagues examined the expression of D_2 receptor and identified three forms of the D_2 receptor gene (*drd2a*, *drd2b* and *drd2c*) (Boehmler et al., 2004). The three forms of the D_2 receptor gene is a due to a gene duplication event that resulted in the evolution of isoforms of the gene (Boehmler et al., 2004). These are differentially expressed in the nervous system: by 5 dpf, *drd2a* is found across the nervous

system with prominent staining in the diencephalon, hindbrain and tectum, whilst *drd2b* is expressed in telencephalon, diencephalon, hindbrain and spinal cord (Boehmler et al., 2004). The expression of *drd2c* is found across the nervous system as well as in the ganglion and intermediate cell layers of the retina (Boehmler et al., 2004). The D_3 receptor gene (*drd3*) appears to be diffusely expressed throughout the zebrafish nervous system (Boehmler et al., 2004)

Another study by Boehmler and colleagues identified three separate isoforms of the D_4 receptor gene in zebrafish. Similar to the D_2 receptor gene, a gene duplication even resulted in the three isoforms of the D_4 receptor gene (Boehmler et al., 2004, Boehmler et al., 2007). These three isoforms were originally known as *drd4a, drd4b* and *drd4c* (Boehmler et al., 2007) although they have recently been renamed *drd4b* and *drd4c* as *drd4-rs* and *drd4b,* respectively (www.ZFIN.org). Examination of *drd4a* expression has revealed it is first detected at 24 hpf, and by 5 dpf *drda* is strongly expressed in the retina but with a low level of expression throughout the brain (Boehmler et al., 2007). Expression of *drd4-rs* has been detected from 24 hpf in the forebrain and by 36 dpf expression is also found in the tegmentum and otic vesicle (Boehmler et al., 2007). By 5 dpf, *drd4-rs* has been detected in the same regions as well as the nuclei of the rostral spinal cord (Boehmler et al., 2007). Finally, *drd4b* appears to be the first D4 receptor to be expressed, with transcript first detected at 15 hpf in the spinal cord (Boehmler et al., 2007). At 24 hpf, *drd4b* is found in the diencephalon and spinal cord, however, at 5 dpf a basal level of *drd4b* is found across the nervous system with prominent expression in the retina (Boehmler et al., 2007).

In sum, zebrafish possess D_1-like and D_2-like receptors, however, D_5 receptor has not been identified in zebrafish. Due to gene duplication events, there are multiple forms of the D_2 receptor and D_4 receptor genes (Boehmler et al., 2007, Boehmler et al., 2004). DA receptors are found across the zebrafish nervous system from embryonic stages. DA receptors have distinct expression patterns across the brain and spinal cord.

1.9   Subpallial dopaminergic neurons

As previously mentioned, the zebrafish subpallium contains a population of DAergic neurons (Schweitzer et al., 2012, Mahler et al., 2010, McLean and Fetcho, 2004a) that are first observed at around 12 hpf and become TH positive at approximately 2 dpf (Figure 1:7) (Mahler et al., 2010). Whilst these neurons have received limited attention, anatomical studies have shown that they are small unipolar cells that by 4 dpf project throughout the telencephalon with dense arborisation fields (Tay et al., 2011). In addition, a proportion of these cells project to the contralateral hemisphere before turning to project posteriorly to the thalamus and hypothalamus (Tay et al., 2011).

Genetic studies have suggested the subpallium is homologous the mammalian striatum (Mueller et al., 2008, Ganz et al., 2012, Ganz et al., 2015). Additionally, it has been shown that the primary source of DA input to the putative striatum is from the subpallial DAergic neurons rather than the DC2/4 cluster that was suggest by the early work of Rink and Wullimann (Schweitzer et al., 2012, Rink and Wullimann, 2001, Tay et al., 2011). Since the subpallial DAergic neurons innervate the putative striatum, these neurons could be functionally equivalent to the mammalian midbrain DAergic neurons. However, although the morphology of subpallial DAergic neurons has been investigated, physiological and functional studies have yet to be undertaken. In this thesis I address this problem to examine the functional relevance of these cells.

1.10   Aims and objectives

The aim of this thesis is to characterise the subpallial DAergic neurons during early development and delineate the role of these neurons in zebrafish behaviour. It has been hypothesised that the subpallial DAergic neurons are physiologically equivalent to the mammalian midbrain DAergic neurons, to address this hypothesis, the anatomical and physiological properties of subpallial DAergic neurons are first examined in early-stage zebrafish (Chapter 3). Furthermore, as it has been proposed that subpallial DAergic neurons are functionally homologous to that of the mammalian midbrain DAergic neurons, the physiological properties, activity patterns and functional role of these neurons was therefore examined during locomotion, anxiety and foraging behaviours (Chapter 4). Finally, it has been suggested subpallial DAergic neurons are involved in the processing of aversive stimuli. To address this, the functional role of subpallial DAergic neurons in zebrafish startle behaviour was studied (Chapter 5).

Methods

2.1   Zebrafish husbandry

Adult zebrafish were maintained in accordance with established procedures described by Westerfield, 2000 and in compliance with the Animals (Scientific Procedures) Act 1986 (ASPA). Adult zebrafish were housed at the aquatic's facility within the University of Leicester's animal facility. Zebrafish were kept at 28.5ºC, on a 14:10 light: dark cycle. Husbandry duties of adult zebrafish were carried out by technician employed by the animal facility. Adult zebrafish were fed a combination of brine shrimp and dry granular food (ZMsystems) twice a day as described by Westerfield, 2000. Adult Tg(ETvmat2:GFP) zebrafish (Wen et al., 2008) were incrossed to obtain embryos in accordance with established procedures described by Westerfield, 2000. Upon fertilisation, embryos were collected and incubated in egg water (1.5ml of stock aquarium salts per litre of dH_2O) at 28.5ºC. Developing zebrafish were housed in an incubator on a 14:10 light: dark cycle until the required developmental stage. All experiments were conducted on larval Tg(ETvmat2:GFP) zebrafish at 2, 3, 4, 5 and 5.5 dpf, which were staged in accordance with (Kimmel et al., 1995). Tg(ETvmat2:GFP) zebrafish developed slower than wild type fish when raised at 28.5ºC. Prior to experiments, zebrafish were visually examined to determine their mouth was not open. Subsequently, only non-protected larval zebrafish were used for experiments.

2.2   Electrophysiological reagents

2.2.1   Extracellular solutions

For all electrophysiological, juxtacellular and retrograde labelling studies preparations were continuously perfused with Evans extracellular saline containing D-tubocurarine to block contraction of axial swim muscles (Table 2.1)

When investigating spontaneous miniature postsynaptic currents (mPSCs), 1 µM of tetrodotoxin (TTX; HelloBio) was added to the Evan's extracellular saline to

abolish action potentials mediated by voltage-gated sodium channels. Moreover, when isolating glutamatergic mPSCs, Mg^{2+} was excluded from the Evan's extracellular saline to alleviate block the N-Methyl-D-aspartic acid (NMDA) receptors at hyperpolarised holding potentials.

Table 2.1 Evan's extracellular saline

Constituent	Concentration (mM)	Supplier
NaCl	123	Fisher Scientific
KCl	2.9	Fisher Scientific
$CaCl_2$	2.1	Fisher Scientific
$MgCl_2$	1.2	Fisher Scientific
HEPES	10	Melford
Glucose	10	Fisher Scientific
D-Tubocurarine	0.01	Chem Cruz

pH adjusted to 7.8 using sodium hydroxide (NaOH).

In order to investigate action potential kinetics during whole-cell current-clamp experiments, 1 mM of kynurenic acid (KYN; HelloBio) and 100 µM of picrotoxin (PIC; Sigma) was added to the Evan's extracellular saline to abolish synaptic transmission.

2.2.2   Intracellular solutions

Intracellular solutions used during the course of this study are listed in **Error! Reference source not found.** - **Error! Reference source not found.**. Sulforhodamine B was routinely added to all intracellular solutions to visualise the neuron post experimentation with epifluorescence microscopy.

Table 2.2 K-gluconate intracellular solution

Constituent	Concentration (mM)	Supplier
D-Gluconic acid	126	Acrose Organics
KCl	6	Fisher Scientific
NaCl	10	Fisher Scientific
$MgCl_2$	2	Fisher Scientific
EGTA	10	Sigma
HEPES	10	Melford
Na_2ATP	4	Sigma
NA_2GTP	0.2	Sigma

pH adjusted to 7.2 with potassium hydroxide (KOH) (Tong and McDearmid, 2012).

Table 2.3 Cesium Chloride intracellular solution

Constituent	Concentration (mM)	Supplier
CsCl	135	Sigma
$MgCl_2$	2	Fisher Scientific
EGTA	10	Sigma
HEPES	10	Melford
Na_2ATP	4	Sigma
Na_2GTP	0.2	Sigma

pH adjusted to 7.3 with cesium hydroxide (CsOH) (Jay et al., 2015).

Table 2.4 Low chloride intracellular solution

Constituent	Concentration (mM)	Supplier
K-Gluconate	125	Acrose Organics
$MgCl_2$	2.5	Fisher Scientific
EGTA	10	Sigma
HEPES	10	Melford
Na_2ATP	4	Sigma
NA_2GTP	0.2	Sigma

pH adjusted to 7.3 with KOH.

2.3 Electrophysiology

2.3.1 Fish preparations

For electrophysiological experiments, zebrafish were anaesthetised with 0.02 % MS-222 (Sigma) dissolved in Evan's extracellular saline before being secured laterally to a sylgard lined petri dish by inserting 25 µm diameter tungsten pins inserted through the notochord and jaw. In most experiments, the left eye was removed, along with skin covering the forebrain to expose the underlying telencephalon (Figure 2:1A). For electrophysiological experiments in which visual stimuli were presented, larval zebrafish were secured to the sylgard lined petri dish allowing the specimen to lie upright so that the visual field was not obstructed. In these cases, the dissection was modified to ensure that both eyes remained intact. Here, a small region of dorsal skin lying between both eyes was removed using a sharp glass electrode.

2.3.2 Electrophysiological methods

Following fish preparation, fish were transferred to the patch-clamp setup and perfused with Evan's extracellular saline containing 10 µM D-tubocurarine and 10 mM glucose (Table 2.1). Standard patch-clamp techniques (extracellular and whole-cell) were used to investigate the electrophysiological properties of subpallial DAergic neurons. Patch-clamp electrodes were pulled from filamented borosilicate glass rods (1.5 mm outer diameter, 0.06 mm inner diameter; Harvard Apparatus, UK) with a P-80 micropipette puller (Sutter Instrument, USA). For whole-cell records, glass pipettes had the electrode resistance = 9 – 13 MΩ. Whilst extracellular recordings, juxtacellular and retrograde labelling experiments, the electrode resistance was 5 – 10 MΩ. Targeted recording of subpallial DAergic neurons in Tg(ETvmat2:GFP) larvae was achieved by using fluorescent microscopy features of the patch-clamp rig.
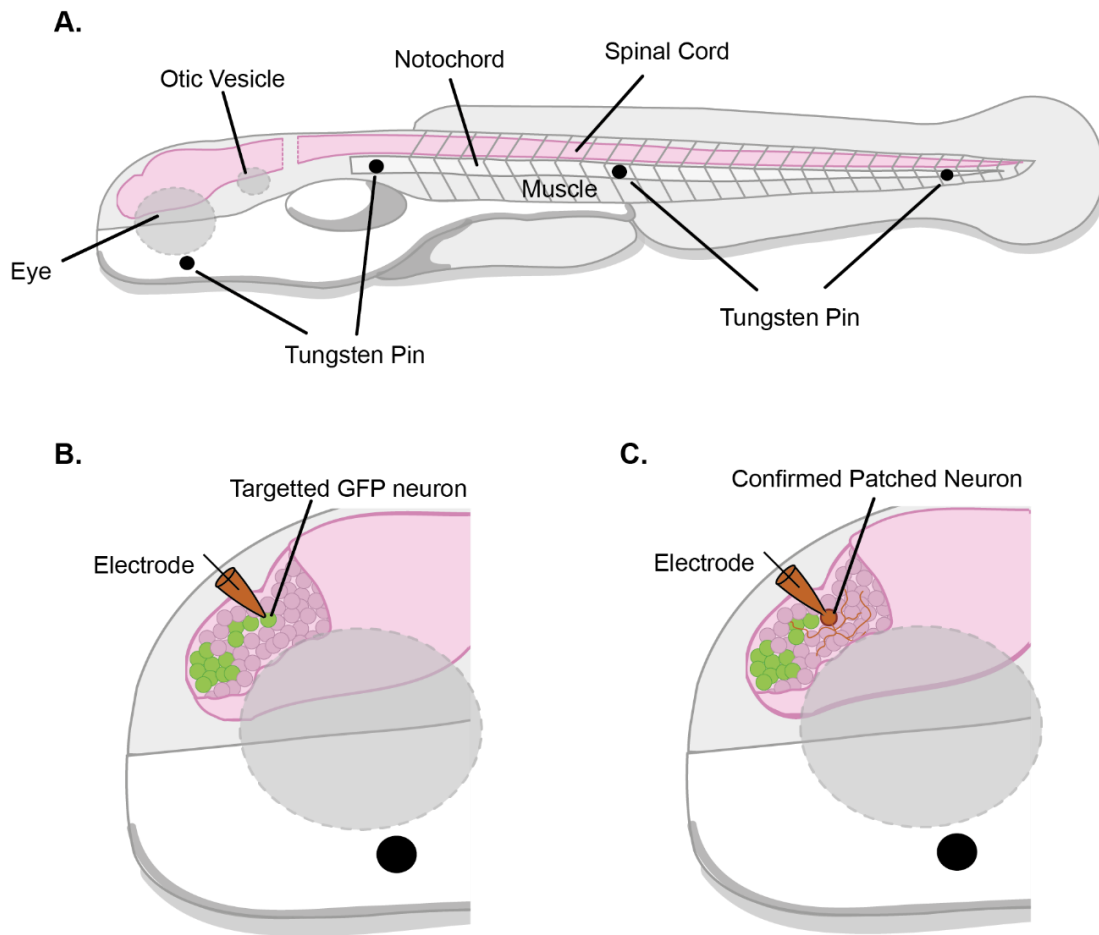
Figure 2:1 Standard dissection and electrophysiological preparation. A: Larval zebrafish were pinned to sylgard dish by the use of tungsten pins being inserted through the notochord and developing lower jaw. **B:** During physiological analysis, GFP positive neurons were visually targeted. **C:** Whole-cell patch-clamp confirmation enables the dialysis of fluorescent dye and permits visualisation of cell morphology.

2.3.2.1 Whole cell recording

Following specimen preparation, glass micropipettes were filled with the appropriate intracellular solution (see section: 2.2.2) and secured to a Biologic head stage connected to an RK-400 amplifier (Intracell, Shepreth, England). Positive pressure was applied to the tip of the micropipette during approach to the preparation. Upon contact, pressure was neutralised, and pulses of negative pressure were applied to the micropipette to obtain a giga-Ohm seal. A holding potential of -65 mV was applied to the electrode to facilitate seal formation. Subsequently, negative pressure was applied until whole-cell access was

achieved. On completion of experiments, cell identity was confirmed by visualising sulforhodamine B fluorescence under 540 nm wavelength fluorescent light.

To study glutamatergic mPSCs, micropipettes were filled with a K-Gluconate solution (**Error! Reference source not found.**) and the 1 µM TTX was added to the extracellular saline. For these recordings, Mg^{2+} in the Evans extracellular solution was replaced with equimolar $CaCl_2$. To isolate glutamatergic mPSCs, 100 µM PIC was added to the Evan's extracellular solution to block GABAergic mPSCs. Here, cells were voltage clamped at -65 mV, and 1mM KYN was added at the end of experiments to confirm that mPSCs were glutamatergic. To study GABAergic mPSCs, the electrode was filled with a CsCl intracellular solution (Table 2.3) and cells were held at -70 mV to allow the GABAergic mPSCs to be resolved as large inward currents. GABAergic mPSCs were isolated by the addition of 1 mM KYN to the Evans solution to abolish glutamatergic inputs. The presence of GABAergic inputs were confirmed by the application of 100 µM PIC to abolish the presumably GABAergic currents.

To examine the firing properties of subpallial DAergic neurons, whole-cell current clamp recordings were performed using an electrode filled with low chloride intracellular solution (**Error! Reference source not found.**). The addition of 1 mM KYN and 100 µM PIC to the Evans extracellular saline allowed the blocking of synaptic input. Therefore, action potential kinetics could be resolved without noise generated by synaptic input. In this configuration, neurons were subjected to depolarising current steps spanning 0 to 30 pA at 1 pA step increments. Neurons were also subjected to hyperpolarising current steps ranging from 0 to -50 pA to investigate I_h currents. In this case, step increments were 5pA in amplitude.

2.3.2.2   Extracellular recording

Extracellular recordings, also known as loose patch recordings, were used to non-invasively characterise subpallial DAergic neuron firing activity. During extracellular recordings, an electrode containing Evan's extracellular solution was used. Electrodes were positioned over a singular subpallial GFP positive cell, and

negative pressure was applied until a low-resistance seal (15 to 50 MΩ) was obtained.

2.3.2.3 Data Acquisition

Data was acquired using an RK-400 amplifier (Intracell, Shepreth, England) and A-D converter connected to a PC running WinEDR (V3.1.3) and WinWCP (V5.1.6; Strathclyde Electrophysiology Software). Raw traces were acquired at 10 – 20 kHz. During whole-cell recordings, traces were filtered using low pass filter at 10 kHz, and a bandpass filter between 1 and 4 kHz was used for loose patch recordings.

2.4 Fast-scan Cyclic Voltammetry

2.4.1.1 FSCV Equipment

The fast-scan cyclic voltammetry (FSCV) equipment was integrated into the patch-clamp rig and was composed of a recording bath, carbon fibre recording electrodes and an Ag/AgCl reference electrode. Both electrodes were connected to a potentiostat, head stage, amplifier and a computer running TarHeel (Chapel Hill, University of North Carolina) voltammetry software.

2.4.1.2 Carbon fibre electrode generation

Electrodes were generated inhouse as described in Jones et al., (2015). Briefly, a carbon fibre rod was aspirated into a borosilicate glass capillary (World Precision Instruments, 100 mm length, 1/0.58 mm OD/ID). The capillary was pulled using a vertical needle puller (PE-21, Narishige). The exposed carbon fibre at the tip of the electrode was cut to 100 µm in length. A wire coated in silver conductive paint (Coating Silver Print II, GC Electronics) was inserted into the glass electrode. The silver-coated wire was connected to a gold pin (Newark) and secured to the glass electrode using heat shrink-wrap.

2.4.1.3 FSCV procedure

The carbon fibre recording electrode was lowered into the subpallium using a micromanipulator. The electrode was held at -0.4 V and a triangular voltage waveform was applied to the electrode (-0.4 to +1.3 to –0.4 V, 400 V·s^{-1}; "scan") using TarHeel software. With this waveform, DA oxidizes at ~ +0.6 V (visualised by a peak) and shows a single reduction peak at ~ -0.2 V.

Each recording of analyte release within the subpallium lasted for 2 minutes. During these recordings, the triangular waveform scans were applied at a frequency of 10 Hz. During rotifer exposure experiments, baseline activity was recorded for 2 minutes, after which the inflow was switched to a secondary inflow filled with Evans extracellular solution that contained rotifers. Subsequent recordings of analyte released were conducted for 4 minutes. Following this, a further 4 minutes of recordings were gained during the wash using original Evan's extracellular saline to wash the rotifers out of the bath. After the recording session, a two-minute recording was gained whilst 5 µM DA was added to the bath solution to gain a concentration-voltage reference.

2.5 Juxtacellular labelling

To label neurons for morphological study, electrodes were filled with Evan's extracellular saline containing 0.5 % neurobiotin (Vector Laboratories). The glass pipettes had the electrode resistance = 7 – 10 MΩ. The electrode was placed on a cell, and a low resistant seal (15 to 50 MΩ) was formed. Subsequently, 500ms 1nA current pulses were applied to the pipette at a frequency of 0.5 Hz for 45 minutes to facilitate the uptake of neurobiotin into the attached cell.

2.6 Retrograde labelling

Retrograde labelling of subpallial afferents was achieved using electroporation. Here, a glass pipette pulled from filamented borosilicate glass rods (1.5 mm outer diameter, 0.06 mm inner diameter; Harvard Apparatus, UK) containing 2% neurobiotin tracer was connected to a Grass S88 Stimulator (Grass Instrument Company, MA, USA) was positioned in close proximity to the DAergic neurons.

Axons were then electroporated with 2-second trains of 5 V pulses at a rate of 0.5 Hz. Trains were repeated 8 times at 1-minute intervals. After cells were electroporated, specimens were left for 5 hours before being subjected to streptavidin histochemistry (see subsection: 2.7.3).

2.7 Histochemistry

Larvae were anaesthetised in 0.02 % MS-222 and fixed in 4 % paraformaldehyde (PFA; Fisher Scientific) dissolved in phosphate buffer solution (PBS; Fisher Scientific) at room temperature up to 90 minutes for 2 dpf fish, and up to 120 minutes for 5 dpf fish. Following fixation, specimens were repeatedly washed using PBS containing 0.1 % Triton-X 100 (PBS-TX; Fisher Scientific) for 45 minutes.

Table 2.5 Primary and secondary antibodies used for immunohistochemistry

Antibody	Description	Ratio	Supplier
Anti-TH	Mouse, clone LNC1, Anti-Tyrosine Hydroxylase Antibody	1:100	Merck Millipore
Anti-pERK	Phospho-p44/42 MAPK (Erk1/2) XP Rabbit mAB	1:100	Cell Signaling technology
CY5 goat, anti-mouse	Goat, Anti-mouse secondary Antibody with CY5 conjugate	1:200	Fisher Scientific
Cy5 goat, anti-rabbit	Goat, Anti-rabbit IgG (h+l) with CY5 conjugate	1:200	Invitrogen

2.7.1 Anti-tyrosine hydroxylase immunohistochemistry

To investigate TH positive neurons, fixed tissue was placed in blocking solution (**Error! Reference source not found.**) for 60 minutes. Primary antibody (anti-TH; Table 2.5) was added to the blocking solution (1:100) and incubated at room temperature overnight. The primary antibody was subsequently removed by 3x 15 minutes washes with PBS-TX. Specimens were incubated for a further 40 minutes in blocking solution before the addition of the secondary antibody (CY5,

Goat anti-mouse; 1:200, Table 2.5) for 4 hours. Specimens were again washed in PBS-TX to remove the secondary antibody. Preparations were then cleared in 60% glycerol before mounting on microscope slides.

Table 2.6 Blocking buffer solution

Constituent	Concentration (%)	Supplier
Milk powder	3	Marvel Milk
DMSO	1	Fisher Scientific
Triton-X 100	0.1	Fisher Scientific

Dissolved in PBS.

2.7.2 Anti-pERK immunohistochemistry

To investigate pERK expression, fixed tissue underwent antigen retrieval in 150 mM Tris-HCl (pH = 8.6; Melford) for 15 minutes at 70°C. Following antigen retrieval, larvae were washed in PBS-TX for 15 minutes and subsequently permeabilized in 0.05% Trypsin-EDTA (Gibco) for 45 minutes (on ice). Trypsin-EDTA was removed by subsequent washes using PBS-TX for a further 15 minutes. Specimens were then incubated in blocking solution (see **Error! Reference source not found.**) for 60 minutes. Primary antibody (anti-pERK; Table 2.5) was added to blocking solution (1:100) and incubated at room temperature overnight. The primary antibody was removed by subsequent washes with PBS-TX for 45 minutes. Larvae were incubated for a further 40 minutes in blocking solution before the addition of the secondary antibody (CY5, goat anti-rabbit; 1:200; Table 2.5) and left overnight at room temperature. Specimens were washed in PBS-TX for 45 minutes to remove the secondary antibody. All immunohistochemistry preparations were cleared in 60% glycerol before mounting on microscope slides.

2.7.3 Streptavidin histochemistry

To investigate the localisation of neurobiotin containing cells following juxtacellular and retrograde labelling procedures, specimens were fixed using methods mentioned in sections 2.7, and incubated overnight with Cy3-conjugated

streptavidin (1:100; Sigma) in PBS-TX. Tissue was subsequently washed in PBS-TX for 45 minutes before being cleared in 60% glycerol and mounted on microscope slides.

2.8 Image acquisition

Confocal images were captured using an Olympus FluoView FV1000 laser scanning confocal microscope. Images were captured in 0.50 to 3 μm z-stack increments. GFP expression was visualised using a 488 nm wavelength laser. TH expression was imaged using an anti-TH antibody and a CY5 conjugated secondary antibody, which was visualised using a 635 nm wavelength laser. For preparations subjected to anti-pERK staining, images were taken of anti-pERK antibody and a CY5-conjugated secondary antibody, which was visualised using a 635 nm wavelength laser. Specimens that underwent streptavidin histochemistry were imaged using CY3-conjugate streptavidin and visualised using a 559 nm wavelength laser.

2.9 Laser ablation

For behavioural studies, 3 dpf ETvmat2:GFP embryos were embedded in 1.5 % low melting point agarose dissolved in embryo medium containing 0.02 % MS-222. Using an Olympus FluoView FV1000 confocal laser scanning microscope, subpallial GFP positive neurons were targeted for laser ablation by defining a region of interest within the FluoView FV1000 software. Fluorescent cells were irradiated for 50 seconds with both a UV (405 nm, 50 mW) laser set to 99 % power and an Argon (488 nm, 40 mW) laser at 12% power. Control fish were given a sham procedure of embedding in the MS-222 agarose medium. Following ablation, zebrafish were removed from the agarose and allowed to recover for 48 hours. Successful ablation was confirmed once behavioural recording had been completed by anti-TH immunohistochemistry in fixed specimens at 5 dpf.

2.10   Behaviour

Individual 5 dpf larval zebrafish were transferred to a behavioural arena, within a behavioural chamber that contained an infrared light source and an overhead camera (Point Grey DragonFly 2). The chamber also contained a fibre optic white light source to control the ambient lighting of the behavioural chamber (Figure 2:2A). Fish were allowed to acclimatise for 5 minutes before behaviour was recorded. Digital video (audio video interleave (AVI) format) recordings were acquired at 15 frames per second (FPS) and captured using Flycap2 software. Unless otherwise stated, recordings were captured for 5 minutes.
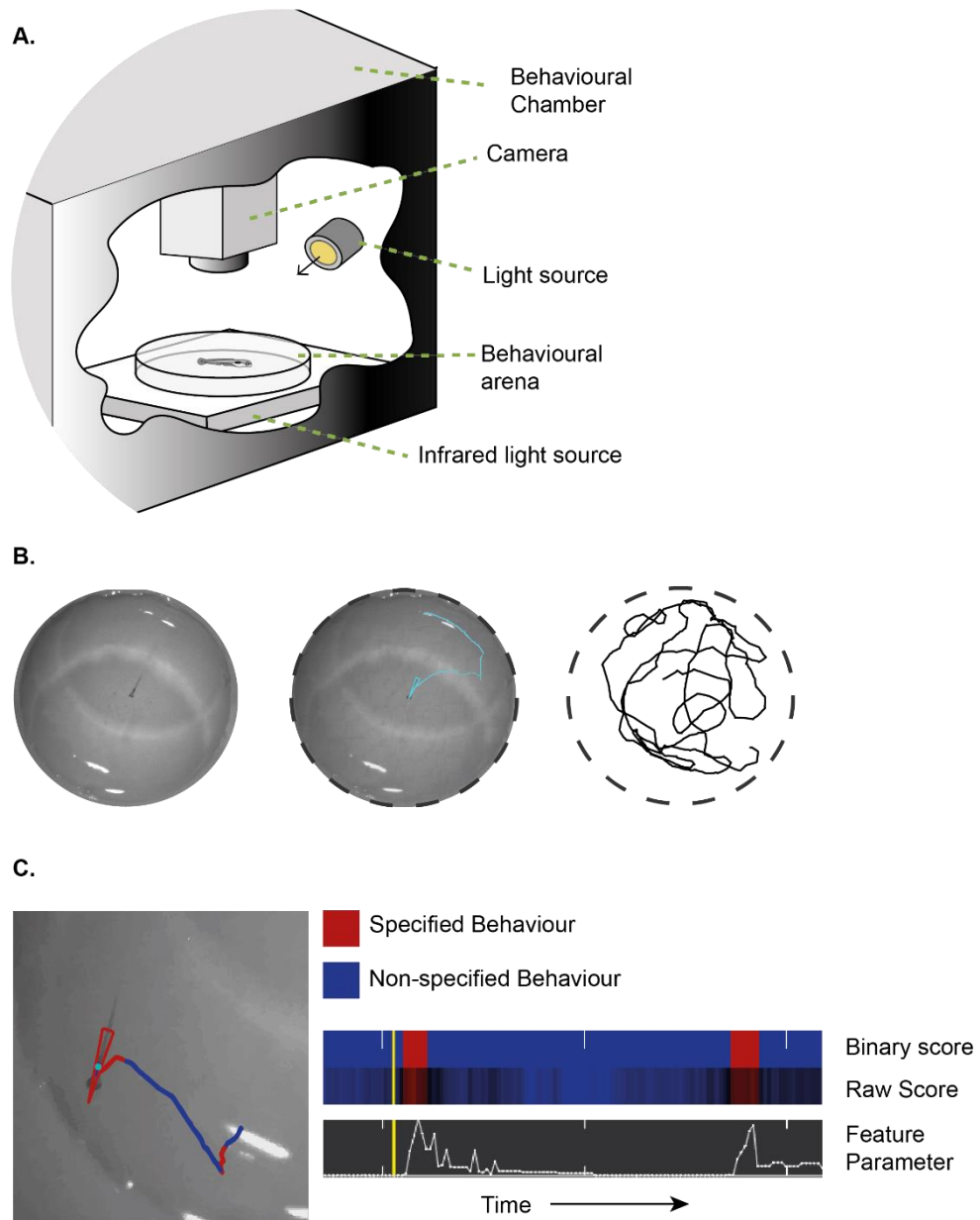
Figure 2:2 Behavioural equipment setup and analysis. A: Larval zebrafish at 5 dpf were placed in a behavioural arena within the behavioural chamber on top of an infrared light source with an overhead camera and a fibre optic light source to control the illumination of the chamber. **B:** Recorded AVI files (left) were processed in VirtualDub and Ctrax to quantify positional information and orientation (middle). Traces of tracking data was generated in MATLAB (right) to illustration swimming behaviours of zebrafish. **C:** Ctrax data was imported into JAABA to categorise specified behaviours (red) and non-specified behaviours (blue).

In order to investigate anxiety-related behaviours such as thigmotaxis and place preference, larvae were placed in a 55 mm diameter dish and allowed to acclimatise for 5 minutes. The dish was placed in an arena illuminated with a fibre

optic light white light source (300 lux) for 5 minutes. Subsequently, the light source was switched off and behaviour recorded for a further 5 minutes in darkness (0 lux). To investigate place preference, zebrafish were placed in a 55 mm diameter dish, in which half of the dish was darkened using black electrical tape. Zebrafish place preference behaviour was recorded for 10 minutes.

2.10.1   Optokinetic reflex

Optokinetic reflex (OKR) assays were used to investigate zebrafish eye movements in response to visual stimuli. To record eye rotation zebrafish were embedded in 3% methylcellulose (Sigma) and orientated in an upright position in a glass arena 10mm in diameter. This arena was placed in a larger 70mm glass arena, and fish were allowed to acclimatise for 5 minutes, after which stimuli were projected onto the outer arena wall. The OKR stimuli were generated using an open-source MATLAB suite described by Scheetz et al., (2018). The OKR stimulus was a grating stimulus and was projected onto the wall of the outer arena. Eye rotational responses to this stimulus were recorded at 50 FPS. The stimulus grated at a spatial frequency of 10 cycles per 360° at an angular velocity of 30 °/s. The grating stimulus moved in one direction and alternated direction every 30 seconds.

2.10.2   Foraging behaviour assay

For specimen subjected to foraging experiments, 5 dpf larvae were placed in a 25 mm agarose dish and recorded for 15 minutes at 30 FPS. Low saline rotifers (ZMsystems) were added to the embryo saline as a natural prey stimulus to trigger foraging behaviours. To visualise free moving rotifers and larval zebrafish, the behavioural arena was placed on a black surface, and fibre optic lights were angled at 45 º towards the dish to illuminate the arena (70 lux) (Bianco et al., 2011b).

2.10.3   Acoustic startle response

In order to investigate the startle response of larval zebrafish, zebrafish were placed in a 25 mm diameter agarose dish and acclimatised for 10 minutes. Zebrafish were recorded for 40 seconds, and bouts of startle responses were captured at 500 FPS using the overhead camera. A speaker underneath the behavioural dish projected a 500 Hz acoustic pulse at 70dB after 10 seconds and repeated a further 2 times at 10-second intervals. When zebrafish were not in the behavioural arena, they were kept in another room to limit pre-exposure to the acoustic stimuli.

2.10.4   Virtually evoked startle response assay

Larval zebrafish were placed in a small glass dish that was 30 mm in height and 10 mm diameter (Figure 5:11A). The lower 20 mm contained sylgard 184 to restrict the vertical swimming space to the upper quadrant. Zebrafish were placed into the dish with system water and acclimatised for 5 minutes prior to any experiment. The small dish was placed in the centre of 70 mm diameter glass arena that was filled with system water upon the infrared light source. A sheet of 60 gms tracing paper was affixed to the outer surface of the 70 mm diameter arena to create a screen for the looming stimuli to be projected onto. Looming stimuli were generated using Psychtoolbox within MATLAB and projected onto the screen using a 100-lumen portable DLP pico projector (iXunGo, Guangdong, China). The projector was placed 15 cm away from the outer arena wall. The size of virtual stimuli was defined by visual angle and calculated using Equation 2.1

$$\theta = 2\arctan\left(\frac{S}{2D}\right)$$

Equation 2.1 Visual angle calculation. S = Object size (mm); D = Distance from object (mm).

Zebrafish visually evoked startle responses were triggered using simulated looming dark squares. Looming stimuli represented an approaching predator and defined by an increase in diameter size and therefore, the visual angle (Figure 5:11C). Free swimming zebrafish were exposed to a looming stimulus. The looming stimulus approached at a constant velocity but expanded at an exponential rate to represent to a realistic approaching stimuli (Matheson et al., 2004, Gabbiani et al., 1999, Bhattacharyya et al., 2017). MATLAB scripts used to generate the realistic looming stimuli were provided by Prof M. MacIver, and experimental protocol was replicated from Bhattacharyya et al., (2017).

Looming stimuli comprised a black object that expanded over time (Figure 5:11). The realistic looming stimulus (constant approach velocity) was defined by the *l/v* ratio, an indicator of angular (θ) expansion over time. The *l/v* ratio is determined as the ratio between half the size of the approaching object (*L*) and the approach velocity (*V*) (Matheson et al., 2004, Bhattacharyya et al., 2017, Temizer et al., 2015). The *l/v* ratio is defined as the angular size of the looming stimuli that is determined by the *l/v* ratio initially expands slowly and then expands rapidly as the object reaches collision (object reaches the visual angle of 180º).

Four looming stimuli of variable approach velocities were presented to zebrafish. The approach velocities of these stimuli included; *l/v* = 0.31, *l/v* = 0.62, *l/v* = 1.25 and *l/v* = 2.5 s, which correspond to approach velocities of 32 mm/s, 16 mm/s, 8 mm/s and 4 mm/s, respectively. Each stimulus was presented to the zebrafish 3 times with 2 minutes interval between the stimulus presentations. Bouts of visually evoked startle behaviours during both constant velocity and linear expanding experiments were captured at 500 FPS using the overhead camera.

2.11   Analysis

2.11.1   Neuron morphology

Juxtacellular experiments reveal the morphology of subpallial DAergic neurons at 2, 3 and 5 dpf. Images of neurobiotin labelled neurons were captured using the Olympus FV1000 confocal microscope. Acquired images were analysed offline using the ImageJ plugin "Simple Neurite Tracer".

2.11.2   Electrophysiology

Electrophysiological recordings were acquired by WinEDR and WinWCP software. .EDR and .WCP files were exported to Axon format. All electrophysiological analyses were conducted offline using Clampfit (Molecular Devices; V10.6). For the analysis of mPSCs, the template search functions were used to identify populations of spontaneous glutamatergic and GABAergic mPSCs. Captured events were manually examined, and inaccurate events (such as fluctuations in baseline noise) were excluded. Event frequencies were determined by counting the number over 300 seconds. For analysis of subpallial DAergic neuron firing activity during extracellular and intracellular recordings, events were identified using Clampfit's threshold detection functions. For fast-scan cyclic voltammetry, electrochemical data were acquired by TarHeel_bob4 software. Subsequent recordings were analysed offline using TarHeelCV.

2.11.3   Behaviour

2.11.3.1   Automated analysis

Compressed digital video AVI files were uncompressed using VirtualDub (V1.10.4). Video colour depth was changed to 'Luminance only (Y8)' and 'No Audio' was specified for the file. The video brightness and contrast were further processed to maximise contrast between specimen and arena background. The uncompressed AVI files were subsequently converted to micro fly movie format (ufmf: V1.0.0.0) using any2ufmf (http://ctrax.sourceforge.net/any2ufmf.html). The

ufmf video files were subsequently imported into California Institute of Technology Fly Tracker (Ctrax; V0.5.16). Video files were processed in Ctrax. Tracking data such as co-ordinates and orientation were obtained for the duration of the recording and extracted in MATLAB format files (Figure 2:2B; left and central panel). Tracking data was reviewed in MATLAB (VR2016a), and any errors were corrected using the 'FixErrors' MATLAB graphical user interface (GUI).To analyse swimming distance and velocity, reviewed Ctrax-derived data was extracted and processed in R-studio (V3.2.0; Figure 2:2B, right panel). Swimming distance, velocity and swimming trajectories were analysed using R script from Jay et al. (2015).

2.11.3.2 Behaviour classification

To analyse specific behaviours exhibit by larva reviewed Ctrax data was imported into Janelia Automatic Animal Behavior Annotator (JAABA; V0.5.0). Using JAABA, the reviewed Ctrax data was used to classify behaviours, e.g. Beat-glide swimming, thigmotaxis and startle response. For JAABA to identify episodes of a specific behaviour, JAABA required an initial training period. During this training period, example (s) of a given behaviour and non-behaviour were manually labelled. Once a behaviour was classified, the machine learning algorithm was executed to identify the behaviour across the video files. Raw data relating to specified data was exported as an excel file for statistical analysis (see subsection 2.11.4).

2.11.3.3 ImageJ analysis

Foraging and startle response kinetics that could not be quantified using the automated software of Ctrax and JAABA were analysed in ImageJ. For startle response analysis, maximal C-bend and counter-bend angles were measured manually using the ImageJ angle tool. To analyse eye movements during free-swimming foraging assays, AVI files were processed in ImageJ. The angle of the eye from the midline of the zebrafish was measured manually for each eye using the ImageJ angle tool.

2.11.3.4   OKR analysis

The analysis of the OKR was conducted using the automated processing of an open-source Matlab suite described in Scheetz et al., (2018). OKR analysis software was used to obtain the orientation of each eye for the duration of the video. Raw traces of the ocular angles were generated automatically from the software. Saccade frequency was extracted using the OKR analysis software in Matlab.

2.11.4   Statistics

All statistical analyses were conducted in Graphpad Prism 7. Gaussian distribution was first examined by the use of the Shapiro-Wilk normality test to determine the appropriate statistical approach (parametric or non-parametric). Data that was determined to be parametric or non-parametric is graphically presented as bar chart or box and whisker plot, respectively (see section 2.11.5). To examine statistical significance, the two-tailed Student's t-test or one-way ANOVA were typically used on normally disturbed data. Non-normally distributed data were statistically analysed using Mann Whitney U test, Kruskal-Wallis test or the Friedman test (paired data). Levene's test was used to compare the variation in the orientation change of control and ablated fish. Two-way ANOVA was used compare multiple stimuli between control and ablated fish. Subsequently a Sidak correction was applied to account for multiple comparisons. Statistical significance is reported as: $*p < 0.05$; $** p < 0.01$, $*** p < 0.001$ and $**** p < 0.0001$.

2.11.5   Data presentation

Results within the figures were generated primarily using Graphpad Prism 7. Unless otherwise stated, bars in bar charts represent the mean, and error bars represent standard error of the mean (SEM). Similarly, for group plots, filled circles represent the mean and the SEM. For box and whisker plots, the internal line represents the median and circles represent raw data points. Upper and lower boundaries of the box correspond to the first and third quartiles and the

whiskers extended to the 1.5x the interquartile ranges. For XY plots, the circles represent raw data points, and the lines represent line of best fit for each condition. Zebrafish swimming traces were generated using R studio using Ctrax data, and plots represent the trajectory of an individual fish. Polar plots were generated in Origin 2015 to illustrate change in orientation, and each line represents the trajectory of a single response from a fish from the looming stimuli. All figures were created in Adobe Illustrator.

CHAPTER 3

The Developmental Properties of Subpallial Dopaminergic Neurons

3.1   Introduction

Our knowledge of the function of DAergic neurons is primarily based on research conducted on mammalian midbrain DAergic neurons. To gain a holistic understanding of these cells, electrophysiological approaches are needed to delineate "how" and "when" DA neurons work. However, current physiological approaches have significant technical limitations. Due to the location of midbrain DAergic neurons, intracellular access cannot be readily gained to delineate "how" these neurons work *in vivo*; therefore, electrophysiological recordings are typically conducted in slice culture. Furthermore, to understand "when" these neurons are active, *in vivo* studies are required to delineate the sensory mechanisms that control DA neuron firing. Therefore, both *in vivo* and *ex vivo* experimental procedures are required fully understand the physiology and function of DA neurons. Early-stage zebrafish is are a useful model for studying the vertebrate nervous system and can overcome the technical limitations associated with mammalian physiological studies (see section 1.5). Due to the size of early-zebrafish, whole-cell patch clamp techniques can be used *in vivo* to visually target DAergic neuron*.* Therefore, "how" and "when" DAergic neurons work can be conducted *in vivo.*

The zebrafish nervous system contains eleven DA clusters, each of which is thought to correspond to an equivalent mammalian DAergic population (Parker et al., 2013). The mammalian midbrain DAergic neurons projects to the striatum as well as the nucleus accumbens, amygdala and frontal cortex (Parker et al., 2013). Whilst there are no DAergic neurons in the zebrafish midbrain, there are, however, a cluster of local DA neurons in the subpallium, the putative striatum (ventral telencephalon) (McLean and Fetcho, 2004a, Tay et al., 2011), that are suggested to be equivalent to the mammalian nigrostriatal neurons (Wullimann and Mueller, 2004, Wullimann and Rink, 2002). This raises the prospect that zebrafish subpallial DAergic neurons could be a model for studying nigrostriatal neurons. However, to date no functional or physiological studies have been conducted to delineate the function of these cells. In this chapter, I have described the physiological properties of subpallial DAergic neurons with an aim to understand if their physiological characteristics are similar to that of the

mammalian nigrostriatal cells. To determine if early-stage zebrafish can be used as a model to study these neurons, their properties have been examined across early development (2 – 5 dpf) to delineate when subpallial DAergic neurons mature and are functionally active. Below, I will discuss an overview of mammalian DA systems and review the physiological studies of mammalian DA neurons to understand the features found in these neurons.

Within this chapter, I have conducted anatomical studies of the subpallial DAergic neurons to examine the development of their morphology and input to assess when they come wired in. Furthermore, I have examined the development of their intrinsic excitability and firing properties of subpallial DAergic neurons in early-stage zebrafish to determine when they are integrated and functional.

3.1.1   Mammalian dopaminergic neurons

There are ten DAergic populations in the mammalian brain (A8 – A17). Eight of these are located in the midbrain/mesencephalon (A8 – A15) (Matsui, 2017, Smeets and Gonzalez, 2000) whilst the remaining are found in the olfactory bulb (A16) and the retina (A17) (Matsui, 2017, Smeets and Gonzalez, 2000). Our understanding of the physiology of DAergic is largely derived from research conducted on midbrain DAergic neurons, specifically the SNc (A9) and VTA (A10) clusters. Early investigations of mammalian DAergic neurons suggested these cells possess a uniform molecular and physiological identity, however, with developing technology and single-cell analysis, evidence now suggests that midbrain DAergic neurons are physiologically heterogeneous (Anderegg et al., 2015, Tapia et al., 2018).

DAergic neurons can be identified by the expression of several genes, including TH, VMAT2, AADC, DAT and D_2 receptors (Eiden and Weihe, 2011, Himi et al., 1995, Smits et al., 2013, Ikemoto et al., 1998). TH and AADC are enzymes involved in the production of DA, and therefore ideal markers for identifying DAergic neurons; however, they are not specific DAergic neuron markers as they are also expressed in NAergic neurons which synthesis DA as a substrate for NA production (Wassall et al., 2009, Daubner et al., 2011). DA and NA neurons can be distinguished by the expression of DβH, an enzyme which converts DA into

NA and therefore is found in NAergic neurons (Issidorides et al., 2004) (see subsection 1.1). Furthermore, DAergic neurons can be identified by the aminergic marker VMAT2 (Eiden and Weihe, 2011). However, as VMAT2 transports the monoamine neurotransmitters including DA, serotonin, histamine and NA (Eiden and Weihe, 2011) into synaptic vesicles (Nirenberg et al., 1996a, Merickel et al., 1995, Gonzalez et al., 1994). Cells that co-express VMAT2 and TH have been used to identify midbrain DAergic neurons (Nirenberg et al., 1996a). However, the levels of VMAT2 expression have been shown to heterogeneous, with the SNc expressing higher levels of VMAT2 than the VTA neurons (Reyes et al., 2013). Together, this suggests there are no universal markers for DAergic neurons. Since NAergic neurons express both TH and DβH, DA neurons can be identified by the expression of TH and the lack of DβH.

Once DA is released into the synaptic cleft, DAT is responsible for reuptake into presynaptic terminals where it is recycled for release or degrade (Giros et al., 1992, Nirenberg et al., 1996b, McHugh and Buckley, 2015). Both D_2 receptor and DAT expression have been observed in the midbrain DAergic neurons as well as the DAergic neurons of the hypothalamus (Stagkourakis et al., 2019, Stagkourakis et al., 2018, Benskey et al., 2012, Revay et al., 1996, Demaria et al., 2000, Meister and Elde, 1993, Stagkourakis et al., 2016). Conversely, the A11 DAergic group express VMAT2 but lack D_2 receptors and DAT (Koblinger et al., 2014a). Without DAT, A11 DAergic neurons are thought to be incapable of regulating DA transmission by reuptake in the same way as SNc and VTA neurons (Koblinger et al., 2014a). Additionally, these neurons cannot be regulated by D_2 autoreceptors. Therefore, DA neurons are active for longer and DA will persist in the synaptic cleft, prolonging the postsynaptic activation of DA receptors.

In sum, although DAergic neurons can be identified by their gene expression profiles, the molecular identity of DAergic neurons is heterogeneous. Therefore, there is no universal set of molecular markers expressed by DAergic neurons. However, DAergic neurons can be identified by the expression of specific genes.

3.1.1.1 Intrinsic excitability and firing patterns of mammalian dopaminergic neurons

Classical studies examining midbrain DAergic neuron excitability (Grace and Bunney, 1984b, Grace and Bunney, 1984a, Grace and Onn, 1989) have identified a number of stereotyped physiological characteristics associated with these cells: broad action potentials characterised by a long half-width (>2ms), cobalt-sensitive calcium currents that drive low threshold depolarisation (Grace and Bunney, 1984b, Grace and Bunney, 1984a, Grace and Onn, 1989), as well as calcium-activated BK channels and Kv2 channels, which are activated during the depolarisation and drive repolarisation (Gantz et al., 2018, Bean, 2007, Kimm et al., 2015) (Figure 3:1). Midbrain DAergic neurons exhibit an after hyperpolarisation (AHP), characterised by a negative shift in membrane potential that inhibits spiking and is dependent on T-type calcium channels and calcium-sensitive potassium channels such as SK channels (Grace and Bunney, 1984b, Evans and Khaliq, 2015, Gantz et al., 2018, Bean, 2007).
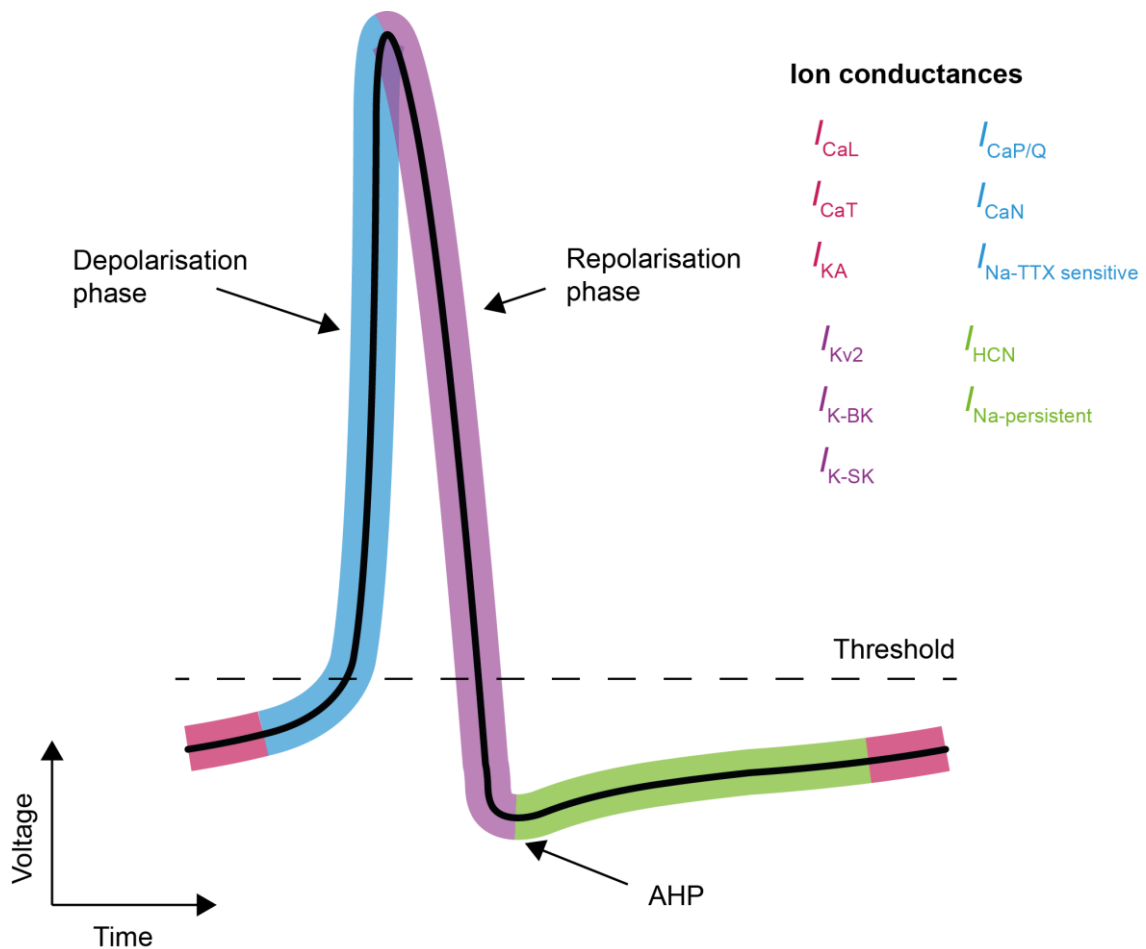
Figure 3:1 Ionic currents underlying action potential wave form. Ion conductances that underlie the generation of action potentials in DA neurons, with the focus to the phases of the waveform. Abbreviations: CaL, L-type calcium channel; CaN, N-type calcium channel; CaP/Q, P/Q calcium channel; CaT, T-type calcium channel; HCN, hyperpolarization-activated cyclic nucleotide-gated channel; I_{Na}-*TTX* sensitive, voltage-dependent sodium current; K-BK, large-conductance calcium-activated potassium (BK) channel; K-SK, small-conductance calcium-activated potassium (SK) channel; Kv2, voltage-gated Kv2 channel. Redrawn and adapted from Gantz et al., (2018), and Bean, (2007).

Early research into the midbrain DAergic neurons revealed these neurons exhibited two types of firing patterns; autonomous and burst firing (Grace and Bunney, 1984a, Grace and Bunney, 1984b, Grace and Onn, 1989). At rest, DAergic neurons exhibit autonomous spiking, characterised by a low firing frequency of approximately 1 – 10Hz (Grace and Bunney, 1984a, Grace and Bunney, 1984b, Grace and Onn, 1989) (see section 3.1.1.2), whilst burst firing pattern is driven by synaptic input and was characterised by repetitive spiking up to a frequency of approximately 50Hz (Overton and Clark, 1997, Hyland et al., 2002) (see section 3.1.1.3). Alongside these dual firing patterns, classical studies

of revealed a variety of physiological features that were used to identify DAergic neurons. These include the presence of presynaptic D_2 autoreceptors, thereby regulating the firing activity of these cells (Ford, 2014, Stagkourakis et al., 2016) (see subsection 3.1.2). As mentioned earlier, another feature of mammalian midbrain DAergic neurons is the presence of an I_h current, which can be identified by a sag potential when the neurons are hyperpolarised (He et al., 2014, Carbone et al., 2017, Okamoto et al., 2006) (see subsection 3.1.3).

3.1.1.2   Autonomous firing

Autonomous firing, or 'pacemaker activity', is characterised by the rhythmic slow membrane oscillations that are sufficient to drive action potentials and persists when synaptic input is blocked (Grace and Bunney, 1984a, Grace and Bunney, 1984b, Grace and Onn, 1989, Guzman et al., 2009, Liss et al., 2001). Such activity is driven by an ensemble of sodium, potassium and calcium currents in midbrain DAergic neurons (Khaliq and Bean, 2010, Canavier et al., 2016, Khaliq and Bean, 2008). Application of TTX is sufficient to abolish action potentials but not membrane oscillations in VTA neurons, suggesting a lack of requirement for voltage gated sodium currents (Grace and Onn, 1989). Khaliq and colleagues found the non-voltage dependent sodium currents in VTA neurons that maintain the neurons above resting membrane potential, substituting external sodium with N-methyl-D-glucamine (NMDG) revealed a TTX-sensitive persistent sodium current (INaP) that drives the neurons to threshold (Khaliq and Bean, 2010). By contrast, autonomous firing activity of SNc neurons is not driven by sodium currents. Rather, SNc neurons appear to have a higher density of nifedipine-sensitive $Ca_v1.3$ L-type calcium channels and application of this drug abolishes subthreshold membrane oscillations in these neurons (Chan et al., 2007, Putzier et al., 2009, Philippart et al., 2016). Together, this suggests the subthreshold calcium conductances drive membrane oscillations in SNc neurons (Philippart et al., 2016).

Mammalian DAergic neurons often possess an I_h current (hyperpolarisation-activated inward current; see subsection 3.1.3), which has also been implicated in the generation of autonomous firing (Maccaferri and McBain, 1996, Okamoto et al., 2006, Funahashi et al., 2003). This current is mediated by

hyperpolarisation-activated cyclic nucleotide-gated (HCN) cation ion channels. As the name suggests HCN channels are activated by membrane hyperpolarisation. The central pore conducts cations to generate a slow membrane depolarisation, gradually pushing the membrane towards threshold (Pape, 1996, He et al., 2014). In DAergic neurons that possess HCN channels, the action potential AHP is sufficient to generate an I_h current drive cyclical firing in the absence of synaptic transmission (Okamoto et al., 2006). Blocking I_h can decrease the autonomous firing SNc and VTA neurons (Krashia et al., 2017) through attenuation of rebound depolarisation following the AHP (Gambardella et al., 2012). Autonomous firing can be restored to by the injection of depolarising current into the neuron (Gambardella et al., 2012). Therefore, the I_h current is not necessary for autonomous firing but facilitates this firing pattern in DAergic neurons.

Autonomous firing has also been observed in olfactory bulb (A16) DA neurons. Here activity is driven by voltage-dependent sodium, potassium and calcium and I_h currents (Pignatelli et al., 2005, Pignatelli et al., 2013). Tuberoinfundibular dopamine (TIDA) neurons of the hypothalamus (A12 cluster) can be divided into two subpopulations based on rhythmic burst firing and the other non-burst firing (Zhang and van den Pol, 2015). Lyons and colleagues suggested oscillatory bursting TIDA cells exhibit electrically coupled rhythmic oscillations that coordinates this activity (Lyons et al., 2010). Recent work has shown that membrane oscillations driving rhythmic bursting occur independently of synaptic input and the application of a T-type calcium channel blocker and an antagonist of A-type potassium channels inhibited the slow depolarisation phase of the membrane oscillation and generated irregular bursting in TIDA cells, respectively (Zhang and van den Pol, 2015). This suggests the rhythmic membrane oscillations are driven by a calcium current and controlled by voltage-dependent A-type potassium channels.

It is also believed that the conductances underpinning subthreshold membrane oscillations differ with respect to developmental stage (Costa, 2014, Dreher et al., 2008, Marti et al., 2009, Vogt Weisenhorn et al., 2016). During maturation, the SNc neurons exhibit a physiological shift with age, at juvenile stage (P17) the subthreshold membrane oscillations of SNc neurons are driven by sodium

currents, however, calcium currents appear to become more important for membrane oscillation generation in older animals (Chan et al., 2007). These neurons of SNc have an increased susceptibility to degeneration in Parkinson's disease (Surmeier et al., 2017). One possible reason for this is that the high density of L-type calcium channels found in SNc neurons may chronically increase calcium load when compared to the neighbouring DAergic neurons of the VTA (Guzman et al., 2009). This increase in calcium signalling may induce oxidative stress and contribute to the degeneration of SNc neurons (Guzman et al., 2010, Dias et al., 2013).

3.1.1.3   Burst firing

Burst firing in DAergic neurons is typically characterised by brief bouts of high-frequency spiking (Grace and Bunney, 1984a, Shepard and Stump, 1999, Overton and Clark, 1997), resulting in the phasic release of DA. Classical studies of SNc DAergic neurons defined burst firing as two or more spikes with the initial interspike interval (ISI) of less than 80 ms, but as the burst progresses the subsequent ISI between spikes increases until it becomes greater than 160 ms (Grace and Bunney, 1984a). The 80/160ms criteria was classically used to identify burst firing in DAergic neurons, however, the diversity in the physiology properties of DAergic neurons has resulted in alternative detection methods (Paladini and Roeper, 2014).

There are multiple models for the mechanism of burst firing in these cells (Morikawa and Paladini, 2011). Injection of depolarising current into DAergic neurons cultured in vitro can elicit bursts (Blythe et al., 2009, Blythe et al., 2007, Deister et al., 2009, Morikawa and Paladini, 2011), suggesting depolarising input evokes this response. In support of this premise, sensory stimulation can evoke burst firing *in vivo* (Horvitz et al., 1997) suggesting synaptic transmission underpins bursting in the intact CNS. Blockade of NMDAs receptor is sufficient to attenuate burst firing, suggesting that this response is driven by excitatory glutamatergic afferents (Overton and Clark, 1992, Zweifel et al., 2009, Chergui et al., 1993).

Whilst synaptic input is required to initiate burst firing, intrinsic membrane properties help to maintain high frequency firing during a burst. Application of

EGTA, a calcium chelator abolishes bursting whilst dialysis with calcium during patch-clamp recording evokes bursting in SNc neurons (Grace and Bunney, 1984a). By contrast, application of apamin, an SK_{ca} channel antagonist also induces bursting in DA neurons (Shepard and Stump, 1999). Similarly, block of potassium currents with intracellular caesium generates bursts in DA neurons (Mercuri et al., 1994). These neurons can generate plateau potential, a stable prolonged depolarisation of the membrane potential that can facilitate successive firing activity without sustained synaptic input (Kiehn and Eken, 1998). Calcium currents have been shown to produce the plateau potential, application of Nifedipine, the antagonist of the L-type calcium channels, abolishes the plateau potential and inhibits burst firing in DA neurons (Shepard and Stump, 1999). Activation of these L-type calcium channels by Bay K8644 can induce bursting in DA neurons (Zhang et al., 2005). The plateau potential of DA neurons is dependent on high threshold calcium currents, which are activated by NMDA receptors (Overton and Clark, 1997). Therefore, burst firing of DAergic neurons is driven by the interaction of excitatory synaptic input and intracellular calcium currents.

Burst firing is not just a physiological feature of DAergic neurons of the SNc and VTA: rhythmic bursting has also been observed in hypothalamic DAergic neurons (A12 cluster). However, here bursting is not driven by synaptic input (Zhang and van den Pol, 2015). Instead, these neurons generate slow rhythmic membrane oscillations, in which slow depolarisation of the membrane potential is driven by T-type calcium, and A-type potassium channels inhibit these oscillations (Zhang and van den Pol, 2015). Rhythmic burst firing is dependent on membrane oscillation exhibited by hypothalamic DAergic neurons (Zhang and van den Pol, 2015) rather than the interaction of synaptic input and plateau potential that is seen in the VTA and SNc. Additionally, Injection of depolarising current can trigger high-frequency firing, up to 28 Hz in some olfactory DAergic neurons (Chand et al., 2015); however, these neurons only exhibit autonomous firing (Pignatelli et al., 2005).

In sum, studies have shown DAergic can generate high-frequency firing patterns known of burst firing. However, burst firing pattern is not conserved between all DA populations, whilst subpopulations can generate high-frequency spike chains,

they are not driven by the same intrinsic mechanisms. Thus, the firing properties of DAergic neurons are heterogeneous.

3.1.2 Presynaptic expression of D_2 receptors can modulate dopamine neuron activity

A traditional physiological feature of mammalian midbrain DAergic neurons is autoregulation by the expression of presynaptic D_2 receptors (Ford, 2014). These activate G protein-coupled inwardly-rectifying potassium (GIRK) channels (Rifkin et al., 2018, McCall et al., 2019, Lalive et al., 2014), resulting in membrane hyperpolarisation (Groves et al., 1975, Luscher and Malenka, 2011, Cruz et al., 2004). In addition, through inhibition of AC (Beaulieu and Gainetdinov, 2011), D_2 reduces cAMP-PKA mediated phosphorylation of TH (Ford, 2014, Wolf and Roth, 1990), thereby reducing DA synthesis (Anzalone et al., 2012, Ford, 2014).

Activation of D_2 autoreceptors can also regulate membrane excitability through GIRK channels, which hyperpolarise the DAergic neurons. Activation of these receptors reduces firing activity of VTA and SNc DA neurons in these regions (Bunney and Aghajanian, 1974, Beckstead et al., 2007). Additionally, D_2 autoreceptor reduces DA transmission by inhibiting voltage-gated calcium channels, therefore inhibiting calcium influx, which promotes synaptic transmission by facilitating vesicle fusion (Phillips and Stamford, 2000, Sudhof, 2012). D_2 receptor null animals have reduced DA levels and exhibit reduced locomotive and reward seeking behaviours (Welter et al., 2007, Kelly et al., 1998). Together, this suggests D_2 receptors have a role in negatively regulating DA levels in the brain. This ensures pathological levels do not occur.

Classically, D_2 autoreceptor inhibition was used as a physiological marker to identify DAergic neurons (Lacey et al., 1987). However, the development of technology that allows single-cell analysis, such as electrophysiology and RNAseq, has shown that not all DAergic neurons exhibit this property. For example, VTA neurons of the mesocortical pathway do not possess physiological responses to D_2 autoreceptor agonism (Lammel et al., 2008). Similarly, unlike those projecting to the striatum, amygdaloid projecting VTA neurons are not hyperpolarised by D_2 receptor agonists (Margolis et al., 2008). Beyond the

midbrain, the D_2 autoreceptor function of TIDA cells is controversial, and early investigations could not determine the presence of D_2 autoreceptors in these neurons (Timmerman et al., 1995), although recent work has challenged this view (Stagkourakis et al., 2016). Studies have shown that the spinal cord projecting A11 DAergic population lack presynaptic D_2 receptors (Pappas et al., 2008). This has been suggested to contribute to disorders such as restless leg syndrome (Pappas et al., 2008). In sum, early studies used D_2 autoreceptor inhibition to identify DA neurons; however, D_2 autoreceptors are not conserved between all DAergic neurons and subpopulations of DAergic neurons exhibit different sensitivities to DA. Therefore, not all DA neurons require autoreceptors to regulate their activity.

3.1.3 Sag potential and I_h current in mammalian dopaminergic neurons

As previously discussed, the I_h current is a hyperpolarisation-activated current that is generated by the HCN cation ion channel (He et al., 2014). These channels conduct potassium and sodium ions (Funahashi et al., 2003, Angelo and Margrie, 2011, Banks et al., 1993), resulting in an initial rapid and subsequent steady-state depolarisation (Pape, 1996). The electrophysiological property of this rebound depolarisation generated by the I_h current is also referred to as a "sag" potential (Maccaferri and McBain, 1996). The presence of this current was traditionally used to identify DAergic neurons as initial studies revealed its presence in SNc, VTA and olfactory bulb DA neurons. However, some DAergic cells, such as TIDA neurons do not generate sag potentials (Grace and Onn, 1989, Lammel et al., 2008, Pignatelli et al., 2013, Lyons et al., 2010). Therefore, whilst I_h was believed to be a common feature of DA neurons, it now appears that this channel is not ubiquitously expressed in this cell population.

The I_h current can be attenuated by the application of ZD7288 (Seutin et al., 2001), and blocking this current can perturb autonomous firing (see subsection 3.1.1.2). Autonomous firing activity can be restored to these neurons by depolarising the resting membrane potential whilst in the presence of ZD7288 (Gambardella et al., 2012). Therefore, the I_h is not necessary for autonomous firing to occur, but the current facilitates autonomous firing in DAergic neurons by

depolarising the membrane to a voltage that activates ion channels that drive currents such as INaP.

The I_h current has been observed in multiple DAergic populations, however, studies have shown this property is heterogeneous between DAergic neurons. VTA and SNc DA populations exhibit differences in the I_h current, sag potential amplitude, as well as rebound delay (Neuhoff et al., 2002). SNc neurons exhibit larger amplitude sag potentials that DAergic neurons of the VTA (Neuhoff et al., 2002, Lammel et al., 2008). One suggestion for the variation is that the ion channels that drive the I_h current are differentially expressed between DAergic neurons groups, however, other factors may affect the sag potential kinetics such as HCN subunit expression (Neuhoff et al., 2002).

3.1.4   Zebrafish dopaminergic neurons

The zebrafish DAergic system is restricted to the zebrafish forebrain, which consists of eleven populations (Schweitzer et al., 2012) (Figure 1:6). The DAergic clusters found in the diencephalon include the preoptic cluster, the posterior tuberculum groups (DC1 to DC7) and the pretectal cluster (Mahler et al., 2010, Rink and Wullimann, 2002b). The DAergic neurons in the diencephalon can be identified based on soma morphology and location across the diencephalic DAergic clusters (Schweitzer et al., 2012). DC1, DC6 and pretectal DAergic neurons have a small round morphology, whilst DC2 and DC4 are large pear-shaped neurons, and the final morphology observed is a bipolar liquor-contacting neuron and found in the DC3, 5 and 7 clusters (Rink and Wullimann, 2002b). The preoptic DAergic neurons can be divided into two morphologies, the most rostral are oval-shaped unipolar neurons, whilst the caudal neurons were larger and had a descending unipolar projection (McLean and Fetcho, 2004a). The DAergic neurons of the olfactory bulb and subpallium have similar soma morphology, small, unipolar and ovoid (McLean and Fetcho, 2004a).

3.1.4.1 Physiological properties of dopaminergic neurons in early-stage zebrafish

Currently, we know relatively little about DA neuron physiology in zebrafish. However, patch-clamp studies of the DDNs in the posterior tuberculum have shown that these cells possess many of the physiological features observed in mammalian midbrain DAergic neurons (Jay et al., 2015). DDNs were found to have broad action potentials and were capable of high frequency firing patterns that resembled burst firing (Jay, 2015). Physiological recordings of the zebrafish DC2/4 neuron clusters in the presence of synaptic blockers have shown that these cells exhibit autonomous firing (Jay et al., 2015). Furthermore, the application of KYN and PIC revealed slow membrane oscillations, that were abolished by the application of TTX (Jay et al., 2015). The conductances driving autonomous firing in DC2/4 neurons were voltage-dependent, and since the application of TTX abolished membrane oscillations, Jay and colleagues suggested the autonomous firing activity of DC2/4 clusters is generated by voltage-gated sodium channels (Jay et al., 2015).

Further examination of the physiological features of DC2/4 neurons found they do not exhibit a sag potential when subjected to hyperpolarising current injection (Jay, 2015). Therefore, these neurons do not possess an I_h current. Additionally, physiological recordings of DC2/4 clusters revealed these neurons exhibit D_2 autoreceptor inhibition (Jay, 2015). Similar to that of the mammalian DAergic neurons, application of DA during physiological records attenuates firing activity and hyperpolarises the membrane potential an effect that is blocked by preincubation with the D_2 receptor antagonist raclopride (Jay et al., 2015, Jay, 2015).

In sum, physiological analysis of the DDNs revealed the DC2/4 cluster exhibit multiple physiological features of mammalian midbrain DAergic neurons. DC2/4 cluster possesses broad action potentials and exhibits both burst and autonomous firing patterns. The DC2/4 cluster also exhibits D_2 autoreceptor inhibition, a feature observed in most mammalian midbrain DAergic neurons. However, the DC2/4 cluster does not exhibit a sag potential or I_h current; a physiological feature traditionally used to identify mammalian DAergic neurons.

Together, this suggests that traditional physiological features of mammalian DAergic neurons are conserved across species and observed in zebrafish, but unique molecular identities of DA neurons can give rise to distinct physiological features exhibited by DA populations.

3.1.4.2 Zebrafish subpallial dopaminergic neurons

To date, investigations into the subpallial DAergic neurons have been limited to morphological and anatomical studies. Morphological studies have revealed these neurons to be small unipolar neurons that project ventrolaterally (McLean and Fetcho, 2004a, Tay et al., 2011). One study found that the subpallial DAergic neurons project locally with dense arbours, with a percentage of these neurons projecting contralaterally and to the thalamus and hypothalamus (Tay et al., 2011). Additionally, anatomical studies have also investigated subpallial afferents in adult zebrafish. Rink and colleagues found the subpallium is innervated by the olfactory bulb, pallium, preoptic region, thalamus, posterior tuberculum, hypothalamus and hindbrain regions including the nucleus of medial longitudinal fascicle (nMLF), raphe, locus coeruleus (Rink and Wullimann, 2004, Rink and Wullimann, 2002a, Rink and Wullimann, 2002b, Rink and Wullimann, 2001). However, these studies did not investigate the subpallial DAergic neurons afferents exclusively.

In adult zebrafish, there have been a limited number of physiological investigations of the subpallial DAergic neurons. Fast-scan cyclic voltammetry (FSCV) was able to detect DA release within the subpallium when electrically stimulated *ex vivo* (Shin et al., 2017, Jones et al., 2015, Field et al., 2018). However, these studies only examined DA release in the telencephalon, the physiological features and firing activity of the subpallial DAergic neurons has not been examined. I aim to address the lack of physiological analysis within the literature and characterise the physiology of subpallial DAergic neurons of early-stage zebrafish.

3.2   Aims and Objectives

In this chapter, I aim to better understand the subpallial DAergic neurons of early-stage zebrafish by characterising the morphological and physiological properties of these cells across early zebrafish development. Of note to this thesis, these properties were examined in 2 to 5 dpf zebrafish. I hypothesise that the subpallial DAergic neurons are physiologically homologous to the DAergic neurons of the SNc. To address this, I examine morphological development of these cells. Additionally, I use whole-cell patch-clamp techniques to examine the development of synaptic input, intrinsic excitability and endogenous firing patterns to delineate their functional maturation. The data presented in this chapter demonstrates the ontogeny of morphological and physiological properties of subpallial DAergic neurons change rapidly during early development.

3.3　　Results

3.3.1　Identification of subpallial dopaminergic neurons during early development

First, I sought to identify and characterise subpallial DAergic neurons in the brain of Tg(ETvmat2:GFP) fish, which express GFP in all aminergic neurons (Wen et al., 2008). To do this, I examined the co-localisation of *th* and GFP *in the* telencephalon of these fish. There are two spatially segregated clusters of *th* positive cells in the telencephalon: one located in the olfactory bulb and the other in the neighbouring subpallium (Yamamoto et al., 2010a). As previous studies have shown that *th* positive neurons are first observed in the subpallium at 48 hpf (Mahler et al., 2010), I restricted my studies to developmental periods beyond this stage. Immunohistochemical analysis revealed that, in agreement with previous studies (Wen et al., 2008, Sallinen et al., 2009, McLean and Fetcho, 2004a, Tay et al., 2011), a cluster of *vmat2, th* positive neurons were observed in the subpallium between 2 and 5 dpf (Figure 3:2B-F).

As mentioned previously, there is no unique marker of DAergic neurons (Eiden and Weihe, 2011) as *th* is also expressed in NAergic cells. However, the distribution of NAergic neurons has been mapped previously using DβH immunohistochemistry (Tay et al., 2011, Schweitzer et al., 2012, Filippi et al., 2010). Based on these findings, NAergic neurons are restricted to the hindbrain, strongly suggesting that forebrain TH neurons are exclusively DAergic (Holzschuh et al., 2003, Schweitzer et al., 2012, Filippi et al., 2010). In this study I used *vmat2* as a marker for DAergic cells, which also labels NAergic, serotonergic and histaminergic cells. Histaminergic neurons are restricted to the hypothalamus, and serotonergic neurons are only found in the ventral diencephalon, caudal hypothalamus and raphe (Sundvik and Panula, 2012, Ren et al., 2013, McLean and Fetcho, 2004a). Taken together, it can be assumed the caudal cluster of *th* and *vmat2* co-expressing neurons in the telencephalon are DAergic.

A.
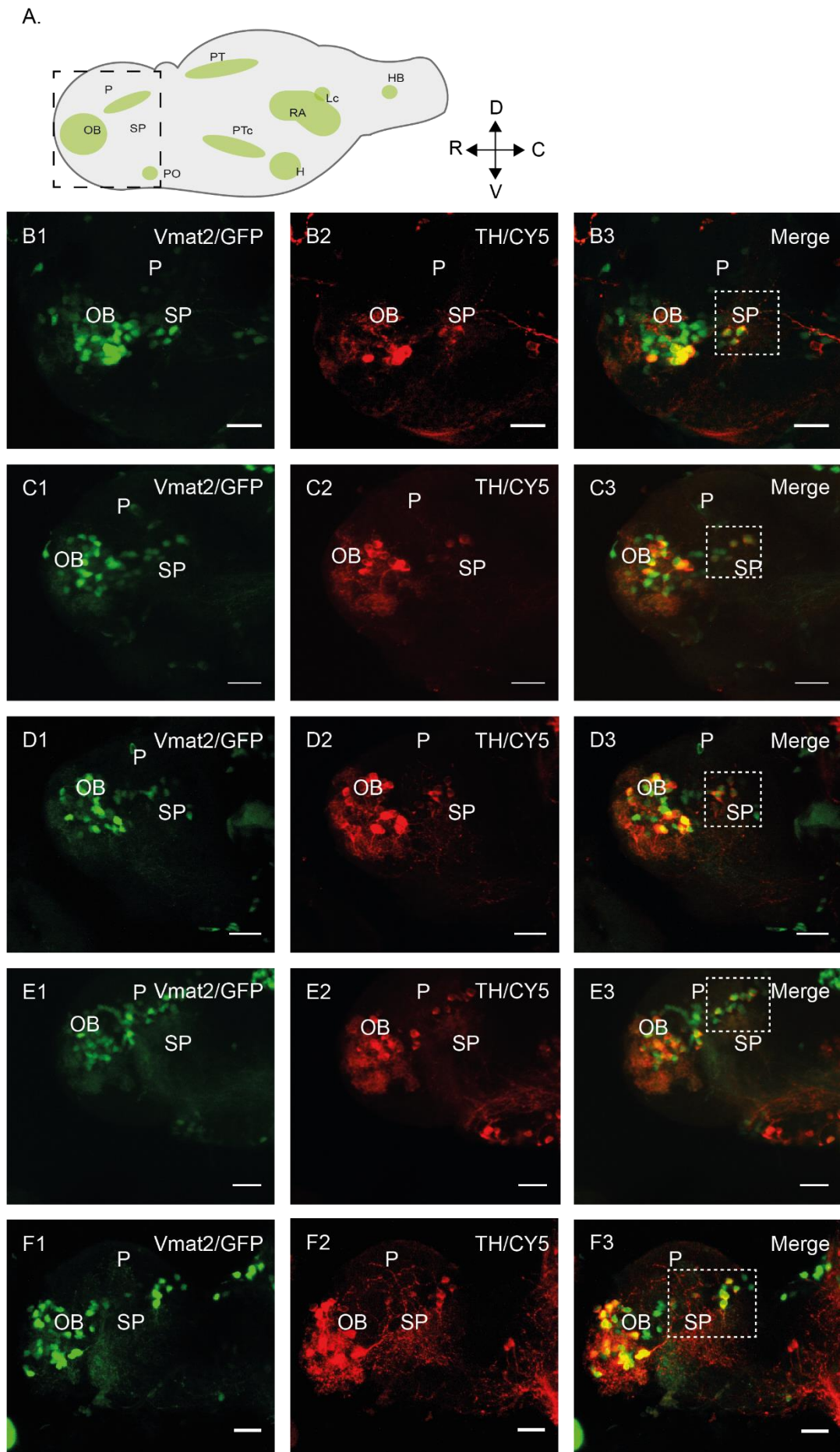
Figure 3:2 Visualisation of TH positive neurons of the zebrafish telencephalon. A: Schematic illustration of zebrafish brain (lateral) representing Vmat2/GFP expression (green). Dashed line represents the region of interest in subsequent confocal images. Orientation is indicated in panel (**A**); R = rostral, C = caudal, D = dorsal and V = ventral. **B–E:** Images illustrating immunohistochemical staining of TH positive neurons in zebrafish telencephalon and visualised by confocal microscopy. Left column: Vmat2/GFP expression (green). Middle column: Anti-TH (red). Right column: merge of green and red channels. **B1–3:** Lateral view of telencephalon (2 dpf). **C1–3:** Lateral view of telencephalon (3 dpf). **D1–3:** Lateral view of telencephalon (4 dpf). **E1–3:** Lateral view of telencephalon (5 dpf). **F1–3:** Lateral view of telencephalon (5.5 dpf). Abbreviations; olfactory bulb (OB), subpallium (SP), pallium (P), preoptic (PO), posterior tuberculum (PTc), hypothalamus (H), pretectum (PT), locus coeruleus (LC), raphe nucleus (RA) and hindbrain (HB). Scale bar 20µm.

Analysis revealed that the number of *th*-positive neurons in each hemisphere of the subpallium increased between 2 and 3 dpf but remained constant thereafter (2 dpf = 3.75 ± 1.04, n_{fish} = 8; 3 dpf = 7 ± 1.16, n_{fish} = 7; 4 dpf = 8 ± 0.93, n_{fish} =8; 5 dpf = 8.29 ± 1.38, n_{fish} = 7; 5.5 dpf = 9.38 ± 1.99, n_{fish} =8, p = 0.0001, Kruskal-Wallis test; Figure 3:3A). During this period, soma diameter gradually increased until plateauing at 4 dpf (2 dpf = 5.96 ± 0.52µm, n_{fish} = 8; 3 dpf = 6.42 ± 0.62µm, n_{fish} = 7; 4 dpf = 7.11 ± 0.58µm, n_{fish} =8 ; 5 dpf = 6.67 ± 0.42µm, n_{fish} = 7; 5.5 dpf = 7.36 ± 0.74µm, n_{fish} =8, p = 0.0004, one way ANOVA; Figure 3:3B).
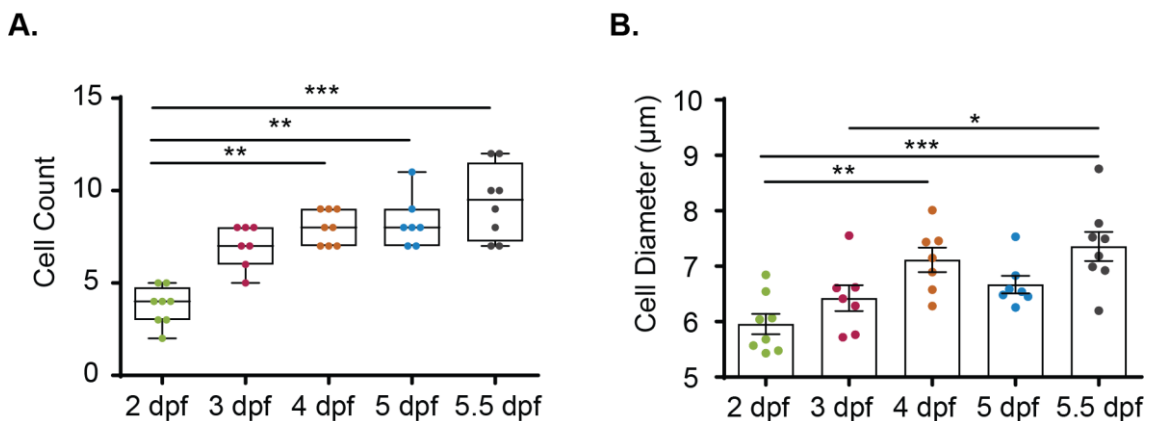
Figure 3:3 Tyrosine hydroxylase neuron measurements during early development. A: Box and whisker plots of TH positive neuron cell count. **B:** Bar chart comparing the soma diameter of TH positive neurons at developmental stages 2 to 5.5 dpf. *P < 0.05, **P < 0.005, ***P < 0.0005.

3.3.2   Ontogeny of subpallial dopaminergic neuron morphology

Tay and colleagues have previously investigated the morphology of subpallial DAergic neurons at 4 dpf, finding that the majority of these neurons arborize locally within the telencephalon (Tay et al., 2011). However, a small proportion also extends processes to posterior tubercular, thalamic and hypothalamic regions (Tay et al., 2011). To examine the ontogeny of subpallial DAergic neurons, I performed juxtacellular neurobiotin labelling of these cells across 2-5 dpf. Imaging of individually neurobiotin labelled neurons revealed that neurites could be identified across all ages studied (Figure 3:4). Juxtacellular labelling revealed that subpallial DAergic neurons arborize locally in close proximity to the cell body (Figure 3:4). I also identified descending projections entering the diencephalon in 5 dpf zebrafish (Figure 3:5). To quantify the development of the subpallial DAergic neurons' Sholl intersection profiles at 2, 3 and 5 dpf (Figure 3:4D). The Sholl intersection profile quantifies the number of times a neurite intersects a hypothetical sphere of a given radius, with the centre of the sphere being the soma (Bird and Cuntz, 2019). Sholl analysis of 2 and 3 dpf neurons revealed a low number of intersections, and therefore a low density of arborisation proximal to the some (Figure 3:4D). At 5 dpf Sholl analysis revealed an increase in the number of intersections, when compared to 2 and 3 dpf neurons (see Table 3.1 Two-way ANOVA of Sholl analysis and Table 3.2 for multiple comparisons for Sholl analysis, Figure 3:4C/D).

Analysis of cumulative neurite length revealed an increase across early development (2 dpf = 150.4 ± 120.2µm, n_{fish} = 6, n_{cells} = 6; 3 dpf = 421.8 ± 174.6µm, n_{fish} = 6, n_{cells} = 6; 5 dpf = 827.0 ± 328.4µm, n_{fish} = 5, n_{cells} = 5; p = 0.0006, one-way ANOVA; Figure 3:4E). Together, with the Sholl analysis, the results show an increase in the number of arbours and arbour length, suggesting the cytoarchitecture of subpallial DAergic neuron becomes more complex during early development, as suggested by previous findings (Tay et al., 2011). Together, these results suggest the dendritic arbours of subpallial DAergic neurons increases as they mature
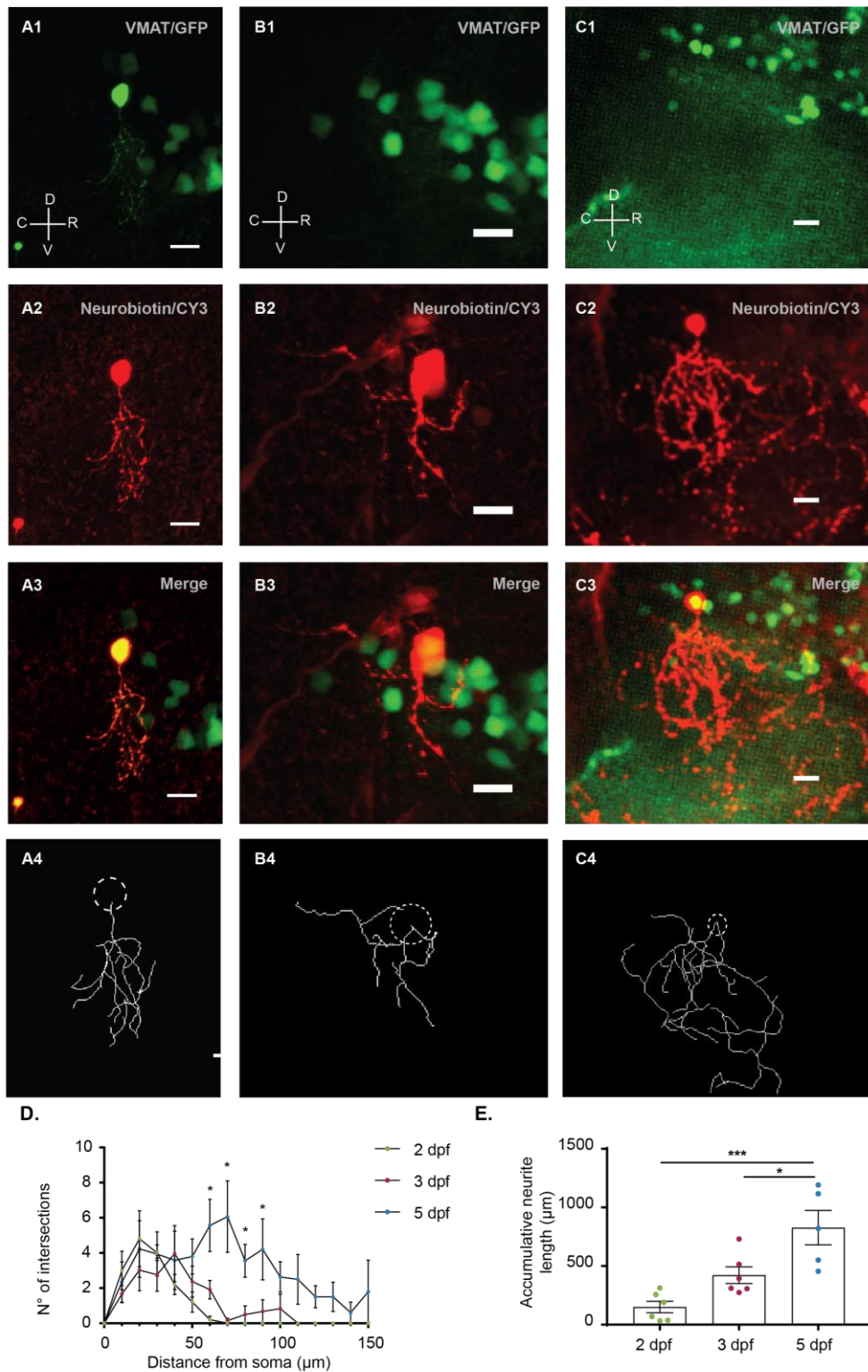
Figure 3:4 Juxtacellular labelling of subpallial DAergic neurons (2, 3 and 5 dpf) A-C: Images illustrating streptavidin histochemical staining of neurobiotin juxtacellular labelled neurons in the subpallium and visualised by confocal microscopy. Upper column: Vmat2/GFP expression (green). Middle column: Neurobiotin (red). Lower column: merge of green and red channels. Orientation is indicated in upper panel; R = rostral, C = caudal, D = dorsal and V = ventral.

A1–3: Neuron morphology of subpallial DAergic neuron at 2 dpf. **B1–3:** Morphology of subpallial DAergic neuron at 3 dpf. **C1–3:** Morphology of subpallial DAergic neuron at 5 dpf. **D:** Bar chart comparing the cumulative dendritic arbour length at 2, 3 and 5 dpf. **E:** Bar chart comparing the average neurite length. Scale bar: 10µm. *P < 0.05, ***P < 0.0005.

Table 3.1 Two-way ANOVA of Sholl analysis

	DF	MS	F (DFn, DFd)	P value
Interaction	30	6.424	F (30, 195) = 1.924	P=0.0045**
Distance	15	24.87	F (15, 195) = 7.449	P<0.0001****
Age	2	104.2	F (2, 13) = 6.531	P=0.0109*
Subjects (matching)	13	15.95	F (13, 195) = 4.776	P<0.0001****
Residual	195	3.339		

* P < 0.05, ** P < 0.005, **** P < 0.0001

Table 3.2 Tukey multiple comparison analysis

	Diff. in mean	DF	P value
_10µm_			
2 dpf vs 3 dpf	1.336	208	0.5237
2 dpf vs 5 dpf	0.6623	208	0.8639
3 dpf vs 5 dpf	-0.6739	208	0.8477
_20µm_			
2 dpf vs 3 dpf	1.778	208	0.3196
2 dpf vs 5 dpf	0.5736	208	0.8960
3 dpf vs 5 dpf	-1.204	208	0.5909
_30µm_			
2 dpf vs 3 dpf	1.238	208	0.5738
2 dpf vs 5 dpf	0.05973	208	0.9988
3 dpf vs 5 dpf	-1.178	208	0.6044
_40µm_			
2 dpf vs 3 dpf	-1.759	208	0.3272
2 dpf vs 5 dpf	-1.376	208	0.5333
3 dpf vs 5 dpf	0.3837	208	0.9478
_50µm_			
2 dpf vs 3 dpf	-1.168	208	0.6094
2 dpf vs 5 dpf	-2.598	208	0.1095
3 dpf vs 5 dpf	-1.429	208	0.4772
_60µm_			
2 dpf vs 3 dpf	-1.71	208	0.3477
2 dpf vs 5 dpf	-5.362	208	0.0001****
3 dpf vs 5 dpf	-3.652	208	0.0093*

62

70µm

2 dpf vs 3 dpf	-0.1494	208	0.9919
2 dpf vs 5 dpf	-6.065	208	<0.0001****
3 dpf vs 5 dpf	-5.916	208	<0.0001****

80µm

2 dpf vs 3 dpf	-0.4937	208	0.9151
2 dpf vs 5 dpf	-3.557	208	0.0168*
3 dpf vs 5 dpf	-3.063	208	0.0360*

90µm

2 dpf vs 3 dpf	-0.6714	208	0.8487
2 dpf vs 5 dpf	-4.201	208	0.0036**
3 dpf vs 5 dpf	-3.53	208	0.0125*

100µm

2 dpf vs 3 dpf	-0.8325	208	0.7773
2 dpf vs 5 dpf	-2.626	208	0.1044
3 dpf vs 5 dpf	-1.793	208	0.3134

110µm

2 dpf vs 3 dpf	0	208	>0.9999
2 dpf vs 5 dpf	-2.496	208	0.1294
3 dpf vs 5 dpf	-2.496	208	0.1078

120µm

2 dpf vs 3 dpf	0	208	>0.9999
2 dpf vs 5 dpf	-1.507	208	0.4707
3 dpf vs 5 dpf	-1.507	208	0.4398

130µm

2 dpf vs 3 dpf	0	208	>0.9999
2 dpf vs 5 dpf	-1.5	208	0.4738
3 dpf vs 5 dpf	-1.5	208	0.4429

140µm

2 dpf vs 3 dpf	0	208	>0.9999
2 dpf vs 5 dpf	-0.6039	208	0.8854
3 dpf vs 5 dpf	-0.6039	208	0.8757

150µm

2 dpf vs 3 dpf	0	208	>0.9999
2 dpf vs 5 dpf	-1.794	208	0.3447
3 dpf vs 5 dpf	-1.794	208	0.3132

* P < 0.05, ** P < 0.005, *** P < 0.0005, **** P < 0.0001

At 2 and 3 dpf subpallial DAergic neurons, labelled neurons only possessed local arbours. However by 5 dpf two morphologies were observed: those that only arbourise locally (n = 5; Figure 3:5A/B) and those that had local and long-range projections to regions caudal to the subpallium (n = 1; Figure 3:5C). This is consistent with the literature, in which Tay and colleagues observed similar projection patterns in 4 dpf subpallial DAergic neurons, with 20% of subpallial DAergic neurons projecting to the thalamus and 30% to the hypothalamus (Tay

et al., 2011). If the subpallial DAergic neurons labelled at 5 dpf are the same as observed by Tay and colleagues, it can be assumed these neurons project to the thalamus and hypothalamus. Together, this suggests the architecture of subpallial DAergic neurons expands rapidly during early development, and by 5 dpf, these neurons innervate structures outside the telencephalon.
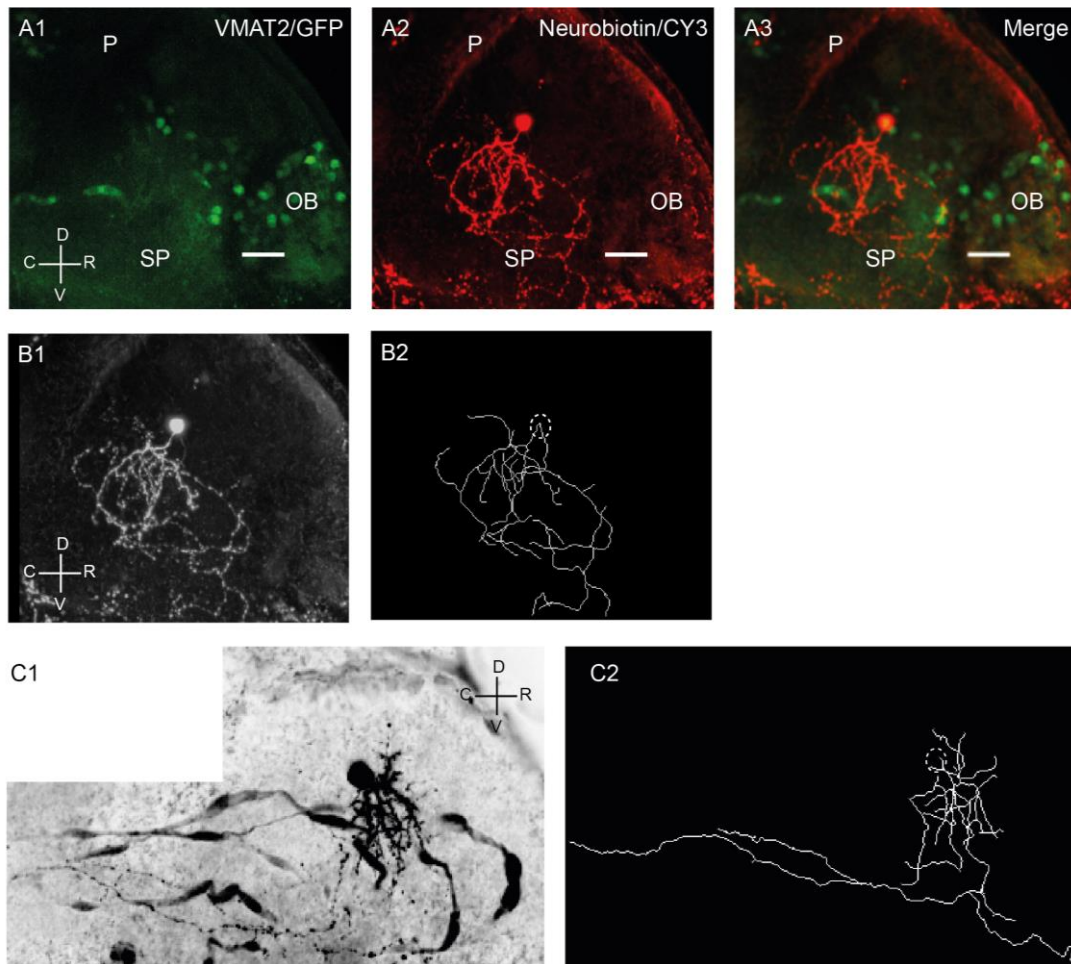
Figure 3:5 Subpallial DAergic neurons have two morphologies at 5 dpf, local arbours and descending projections A1–A3: Confocal images of neurobiotin labelled neurons at 5 dpf with local arbours Left column: Vmat2/GFP expression (green). Middle column: neurobiotin (red). Right column: merge of green and red channels. **B1:** Confocal image of 5 dpf subpallial DAergic neuron with arbours restricted to the telencephalon and representative line z stack of neurites line (**B2**). **C1:** Confocal image of 5 dpf subpallial DAergic neuron with local arbours and descending projections and representative line z stack of

neurites (**C2**). Orientation is indicated in panel (**A1, B1** and **C1**); R = rostral, C = caudal, D = dorsal and V = ventral. Scale bar 20µm (**A -B**) and 50µm (**C**).

3.3.3　　　The ontogeny of input to the subpallium

Previous studies have shown that the adult subpallium receives input from a number of brain regions, including the telencephalon, diencephalon and hindbrain (Rink and Wullimann, 2004). To understand the innervation patterns of this region during earlier development, I examined subpallial afferents by electroporating DAergic neurons in this region at 2, 3 and 5 dpf. This resulted in the uptake and retrograde transport of neurobiotin to the cell body in regions innervated by subpallial DAergic neurons (Figure 3:6). Neurobiotin labelled neurons were found locally within the subpallium, proximal to the subpallial DAergic neurons (Figure 3:7B). Further caudal, a labelled neuron was identified lateral to the raphe (RA) within the hindbrain in 2 fish (n_{fish} = 2 of 8, Figure 3:7C). This data suggests subpallial DAergic neurons at 2 dpf receives limited input, with a few labelled cells proximal to the electroporation site and distal cell labelled in the hindbrain.

A.

B.

C.
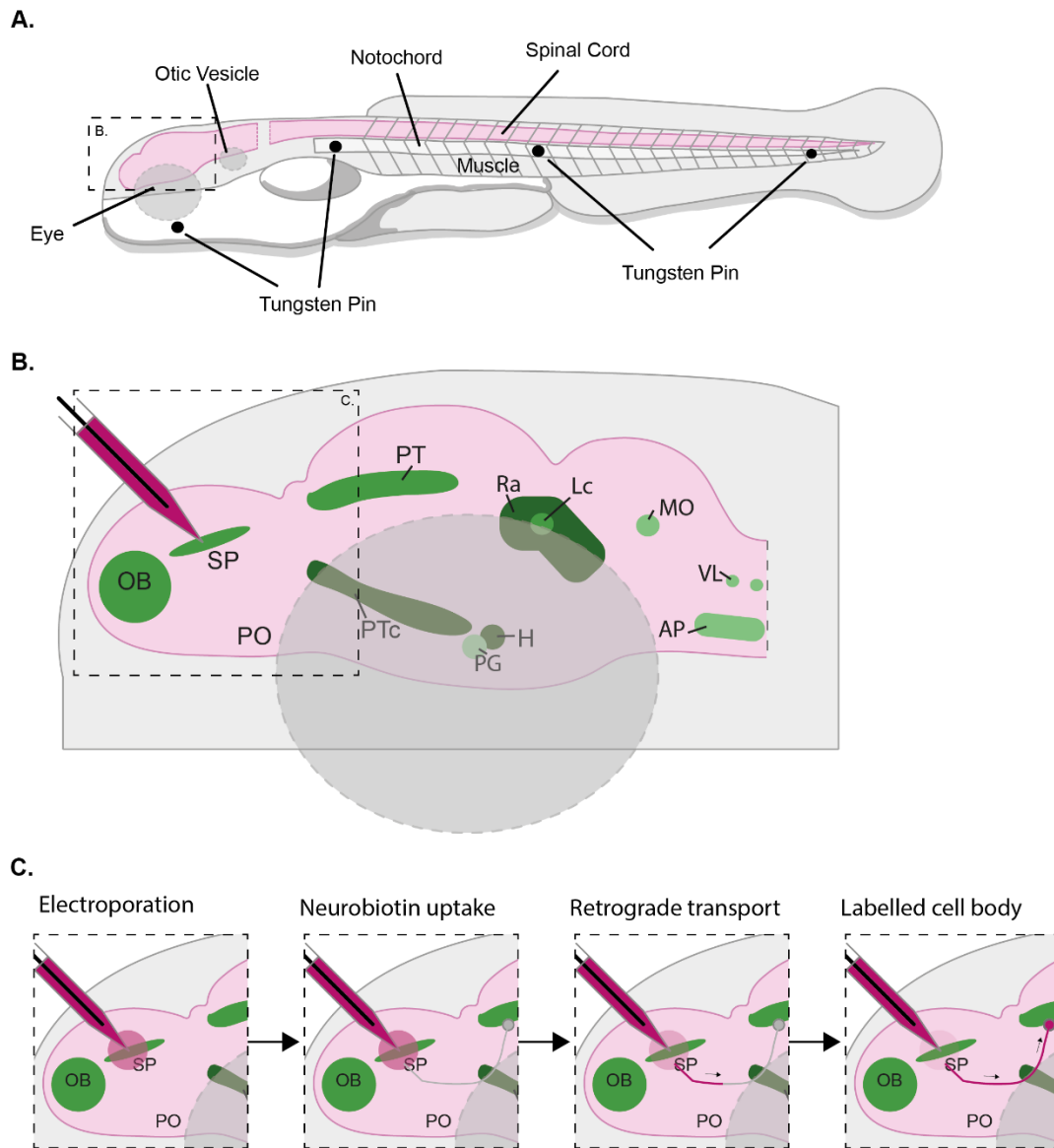
Figure 3:6 Illustration of the retrograde labelling technique of subpallial DAergic neurons. A: Larval zebrafish were pinned to sylgard dish by the use of tungsten pins being inserted through the notochord and developing lower jaw. **B:** GFP positive neurons in the subpallium were visually targeted with an neurobiotin filled electrode and were electroporated. **C:** Area around the subpallial DAergic neurons were electroporated, neurobiotin was taken up by afferent projections. Subsequently, the neurobiotin is retrogradely transported along the axon to the cell body. Labelled cell bodies were visualised using streptavidin histochemistry. Arrowheads show the direction of the retrograde transport of neurobiotin **(C)**. Abbreviations; olfactory bulb (OB), subpallium (SP), posterior tuberculum (PTc), hypothalamus (H), pretectum (PT), raphe nucleus (RA) and hindbrain (HB).

A. Schematic Diagram
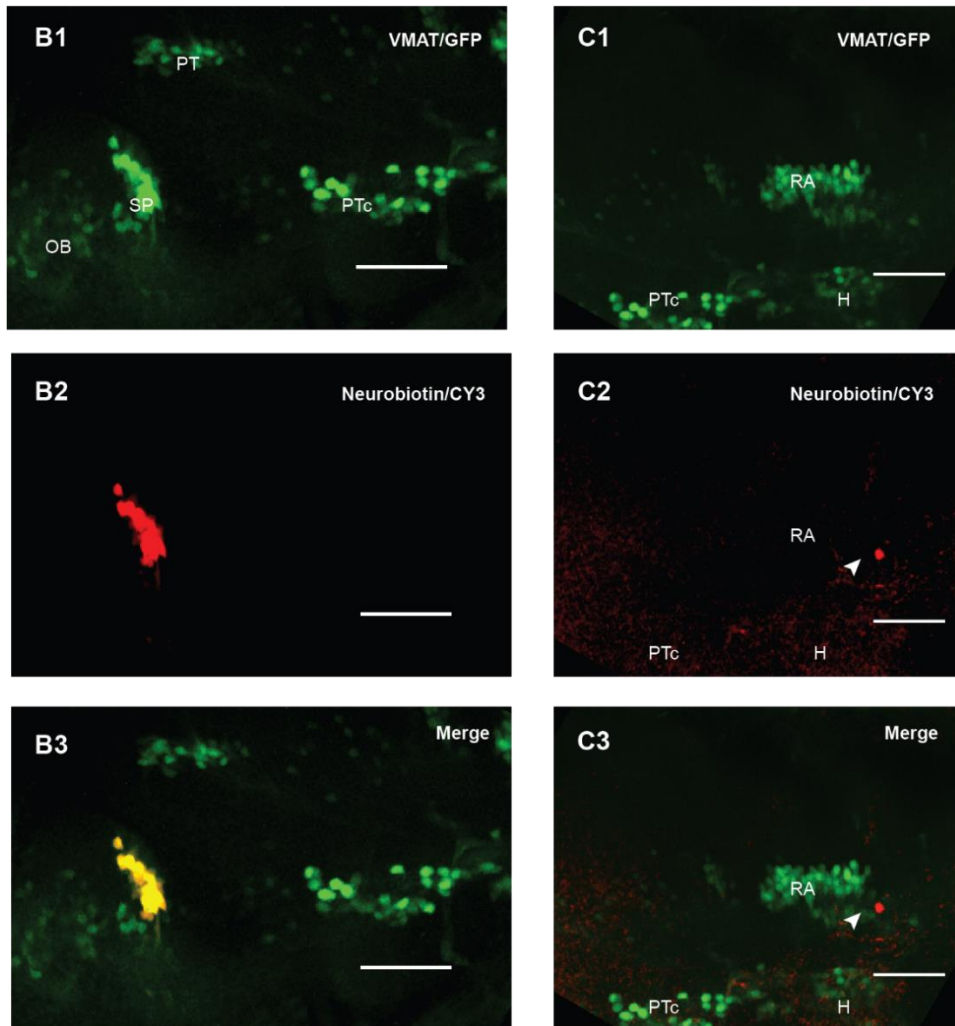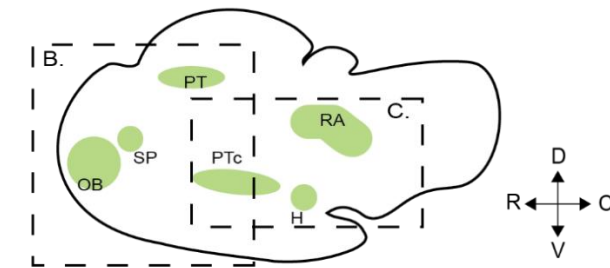
Figure 3:7 Retrograde labelling of subpallial DAergic neurons at 2 dpf A: Illustration of the zebrafish brain at 2 dpf, showing the distribution of VMAT2 expressing cells in ETvmat2:GFP fish. Orientation is indicated in panel (**A**); R = rostral, C = caudal, D = dorsal and V = ventral. **B–C:** VMAT2/GFP (green) expression, neurobiotin labelling (red) and merge channels for the rostral region **(B1–3)**, caudal aspect of the brain **(C1–3).** Abbreviations; olfactory bulb (OB), subpallium (SP), posterior tuberculum (PTc), hypothalamus (H), pretectum (PT), raphe nucleus (RA) and hindbrain (HB). Arrowheads point to neurobiotin labelled cells. Scale bar: 50μm.

By contrast, retrograde labelling at 3 dpf revealed neurons scattered through various compartments of the zebrafish brain (n_{fish} = 8; Figure 3:8A). Specifically, labelled cells were found in the preoptic region (Figure 3:8B) the ventral diencephalon, the posterior tuberculum (Figure 3:8C), the pretectal region of the dorsal diencephalon (Figure 3:8D) and the hindbrain (Figure 3:8E).
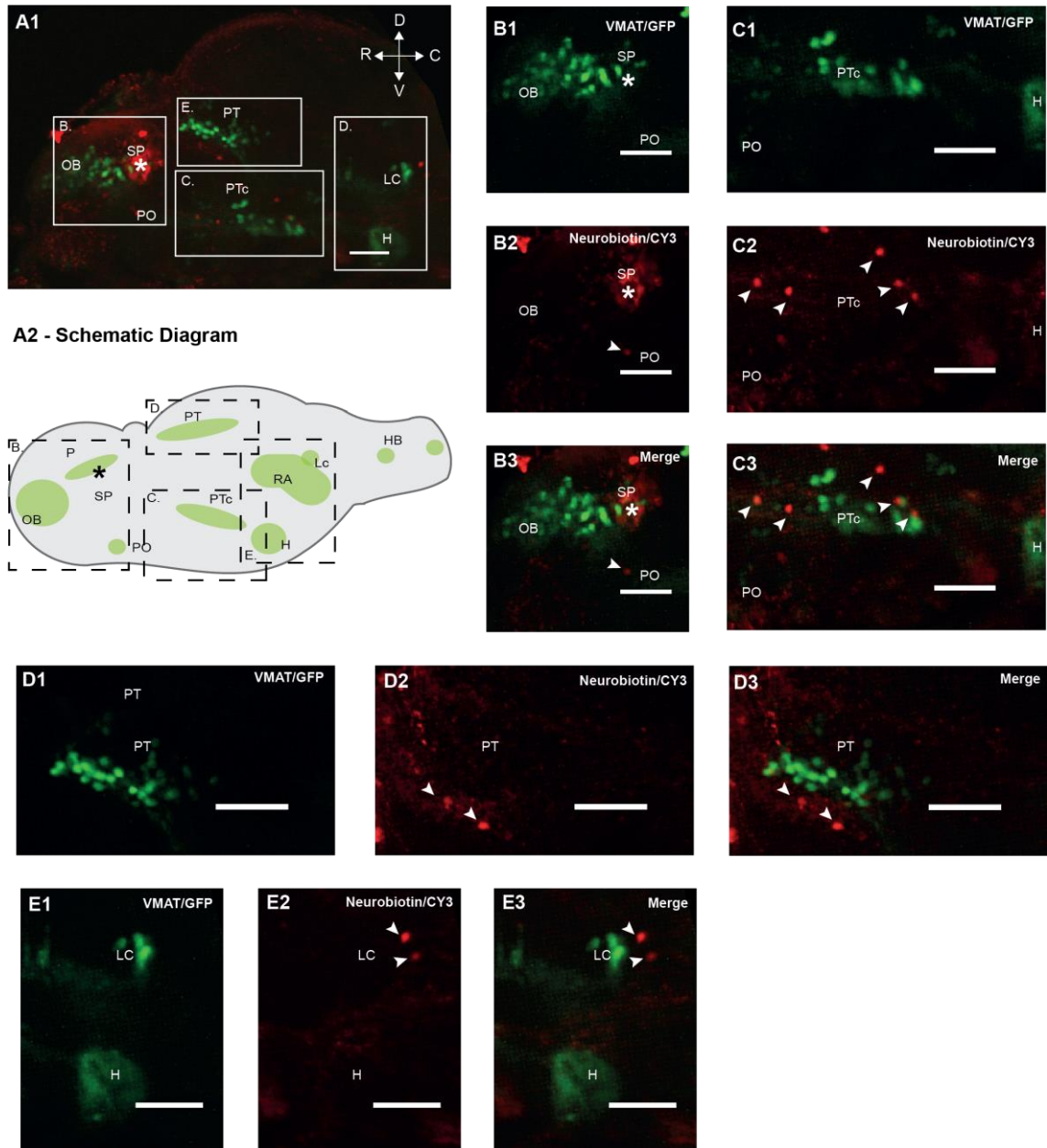
Figure 3:8 Retrograde labelling of subpallial DAergic neurons at 3 dpf. A–E: Images illustrating neurobiotin retrograde labelling of subpallial projecting neurons in tg(ETvmat2:GFP) fish and visualised using confocal microscopy. * = electroporation site. Orientation is indicated in panel (**A1**); R = rostral, C = caudal, D = dorsal and V = ventral. **A1:** Lateral overview of the larval brain at 3 dpf,

stained for neurobiotin (red) in VMAT2/GFP expressing fish (green). **A2:** Schematic overview of larval zebrafish brain showing distribution of Vmat2 expression in ETvmat2:GFP fish. **B–E:** VMAT2/GFP (green) expression, neurobiotin labelling (red) and merge channels for telencephalon **(B1–3)**, posterior tuberculum **(C1–3)**, pretectum **(D1–3)** and rostral hindbrain **(E1–3)**. Abbreviations; olfactory bulb (OB), subpallium (SP), pallium (P), preoptic (PO), posterior tuberculum (PTc), hypothalamus (H), pretectum (PT), locus coeruleus (LC), raphe nucleus (RA) and hindbrain (HB). Arrowheads point to neurobiotin labelled cells. Scale bar: 50µm.

At 5 dpf ($n_{fish} = 9$), a similar distribution of cells was seen, with neurobiotin labelled neurons scattered through the preoptic, posterior tubercular, pretectal and locus coeruleus regions (Figure 3:9). In addition, labelled neurons were also found in the hypothalamus and anterior to the RA (Figure 3:9D). Furthermore, labelled neurons in the preoptic, posterior tubercular, pretectal and hypothalamus were found in to be ipsilateral when images were taken dorsally and ventrally (Figure 3:10A/B). However, dorsal and ventral images revealed neurobiotin labelled neurons in the contralateral subpallium and ventral diencephalon (Figure 3:10A/B). The location of these labelled neurons are summarised in Figure 3:10C. A summary illustration of labelled subpallial afferents can be observed in Figure 3:11. In sum, afferents terminating in the subpallium can be observed from 3 dpf onwards. By 5 dpf, subpallial afferents were identified throughout the zebrafish brain, including forebrain regions: telencephalon and diencephalon as well as midbrain and hindbrain regions.
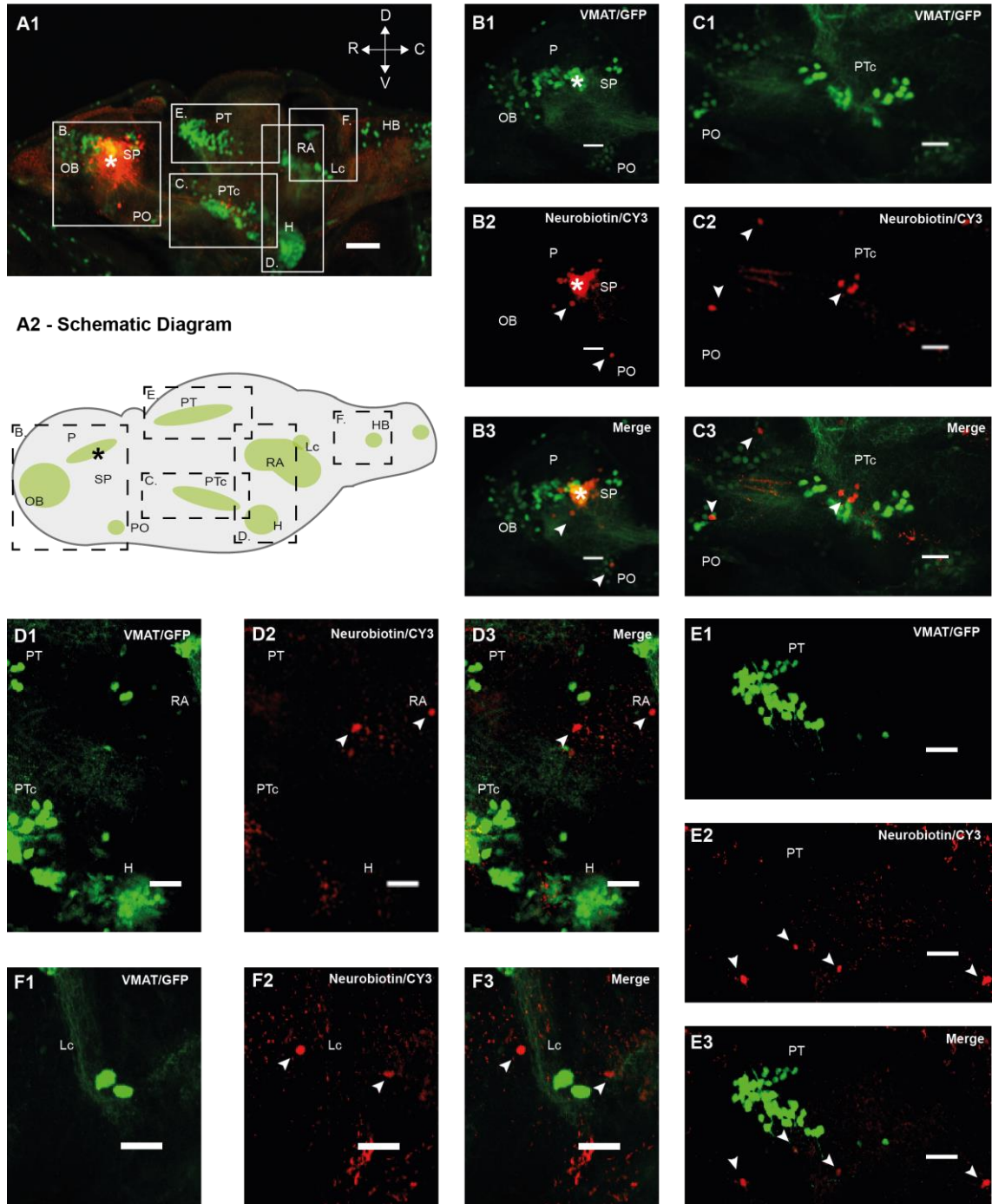
Figure 3:9 Retrograde labelling of subpallial DAergic neurons at 5 dpf (lateral view). A–F: Images illustrating neurobiotin retrograde labelling of subpallial projecting neurons in tg(ETvmat2:GFP) fish and visualised using confocal microscopy. * = electroporation site. Orientation is indicated in panel (**A1**); R = rostral, C = caudal, D = dorsal and V = ventral. **A1:** Lateral overview of the larval brain at 5 dpf, stained for neurobiotin (red) in VMAT2/GFP expressing fish (green). **A2:** Schematic overview of larval zebrafish brain showing the distribution of VMAT2 expression in ETvmat2:GFP fish. **B–F:** VMAT2/GFP expression (green), neurobiotin labelling (red) and merge channels for telencephalon **(B1–3)**, posterior tuberculum **(C1–3)**, rostral hindbrain **(D1–3)**, pretectum **(E1–3)** and caudal hindbrain **(F1–3)**. Abbreviations: Olfactory bulb

(OB), subpallium (SP), pallium (P), preoptic (PO), posterior tuberculum (PTc), hypothalamus (H), pretectum (PT), locus coeruleus (LC), raphe nucleus (RA) and hindbrain (HB). Scale bar: 50µm **(A1)**. Scale bar: 20 µm **(B–F)**.
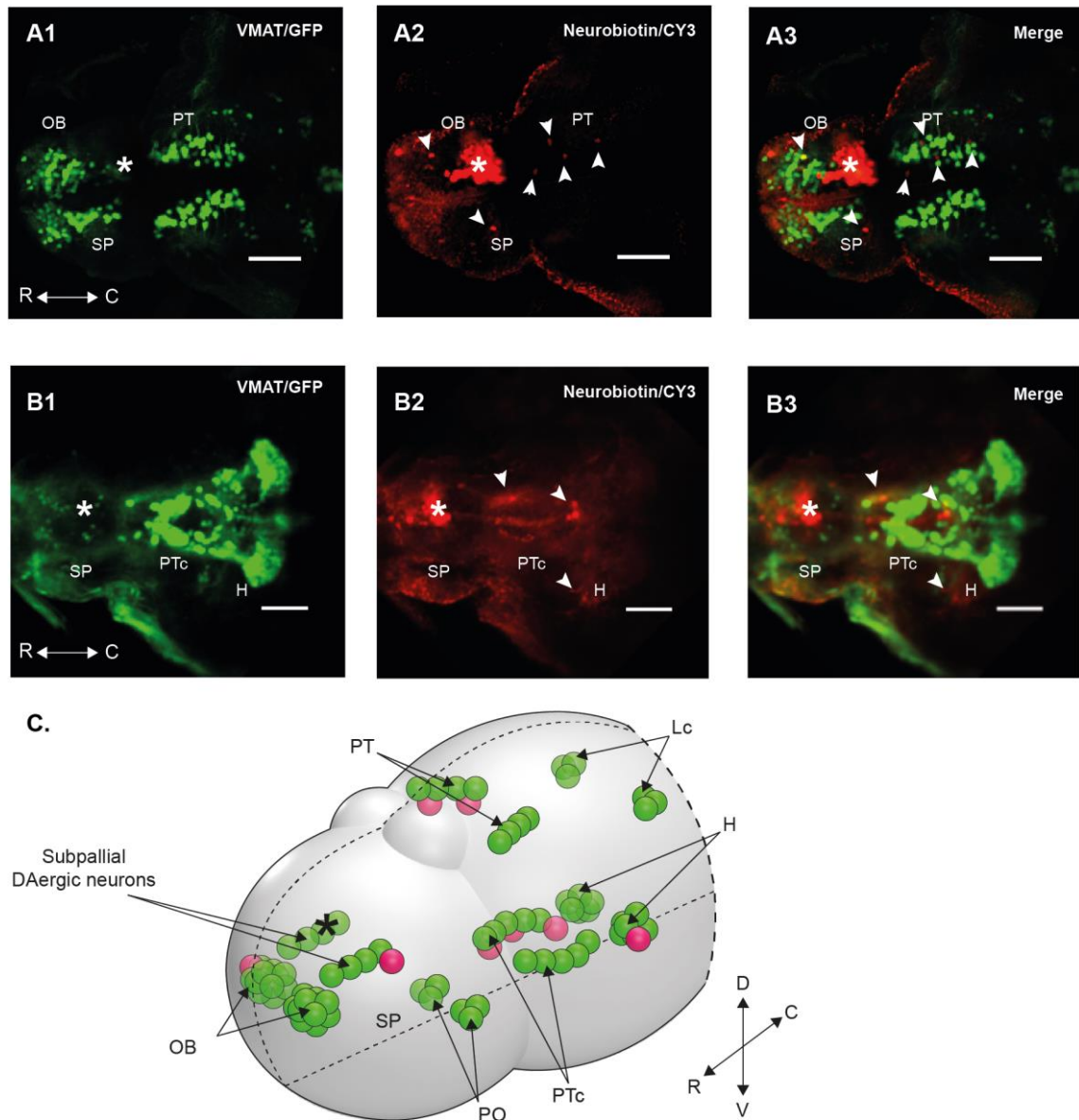
Figure 3:10 Retrograde labelling of subpallial DAergic neurons at 5 dpf (dorsal and ventral views). A–B: Images illustrating neurobiotin retrograde labelling of subpallial DAergic neurons from dorsal **(A)** and ventral **(B)** views. * = electroporation site. Left column: Vmat2/GFP expression (green). Middle column: neurobiotin (red). Right column: merge of green and red channels. Arrowheads point to neurobiotin labelled cells. Orientation is indicated in panel **(A1/B1)**; R = rostral, and C = caudal. **C:** Schematic illustration summarising the neurobiotin labelled cells in panels **(A+B)**. Green cells represet Vmat2 positive cells and

neurobiotin labelled cells are red. Orientation is indicated in the panel; R = rostral, C = caudal, D = dorsal and V = ventral. Abbreviations: Olfactory bulb (OB), subpallium (SP), preoptic (PO), posterior tuberculum (PTc), hypothalamus (H), pretectum (PT), locus coeruleus (LC).
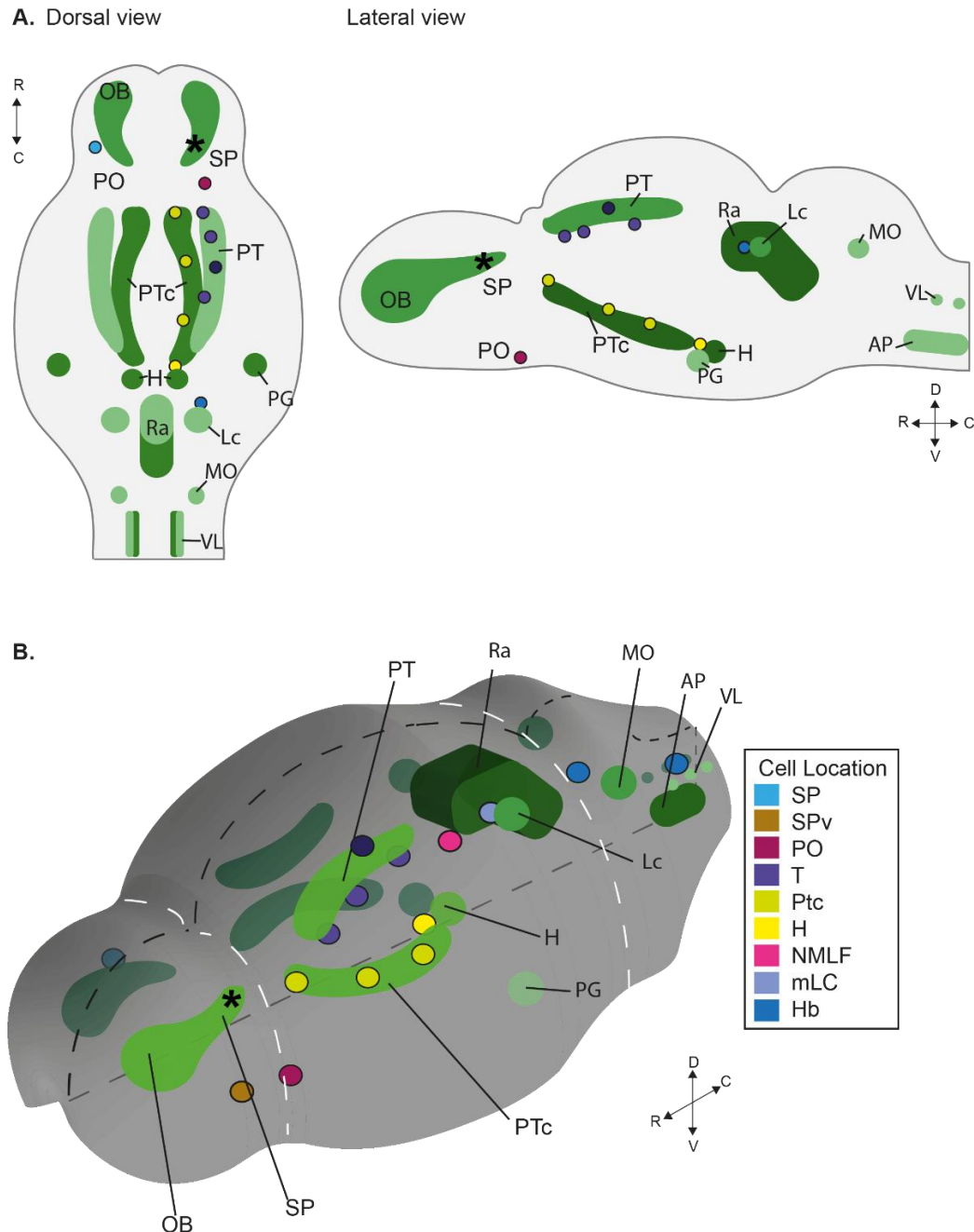
Figure 3:11 Schematic illustration of retrograde labelling at 5 dpf. A: Schematic illustration of the location of retrogradely labelled neurobiotin retrograde labelled neurons locations from dorsal (left) and lateral (right) views. **B:** 3D schematic summary of retrograde labelled neurons. * = electroporation

site. Abbreviations: Olfactory bulb (OB), subpallium (SP) ventral subpallium (SPv), preoptic (PO), posterior tuberculum (PTc), hypothalamus (H), pretectum (PT), thalamic nuclei (T), nucleus of the medial longitudinal fasciculus (NMLF), medial to locus coeruleus (mLC), locus coeruleus (LC), raphe nucleus (RA) and hindbrain (HB), medulla oblangata (MO), Area Postrema (AP). Orientation is indicated in panel, R = rostral C = caudal, D = dorsal and V = ventral.

Having shown that the subpallium receives afferent input from the telencephalon, pretectum, posterior tuberculum, hypothalamus and the hindbrain during early stages of development, I next sought to determine whether subpallial DAergic neurons receive synaptic input during these stages of development. To do this, whole-cell voltage-clamp was used to isolate miniature postsynaptic currents (mPSCs) in subpallial DAergic neurons. Attempts to record from 2 dpf neurons were unsuccessful. However, recordings could be routinely acquired from neurons of 3 and 5 dpf fish. At both stages studied, application of PIC isolated a population mPSCs that were abolished by subsequent application of KYN (Figure 3:12A, B), suggesting they originated from glutamatergic synapses. Conversely, application of KYN revealed a population of mPSCs that were abolished by the subsequent application of PIC (Figure 3:12A, B), suggesting they were mediated by GABA.

Comparison of glutamatergic and GABAergic mPSC revealed different kinetic properties: at 5 dpf, KYN-sensitive glutamatergic inputs and PIC-sensitive GABAergic mPSCs had similar rise times (Glutamatergic = 4.944 ± 0.9092 ms, n_{fish} = 7, n_{cells} = 7; GABAergic = 4.128 ± 1.572 ms, n_{fish} = 8; p = 0.2500, unpaired t test, Figure 3:13A) but glutamatergic mPSCs had a shorter decay (Glutamatergic = 14.93 ± 0.8244 ms, n_{fish} = 7, n_{cells} = 7; GABAergic = 34.30 ± 5.20 ms, n_{fish} = 8, n_{cells} = 8; p < 0.0001, unpaired t test, Figure 3:13B). Additionally, glutamatergic mPSCs occurred at a higher frequency compared to the GABAergic mPSCs of subpallial DAergic neurons (Glutamatergic = 1.614 ± 0.7804 Hz, n_{fish} = 7, n_{cells} = 7; GABAergic = 0.2595 ± 0.3556 Hz, n_{fish} = 8, n_{cells} = 8; p = 0.0003, Mann-Whitney test, Figure 3:13C). The differences in decay time exhibit by these two populations supports the argument that these populations are two distinct mPSC populations in origin.
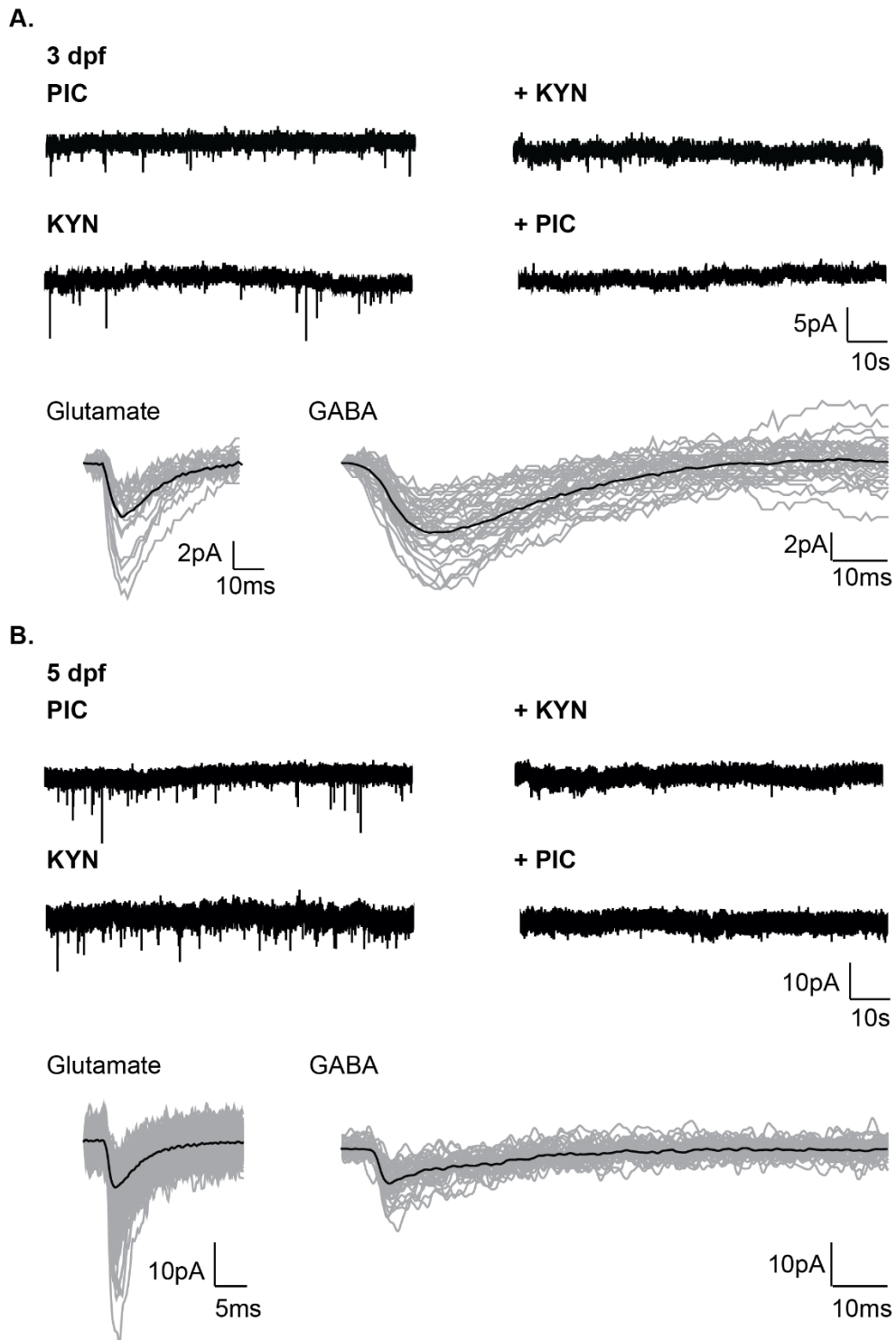
Figure 3:12 Development and identification of synaptic input. Identified spontaneous synaptic inputs at 3 **(A)** and 5 **(B)** dpf. At 3 and 5 dpf, application of picrotoxin (PIC) during whole-cell voltage-clamp recordings of TTX-treated subpallial DAergic neuron *in vivo* isolated a population of kynurenic acid (KYN) sensitive mPSCs (presumably glutamatergic), holding potential at -65mV. At 3 and 5 dpf, the application of KYN isolated another population of PIC sensitive mPSCs (presumably GABAergic), holding potential at -70mV. Bottom traces **(A-**

B) overlays of isolated mPSC events on an expanded time scale, the black line represents the average trace.
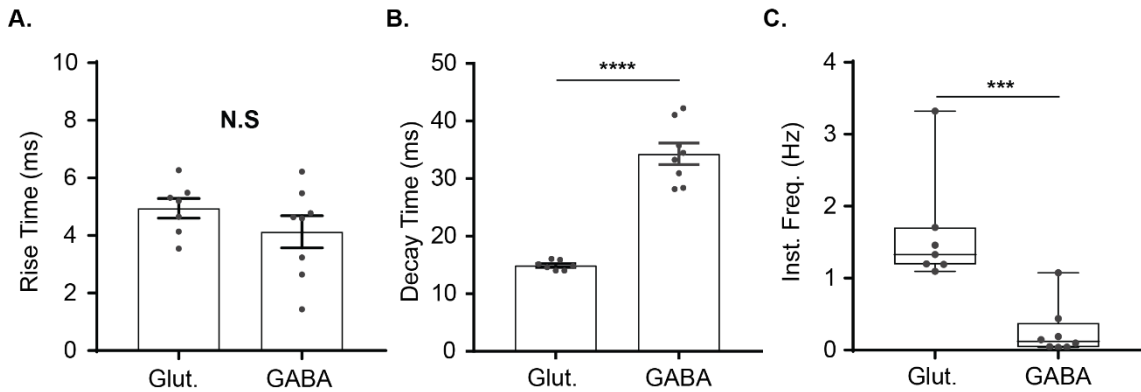
Figure 3:13 Isolated glutamatergic and GABAergic mPSC kinetics at 5 dpf. Bar chart and distribution plot of glutamatergic and GABAergic rise times **(A)** and decay time **(B)**. Box and whisker plot of the instantaneous frequency of spontaneous glutamatergic and GABAergic mPSCs **(C)**. ***P < 0.0005, ****P < 0.0001, N.S = not significant.

Developmentally-related changes in receptor number, clustering and subunit composition often results in a sharpening of PSC kinetics (Gonzalez-Forero and Alvarez, 2005, Hall and Sanes, 1993). Therefore, I asked if mPSC parameters change across the period of study. Comparison of glutamatergic mPSCs revealed that these currents had similar amplitudes (3 dpf = -3.06 ± 0.57 pA, n_{fish} = 7, n_{cells} = 7; 5 DPF = -5.636 ± 3.147 pA, n_{fish} = 7, n_{cells} = 7; p = 0.3829, Mann-Whitney test, Figure 3:14A), rise times (3 dpf = 4.94 ± 0.91 ms, n_{fish} = 7, n_{cells} = 7; 5 DPF = 4.52 ± 0.35 ms, n_{fish} = 7, n_{cells} = 7; p < 0.2683, unpaired t test, Figure 3:14B) and decay times (3 dpf = 14.27 ± 2.48 ms, n_{fish} = 7, n_{cells} = 7; 5 DPF = 14.93 ± 0.82 ms, n_{fish} = 7, n_{cells} = 7; p = 0.5191, unpaired t test, Figure 3:14C) at 3 and 5 dpf.

Examination of GABAergic mPSCs revealed no difference in amplitude (3 dpf = -4.268 ± 1.55 pA, n_{fish} = 6, n_{cells} = 6; 5 DPF = -5.636 ± 3.147 pA, n_{fish} = 8, n_{cells} = 8; p = 0.2284, Mann-Whitney test, Figure 3:14D), However, rise time decreased (3 dpf = 8.314 ± 0.918 ms, n_{fish} = 6, n_{cells} = 6; 5 DPF = 4.128 ± 1.572 ms, n_{fish} = 8,

n_{cells} = 8; p < 0.0001, unpaired t test, Figure 3:14E). in addition to the decay time decreasing during development (3 dpf = 43.84 ± 4.547 ms, n_{fish} = 6, n_{cells} = 6; 5 DPF = 34.30 ± 5.20 ms, n_{fish} = 8, n_{cells} = 8; p = 0.0048, unpaired t test, Figure 3:14F). The decrease in the rise and decay time of GABAergic neurons shows a faster activation kinetics, suggesting maturation of the GABAergic synapse. In sum, these experiments isolated glutamatergic and GABAergic synaptic inputs during early developments, suggesting the subpallial DAergic neurons receive glutamatergic and GABAergic input from 3 dpf.
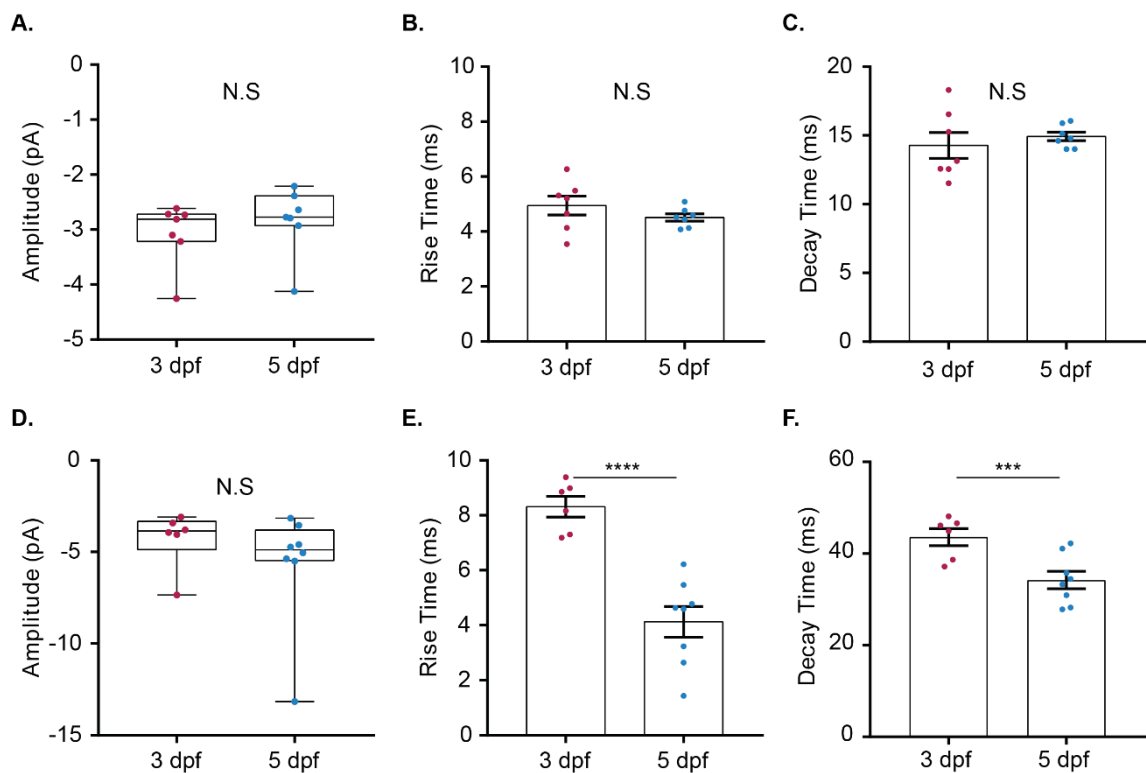
Figure 3:14 Comparison of mPSC kinetics during development. Bar chart and distribution plot of glutamatergic mPSC at 3 and 5 dpf comparing amplitude (**A**), rise time (**B**), decay time (**C**). Comparison of GABAergic mPSC at 3 and 5 dpf comparing amplitude (**D**), rise time (**E**), decay time (**F**). ** P < 0.005, ****P < 0.0001, N.S = not significant.

3.3.4   Characterisation of intrinsic excitability

So far, I have shown that subpallial DAergic neurons undergo extensive morphological maturation and receive synaptic input during early periods of development. Next, I sought to determine if the subpallial DAergic neurons are also capable of generating action potentials during this developmental period.

3.3.4.1   Response to depolarising current

In order to examine the intrinsic excitability of the subpallial DAergic neurons, 1 pA current steps were applied to subpallial DA neurons during voltage recordings. At rheobase current, single broad action potentials could be evoked at 3 dpf (n_{fish} = 10, n_{cells} = 10) and 5 dpf (n_{fish} = 7, n_{cells} = 7; Figure 3:15A). However, only one recording could be acquired from 2 dpf neurons. In this cell, unitary action potentials was observed in response to suprathreshold current injection (n_{fish} = 1, n_{cells} = 1; Figure 3:15A). Comparison of 3 and 5 dpf neurons revealed that threshold potential did not changed with respect to age (3 dpf = -29.55 ± 4.76mV, n_{fish} = 10, n_{cells} = 10; 5 dpf = -33.62 ± 2.79mV, n_{fish} = 7, n_{cells} = 7; p = 0.061, unpaired t test; Figure 3:15B). Examination of action potentials in neurons of 3 and 5 dpf fish revealed a larger spike amplitude (3 dpf = 24.72 ± 5.02mV, n_{fish} = 10, n_{cells} = 10; 5 dpf = 30.58 ± 4.37mV, n_{fish} = 7, n_{cells} = 7; p = 0.0248, unpaired t test; Figure 3:15C) but no difference in half-width (3 dpf = 11.82 ± 3.06ms, n_{fish} = 10, n_{cells} = 10; 5 dpf = 9.71 ± 6.59ms, n_{fish} = 7, n_{cells} = 7; p = 0.2002, unpaired t test; Figure 3:15D).

A.
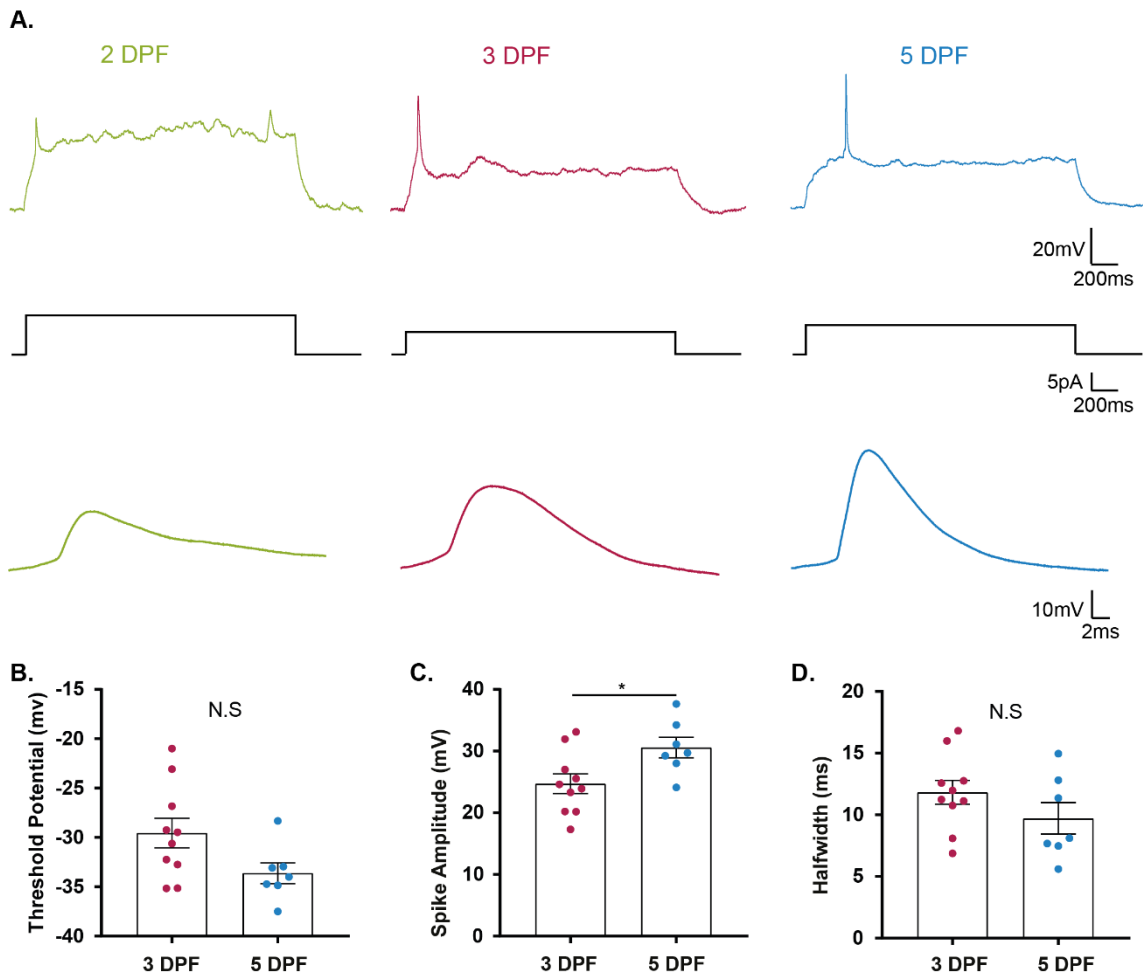
Figure 3:15 Activity patterns of subpallial DAergic neurons in response to rheobase current injection. A: Representative whole-cell patch-clamp recordings in response to rheobase current from subpallial DAergic neurons at 2 dpf (left), 3 dpf (central) and 5 dpf (right) ages. Bottom traces represent a single action potential over an expanded time scale. Neurons were subjected to current steps of 1pA, and the lower traces show rheobase current. Note subpallial DAergic at 2 dpf are fragile and unable to gain significant replicates for analysis and this 2 dpf has been included as an example. **B–D:** Bar charts comparing the action potential threshold **(B)**, spike amplitude **(C)** and spike half-width **(D)**. N.S = no significant difference.

Injection of depolarising current into subpallial DAergic neurons could elicit repetitive firing in these neurons at both 3 and 5 dpf (Figure 3:16A). Repetitive spiking was seen in the majority of neurons at 3 dpf (n_{cells} = 7 of 10) and all neurons at 5 dpf (n_{cells} = 7 of 7; Figure 3:16A). Whilst there was no difference in action potential waveform at 3 and 5 dpf, at 1.5 x rheobase, instantaneous spike frequency increased at 5 dpf when compared 3 dpf (3 dpf = 3.496 ± 1.735 Hz,

n_{fish} = 10, n_{cells} = 7; 5 dpf = 7.259 ± 2.58 Hz, n_{fish} = 7, n_{cells} = 7; p = 0.0076, unpaired t test; Figure 3:16B).

A.

B.
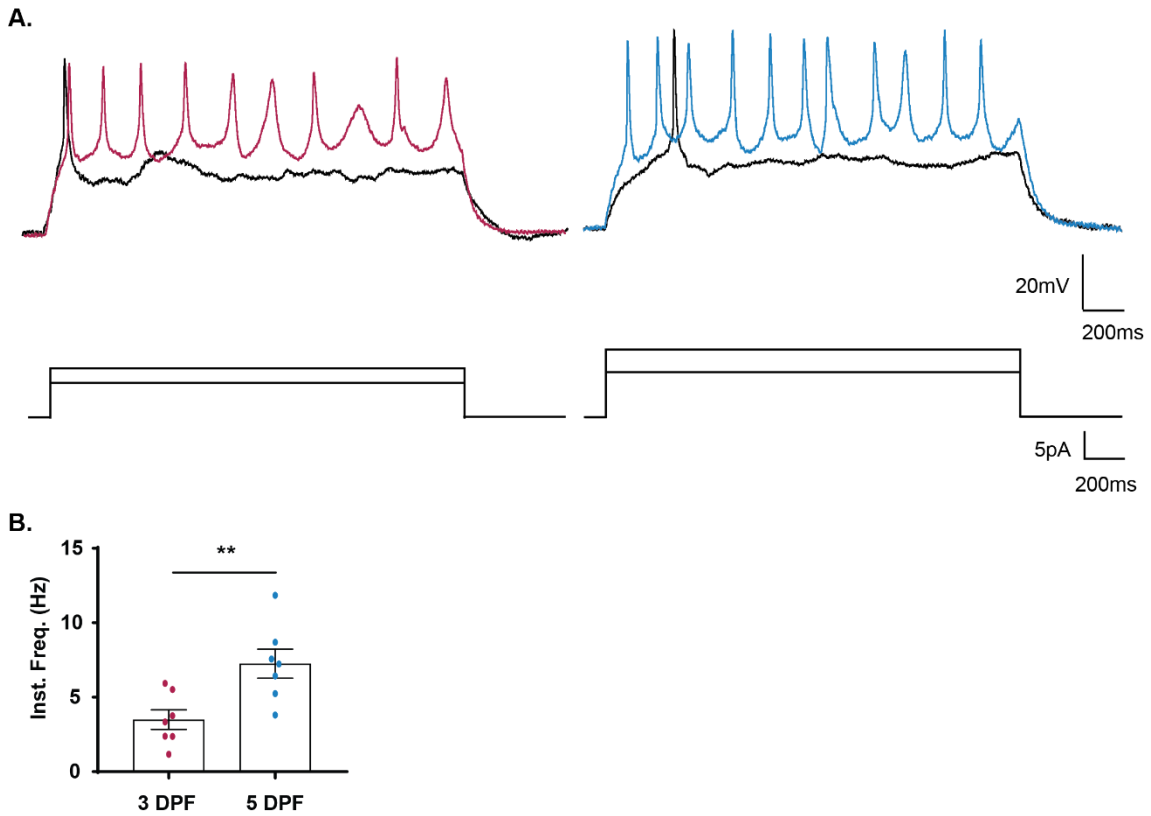
Figure 3:16 Subpallial DAergic neurons exhibit repetitive spiking. A: Representative whole-cell patch-clamp recordings in response to 1 x rheobase (black line) and 1.5 x rheobase (colour line) current injection from subpallial DAergic neurons at 3 dpf (left) and 5 dpf (right). Bottom traces represent current injection traces, 1 x rheobase (black line) and 1.5 x rheobase (colour line) **B:** Bar chart comparing average action potential instantaneous frequency of 3 and 5 dpf neurons at 1.5 x rheobase. **P<0.005.

Table 3.3 Two-way ANOVA of consecutive action potential Amplitude

	DF	MS	F (DFn, DFd)	P value
Interaction	1	1.351	F (1, 9) = 0.3942	P=0.5457
A.P. Number	1	321.2	F (1, 9) = 93.74	P<0.0001****
Age	1	252.7	F (1, 9) = 4.667	P=0.0590
Residual	9	3.427		

**** P < 0.0001

Table 3.4 Consecutive action potential Amplitude - Sidak multiple comparison analysis

1st – 4th Action potential	Diff. in mean	DF	P value
3 dpf	8.172	9	0.0001****
5 dpf	7.177	9	0.0002***

*** P < 0.0005, **** P < 0.0001

Additionally, the injection of current evoked repetitive spiking in both 3 dpf and 5 dpf (Figure 3:17A, B). Consecutive spikes showed a progressive decrease in spike amplitude (Figure 3:17C). Comparison of spike amplitude of the 1st and 4th action potentials revealed a decrease in successive action potentials (see Table 3.3 and Table 3.4 for two-way ANOVA and multiple comparisons analysis; Figure 3:17D) and examination of consecutive spikes suggested a progressive increase in spike half-width (Figure 3:17E). However, comparison of the spike halfwidth of consecutive action potentials revealed there was no difference between 3 and 5 dpf fish (see Table 3.5 for two-way ANOVA; Figure 3:17F). In sum, my data suggest that subpallial DAergic neurons generate spike trains on current injection from early larval stages.
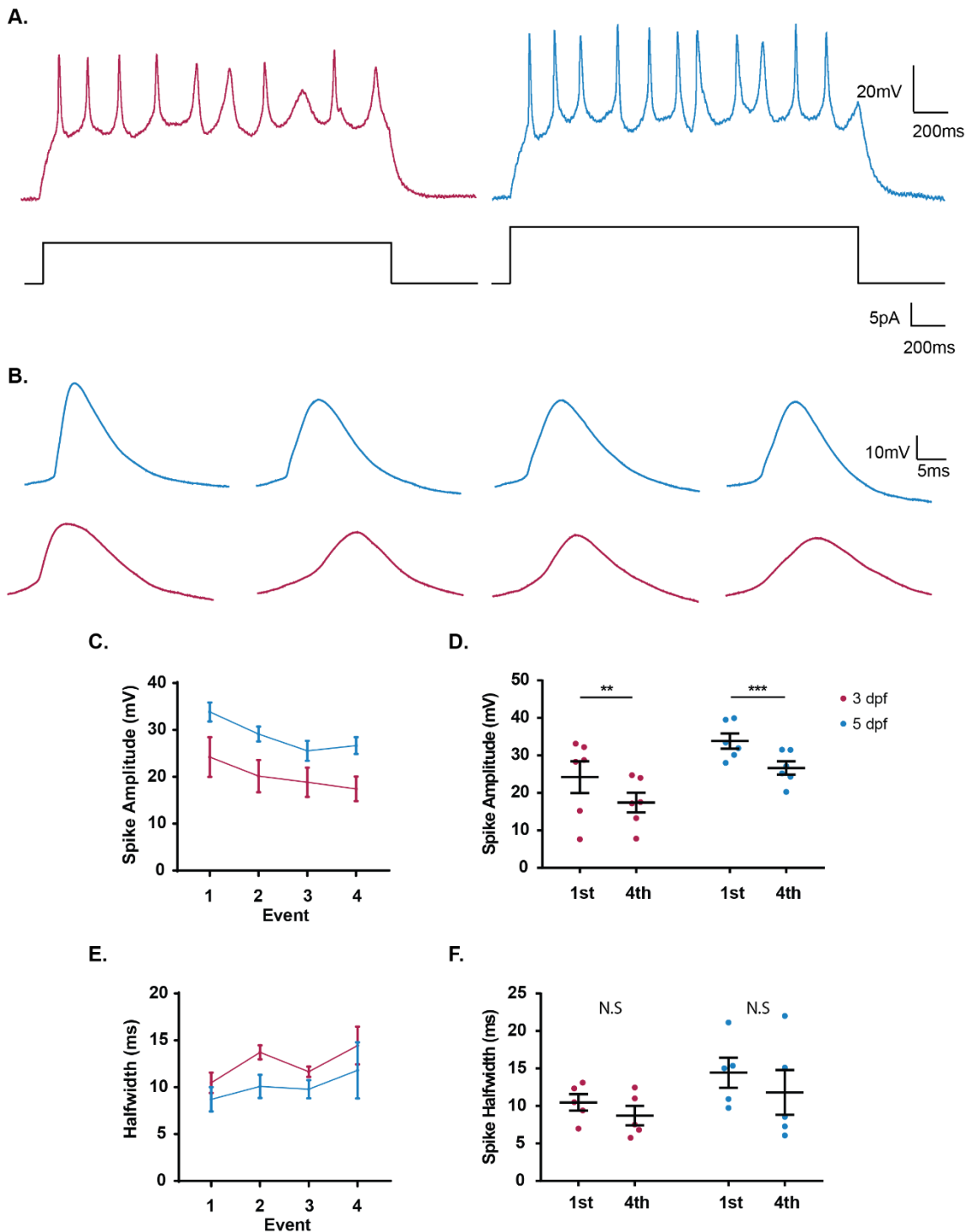
Figure 3:17 Action potential waveforms during 1.5 x Rheobase current injection. A: Representative whole-cell patch-clamp recordings in response to 1.5 x rheobase current injection from subpallial DAergic neurons at 3 dpf (left) and 5 dpf (right). Bottom traces represent current injection traces. **B**: Initial 4 action potentials from traces in Figure 3:17A at 3 dpf (lower panel) and 5 dpf (upper panel). **C**: Line graph illustrating the change in amplitude of the first four action potentials of 3 and 5 dpf neurons. **D**: Separated scatter plot comparing the spike amplitudes of the first and fourth action potentials of 3 and 5 dpf neurons at 1.5 x rheobase. **E**: Line graph illustrating the change in spike half-width first four

action potentials of 3 and 5 dpf neurons. **F**: Separated scatter plot comparing the half-width of the first and fourth action potentials of 3 and 5 dpf neurons at 1.5 x rheobase. **P<0.005; ***P<0.0005; N.S = no significant difference.

Table 3.5 Two-way ANOVA of consecutive action potential half-width

	DF	MS	F (DFn, DFd)	P value
Interaction	1	0.9592	F (1, 8) = 0.06595	P= 0.8038
A.P. Number	1	24.16	F (1, 8) = 1.661	P= 0.2335
Age	1	62.38	F (1, 8) = 2.493	P= 0.1530
Residual	8	14.54		

3.3.4.2   Application of hyperpolarising current injection

A typical feature of mammalian DAergic neurons is the presence of an I_h, which can be visualised by the presence of a rebound depolarisation, also known as a sag potential. The I_h is activated when a neuron is hyperpolarised, and it has been observed in the DAergic neurons of the SNc, VTA and olfactory bulb (Grace and Bunney, 1984a, Grace and Bunney, 1984b, Pignatelli et al., 2013). To investigate the presence of I_h in subpallial DAergic neurons, hyperpolarising current was applied into these cells during whole-cell recordings. At both 3 dpf (n_{fish} = 10, n_{cells} = 10) and 5 dpf (n_{fish} = 7, n_{cells} = 7), injection of hyperpolarising current steps failed to activate I_h, as observed by the lack of sag potential (Figure 3:18A). However, rebound spikes were often observed at 5 dpf (Figure 3:18B). The lack of sag potential suggests the subpallial DAergic neurons do not possess I_h.
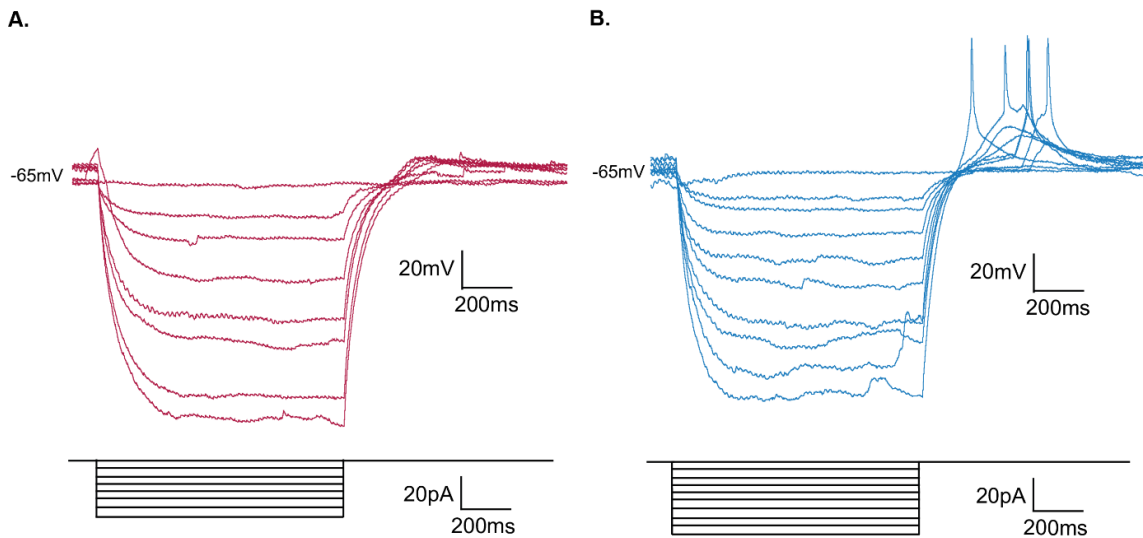
Figure 3:18 Activity patterns of subpallial DAergic neurons in response to hyperpolarising current injection. A–B: Representative whole-cell patch-clamp recordings in response to hyperpolarising current injection in subpallial DAergic neurons at 3 dpf **(A)** and 5 dpf **(B)**. Resting membrane potential -65 mV. Bottom traces represent current traces.

3.3.5   The development of endogenous firing activity

Having found that subpallial DAergic neurons are intrinsically excitable during early development, I next sought to determine whether subpallial DAergic neurons exhibit endogenous firing activity during early stages of development. Extracellular recordings of subpallial DAergic neurons revealed endogenous firing activity at 2 dpf (n_{fish} = 9), 3 dpf (n_{fish} = 9) and 5 dpf (n_{fish} = 8; Figure 3:19A). The instantaneous frequency of firing activity increased significantly between 2 and 5 dpf (2 dpf = 1.51 ± 1.02Hz, n_{fish} = 9, n_{cells} = 9; 3 dpf = 1.52 ± 1.24Hz, n_{fish} = 9, n_{cells} = 9; 5 dpf = 3.81 ± 1.90Hz, n_{fish} = 8, n_{cells} = 8; p = 0.0035, one-way ANOVA; Figure 3:19B). Consistent with results seen in Figure 3:16C, extracellular recordings at 5 dpf exhibited higher firing frequencies when compared with 2 or 3 dpf neurons.

Examination of loose patch recording revealed changes in spike amplitudes (Figure 3:19A). These recordings are of singular high input resistant neurons using cell attached mode with a low resistant seal, therefore, fluctuations in spike amplitude are unlikely to be attributable to noise from other neurons. Studies have found similar results and suggested the changes to the amplitudes are due to

changes in the seal and the interaction with the electrode (Shmoel et al., 2016). Furthermore, the firing frequency and spike amplitudes of high input resistant neurons are affected by mechanical stress during loose patch recordings (Alcami et al., 2012).
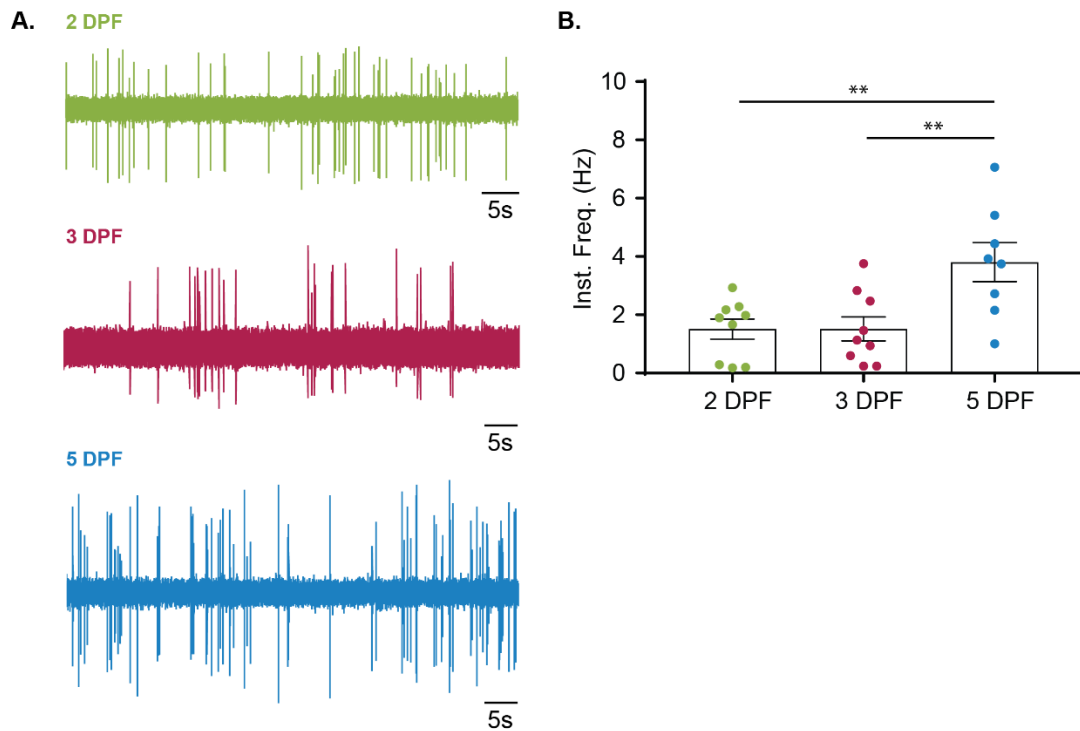
Figure 3:19 Endogenous firing activity of subpallial DAergic neurons. A: Representative extracellular recordings of endogenous firing activity of subpallial DAergic neurons at 2 dpf (upper trace), 3 dpf (middle trace) and 5 dpf (lower trace). **B:** Box and whisker plot comparing the instantaneous frequency firing activity detected by extracellular recordings. **P<0.005.

3.3.5.1   Firing activity of subpallial dopaminergic neurons is synaptically driven

As some mammalian DAergic neurons and zebrafish DDNs have been shown to exhibit autonomous firing (Lammel et al., 2008, Grace and Onn, 1989, Jay et al., 2015), I therefore asked if subpallial DAergic neurons exhibited this type of firing activity. To do this I performed whole-cell current-clamp recordings of subpallial DAergic neurons at 5 dpf (Figure 3:20A; upper trace). After obtaining a recording,

1 mM KYN and 100 µM PIC was added to the extracellular saline to block both glutamatergic and GABAergic input, respectively. Subsequent application of the synaptic blockers abolished the endogenous firing activity of subpallial DAergic neurons (baseline = 1.774 ± 1.305Hz, n_{fish} = 7, n_{cells} = 7; synaptic blockers = 0.00 ± 0.00 Hz, n_{fish} = 7, n_{cells} = 7; p = 0.0114, paired t-test; Figure 3:20A lower trace & B). These results suggest that the firing activity of subpallial DAergic neurons is synaptically driven and they do not exhibit autonomous firing.
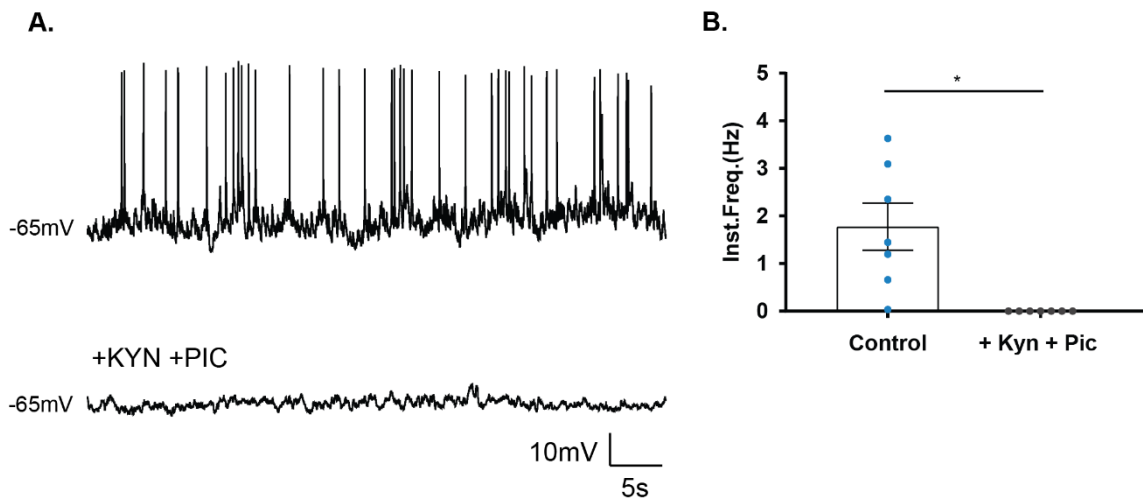
Figure 3:20 Endogenous firing activity is synaptically driven at 5 dpf. A: Representative whole-cell patch-clamp recordings of endogenous firing activity of subpallial DAergic neurons 5 dpf (upper trace) and in the presence of KYN and PIC (lower trace). **B:** Representative activity recording of subpallial DAergic neurons in response to current injection (upper panel) after the application of KYN and PIC. The lower panel represents the current injection trace. **C:** Box and whisker plot comparing the instantaneous frequency of endogenous firing activity of 5 dpf neurons. *P<0.05.

3.3.5.2 Exposure to dopamine reduces firing activity of subpallial dopaminergic neurons

Mammalian DAergic neurons exhibit D_2 autoreceptor-mediated inhibition (Stagkourakis et al., 2016, Lammel et al., 2008, Grace and Onn, 1989), and this feature has also been found in zebrafish DDNs (Jay et al., 2015). I next asked if subpallial DAergic neurons displayed D_2 autoreceptor-mediated inhibition. To do this, neurons were exposed to 5µM of DA. Loose patch recordings revealed the application of DA reversibly reduced firing frequency of subpallial DAergic neurons (Figure 3:21A) (Control = 5.69 ± 0.65Hz; DA = 2.29 ± 1.15Hz, wash = 5.94 ± 2.21Hz, $n_{fish} = 5$, $n_{cells} = 5$; p = 0.0279, RM one-way ANOVA; Figure 3:21B). These results suggest that subpallial DAergic neurons possess autoreceptors which supress neuronal firing. To confirm if the inhibition of subpallial DAergic neurons is mediated by D_2 autoreceptors, further studies using preincubation D_2 receptor antagonist prior to DA application are required. Additionally, using immunohistochemistry to stain for D_2 receptor on subpallial DAergic neurons would demonstrate if these neurons express presynaptic D_2 receptors.
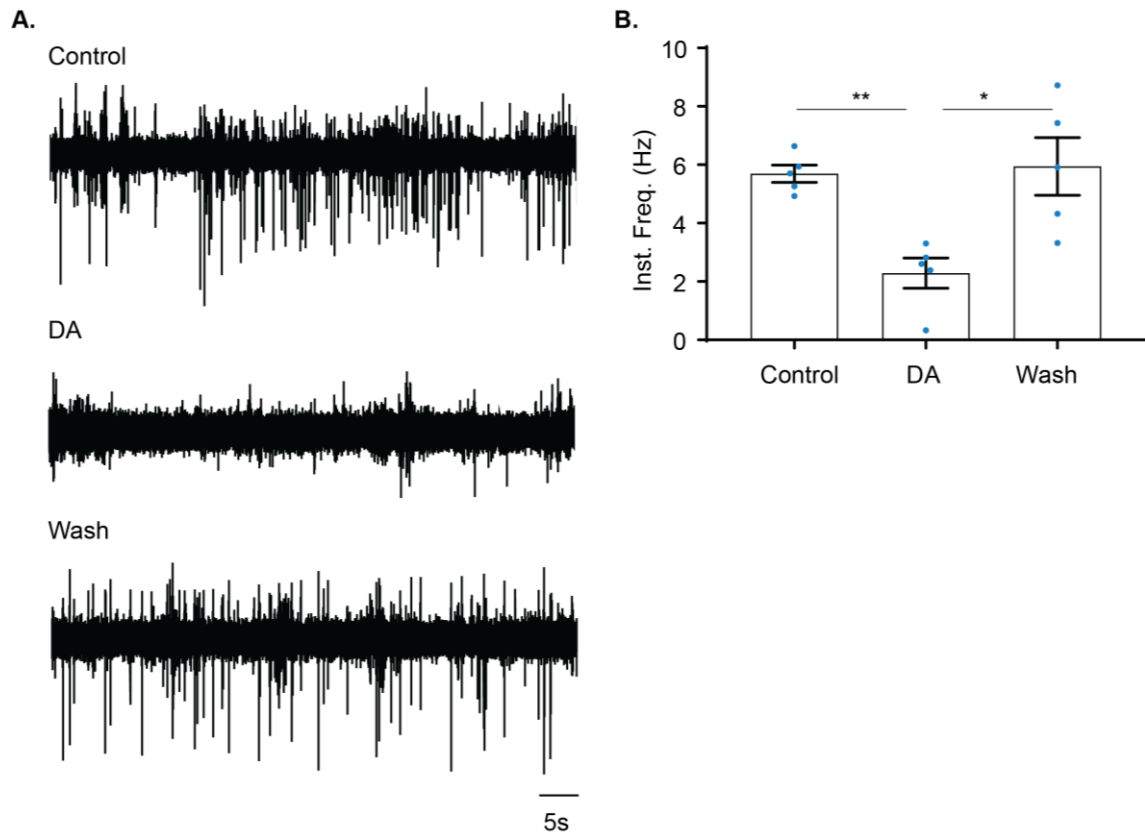
Figure 3:21 DA application reduces subpallial DAergic neuron activity. A: Representative loose patch recordings of firing activity of subpallial DAergic neurons 5 dpf (upper trace) and in the presence of 5µM DA (middle trace) and in wash (lower trace) condition. **B:** Bar chart comparing the instantaneous frequency during control, DA treatment and wash condition. * $P<0.05$, ** $P<0.005$.

3.4 Discussion

In this chapter, I have examined the development of subpallial DAergic neurons during early periods of zebrafish development. The results presented in this chapter demonstrate three key findings. Firstly, these neurons undergo rapid morphological changes during late embryonic and early larval life; second, they receive excitatory and inhibitory synaptic input from as early as 3 dpf and; third, they are intrinsically excitable and exhibit synaptically driving firing activity from late embryonic life.

3.4.1 Morphogenesis of subpallial dopaminergic neurons

To examine the morphology of subpallial DAergic neurons during early development, I performed single-cell labelling using neurobiotin juxtacellular labelling and streptavidin histochemistry to visualise the cytoarchitecture of subpallial DAergic neurons. These experiments revealed that at 2 and 3 dpf subpallial DAergic neurons possess ventrolateral projections proximal to the soma that are restricted to the subpallium. At 5 dpf, large arbours were seen that primarily innervated the subpallium. However, a proportion of these neurons possess descending projections that enter the diencephalon at 5 dpf. This was to be expected, as previous studies found subpallial DAergic neurons projected ventrolaterally and then arbourise extensively, a subpopulation of subpallial DAergic neurons was also found to project to the thalamus and hypothalamus (Tay et al., 2011, McLean and Fetcho, 2004a). Interestingly, I observed also a population of subpallial DAergic neurons that also possessed descending projections in which they extended axons posteriorly towards the diencephalon. Limitations associated with staining prevents me from determining where these axons terminated. However, previous studies suggest these most likely innervated thalamic and hypothalamic regions (Tay et al., 2011). However, further research is needed to determine whether this is indeed the case for the neurons labelled in this study.

Based on my anatomical evidence, can anything be inferred about the functional role of subpallial DAergic neurons? Genetic studies have suggested ventral and

dorsal aspects of the subpallium are homologous to the mammalian striatum and extended amygdala respectively (Mueller et al., 2008, Osorio et al., 2010, Wullimann, 2009, Wullimann and Mueller, 2004, Wullimann and Rink, 2002, Ganz et al., 2012, Perathoner et al., 2016, O'Connell and Hofmann, 2011). Therefore, locally projecting DAergic neurons may be functionally equivalent to nigrostriatal neurons of the mammalian brain. To determine if this is the case ablation of subpallial DAergic could be used to if these neurons have a similar role in locomotion. Since SNc neurons have a role in modulating locomotion and loss of these neurons cause Parkinson's disease like symptoms, ablating subpallial DAergic neurons may have a similar effect of zebrafish locomotion. The role of subpallial DAergic neurons in locomotion will be addressed in chapter 4.

3.4.2   Development of synaptic input to subpallial dopaminergic neurons

Electroporation of subpallium DAergic neurons allowed me to study developmental morphology (Figure 3:6). I found labelled cells in the olfactory bulb and contralateral subpallium. This is consistent with the literature, retrograde labelling studies conducted in adult zebrafish, found labelled neurons in the ventral telencephalon, Vs, Vp and olfactory bulb (Rink and Wullimann, 2004, Rink and Wullimann, 2002a, Rink and Wullimann, 2002b). However, these studies found the ventral telencephalon was innervated by the pallium, the putative hippocampus and amygdala. Together, this would suggest the ventral telencephalon of adults receives input from putative striatum, hippocampus, amygdala and extended amygdala, as well as the olfactory bulb (Rink and Wullimann, 2004, Rink and Wullimann, 2002a, Rink and Wullimann, 2002b, Perathoner et al., 2016, O'Connell and Hofmann, 2011, Mueller et al., 2011, Ganz et al., 2015). The experiments I conducted did not find the pallial input. One explanation for this is that subpallium and pallium are transient structures that become the ventral and dorsal telencephalon later in development; therefore, these structures are still developing, and the connectome is not complete. Evidence supporting this argument includes studies investigating learning and memory, which are conducted from 7 dpf onwards. Social behaviours, learning and operant conditioning are examined in older fish, when they are juvenile

(Roberts et al., 2013). Pallial lesions can disrupt memory and learnt behaviours in other teleost fish (Portavella et al., 2002). Therefore, it could be assumed that functional connections from the pallium develop later in development and which is why subpallial afferents from the pallium are not present at 5 dpf.

In larval zebrafish, subpallial afferents were found in the posterior tuberculum-pretectum border as early as 3 dpf. The posterior tuberculum-pretectum border corresponds to the thalamus in adult zebrafish, and this structure integrates, processes and relays sensory input (Roberts et al., 2013). The zebrafish thalamus has been shown to filter visual information, specifically changes in luminescence (Heap et al., 2018b), and this structure is an integral part of the ascending visual and auditory pathway (Roberts et al., 2013, Mueller, 2012). The thalamic connections I observed in early-stage zebrafish are consistent with reports in the literature: Rink and colleagues found subpallial afferents originating in the thalamus in adult fish (Rink and Wullimann, 2004, Rink and Wullimann, 2002a, Rink and Wullimann, 2002b). Interestingly, similar thalamic-subpallial connections have been observed in goldfish (Northcutt, 2006). Together, these studies suggest the teleost subpallium receives input from the thalamus and these connections develop as early as 3 dpf in zebrafish. Since the subpallium receives input from the thalamus early in development, it could be assumed the subpallial DAergic neurons receive sensory input from a thalamic relay; however, functional studies are required to determine if these neurons receive sensory information.

During early larval stages, subpallial afferents were found in the preoptic area, the posterior tuberculum and hypothalamus from 3 dpf. Similar observations were found in adult zebrafish; retrograde labelling studies found the ventral telencephalon received input from the preoptic area, posterior tuberculum as well as multiple regions of the hypothalamus (Rink and Wullimann, 2004, Rink and Wullimann, 2002a, Rink and Wullimann, 2002b). Interestingly, these studies found ascending DAergic projections from the posterior tuberculum and suggested these DAergic neurons are homologous to the neurons in VTA and SNc (Rink and Wullimann, 2002a). However, the experiments I conducted did not find any subpallial afferents that originated from *vmat2*/gfp positive neurons in the posterior tuberculum. This suggests the subpallial DAergic neurons do not

receive input from DAergic neurons of the posterior tuberculum. One explanation is that these neurons do not innervate the dorsal aspect of the subpallium, where the cell bodies of the subpallial DAergic neurons reside and was the location of the electroporation site. Evidence supporting this argument is a study by Tay and colleagues, in which they examined the projectome of zebrafish catecholamine neurons found the ascending projections originated from DC2/4; however, these neurons do not innervate the subpallium extensively and were restricted to the ventral aspect of the subpallium (Tay et al., 2011). Another explanation may be that, due to technical limitations, the electroporation was proximal to the soma and did not label the subpallial afferents that innervate the subpallial DAergic neurons projections.

My retrograde labelling experiments also revealed that the subpallium receives input from the hindbrain from 2 dpf onwards. These neurons were found close to the locus coeruleus and raphe at 2, 3 and 5 dpf. Similarly, Rink and Wullimann found the ventral telencephalon of adult zebrafish received input from the hindbrain, however, they found input specific structures, including the nMLF, dorsal tegmental, superior reticular nucleus, superior raphe and locus coeruleus (Rink and Wullimann, 2004, Rink and Wullimann, 2002a, Rink and Wullimann, 2002b). These studies suggest the ventral telencephalon receives a range of cholinergic, noradrenergic and serotonergic input from across the hindbrain. Whilst these studies found input from these regions in adult fish, I only found a subset in larval zebrafish. One explanation for this discrepancy is these connections have not fully developed in early-stage zebrafish. Another explanation is that different labelling techniques were used: I electroporated locally to the subpallial DAergic neurons, which reside in the dorsal aspect of the subpallium, whilst Rink and Wullimann used DiI-labelling to identify the afferent nuclei to both ventral and dorsal aspects of the ventral telencephalon. Subpallial DAergic neurons are restricted to the dorsal aspect of the ventral telencephalon of adult zebrafish (Yamamoto et al., 2010a), therefore, only a subset of afferent nuclei identified by Rink and Wullimann may innervate this region (Figure 3:22) (Rink and Wullimann, 2004, Rink and Wullimann, 2002a, Rink and Wullimann, 2002b). Evidence supporting this includes a study investigating the catecholamine projectome. Rink and Wullimann found NAergic neurons of the

locus coeruleus innervate the ventral telencephalon; however, Tay and colleagues examined the morphology of these NAergic neurons and found their projections innervate the ventral aspect of the subpallium (Figure 3:22) (Tay et al., 2011, Rink and Wullimann, 2002a). Therefore, the NAergic afferents were not electroporated as they do not project to the dorsal aspect of the subpallium, where the subpallial DAergic neurons are located. This suggests the subpallial DAergic neurons are not innervated by NAergic neurons. However, subpallial DAergic neurons innervate the subpallium extensively, and NAergic neurons could modulate DAergic synapse in these regions.
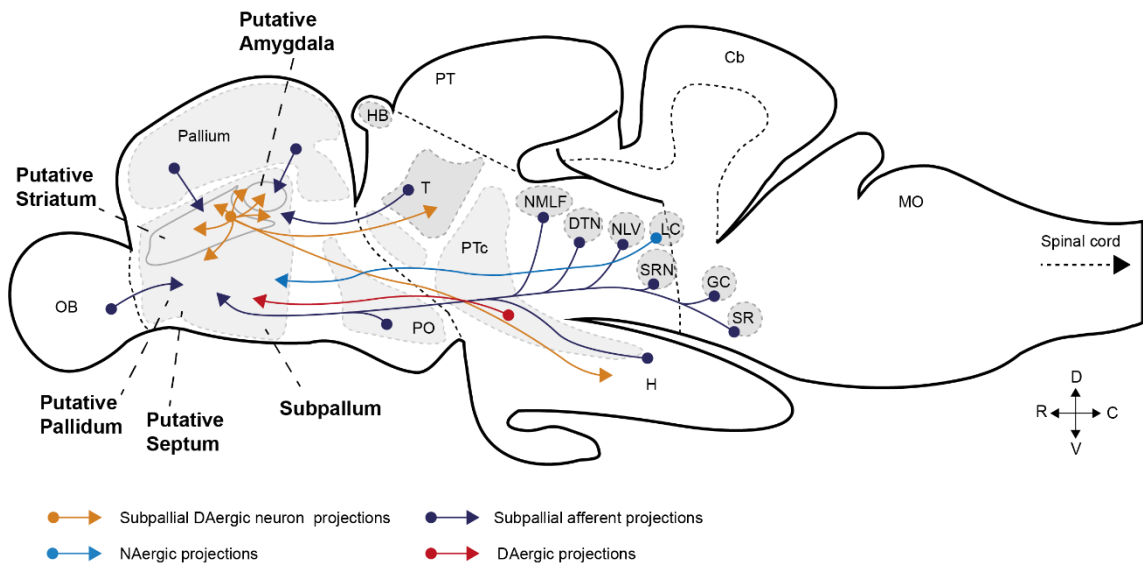
Figure 3:22 Schematic illustration of the connectome of subpallial DAergic neurons. Schematic illustration of the afferent projections to the subpallium (navy arrows), as well as the ascending DAergic projections originating from the DDNs (red arrow) and the NAergic projection originating from the LC (blue). The projections of the subpallial DAergic neurons are shown by orange arrows. Orientation is indicated in the panel; R = rostral, C = caudal, D = dorsal and V = ventral. Abbreviations: Olfactory bulb (OB), cerebellum (Cb) subpallium (SP), preoptic (PO), posterior tuberculum (PTc), hypothalamus (H), pretectum (PT), thalamic nuclei (T), nucleus of the medial longitudinal fasciculus (NMLF), griseum centrale (GC), dorsal tegmental nucleus (DTN), nucleus lateralis valvulae (NLV), superior reticular nucleus (SRN), superior raphe (SR), locus coeruleus (LC), habenular (HB) and medulla oblangata (MO). Redrawn from Tay et al., (2011) and Rink and Wullimann (2002).

In sum, the subpallium receives input early in development, and these afferent processes change rapidly. I observed input originating from the putative striatum and extended amygdala during early development, this suggests the subpallial DAergic neurons receive input from these regions. Furthermore, similar findings have been observed in adult zebrafish. Additionally, I observed afferent nuclei in the olfactory bulb and thalamus, and these afferent nuclei were labelled in adult retrograde labelling studies (Rink and Wullimann, 2002b). Furthermore, I found subpallial afferents originating from the posterior tuberculum, hypothalamus and hindbrain regions as early as 3 dpf. These have also been found in adult zebrafish; however, these studies found additional afferent nuclei (Rink and Wullimann, 2004, Rink and Wullimann, 2002a, Rink and Wullimann, 2002b). These discrepancies could be due to changes to input that appear later in development, or due to differences in retrograde labelling techniques used.

In this chapter, I have also shown that subpallial DAergic neurons receive GABAergic and glutamatergic input from at least 3 dpf. Examination of the kinetics of glutamatergic mPSCs did not differ between 3 and 5 dpf. However, the rise and decay time kinetics of GABAergic mPSCs decreased with age. The kinetics of mPSCs often change during development as synapses mature. The rise time of the GABAergic mPSCs decreased with age, suggesting faster activation of GABAergic receptors. These kinetics are driven by ion channels and receptors, and mPSC kinetics are affected by their densities. During early neuron development, there is low expression of receptors, and they are dispersed across the membrane (Hall and Sanes, 1993). Subsequently, there is slow activation of the receptors on the postsynaptic terminal. During synapse maturation, receptor number increases and clustering occurs (Favuzzi and Rico, 2018, Craig et al., 1994, Hall and Sanes, 1993, Sudhof, 2018). In combination, these changes lead to a decrease in the rise and decay time and an increase in the amplitude of mPSCs (Gonzalez-Forero and Alvarez, 2005, Sutor and Luhmann, 1995, Jang et al., 2010, Kuhlman et al., 2010, Felix and Magnusson, 2016, DuBois et al., 2004).

In sum, the subpallium begins to receive axonal projections from 2 dpf. By 5 dpf, the subpallial afferent largely resembles innervation patterns observed in the adult zebrafish. Examination of functional synaptic input by whole-cell patch-clamp revealed subpallial DAergic neurons receive glutamatergic and GABAergic

input from 3 dpf. Together, this suggests subpallial DAergic neurons have become integrated into the neural circuits.

3.4.3   The ontogeny of intrinsic excitability.

I have shown subpallial DAergic neurons are wired into the CNS; however, i sought to determine if they are capable of releasing DA. This can be inferred by studying the excitable properties of these neurons. Whole-cell patch clamp recordings of subpallial DAergic neurons revealed these cells are intrinsically excitable from 3 dpf. Here, rheobase current evoked broad action potentials. At 5 dpf, the action potential kinetics had similar threshold potential and halfwidth to 3 dpf neurons. However, 5 dpf neurons had larger spike amplitudes suggesting changes in action potential kinetics. Since action potential kinetics are driven by ion channel expression and densities, it could be assumed changes in ion channels and/or their densities. The depolarisation phase of an action potential is driven by TTX-sensitive voltage-gated sodium channels and N-type and P/Q-type calcium channels (Gantz et al., 2018, Bean, 2007). An increase in their expression could result in an increase depolarisation phase and amplitude. Immature neurons typically generate small spikes that are activated at depolarised threshold potentials. During maturation, changes to ion channel expression, densities and subunit composition alter the conductances that drive action potential kinetics (Gao and Ziskind-Conhaim, 1998). The density of both voltage-gated sodium and potassium channels have been observed to increase during early development, leading to a decrease in spike time to peak, width and increased amplitude (Benninger et al., 2003, Gao and Ziskind-Conhaim, 1998).

Analysis of subpallial DAergic neurons revealed they exhibited broad action potentials (~9ms) during early development, whilst the DDNs exhibit shorter action potential durations (~4ms) during this time (Jay, 2015). The subpallial DAergic neurons have relatively broader action potentials when compared to those of the DC2/4 population. One explanation for this is that DC2/4 neurons are more mature since these neurons develop early. DC2/4 are some of the first catecholamine neurons that appear in the zebrafish brain, becoming *th* positive at 20 hpf, whilst subpallial DAergic neurons can only be identified by their *th*

expression at 48 hpf (Mahler et al., 2010). Another explanation is that zebrafish DAergic neurons exhibit heterogeneity with regards to action potential kinetics. Interestingly, studies of mammalian DAergic neurons revealed a high degree of diversity in the action potential duration and amplitude. Subpopulations of VTA neurons that project to the cortex, amygdala and the core of the NAc have broader action potentials (action potential duration ~7ms) compared to the SNc neurons (~4ms) (Lammel et al., 2008). Together, it shows DAergic neurons of zebrafish exhibit similar properties to mammalian DAergic neurons; they both generate broad action potentials and are heterogeneous.

As neurons mature, some develop the capacity to generate repetitive spikes when subjected to constant depolarising current injection. In this chapter, the individual recording of a neuron at 2 dpf, a single spike was observed. This is due to the difficulty of performing whole-cell patch clamp recordings on these neurons. At 3 dpf, injection of suprathreshold current was able to elicit multiple action potentials in the majority (~70%) of subpallial DAergic neurons while at 5 dpf, all recorded neurons exhibited repetitive spike trains of action potentials and had an increase in spike frequency compared to 3 dpf neurons. This suggests that by 5 dpf, subpallial DAergic neurons developed the capacity to fire repetitively. Similar observations have been made in maturing neurons in rodents as well as the DDNs of zebrafish (Jay et al., 2015, Strubing et al., 1995, Lenka et al., 2002, Benninger et al., 2003, Jay, 2015).

In sum, subpallial DAergic neurons are intrinsically excitable during early development. Subpallial DAergic neurons are capable of generating action potentials and exhibit maturation in the action potential waveform. With age, the subpallial DAergic neurons generate trains of spikes, by 5 dpf they are capable of generating higher firing frequencies. Together, this suggests the maturation of the neurons.

3.4.4 Physiological Properties of subpallial dopaminergic neurons.

I examined the subpallial DAergic neurons for the traditional physiological features of mammalian midbrain DAergic neurons, including I_h current and D_2 autoreceptors. However, subpallial DAergic neurons do not exhibit all of the

traditional physiological properties that have been observed in mammalian DAergic neurons. A classical property of mammalian DAergic neurons is the presence of an I_h current, examination of the subpallial DAergic neurons revealed they do not possess an I_h current. A recent study of mammalian DAergic neurons found that this feature is not conversed between all mammalian DAergic populations, mesocortical DA neurons of the VTA did not exhibit a sag potential (Lammel et al., 2008). Interestingly, examination of zebrafish DC2/4 neurons revealed they also lacked an I_h current (Jay, 2015).

The presence of D_2 autoreceptors is another feature used to identify mammalian DAergic neurons. Activation of presynaptically expressed D_2 receptors can activate GIRK channels, which reduces the excitability of the DA neurons (Ford, 2014). Autoreceptor function has been observed in multiple mammalian DAergic neuron populations as well as the zebrafish DC2/4DAergic cluster (Lammel et al., 2008, Jay, 2015). This suggests that the autoreceptor function of DAergic neurons is conserved across species. My work stands in broad agreement with this principle: application of DA to subpallial DAergic neurons decreased the firing activity of these neurons, suggesting activation of presynaptic D_2 receptors typically attenuates firing activity; however, I did not use a specific D_2 antagonist to confirm the DA induced inhibition of firing activity was mediated by D_2 receptors. Interestingly, physiological recordings of zebrafish DC2/4 neurons revealed they exhibited D_2 autoreceptor inhibition (Jay, 2015), demonstrating this physiological feature is conserved across species. However, work in mammals revealed D_2 autoreceptor are not conserved in all DAergic clusters, activation of presynaptic D_2 receptors of the VTA DAergic neurons that project to the amygdala does not abolish firing activity but rather reduces the firing of these neurons (Lammel et al., 2008).

3.4.5   Conclusion

In sum, the findings presented in this chapter confirm that the DAergic neurons of the zebrafish subpallium can be targeted for physiological techniques. These neurons demonstrate fast development in their input, morphology and physiological features between 2 and 5 dpf. The cellular and physiological

properties and activity of subpallial DAergic neurons at 2, 3 and 5 dpf, have been examined and by 5 dpf, subpallial DAergic neurons exhibit chain spiking and endogenous firing. This work lays the foundation to delineating the functional role of subpallial DAergic neurons in awake, free-moving zebrafish.

The Functional Role of Subpallial Dopaminergic Neurons

4.1 Introduction

Our understanding of subpallial DAergic neurons has been limited by a lack of studies investigating this neural population. From anatomical and genetic studies, it has been hypothesised that the zebrafish subpallium is homologous to the mammalian striatum and extended amygdala (Ganz et al., 2012, Perathoner et al., 2016, O'Connell and Hofmann, 2011). Within the subpallium, there is a cluster of DAergic neurons that provide the primary source of DA input to the telencephalon as well as innervate the thalamus and hypothalamus (Tay et al., 2011). Based on these observations, it is hypothesised that the subpallial DAergic neurons may be functionally equivalent to mammalian midbrain DAergic neurons. However, as no functional studies have been conducted, this hypothesis remains untested. In this chapter, I use physiological, imaging and behavioural approaches to determine whether subpallial DAergic neurons are functionally homologous to mammalian midbrain DAergic neurons. Below, I provide an account of the nigrostriatal and mesostriatal pathways in mammals and its role in regulating behaviours before detailing our current understanding of equivalent pathways in zebrafish.

4.1.1 Mammalian striatum

The striatum is a nucleus located in the forebrain and can be structurally and functionally subdivided into dorsal and ventral regions (Dudman and Krakauer, 2016, Yoshimi et al., 2015). The dorsal region of the striatum is composed of the caudate nucleus and putamen and has a role in locomotion and action selection (Grahn et al., 2008, Palmiter, 2008). The caudate nucleus primarily receives cortical input, whilst the putamen receives input from sensorimotor and prefrontal cortex as well as the limbic circuits (Krack et al., 2010, Soares-Cunha et al., 2016b). The ventral striatum contains the NAc and is associated with the reward circuits (Nakanishi et al., 2014, Hikida et al., 2013, Minami et al., 2017). The NAc, which is divided into the core and shell components, receives input from the prefrontal cortex and limbic systems (Soares-Cunha et al., 2016b). Both dorsal

and ventral regions of the striatum are innervated by the midbrain DAergic neurons.

The dorsal striatum is an integral component of the basal ganglia, a group of subcortical nuclei that regulate motor control, as well as motor learning, executive behaviours and emotions (Lanciego et al., 2012). The basal ganglia is composed of the striatum, substantia nigra pars reticulata (SNr), SNc, globus pallidus externus (GPe) and internus (GPi), subthalamic nucleus, thalamus and cortex. The classical model of the basal ganglia circuit is divided into two cortex-basal ganglia-thalamus-cortex loops described as direct and indirect pathways (Kreitzer and Malenka, 2008) (Figure 4:1). The dorsal striatum receives input from the cortex as well as DAergic input from the SNc (Lim et al., 2014). Furthermore, the dorsal striatum innervates the GPe, GPi and SNr (Lanciego et al., 2012).

The ventral aspect of the striatum is a major component of the limbic system, mediating reward, aversion, cognition and motivational salience (Cardinal et al., 2002, Jensen et al., 2003, Heekeren et al., 2007, Meffert et al., 2018, Floresco, 2015). The ventral striatum receives input from the amygdala, thalamus, cortex and hippocampus (Zhu et al., 2016, Choi et al., 2017). Additionally, it receives DAergic input from the VTA as part of the mesolimbic pathway (Reynolds et al., 2001). The ventral striatum innervates the ventral pallidum, globus pallidus, thalamus and the extended amygdala (Morales and Margolis, 2017).

Both dorsal and ventral aspects of the striatum are primarily composed of GABAergic medium spiny projecting neurons (MSNs), cholinergic interneurons as well as a four classes of GABAergic interneurons (Gangarossa et al., 2013, Gerfen, 1988, DiFiglia, 1987, Straub et al., 2016, Tepper et al., 2018). The GABAergic interneurons can be distinguished based on molecular markers and include parvalbumin expressing fast spiking interneurons, tyrosine hydroxylase expressing interneurons, the neuropeptide Y/ somatostatin/ nitric oxide synthase expressing interneurons and calretinin expressing neurons (Tepper et al., 2018). The striatal circuitry is modulated by DA signalling which, when perturbed, cause conditions such addiction, schizophrenia and Parkinson's disease (Berke and Hyman, 2000, Hamid et al., 2016, Deserno et al., 2016, Lotharius and Brundin,

2002, Dauer and Przedborski, 2003). Below, I review the structural and functional studies of the striatum and the role of DA signalling in this region.

4.1.1.1   Medium spiny projecting neurons

MSNs are inhibitory GABAergic neurons that makeup approximately 95% of the striatal grey matter (Plenz and Wickens, 2016). MSNs have been clearly defined and possess stereotypical morphological and physiological characteristics (Ericsson et al., 2011, Bicanic et al., 2017, Gertler et al., 2008). Specifically, these cells have 5-6 primary dendrites projecting from the soma, which branch extensively and are studded with numerous spines (Bicanic et al., 2017, Plenz and Wickens, 2016).

MSNs exhibit episodic spike trains followed by quiescent periods. On current injection these cells show repetitive firing (Plenz and Wickens, 2016, Galarraga et al., 2007, Kimura et al., 1990). The resting membrane potential of MSNs alternates between two subthreshold states, a hyperpolarised 'down-state' and a depolarised 'up-state' (Evans et al., 2013, Wilson and Kawaguchi, 1996). The up-state is dependent on combined cortical and striatal inputs (Surmeier and Kitai, 1997, Carter and Sabatini, 2004, Wilson and Kawaguchi, 1996). When in the up-state MSNs display slow ramp-like depolarisations that is mediated by slowly inactivating A-type K$^+$ channels (I_{As}) (Gabel and Nisenbaum, 1998, Nisenbaum and Wilson, 1995, Nisenbaum et al., 1994, Surmeier et al., 1991). The I_{As} current can persist for seconds and is associated with prolonged spike latency, restricting recurring spiking by delaying depolarisation (Nisenbaum and Wilson, 1995, Nisenbaum et al., 1994, Gabel and Nisenbaum, 1998). The I_{As} current of MSNs is inhibited and activated by D$_1$ and D$_2$ receptor signalling, respectively. Depending on the state of the MSN, DA signalling can affect the excitability of these neurons (see section 4.1.1.3).

MSNs can be segregated into D1-MSN and D2-MSN populations: D1-MSNs can be identified by expression of substance P, dynorphin and D$_1$ receptors (Thibault et al., 2013, Young et al., 1986) while D2-MSNs can be identified by expression of D$_2$ receptors and encephalin (Gerfen et al., 1990). A small population of MSNs also express D$_1$ and D$_2$ receptors, but little is known about the function of these cells (Gagnon et al., 2017). The D1-MSNs and D2-MSNs are functionally and

anatomically differentiated, comprising the direct and indirect striatal pathways, respectively (Gerfen and Surmeier, 2011) (see section 4.1.1.2). These cells are evenly distributed across the dorsal striatum although the caudal aspect of the dorsal striatum has been found to express D_1 receptors only (Gangarossa et al., 2013).

4.1.1.2   The direct and indirect pathways of the dorsal striatum

In the direct pathway, the striatum receives glutamatergic input from the cortex and thalamus, which excite GABAergic neurons projecting to the GPi and SNr. This, in turn, inhibits GABAergic neurons of the GPi/SNr that project to the thalamus and the net result is disinhibition of the thalamus (Freeze et al., 2013). DA input activates D_1 receptors expressed by D1-MSNs, which increases the excitability of D1-MSNs (Gerfen and Surmeier, 2011). Since the D1-MSNs are GABAergic, the increased excitability leads to an increase in inhibitory GABAergic transmission to the GPi/SNr (Freeze et al., 2013). Subsequently, the activity of GABAergic GPi/SNr neurons is reduced, which disinhibits thalamic neurons that are innervated by the GPi/SNr (Figure 4:1). The activation of the direct pathway is thought to promote movement by allowing activation of the thalamocortical loop.

In the indirect pathway, the striatum receives excitatory input from the cortex which in turn excites GABAergic neurons projecting to the GPe. Once activated, these cells inhibit GABAergic GPe neurons that project to the subthalamic nucleus (STN; Figure 4:1) (Morera-Herreras et al., 2012). This loss of inhibition of STN neurons allows excitatory glutamatergic input to activate GPi/SNr GABAergic neurons that project to the thalamus (Lanciego et al., 2012). This, in turn, inhibits the glutamatergic thalamocortical projecting neurons. In the indirect pathway, DA input from the SNc activates D_2 receptors in the striatum and reduces the excitability of the D2-MSNs, which in turn reduces the GABAergic transmission to the GPe (Murer et al., 2000). Subsequently, there is an increase in activity of the GABAergic neurons of the GPe that innervate the STN, therefore, the activity of the STN is reduced. In sum, activation of the indirect pathway leads to increased inhibition of the thalamocortical loop and subsequently inhibits movement.

In Parkinson's disease, DAergic neurons of the SNc are lost. The resulting loss of DA modulation of the striatum perturbs locomotion (Sveinbjornsdottir, 2016, Magrinelli et al., 2016). Optogenetic activation D2-MSNs of the indirect pathway can elicit Parkinson-like symptoms, whilst activation of D_1 receptors rescues the locomotive deficits (Kravitz et al., 2010). Loss of DA input to the direct pathway reduces the activity of D1-MSNs, which reduces inhibition of GPi/SNr neurons and subsequently increases the GABAergic input to the thalamocortical loop (Lanciego et al., 2012). Loss of DAergic input to the indirect pathway increases the excitability of D2-MSNs, inhibiting the GPe (Lanciego et al., 2012) and causes hyperexcitability of the STN, resulting in increased inhibition of the thalamocortical loop (Murer et al., 2000, Calabresi et al., 2014).

Indirect Pathway   **Direct Pathway**
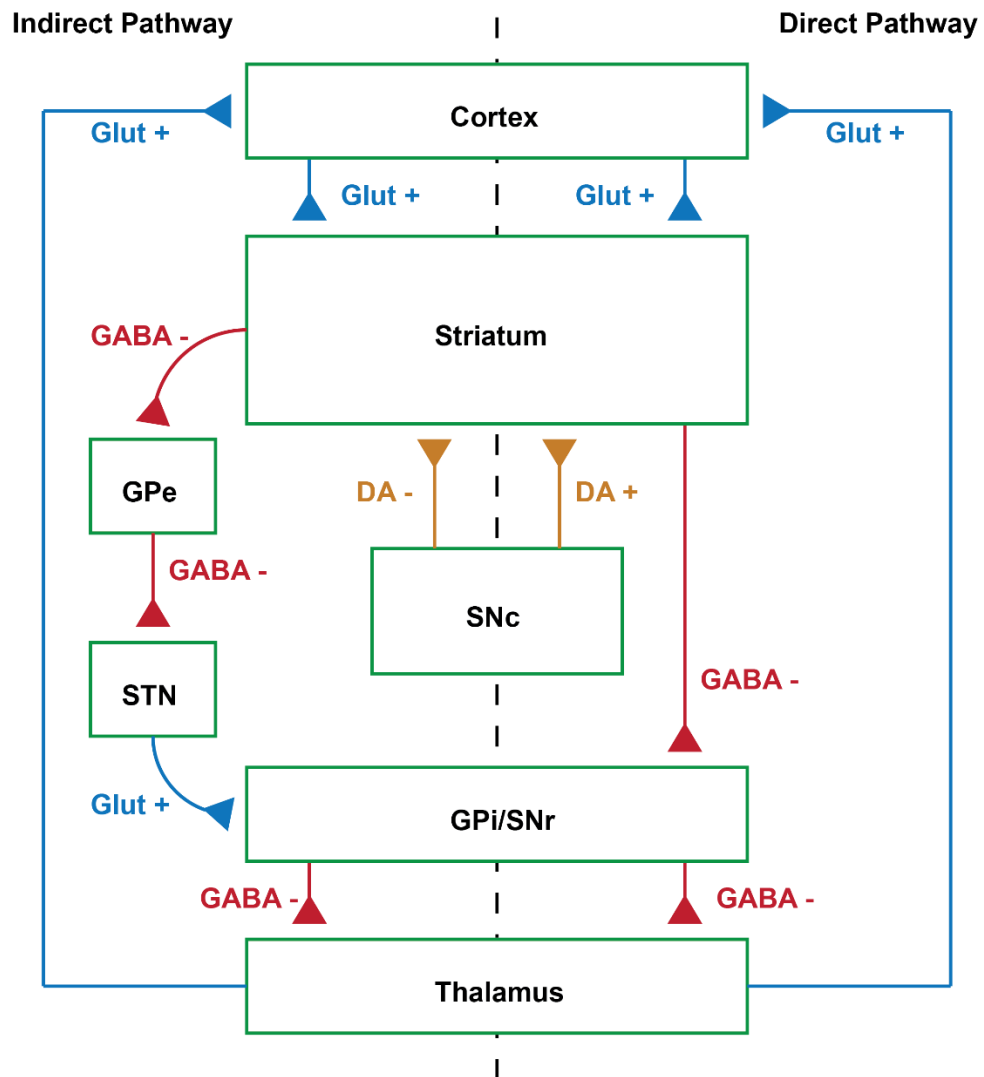
Figure 4:1 Classic model of basal ganglia. Schematic illustration the direct and indirect pathways of the basal ganglia, highlighting the excitatory and inhibitory effects of neurotransmission. Abbreviations: GPe – Globus Pallidus externus, GPi – Globus Pallidus Internus, SNc – Substantia Nigra Pars Compacta, STN – Subthalamic nucleus. Adapted from Morera-Herreras et al., (2012) and Lanciego et al., (2012).

4.1.1.3   Dopamine signalling and medium spiny projecting neurons

DA can modulate D1-MSNs through multiple ion channel targets. Activation of D_1 receptors on D1-MSN has been shown to reduce the I_{As} current (Kitai and Surmeier, 1993, Surmeier and Kitai, 1993). In the up-state, D_1 receptor activation increases the activity in the L-type Ca^{2+} channels, and along with the reduction of the I_{As} current can increase the excitability of the D1-MSNs (Hernandez-Lopez et al., 2000, Plenz and Wickens, 2016, Surmeier et al., 1995). During the downstate, DA activation of D1-MSNs increases I_{Kir} and decrease I_{Na} currents, which in turn

stabilises the hyperpolarisation of the down-state, making the cell less excitable (Surmeier and Kitai, 1993).

Whilst DA stimulation of D1-MSNs increases excitability of the up-state and stability of the down-state, DA input to D2-MSNs has an opposite effect. Activation of D_2 receptors enhances the I_{As} current in the D2-MSNs and decreases the I_{Kir} current. Modulation by DA enhances the probability of transiting from the down-state to up-state (Plenz and Wickens, 2016, Uchimura et al., 1989). In the up-state, D_2 receptor activation decreases L-type Ca^{2+} channel activity, and along with an increase in the I_{As} current can increase the delay in D2-MSN firing activity (Olson et al., 2005, Plenz and Wickens, 2016). In sum, DA transmission modulates the excitability of MSNs.

4.1.2   Dopamine transmission in the ventral striatum

As mentioned above, the ventral striatum is composed of NAc core and shell regions that can be differentiated by their inputs, outputs and immunohistochemical marker expression (Burke et al., 2017). Further subregions can be identified based on their activity and the information they encode (Tsutsui-Kimura et al., 2017a, Ikemoto, 2007, de Jong et al., 2019, Badrinarayan et al., 2012). As with the dorsal aspect of the striatum, the NAc is composed primarily of D1 and D2 MSNs, a smaller population of cholinergic interneurons as well as four classes of GABAergic interneurons. Mesolimbic DA transmission can modulate the activity of the NAc and has been associated with motivational salience, aversive and rewarding cues and various aspects of decision making by (de Jong et al., 2019, Badrinarayan et al., 2012, Yoshimi et al., 2015, Jenni et al., 2017, Tsutsui-Kimura et al., 2017a).

Traditionally, both direct and indirect pathways of the NAc were thought to modulate motivated behaviour such as reward and aversion (Lobo et al., 2010). Here, activation of D1-MSNs (the direct pathway) was thought to increase motivational behaviour and promote reward signalling (Lobo and Nestler, 2011), while indirect pathway activation triggers aversive learning behaviours (Kravitz et al., 2012, Hikida et al., 2010, Lobo et al., 2010). Optogenetic activation of NAc D1-MSNs facilitated conditioned place preference, whilst optogenetic activation

of NAc D2-MSNs attenuated conditioned place preference (Lobo et al., 2010). However, recent studies challenge this functional dichotomy (Soares-Cunha et al., 2016a). Studies have shown that D1 and D2-MSNs can both modulate reward and aversion. Optogenetic studies have shown that activation of both D1 and D2-MSNs had both rewarding and aversive effects on behaviour (Soares-Cunha et al., 2019). Additionally, application of D_1 and D_2 receptor antagonists reduced avoidance behaviours during two-way active avoidance tasks (Boschen et al., 2011, Wietzikoski et al., 2012). It has been suggested that the DAergic population of the VTA are involved in processing both aversive and reward-related information (Lammel et al., 2014). Below, I review the functional studies of the ventral striatum and the role of DA signalling in mammalian striatum.

4.1.2.1 Reward related dopamine transmission in the ventral striatum

Midbrain DAergic neuron activity has been shown to be involved in conveying reward signals and reward-prediction which provides a mechanism by which reward learning can occur (Schultz, 2016, Schultz et al., 2017, Schultz, 1998). Schultz and colleagues describe DA as a reward prediction error (RPE) signal that provides a mechanism of error-driven reinforcement learning (Schultz et al., 2017). Without a predictor, phasic DA release is detected in the striatum when presented with an unexpected reward (Yoshimi et al., 2015, Schultz et al., 2017). During learning and in the context of RPE, phasic DA is released in response to the predictive stimulus of an expected reward and not released when the reward is received. If the value of the reward is equal to the expected reward, then the firing activity of DAergic neurons does not change (Schultz et al., 2017). However, if an expected reward is not received, the firing activity of DA neurons decreases (Schultz et al., 2017). These errors in the RPE reflects a reward value and can promote learning (Schultz, 2016, Keiflin and Janak, 2015).

Phasic DA signalling and RPE is a system that conveys the value of an object as well as encoding information regarding stimuli that predicts future rewards. Changes to phasic DA signalling can alter motivation to work and affect learning (Hamid et al., 2016). Exposure to food rewards causes an increase in DA concentrations in NAc (Biesdorf et al., 2015) and .depletion of NAc DA by neurochemical lesions impairs reward-related behaviours (Bergamini et al.,

106

2016). The pursuit of food rewards can be inhibited by blocking the phasic release of DA in the NAc by inducing tonic firing activity of VTA DAergic neurons (Mikhailova et al., 2016).

Exposure to addictive drugs such as cocaine and amphetamine increases DAergic transmission and enhances learning processes to reinforce reward signals (Koob, 1992, Sulzer, 2011). Amphetamine exposure has several effects on DA transmission, including increased TH activity, decreased MAO activity and DAT inhibition (Sulzer, 2011). Furthermore, cocaine blocks the activity of DAT (Siciliano and Jones, 2017). The net result of amphetamine and cocaine exposure is an increase in extracellular DA in the synaptic cleft by increasing DA concentration available for synaptic release and inhibiting DA reuptake (Carboni et al., 2001).

D1 and D2-MSNs have been shown to be involved in mediating reward (Soares-Cunha et al., 2016b). Knockout of D_1 receptors in mice abolished Pavlovian conditioning (Parker et al., 2010). Additionally, D_1 receptor knockout mice had a reduction in performance during a cocaine self-administration task, suggesting the rewarding effects of cocaine is attenuated in these animals (Caine et al., 2007). Furthermore, D_2 receptor knockout mice exhibited reduced cocaine-induced conditioned place preference (Welter et al., 2007), similar to D_1 receptor knockout mice. Together, these studies suggest both D_1 and D_2 receptors are required for reward. Optogenetic studies into D1 and D2-MSNs further support this argument. Lobo and colleagues found that optogenetic activation of D1-MSNs in the NAc enhanced cocaine place preference in rodents (Lobo et al., 2010). Furthermore, this study also found that optogenetic activation of D2-MSNs in the NAc attenuated cocaine place preference (Lobo et al., 2010).

Together, these findings suggest that loss of phasic DA release is sufficient to perturb reward-related behaviours such as the pursuit of food. It has been suggested that the DAergic reward circuitry is involved in overeating and decreased activity of D_2 receptor is associated with obesity (Stice and Dagher, 2010, Mahapatra, 2010).

4.1.2.2   Dopamine transmission in the ventral striatum and aversion

DA transmission has been well studied in the context of reward-orientated behaviours, however, the role of DA transmission in aversive behaviours remains somewhat controversial. Nonetheless, recent studies have shown that mesolimbic DAergic transmission in the NAc increases in response to aversive stimuli (Matsumoto and Hikosaka, 2009, Soares-Cunha et al., 2016a). Aversive stimuli can enhance DA transmission in the NAc shell, whilst the opposite is observed in the core (Tsutsui-Kimura et al., 2017a, Ikemoto, 2007, de Jong et al., 2019, Badrinarayan et al., 2012). Real-time DA signalling within the NAc core is decreased when rodents are exposed to fear-evoking cues whilst in the ventromedial NAc shell, DA transmission is increased (Badrinarayan et al., 2012, de Jong et al., 2019). In support of this premise, the ventral VTA DAergic neurons encode information about aversive events, these neurons are excited in response to foot shock, whilst the dorsal VTA DAergic neurons only excite to rewarding stimuli (Brischoux et al., 2009). Populations of VTA DAergic neurons that project the medial prefrontal cortex (mPFC) and NAc lateral shell have been observed to increase in activity to aversive stimuli (Lammel et al., 2011). This suggests that the VTA can modulate both aversive and reward behaviours by the segregation of DAergic neurons function based on location and targets.

Classically, it was suggested that the direct and indirect pathways of the ventral striatum modulate reward and aversive behaviours, respectively (Kupchik and Kalivas, 2017). However, recent studies have shown that activation of D1-MSNs can evoke both aversive and reward-orientated behaviours. Excitation D1-MSNs in the ventral NAc shell elicits robust aversive behaviours, whilst in the dorsal NAc shell activation of these neurons induced positive reinforcement of behaviours (Al-Hasani et al., 2015). Application of either D_1 or D_2 receptor antagonist can block amphetamine place preference (Liao, 2008), and D_2 receptor agonist enhances the effects of cocaine during self-administration task (Caine et al., 2002). Together these findings suggest both D1 and D2-MSNs are involved in reward and learning. In support of this premise, D_1 receptor knockout mice exhibited reduced performance in a cocaine self-administration task (Caine et al., 2007). Similarly, mice lacking D_2 receptors exhibited a decrease in the rewarding effects of opiates (Maldonado et al., 1997). Optogenetic activation of NAc D1-

MSNs enhance cocaine place preference (Lobo et al., 2010) and optogenetic inhibition of these neurons suppresses cocaine sensitization (Chandra et al., 2013). Together, these data suggest that both D1 and D2-MSNs in the NAc influences reward behaviours.

The examination into the role of D1 and D2-MSNs in the role of aversion has received relatively little attention (Soares-Cunha et al., 2016b). However, studies have shown that VTA DA neurons that project to the NAc medial shell are activated by aversive stimuli and aversive-predicting cues (de Jong et al., 2019). Blocking D1-MSN activity by application of D_1 receptor antagonists in the NAc shell can block conditioned taste aversion (Fenu et al., 2001, Fenu and Di Chiara, 2003). Similarly, D_1 receptor knockouts attenuate the learning and maintenance of conditioned taste aversion responses (Cannon et al., 2005). Optogenetic inactivation of DAergic neurons induced aversive behaviours and abolishing D_2 receptor in these animals could abolish learnt aversive behaviour (Danjo et al., 2014). This suggests DA signalling is activated by aversive cues and modulates aversive learning.

It has been shown that the activity DAergic neurons from the VTA can be modulated by aversive stimuli, not just reward-like stimuli. Distinct DAergic populations within the VTA have been shown to respond specifically to either reward-like or aversive stimuli (Matsumoto and Hikosaka, 2009, Lammel et al., 2011). Both D_1 receptor and D_2 receptor activation can modulate both aversion and reward, rather than having the dichotomy of a direct and indirect pathway, as seen in the dorsal striatum. However, reward and aversion processing is segregated between the NAc dorsal shell and mediolateral shell, respectively (Nakanishi et al., 2014).

4.1.2.3　Dopamine transmission in the NAc conveys motivational signals

DA signalling has also been associated with motivation (Soares-Cunha et al., 2016a). Incentive salience relates to the presence of a reward and promotes reward-seeking, whilst motivational salience relates to both rewarding and aversive stimuli (Berridge and Robinson, 1998). Bromberg-Martin and colleagues discuss DAergic neurons as having distinct roles in motivation: populations that encode value, which deal with reward/aversive stimuli that drive learning, whilst

another population encode motivational salience to support cognition and general motivation, and are activated by both reward and aversive stimuli (Bromberg-Martin et al., 2010). Evidence supporting role of DA neurons in motivational salience includes the identification of a subpopulation of VTA neurons that projects to the NAc lateral shell in response to both reward and aversive stimuli (Lammel et al., 2011, Matsumoto and Hikosaka, 2009, Matsumoto and Takada, 2013). Additionally, an examination into the DA transmission in the NAc shell was associated with motivational salience (Saddoris et al., 2015).

Early work has suggested that D1-MSNs and D2-MSNs can either promote or decrease motivation, respectively (Flanigan and LeClair, 2017). However, recent studies show that motivation of nonhuman primates can decrease upon the administration of D_1 or D_2 receptor-specific agonists (Marino and Levy, 2019). Investigations into incentive salience revealed optogenetic inhibition of either D1 or D2-MSNs of the ventrolateral striatum is sufficient to reduce performance in goal-directed and food incentive behaviours (Natsubori et al., 2017). Optogenetic activation of D1-MSNs in the NAc has been shown to promote incentive motivation during a self-stimulation task, however, this was not observed with D2-MSNs (Cole et al., 2018). Furthermore, perturbed D2-MSN activity in the ventrolateral striatum perturbs motivation and reduces goal directed behaviours (Tsutsui-Kimura et al., 2017b). Additionally, optogenetic activation D2-MSNs could increase performance during a progressive ratio task, whilst optogenetic inhibition of these neurons can decrease performance (Soares-Cunha et al., 2016a). Together, this data suggests that DA transmission in the NAc is involved in modulating incentive salience and motivation.

DA signalling and motivational salience are associated with both rewarding and aversive stimuli. A population of VTA DAergic neurons are known to respond to both types of stimuli (Lammel et al., 2011, Horvitz, 2000). Similarly, Matsumoto and colleagues found that DA neurons responded to both rewarding and aversive stimuli, as well as the predictive cue of a reward or aversive stimulus (Matsumoto and Hikosaka, 2009). Little is known in the role of these neurons, although Bromberg-Martin and colleagues suggest they encode motivational salience (Bromberg-Martin et al., 2010).

As mention previously, midbrain DAergic neurons exhibit both phasic and tonic DA release that is underpinned by burst and autonomous firing patterns respectively (Grace and Bunney, 1984a, Grace and Bunney, 1984b, Grace and Onn, 1989, Guzman et al., 2009, Liss et al., 2001, Shepard and Stump, 1999, Overton and Clark, 1997). It has been suggested that phasic DA release is typically associated with rewards and learning, and tonic DA transmission conveys motivation levels (Hamid et al., 2016, Salamone and Correa, 2012). One study found that elevated tonic levels of DA release enhanced performance to earn reward but did not affect Pavlovian learning (Cagniard et al., 2006). Similarly, Beeler and colleagues found changes to tonic DA release didn't affect learning, though it did modulate exploitation of reward learning (Beeler et al., 2010). Additionally, computational models of tonic DA release have also suggested a role in motivation and response vigor (Niv et al., 2007). A recent study found infusion of fluropenthixol, the nonselective DA receptor antagonist, reduces performance during an effort-based choice task and decreased response vigor (Bailey et al., 2018). Taken together, these suggest that tonic DA levels are not required for learning, but influence motivation by affecting performance.

Within the mesolimbic pathway, the ventral pallidum (VP) is among multiple circuits that are known to influence motivation. The VP is composed of GABAergic, and to a lesser extent, glutamatergic and cholinergic neurons (Root et al., 2015), and receives input from the NAc and DAergic input from the VTA (Breton et al., 2019). Additionally, GABAergic VP neurons innervate the VTA and inhibit the activity of these neurons (Root et al., 2015). Activation of D_1 receptors increases the excitability of VP neurons, whilst D_2 receptor activation has both inhibitory and excitatory effects (Clark and Bracci, 2018). D_1 receptor agonist in the VP increased the step-through latency during an inhibitory avoidance learning paradigm, which was abolished by the pre-treatment of a D_1 receptor antagonist (Peczely et al., 2014). Similar findings were observed when investigating D_2 receptor activity during inhibitory avoidance learning, activation of these receptors facilitated avoidance learning (Lenard et al., 2017). Taken together, it suggests D_1 and D_2 receptors facilitate inhibitory avoidance learning.

The VP is innervated by both D1 and D2-MSNs (Gong et al., 1999, Castro et al., 2015, Smith et al., 2009), therefore, it can be modulated indirectly by DA transmission in the NAc. A recent study found the D1-MSNs that innervate the VP are necessary for reward-seeking (Pardo-Garcia et al., 2019). Whilst, activation of D_2 receptors in NAc D2-MSNs decreased the inhibitory transmission in the VP, subsequently, this enhanced motivation as measured by a concurrent choice task (Gallo et al., 2018). As mentioned earlier, the VP innervates the VTA with GABAergic projections (Root et al., 2015). A recent study found that the optogenetic activation of NAc D2-MSN projections to the VP, inhibits the VP and subsequently disinhibits VTA DAergic neurons and enhances the motivational response in animals (Soares-Cunha et al., 2018).

In sum, DA signalling to the NAc conveys an array of information associated with reward-orientated behaviours, which can include contextual information such as reward prediction from environmental cues, the value of the reward and the motivational information to pursue a reward. DA transmission can directly modulate neurons to enhance or attenuate motivation signals. However, DA signalling also modulates regions like the VP indirectly to enhance motivation.

4.1.3   The non – mammalian striatum

Evidence derived from studies of the lamprey suggests that the striatum and the components of the basal ganglia, including the direct and indirect pathways, are conserved in amniotes (Stephenson-Jones et al., 2012, Grillner et al., 2013). Below, I will review the anatomical, genetic and functional studies that support this premise.

4.1.3.1   The lamprey striatum and basal ganglia

The components of the basal ganglia are highly conserved across species, throughout the vertebrate phylogeny, nuclei including the striatum, GPi, GPe and STN have been identified in the lamprey forebrain (Stephenson-Jones et al., 2011, Grillner et al., 2013). The organisation of the lamprey striatum is similar to that of mammals, being composed of both GABAergic and cholinergic neurons (Pombal et al., 1997b). Tracing studies showed the putative pallium receives

GABAergic input from the striatum, and electrophysiological recordings showed that neurons of this region exhibit tonic firing properties that persist in the presence of synaptic blockers, a feature found in the mammalian pallium (Stephenson-Jones et al., 2011). Additionally, the putative STN was identified using IHC and whole-cell recordings, and these glutamatergic neurons exhibit spontaneous firing activity with a post-inhibitory rebound spike (Stephenson-Jones et al., 2011). These are stereotypical features associated with the mammalian STN (Bevan and Wilson, 1999). Furthermore, homologs of the SNr and pedunculopontine nucleus have been identified in lamprey using IHC and whole-cell recordings (Stephenson-Jones et al., 2012). Additionally, DAergic neurons have been identified within the mesencephalic nucleus of the tuberculum posterior (NTP) that are suggested to be homologous to the SNc and VTA DAergic neurons of mammals (Perez-Fernandez et al., 2017). Together, these studies have identified homologous nuclei that make up the basal ganglia. These tracing studies suggests nuclei of the putative basal ganglia have a conserved projectome as that of the mammalian counterparts, this includes the ascending DAergic pathways.

Studies have shown that the lamprey striatum has a similar organisation to that of mammals (Pombal et al., 1997b, Robertson et al., 2014, Robertson et al., 2007). Tracing studies found the lamprey striatum projects to the VP. This study also identified DAergic, serotonin, encephalin and substance P immunoreactive fibres in the VP (Stephenson-Jones et al., 2011). Moreover, lamprey striatal neurons have similar electrophysiological properties to mammalian MSNs such as the presence of pronounced inward rectification, driven by a K_{ir} channel as well as the presence of a low-voltage-activated potassium current that contributes to the long delay to spiking (Ericsson et al., 2011). Ericsson and colleagues also observed spiny dendrites in these neurons and suggested these neurons are homologous to the MSNs (Ericsson et al., 2011).

Further evidence, supporting the conserved anatomy and function of lamprey striatum is DA receptor expression and DA neuron projections. As with mammals, the lamprey striatum also expresses DA receptors, including the D_1 and D_2 receptors (Perez-Fernandez et al., 2014). There are two populations of GABAergic neurons in the lamprey striatum that express either the mammalian

direct or indirect pathway markers, substance P or encephalin, respectively (Stephenson-Jones et al., 2011). The striatum receives ascending DAergic input from the NTP (Pombal et al., 1997a, Pombal et al., 1997b). This suggests the ascending DAergic pathways are conserved between mammals and lamprey. Functional examination of the lamprey striatum have shown that the activation of D_1 receptors on GABAergic neurons in this region increases their excitability (Ericsson et al., 2013b, Ericsson et al., 2013a), whilst activation of D_2 receptors has the opposite effect (Robertson et al., 2012). These findings are similar to mammalian studies of the D1 and D2-MSNs within the mammalian striatum (Surmeier et al., 2007). Together, they suggest that there are functionally conserved direct and indirect pathways in the lamprey basal ganglia.

In mammals, depletion of striatal DA input from the midbrain DAergic neurons of the SNc impairs motor behaviours and generate Parkinson's disease-like symptoms (Dauer and Przedborski, 2003). Similar results have been seen in lamprey with chemogenic ablations of NTP neurons causing depletion of striatal DA and locomotor defects including perturbed initiation of movement, decreased locomotion and duration of swim episodes (Thompson et al., 2008). This suggests the lamprey ascending DAergic neurons are functionally equivalent to the mesostriatal pathway in mammals.

In sum, these studies suggest that the basal ganglia and the role of ascending DAergic input is highly conserved, and perturbed DAergic signalling in lamprey generates similar locomotive phenotypes similar to that of Parkinson's disease models. Thus, the striatum and associated DAergic circuits are highly conserved between lamprey and mammals.

4.1.3.2   The striatal homolog in zebrafish

Although they lack comparable anatomical structures, the zebrafish telencephalon exhibits genetic homology to that of mammals (Wullimann and Mueller, 2004, Wullimann and Rink, 2002, Mueller et al., 2008, Osorio et al., 2010, Wullimann, 2009). The adult zebrafish telencephalon can therefore be divided into the putative pallium (dorsal) and subpallium (ventral) based on differentially expressed genes which include Lhx6, Lhx7, Dlx2a, Tbr2 and GAD67 (Mueller et al., 2008, Ganz et al., 2012, Ganz et al., 2015). By contrast, Lhx6,

Lhx7, Dlx2a and GAD67 are expressed differentially across the subpallium (Mueller et al., 2008). The subpallium can be further subdivided based on the combinational expression of genes which have been defined as striatum, pallidum and septum-like regions (Figure 4:2).

The subpallium is a transient structure, and the striatal region of the subpallium is hypothesised to be homologous to the mammalian structure known as the lateral ganglionic eminence (LGE). The LGE is a transient developmental structure that becomes the striatum after development (Deacon et al., 1994, Olsson et al., 1998). The expression pattern of zebrafish genes in the dorsal subpallium include Dlx2a, Lhx6 and GAD67, corresponds to the mammalian gene expression pattern found in the LGE (Mueller et al., 2008). The pallidum-like regions of the subpallium are found the ventral aspect of the dorsal subpallium and genetic analysis has shown the homologous gene expression of Lhx6, Lhx7, Dlx2a, and GAD67 between that of the zebrafish pallidum and the medial ganglionic eminence (MGE) in mammals (Mueller et al., 2008). These genetic studies have defined the topography of zebrafish subpallium to have homologous regions to the mammalian striatum.
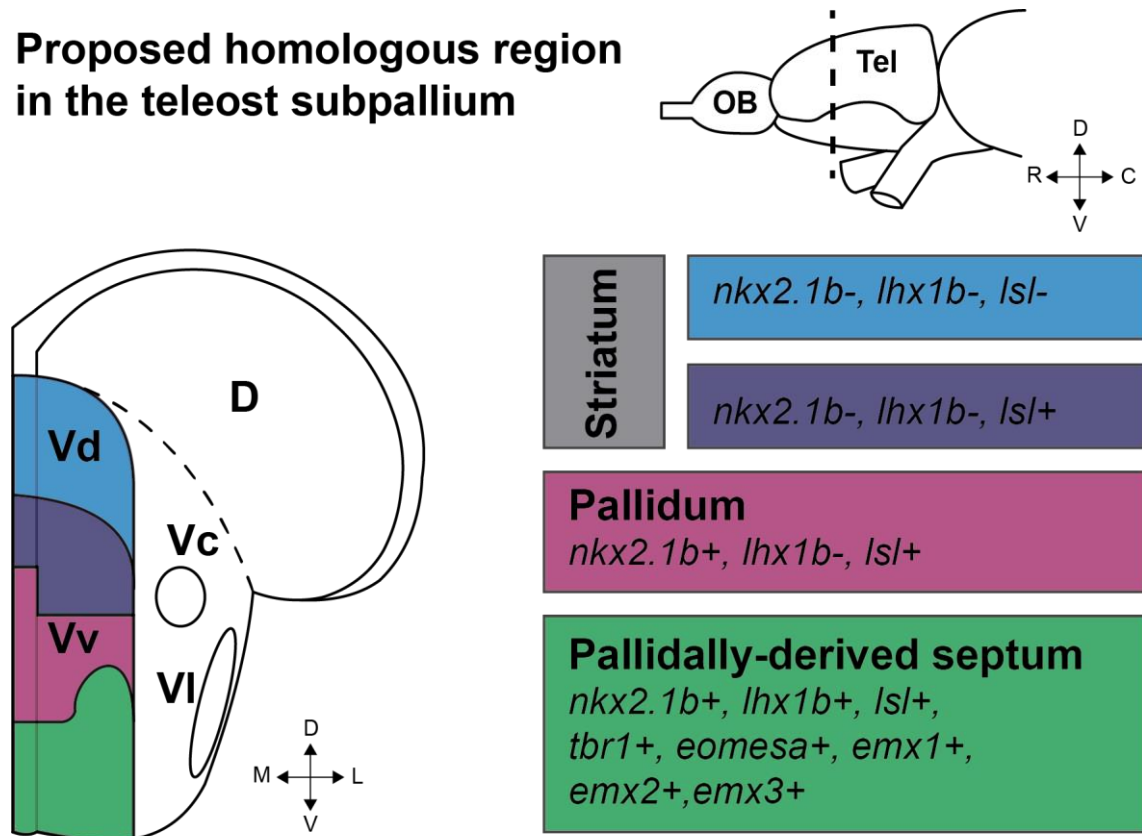
Figure 4:2 Schematic illustration of gene expression across the subdivisions of zebrafish subpallium. Summary of the gene expression in the subpallium of adult zebrafish. Cross-section at the mid-telencephalon level Orientation is indicated in panel; R = rostral, C = caudal, D = dorsal, V = ventral, M = medial and L = lateral. Abbreviation – OB; Olfactory Bulb, Tel; Telencephalon, Vc; central, Vd; dorsal, Vl; lateral, Vv; ventral zones of ventral telencephalon, D; dorsal telencephalon. Redrawn from Ganz et al., (2012).

Anatomic studies have identified clusters of DAergic neurons throughout the zebrafish brain. Two of these, located in the posterior tuberculum, are known as DC2 and DC4 and possess ascending projections that innervate the subpallium (Tay et al., 2011). Based on their projection patterns, it had been previously thought that these neurons are homologous to ascending DAergic projections of both lampreys and mammals (Rink and Wullimann, 2001). These studies have also suggested that the conserved hodology of these neurons could be homologous to the mesostriatal or mesolimbic pathways in zebrafish (Rink and Wullimann, 2002a). However, studies have not been conducted to determine their functional equivalence. As discussed in Chapter 3, there is also a cluster of DAergic neurons in the subpallium. These cells innervate the telencephalon, and

are proposed to be the primary source of DA in the telencephalon (Tay et al., 2011). However, this has yet to be experimentally validated.

In the mammalian and lamprey striatum, GABAergic MSNs can be subdivided on the basis of D_1 receptor and D_2 receptor expression (Robertson et al., 2012, Ericsson et al., 2013b, Levey et al., 1993). The zebrafish brain expresses both D_1 and D_2 receptors, the expression pattern of these receptors have been examined independently (Liu et al., 2007, Boehmler et al., 2004). However, co-expression has not. Therefore, it is currently unknown whether segregated D_1 receptor and D_2 receptor expression is observed in the putative zebrafish striatum, as it is in mammals.

In sum, anatomical and genetic studies of the zebrafish brain suggested genetic homology between the zebrafish forebrain and the mammalian striatum. Hodological studies have suggested there are conserved DAergic projections in zebrafish that could correspond to the putative meso-striatal pathways (Rink and Wullimann, 2001). Nonetheless, no functional or physiological studies have been conducted to support these hypotheses.

4.1.4   Mammalian amygdala

The amygdaloid complex is a structure that is developmentally derived from the pallium and subpallium (O'Connell and Hofmann, 2011). In mammals, this brain region is composed of several interconnected nuclei that are known to be a crucial part of the neural circuitry for emotion, memory, motivation, reward and fear (Gallagher and Chiba, 1996). The heterogeneous nuclei of the amygdala complex can be divided into three groups; the basolateral amygdala, cortical-like and centromedial nuclei but also encompasses the extended amygdala (Sah et al., 2003, Benarroch, 2015). Below, I review the structural and functional studies of the amygdaloid complex and the role of DA signalling in mammals.

4.1.4.1   Basolateral amygdala in mammals

The basolateral nucleus (BLA) is a heterogeneous collection of nuclei, composed of the lateral, basomedial and basolateral nuclei (Yang and Wang, 2017). The BLA is primarily composed of spiny glutamatergic neurons(~80% of the

population)and GABAergic neurons (~20% of the population) (Sah et al., 2003, Duvarci and Pare, 2014, Spampanato et al., 2011). The BLA is innervated by a range of structures including, the thalamus, hippocampus, mPFC midbrain DAergic neurons (Christian et al., 2013, Yang and Wang, 2017, Floresco and Tse, 2007, Rosenkranz and Grace, 1999). However, each BLA nucleus receives input from different regions. The lateral nuclei receives the majority of its input from the thalamus, hippocampus, visual, auditory and somatosensory cortices (Sah et al., 2003, LeDoux, 2007). The basolateral nuclei receive input from hippocampus and the prefrontal cortex (LeDoux, 2007) while the basomedial nuclei receives input from the accessory olfactory tract and the hypothalamus (Sah et al., 2003).

Tracing studies have revealed extensive intra-amygdaloid connections (Sah et al., 2003). There are reciprocal projections between the lateral, basolateral and basomedial nuclei with exception between the basolateral and basomedial nuclei, in which the basomedial nucleus does not innervate the basolateral nucleus (Sah et al., 2003). All three nuclei of the BLA innervate the central amygdaloid nuclei (CeA) (Sah et al., 2003, Yang and Wang, 2017). Examination of BLA output reveals substantial innervation to the medial temporal lobe (LeDoux, 2007). Other studies have shown BLA also innervates the NAc, hypothalamus and extended amygdala (Janak and Tye, 2015, McDonald, 1991, Petrovich et al., 2001).

The BLA has been implicated in reward learning, drug-seeking, fear response and anxiety behaviours, as well as acquisition of conditioned threats (Stamatakis et al., 2014, Fox et al., 2015). Investigations into the role of the BLA in anxiety shows that optogenetic activation of excitatory BLA neurons induces anxiety-like behaviours (Siuda et al., 2016) whilst lesion of the BLA reduces anxiety-like during open field tests (Ranjbar et al., 2017). Evidence supporting the role of the modulation of BLA in anxiety responses comes from studies showing NA in this region promotes anxiety-like behaviours (McCall et al., 2017), whilst depletion of serotonin has the opposite effect (Johnson et al., 2015).

The BLA can modulates circuits such as the NAc, hippocampus and mPFC that are known to be involved in reward learning (Stevenson and Gratton, 2003, Yang and Wang, 2017, Floresco and Tse, 2007). For example, the BLA has been

implicated in Pavlovian conditioning and is required for responding to reward (Cardinal et al., 2002, Sharp, 2017). Lesions to the BLA inhibit cue-induced reinstatement during cocaine self-administration task but not the self-administration for cocaine (See et al., 2003). Additionally, lesions to the BLA blocked the effects of cocaine conditioning, supporting an involvement of the BLA in conditioning. Furthermore, BLA projections to the NAc facilitate reward-seeking behaviours (Ambroggi et al., 2008). In sum, anatomical studies have shown that the BLA receives sensory information, and functional studies have shown the BLA has a role in reward, learning, fear and anxiety behaviours.

4.1.4.2   Mammalian extended amygdala

The extended amygdala is composed of several nuclei that include the CeA and medial amygdaloid nuclei (MeA) and incorporates the bed nucleus of the stria terminalis (BNST) (Ahrens et al., 2018, Shackman and Fox, 2016, Waraczynski, 2016). Morphological and electrophysiological studies suggest the majority of the CeA neurons are GABAergic (Chieng et al., 2006). The CeA can be identified by Lhx6/7, Dlx1/2, GAD67 and Nkx2.1 expression (O'Connell and Hofmann, 2011, Garcia-Lopez et al., 2008). Homologs of these genes are also expressed in the zebrafish pallidum (Ganz et al., 2012) (see subsection 1.7).

The CeA can be divided into its lateral and medial subdivisions (Janak and Tye, 2015). The lateral CeA contains striatal-like MSNs, whilst the medial subdivision contains pallial-like aspiny projection neurons. The lateral aspect of the CeA is innervated by the insular cortex, thalamus, SNc and VTA (Sun et al., 1994, Yasui et al., 1991, Moga et al., 1995, Fallon and Moore, 1978, Veinante and Freund-Mercier, 1998). The medial subdivision receives input from the hypothalamus and periaqueductal gray (PAG) (Fallon and Moore, 1978, Gray and Magnuson, 1992, Veinante and Freund-Mercier, 1998). As mentioned previously, the CeA receives intra-amygdaloid connections from the BLA and serves as a major output of the amygdala (Sah et al., 2003, Yang and Wang, 2017). Anatomical studies have found connections between the lateral and medial subdivisions of the CeA (Sah et al., 2003, Calhoon and Tye, 2015). The main efferent targets of the CeA has been shown to be the hypothalamus, PAG, BNST and modulatory systems including NA and midbrain DAergic circuits (Sah et al., 2003, LeDoux, 2007,

Fadok et al., 2018). In addition to this direct input to the hypothalamus is a polysynaptic pathway that is routed through the BNST (Yamamoto et al., 2018, Lebow and Chen, 2016). It has been suggested the efferent connections influence action selection and influence physiological states (Fadok et al., 2018).

Studies of the CeA and BNST suggest their function is involved in fear and anxiety (Shackman and Fox, 2016, Fox and Shackman, 2019, Newman, 1999, Trimble and Van Elst, 1999). Using functional MRI in humans, activity in the extended amygdala has been shown to be associated with a sustained threat (Torrisi et al., 2018). Whilst this only shows a correlation between amygdala activity and stimulus presentation, partial deletion of the CeA population promotes anxiety as observed by decreased time in the centre of an open arena as well as arms of an elevated plus-maze (Ahrens et al., 2018). Additionally, lesions to the CeA and BNST can attenuate conditioned freezing behaviour as well as impair visual and auditory conditioned startle behaviours (Ahrens et al., 2018, Nader et al., 2001, Zimmerman et al., 2007

, Campeau and Davis, 1995, Hitchcock and Davis, 1986, Hitchcock and Davis, 1987). Moreover, stimulation of the CeA can cause defensive behaviours including freezing (Davis and Whalen, 2000). Together, these studies show that the extended amygdala is active when subjects are presented with threatening stimuli and influence aversive behaviours.

Research into the function of the CeA has also suggested a role in modulation of motivational aspects of reward, appetitive and addictive behaviours (Jennings et al., 2013, Waraczynski, 2006, Koob, 2003, Stamatakis et al., 2014). Whole-brain mapping studies of the rodent brain found that activity in the extended amygdala was associated with predatory hunting, suggesting it may encode motivational values that influence motor output (Comoli et al., 2005). Optogenetic activation of the CeA can enhance incentive motivation to favour reward (Robinson et al., 2014). Moreover, stimulation of the CeA increases attention but also causes freezing behaviour (Davis and Whalen, 2000), whilst inhibition of the CeA decreases freezing (Gozzi et al., 2010). Together, this shows the CeA has a multifaceted role in processing sensory information, and also influencing

behavioural output and decision-making processes that affect fear, reward and motivationally-driven behaviours

The BNST is another component of the extended amygdala that has been suggested to have a role in anxiety and stress responses (Everitt et al., 1999). Evidence supporting this has revealed the BNST is active in response to threat anticipation (Herrmann et al., 2016). Furthermore, optogenetic activation of glutamatergic neurons in the BNST can cause aversive and anxiety-like behaviours while activation of GABAergic neurons in this region elicits rewarding and anxiolytic responses (Jennings et al., 2013). These GABAergic neurons reside in the anteromedial BNST and innervate the VTA, presumably modulating reward and aversion circuits in this region (Kaufling et al., 2017). Together, studies have shown that the activity of the BNST processes threat anticipation, anxiety and stress, which can modulate subsequent behaviours.

4.1.5 The role of dopamine signalling on amygdala function

The amygdala receives a broad DAergic input from the SNc, VTA and retrorubral field (RRF) (Cho and Fudge, 2010, de la Mora et al., 2010). DA receptors have been detected throughout the amygdala, including the BLA, CeA and LA (de la Mora et al., 2010) and D_1 and D_2 receptors are known to be differentially expressed across the amygdaloid nuclei: the BLA expresses a high density of D_1 receptors and a low density of D_2 receptors, whilst the CeA has a low density of D_1 receptors and a high density of D_2 receptors (Perez de la Mora et al., 2012). Other DA receptors such as D_3 and D_4 receptors have also been detected throughout this region (Gurevich and Joyce, 1999, Xiang et al., 2008). Since DA release has been detected in the amygdala by the presentation of aversive stimuli and the administration of addictive drugs such as cocaine (Hurd et al., 1997, Lee et al., 2006), and the disruption of DA transmission to the amygdala can affect this behaviour (Andrzejewski and Ryals, 2016, Fudge and Haber, 2000). It can be assumed DA is an essential modulator of the amygdala. Below, I review the function studies of DA transmission on the amygdaloid complex and behaviour.

4.1.5.1 Dopamine and the basolateral amygdala

As mentioned previously, the BLA has been shown to be involved in fear and anxiety behaviours (Muller et al., 2009). Furthermore, DA signalling in the amygdala can modulate its function, application of a D_1 receptors antagonist within the BLA has an anxiolytic effect and can block fear responses, including freezing and startling behaviours (Ng et al., 2018, Heath et al., 2015, Stevenson and Gratton, 2003). Further studies have shown that DA transmission in the BLA has shown to be involved in fear conditioning. Evidence supporting this comes from studies showing D_1 receptor signalling in the BLA disrupts fear conditioning (Heath et al., 2015) whilst local application of either a D_1 receptor agonist or antagonist impairs fear response suppression during conditioned reward fear safety cue discrimination (Ng et al., 2018). However, modulating D_1 receptor signalling in both the hippocampus and BLA is required for the acquisition of fear conditioning but not consolidation or retrieval of fear memories (Heath et al., 2015). As such, DA signalling to the BLA appears to be involved in modulating anxiety-like behaviours and fear response as well as the learning of fear conditioning.

An examination into the role of D_2 receptor signalling within the BLA has been shown to modulate anxiety and fear behaviours, and specific D_2 receptor antagonism can attenuate freezing responses during a conditioned fear test (de Oliveira et al., 2017). Chemogenic ablation of D_2 receptor expressing DA neurons that innervate the BLA promotes anxiety-like behaviours (Zhang et al., 2017). Additionally, activation of D_2 receptors facilitates fear extinction (Shi et al., 2017). VTA activation of D_2 receptors in the BLA modulates the expression of contextual conditioned freezing (de Souza Caetano et al., 2013). Together, this suggests D_2 receptor signalling in the BLA is involved in evoking aversive behaviours as well as fear-induced conditioning. Therefore, D_2 receptor signalling in these regions may modulate learning.

DA signalling in the amygdala has also been shown to affect decision-making processes and affect risky behaviours. Impulsivity is the impaired control of inappropriate behaviours and is associated with many multiple disordered, including addiction and can perturb decision making. Pharmacological activation

of D_1 receptors in the BLA could increase risky choices, whilst blocking D_1 receptor activity within the BLA by intra-BLA infusion of D_1 receptors antagonist could reduce risky behaviours in rodents (Larkin et al., 2016). Cocaine exposure can reduce impulsive decision making, but BLA injection of the D_1 receptor antagonist SCH23390 could increase impulsivity and application of a D_2 receptor antagonist could reverse the cocaine-induced inhibitory effect on impulsive choice (Li et al., 2015).

4.1.5.2 Dopamine and extended amygdala

The extended amygdala is innervated by DAergic neurons of the VTA, SNc and RRF (Hasue and Shammah-Lagnado, 2002, Cho and Fudge, 2010). Studies have shown the majority of DA fibres in this region innervate the dorsolateral BNST and lateral CeA (Freedman and Cassell, 1994). Similarly, the CeA expresses a very higher density of D_2 receptors compared to D_1 receptors (Perez de la Mora et al., 2012).

Studies have shown that injecting muscimol (a GABA receptor agonist) into the CeA attenuates anxiety-like behaviours (Moreira et al., 2007). VTA stimulation can activate the CeA (Gelowitz and Kokkinidis, 1999); therefore DA transmission can also modulate CeA activity. DA modulation of the CeA has been shown to modulate aversive learning, D_1 receptor signalling in the CeA is involved in the acquisition and expression of fear conditioning (Guarraci et al., 1999a, Guarraci et al., 1999b). Blocking D_2 receptor signalling within the CeA prior to fear conditioning attenuates conditioned freezing behaviours (Guarraci et al., 2000). Together, this suggests DAergic signalling in the CeA is required for fear conditioning.

DA signalling in the CeA can modulate anxiety-like behaviours, modulation of the CeA activity with D_1 receptor agonist or antagonist can have an anxiogenic or anxiolytic effect, respectively (de la Mora et al., 2010). Antagonism of D_1 receptors in the CeA can attenuate fear response such as freezing and startling (Lamont and Kokkinidis, 1998, Guarraci et al., 1999a, Guarraci et al., 1999b). Whilst antagonism of D_2 receptors in the extended amygdala can induce a fear response to threats (De Bundel et al., 2016). Injection of D_2-like receptor antagonists in the CeA evoked increase burying behaviour (Perez de la Mora et

al., 2008). Overexpression of D_1 receptor on amygdaloid neurons has been associated with higher anxiety levels in rats (Rebolledo-Solleiro et al., 2016). Nicotine can trigger an anxiogenic-like response in rats, but the modulation of DA signalling by D_1 receptors and D_2 receptor antagonists attenuates anxiogenic-like behaviours (Zarrindast et al., 2013). Together, these findings show that DA receptor activation modulates anxiety-like behaviours and fear responses. Research by de la Mora and colleagues has suggested that the CeA D_1 receptor activity facilitates behaviours associated with threat recognition, whilst D_2 receptors have a role in adaptive responses to deal with threatening stimuli (de la Mora et al., 2010).

DA signalling within the extended amygdala has been shown to modulate attention and motivation. Chemogenic lesions to the CeA caused animals to have reduced sustained performance in multiple-choice reaction time tasks and other attention test paradigms (Holland et al., 2000). Disruption of DA signalling from the SNc to the CeA perturbed attention and learning (Lee et al., 2006). This suggests DA transmission from the midbrain is required for attention-related activity of the CeA. D_1 receptor antagonism reduced motivational and attentional performance (Smith et al., 2015). Loss of DA input to the CeA or the application D_1 receptor antagonists in the CeA disrupts rodent disengagement behaviour (the ability to stop an ongoing behaviour to interact with a new stimulus) (Smith et al., 2013). Together, DA transmission to the CeA can modulate attention and motivation, and D_1 receptors activity is required for motivation.

DA signalling in the NAc is known to convey rewards and perturbed DA signalling can cause addictive behaviours. Studies have implicated DA signalling to the CeA to be involved in conveying rewards (Douglass et al., 2017b, Lammel et al., 2014, Smith et al., 2015). Blocking D_1 receptor activity reduces the rewarding effects of cocaine, suggesting that DA transmission in the CeA has a role in rewarding behaviours (Laszlo et al., 2018). Blocking of DA transmission via D_1 and D_2 receptor antagonism can perturb the reinforcing effects of neurotensin and block conditioned place preference (Laszlo et al., 2018). Activating D_2 receptor in the CeA can reduce cue evoked drug-seeking behaviours as well as self-administration of cocaine, however, D_1 receptor agonist was not able to block cue evoked drug-seeking behaviours (Thiel et al., 2010). Together, these studies

suggest DA transmission in the CeA conveys rewards as well as being required for the motivational aspect of drug-seeking behaviours. It has been suggested that CeA D_1 receptor activation mediates the attentional functions regarding visual cue detection (Smith et al., 2015).

Evidence also suggests DA modulation of the CeA play a role in impulsive behaviours (Dalley et al., 2008, Trifilieff and Martinez, 2014). Impulsivity is described as the tendency to undertake risky behaviours and is associated with addiction. Loss of D_2 receptors expressed in the CeA can cause an increase in impulsive behaviour, restoration of D_2 receptors can attenuate impulsivity (Kim et al., 2018). Optogenetic activation of D_2 receptors expressed by the GABAergic neurons of the CeA can attenuate impulsive behaviours by inhibiting BNST circuitry (Kim et al., 2018). These results show that DA signalling can directly modulate the extended amygdala and impulsive behaviours.

In sum, the extended amygdala is involved in many behaviours including motivation, attention, fear and anxiety as well as the pursuit of reward. DA signalling to the extended amygdala can modulate the CeA and BNST activity and related behaviours.

4.1.6   The homologous zebrafish extended amygdala

Genetic analysis of the subpallium revealed the supracommissural (Vs) and postcommissural (Vp) regions of dorsal/posterior aspect of the subpallium of the ventral telencephalon has been suggested to be equivalent to the extended amygdala, an area in mammals composed of the BNST and the medial amygdala (O'Connell and Hofmann, 2011) (Figure 4:3A). The differential expression pattern of *nkx2.1b, lhx1* and *lsl* in the caudal aspect of the adult zebrafish subpallium suggest homologous regions to the tetrapod telencephalon (Figure 4:3B/C) (Ganz et al., 2012). This differential gene expression within the ventral subpallium can be divided up into homologous regions, including the dorsal and ventral central amygdala and the BNST (Ganz et al., 2012). The medial amygdala and accessory olfactory systems have been identified in the ventral telencephalon (Biechl et al., 2016).

Genetic studies into the zebrafish subpallium have suggested that this region can be divided up into multiple areas that are homologous to structures including the striatum, pallidum and amygdala (Figure 4:3). Whole-brain mapping has revealed that the subpallium is active when zebrafish are exposed to both food rewards and amphetamines (Randlett et al., 2015, von Trotha et al., 2014). It has also been shown that the subpallium is active when zebrafish are exposed to aversive stimuli (Randlett et al., 2015). Research also suggests that the zebrafish medial amygdala has a role in kin recognition (Biechl et al., 2016). Together, the limited behavioural studies suggest the zebrafish subpallium processes information conveying reward and aversion.
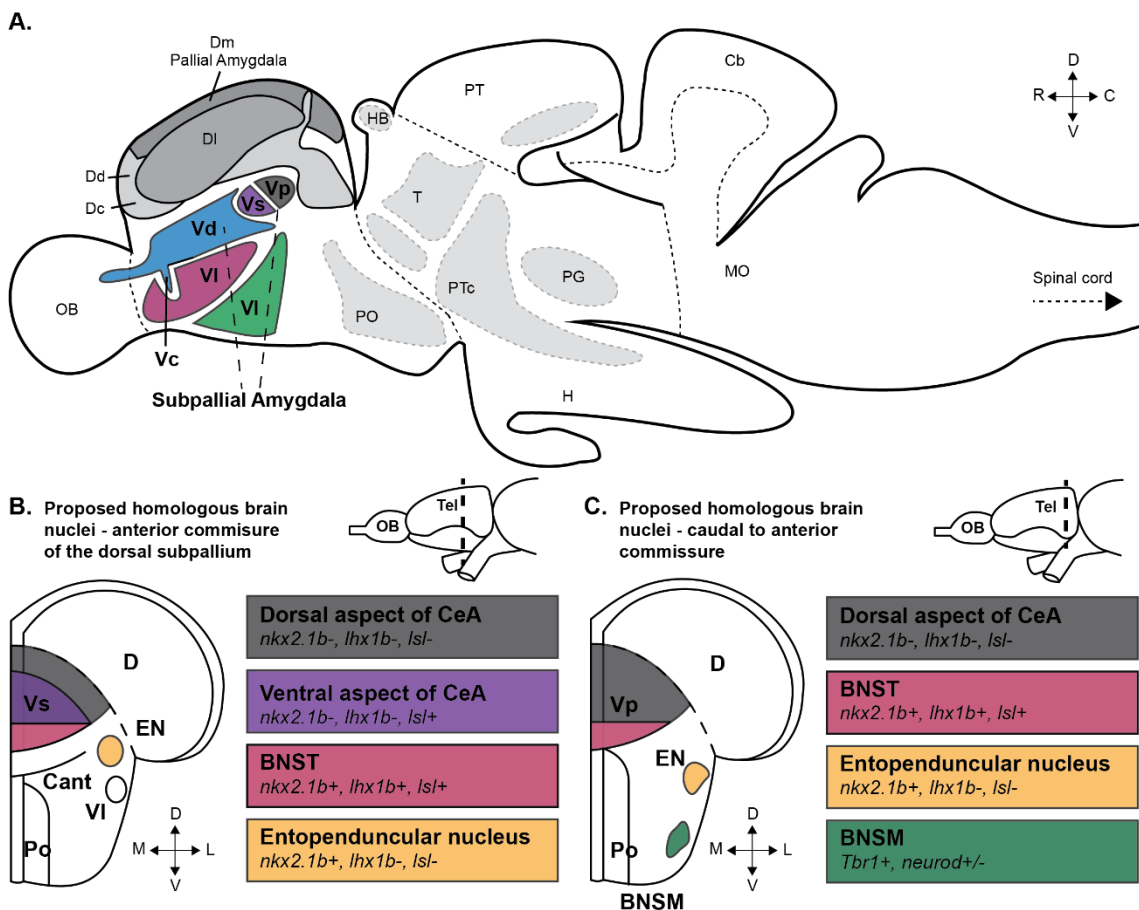
Figure 4:3 Gene expression pattern of the zebrafish putative amygdala. A: Schematic illustration of the sagittal cross-section of the zebrafish amygdala. **B:** Coronal cross-section of the zebrafish subpallium at the anterior commissure, highlighting the CeA, BNST and entopeduncular nucleus and the gene expression pattern. **C:** Illustration of the coronal section of the subpallium posterior to the anterior commissure, highlighting the gene expression the CeA, BNST, Entopenduncular nucleus and BNSM. Orientation is indicated in panel; R

= rostral, C = caudal, D = dorsal, V = ventral, M = medial and L = lateral. Abbreviation: D; Dorsal telencephalon, Dc; central, Dd; dorsal, Dl; lateral, Dm; medial zones of dorsal telencephalon. Hb; habenular, Cb; Cerebellum, MO; Medulla, H; Hypothalamus, T; Thalamus, Tel; telencephalon, PO; preoptic region, PTc; posterior tuberculum, OB; olfactory bulb. Vc; central, Vd; dorsal, Vl; lateral, Vp; postcommissural, Vs; supracommissural, Vv; ventral zones of ventral telencephalon. Adapted from Ganz et al., (2012), and Perathoner et al., (2016).

4.1.7   Dopamine input to the putative amygdala of zebrafish

The zebrafish subpallium receives DA input from two sources; local DAergic neurons within the subpallium, and the DC2/4 group in the posterior tuberculum (Tay et al., 2011). In larval zebrafish, subpallial DAergic neurons are located at the boundary of subpallium and pallium. In adult zebrafish, these neurons are found at the boundaries of the central (Vc), dorsal (Vd) and ventral (Vv) zones of the ventral telencephalon (adult subpallium) of the rostral subpallium and within the supracommissural (Vs) and postcommissural (Vp) zones of the ventral telencephalon (Yamamoto et al., 2010a). The subpallial DAergic neurons arbourise extensively throughout the telencephalon, and it is suggested these neurons are the primary source of DA to telencephalon (Tay et al., 2011). However, there have been no studies conducted to determine the function of the subpallial DAergic neurons to the subpallial amygdala structures.

The second population of DAergic neurons that project to the subpallium was identified by Rink and Wullimann, who found ascending DAergic projections from the DDNs (Rink and Wullimann, 2004, Rink and Wullimann, 2002a, Rink and Wullimann, 2002b). Selective ablation of DC2/4 neurons affects locomotion, and it has been suggested these are functionally homologous to the A11 DAergic cluster (Tay et al., 2011, Jay et al., 2015). A study investigating the projectome of zebrafish DAergic neurons found DC2/4 superficially innervate the ventral aspect of the subpallium (Tay et al., 2011). Since the putative amygdala exists in the dorsal aspect of the subpallium (Ganz et al., 2012), the DC2/4 neurons do not innervate this region. However, this study was conducted in 4 dpf fish and these neurons could still be developing. Unfortunately, the morphology of these neurons has not been studied in older fish. Additionally, their functional role in motivation, reward or aversion has not been examined.

4.2 Aims and Objectives

Previous anatomical and genetic studies suggest that the zebrafish subpallium is homologous to striatal and amygdaloid structures. If this is indeed the case, subpallial DAergic neurons could provide a local source of DA that is functionally equivalent to that originating from the SNc and VTA in mammals. I hypothesise that the subpallial DAergic neurons are functionally equivalent to the mammalian midbrain DAergic neurons and have a role in locomotion, anxiety and foraging. In this chapter, I aim to address this hypothesis by laser ablating these neurons and studying the behavioural effects in early-stage zebrafish. The data presented in this chapter suggests that subpallial DAergic neurons have a key role in regulating foraging behaviours and therefore, share functional roles with VTA neurons in mammals.

4.3   Results

4.3.1   Targeted laser ablation of subpallial dopaminergic neurons

First, I sought to determine if subpallial DAergic neurons can be targeted for selective laser ablation (see section 2.9). To this end, I used Tg(ETvmat2:GFP) fish in which aminergic neurons, including DA neurons of the subpallium, can be visualised from 2 dpf (Wen et al., 2008, Mahler et al., 2010). Previous immunohistochemistry I performed (see section 3.3.1) revealed the number of subpallial DAergic neurons does not change from 3 dpf onwards. Therefore, I asked whether targeted ablation by laser of the subpallial GFP positive neurons at 3 dpf was sufficient to reduce the number of subpallial TH positive neurons at later larval stages. Zebrafish subpallial DA neurons were ablated (see section 2.9 for methods; Figure 4:4A1, B1).

To confirm that the ablation method was successful, fish were raised to 5 dpf before fixation and processing for anti-TH immunohistochemistry (see subsection 2.7.1). This revealed a loss of TH positive neurons within the subpallium at 5 dpf (Figure 4:4A2, B2). These findings show that targeted laser ablation of GPF-positive subpallial DAergic neurons cells at 3 dpf is sufficient to cause selective loss of these cells at 5 dpf. A summary illustration of the selective ablation of subpallial DAergic neurons can be observed in Figure 4:4D.

A.

B.

C.   **D.**
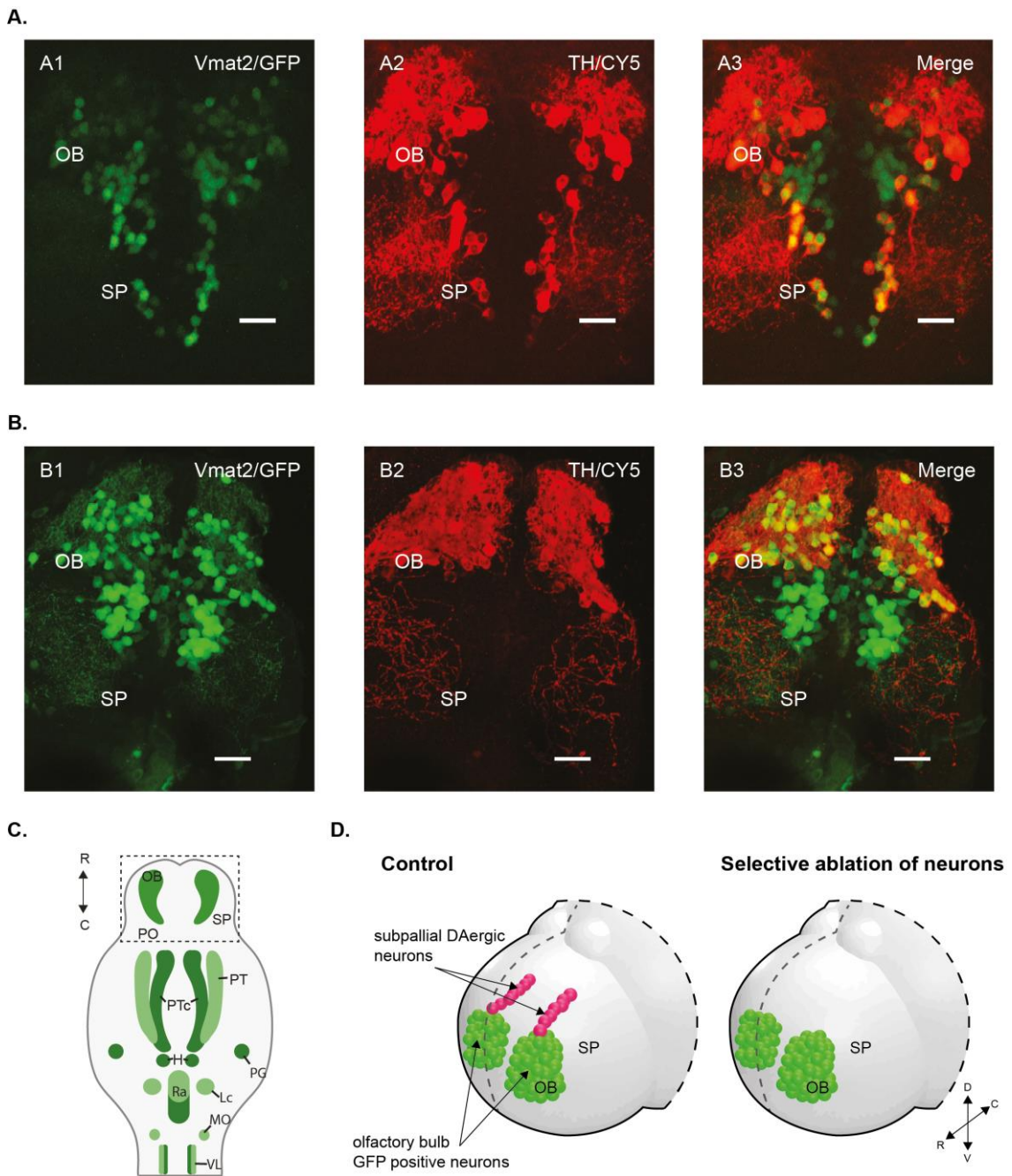
Figure 4:4 Subpallial DAergic neurons can be selective ablated in larval zebrafish. A: Representative confocal images of the subpallium (dorsal view aspect) showing VMAT2/GFP expression (A1), TH immunohistochemical staining (A2) and merged channels (A3) of a control zebrafish at 5 dpf. Orientation is indicated in panel **C. B:** Confocal images of the subpallium in zebrafish subjected to selective ablation, with VMAT2/GFP expression (B1), TH immunohistochemical staining (B2) and merged channels (B3). Orientation is indicated in panel **C. C:** Schematic overview of larval zebrafish brain (dorsal) showing the distribution of Vmat2 expression in ETvmat2:GFP fish. Dash line represents region of focus in confocal images. Orientation: R = rostral and C = caudal. **D:** Schematic 3D illustration of the telencephalon of control zebrafish (left) and the telencephalon with the selective loss of subpallial DAergic neurons (right). Green neurons represent the olfactory bulb Vmat2 positive cells. Red

neurons represent the subpallial DAergic neurons. Orientation is indicated in panel (**A**); R = rostral, C = caudal, D = dorsal and V = ventral. Abbreviations; olfactory bulb (OB), subpallium (SP), preoptic (PO), posterior tuberculum (PTc), hypothalamus (H), pretectum (PT), locus coeruleus (LC), raphe nucleus (RA) and medulla oblangata (MO). Scale bar = 20μm.

4.3.2 Effects of subpallial dopaminergic neuron ablation on locomotion

Next, I sought to determine the behavioural effects of ablating subpallial DAergic neurons on motor behaviour. If subpallial DAergic neurons are homologous to the SNc, then ablating these cells should generate locomotive deficits. To determine if this was the case, free-swimming behaviour was studied in ablated larvae at 5 dpf. At this stage swimming behaviour is characterised by 'beat-glide' swimming which comprises brief bouts of tail beating (beat periods) separated by bouts of inactivity (glide periods) (Saint-Amant and Drapeau, 1998, Buss and Drapeau, 2001). Fish in the control (n_{fish} = 18) and ablated (n_{fish} = 14) conditions exhibited robust beat-glide swimming behaviour (Figure 4:5A) and analysis revealed no significant differences in distance travelled (control = 736.9 ± 463 mm, n_{fish} = 18, ablated = 665.6 ± 411.1 mm, n_{fish} = 14, p = 0.6535, Unpaired t test; Figure 4:5B/D) or swim velocity (control =1.99 ± 1.07 mm/s, n_{fish} = 18, ablated = 1.71 ± 0.98 mm/s, n_{fish} = 14, p = 0.4547, Unpaired t test; Figure 4:5C).

Examination of the beat episodes revealed the proportion of time spent performing beat swimming episodes was similar in control and ablated fish (control= 17.27 ± 13.66%, n_{fish} =18, ablated = 16.56 ± 12.08%, n_{fish} = 14, p = 0.8833, Unpaired t test; Figure 4:6A). Further analysis of this behaviour showed there was no difference in beat durations (control = 0.40 ± 0.15s, n_{fish} = 18, ablated = 0.39 ± 0.11, n_{fish} = 14, p = 0.8534, Mann-Whitney U; Figure 4:6B), peak velocity during beat bouts (control = 15.14 ± 7.29 mm/s, n = 18, ablated = 12.48 ± 4.51 mm/s, n = 14, p = 0.2563, Unpaired t test; Figure 4:6D) or glide duration (control = 2.91 ± 2.77s, n_{fish} = 18, ablated = 1.71 ± 1.12, n_{fish} = 14, p = 0.5118, Mann-Whitney U; Figure 4:6C). Together, these results suggest that subpallial DAergic neurons do not modulate basic parameters of free-swimming behaviour in larval.

A.
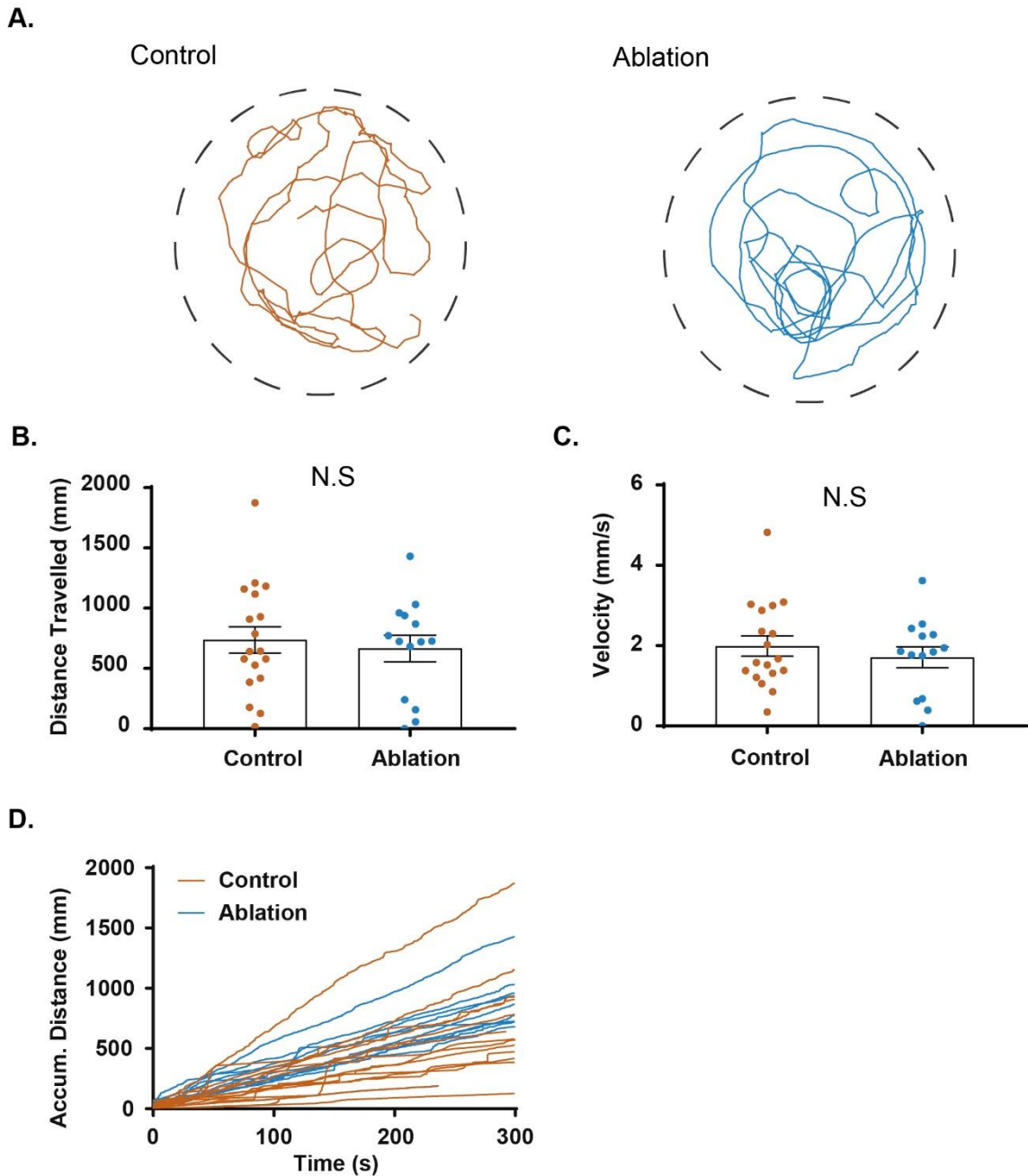
Figure 4:5 Selective loss of subpallial DAergic neurons does not affect locomotion output. A: Representative swimming trajectories of control (left panel) and ablated (right panel) zebrafish at 5 dpf recorded over a 5-minute period. **B:** Box and whisker plot comparing the total distance travelled over 5 minutes of control and ablated fish. **C:** Comparison of the mean swimming velocity of larval zebrafish. **D:** Cumulative distance that individual control (orange) and laser ablated (ultramarine) fish travelled. N.S, no significant difference.
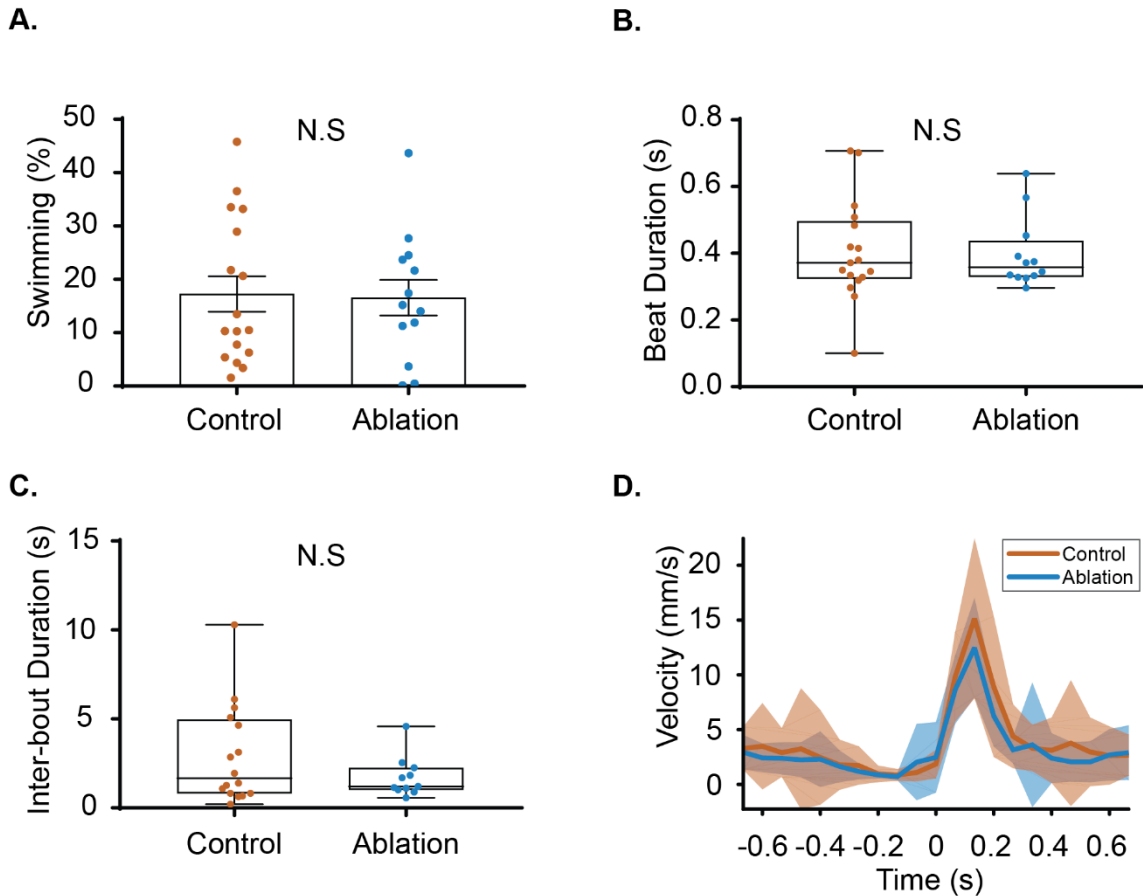
Figure 4:6 Beat-glide swimming kinetics are not affected by the loss of subpallial DAergic neurons. A: Box and whisker plots comparing the percentage of time spent exhibiting beat-glide swimming over 5 minutes of observed swimming. **B:** Comparison of average beat duration of bouts of beat glide swimming. **C:** Comparison of the mean inter-bout duration between episodes of beat-glide swimming. **D:** Plots of average velocity and distribution as a function of time for bouts of beat glide swimming. Zero (0s) marks the onset of the beat event, with a sharp increase in velocity and subsequent decline to baseline during glide events. N.S, no significant difference.

4.3.2.1 Effects of subpallial dopaminergic neuron ablation on the optomotor response

To this point, I have shown the subpallial DAergic neurons do not influence free-swimming behaviour in larval zebrafish. I next asked whether these neurons are involved in sensorimotor integration. The optomotor response (OMR) is an innate behaviour exhibited by zebrafish (Portugues and Engert, 2011) that comprises locomotion in response to a whole-field moving stimulus, such as gratings (Neuhauss et al., 1999, Portugues and Engert, 2011, Roeser and Baier, 2003). Upon presentation of grating stimuli, zebrafish will change orientation and swim in the same direction as the stimulus moves (Figure 4:7). To examine the OMR, zebrafish were placed in an arena that was suspended in a rotating drum and exposed to grating moving in alternating directions and speed.
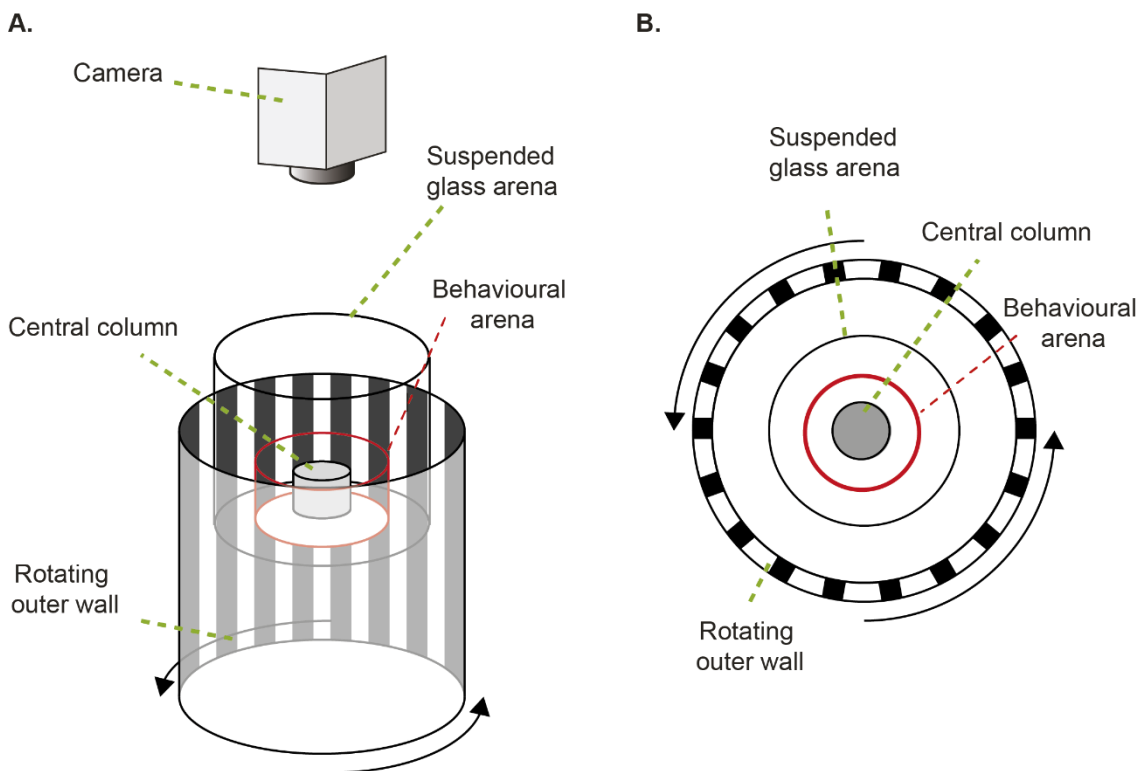
Figure 4:7 Schematic illustration of OMR experimental equipment. A: Larval zebrafish were placed in a glass arena (red outline) suspended on a central opaque column. A digital video camera was placed overhead. The glass arena was suspended in a rotating wall patterned with a black and white striped grating. **B:** Aerial view of equipment, showing outer rotating wall, suspended glass arena and the inner behavioural arena (red outline) with a central column.

When exposed to grating stimuli, the OMR was observed in both control and ablated fish (Figure 4:8A). Closer examination revealed that control and ablated larvae spent a similar proportion of time performing the OMR, regardless of stimulus direction or speed (see Table 4.1 Two-way ANOVA of Time spent performing OMR). Analysis of swimming velocity showed the fish swam at similar velocities regardless of stimulus speed (Figure 4:8B; see Table 4.2 for two-way ANOVA analysis). Furthermore, ablation did not affect distance swum regardless of stimulus speed (Figure 4:8C; see Table 4.3 for two-way ANOVA analysis). Together this data suggests that selective loss of subpallial DAergic neurons does not affect the processing of the visual information and the subsequent modulation of during OMR behaviour.
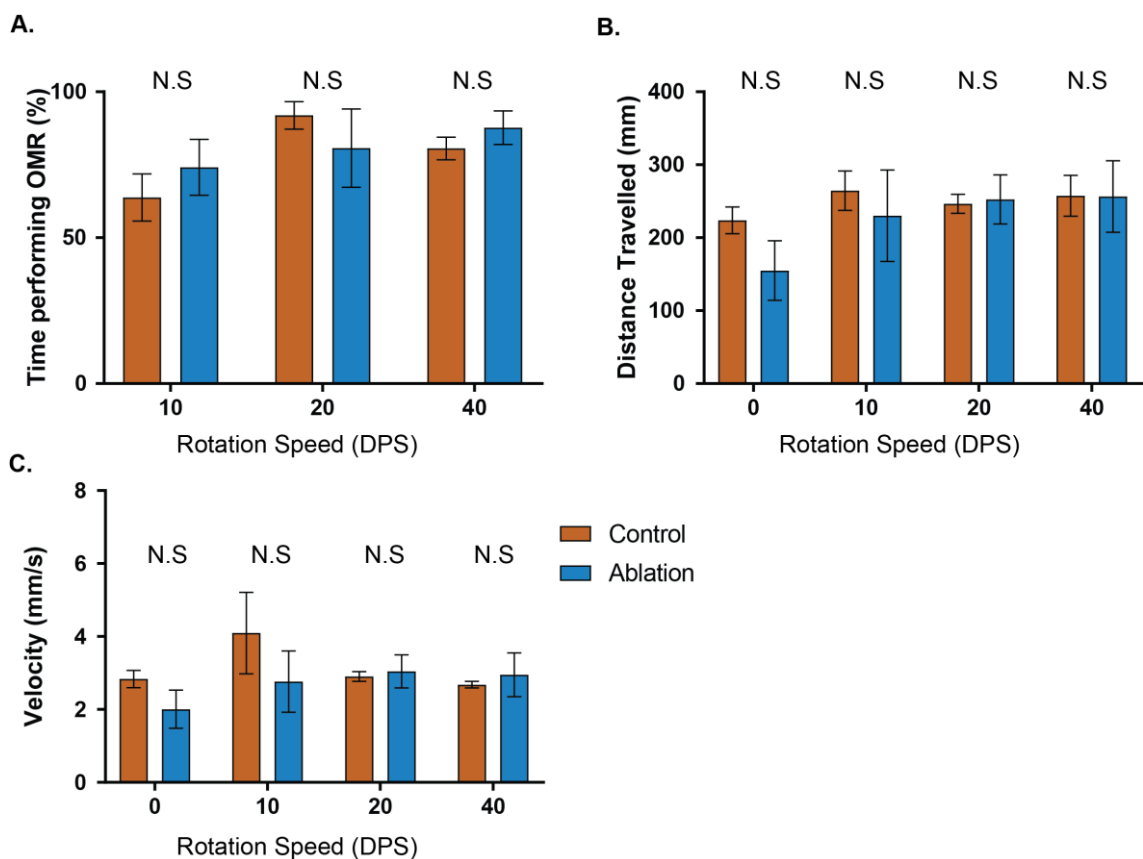
Figure 4:8 Selective loss of subpallial DAergic neurons does not affect OMR. A: Bar chart comparing the percentage of time zebrafish larvae performed OMR to various stimuli. **B:** Bar chart showing the average velocity larval zebrafish swam when presented with alternating direction grating stimuli that varied in

speed. **C:** Bar chart showing the distance travelled when zebrafish were presented with grating stimuli that varied in speed.

Table 4.1 Two-way ANOVA of Time spent performing OMR

	DF	MS	F (DFn, DFd)	P value
Interaction	2	323.6	F (2, 16) = 1.044	P=0.3749
Speed	2	858.1	F (2, 16) = 2.768	P=0.0928
Condition	1	31.24	F (1, 8) = 0.1413	P=0.7167
Residual	16	310		

Table 4.2 Two-way ANOVA of OMR evoked swim velocity

	DF	MS	F (DFn, DFd)	P value
Interaction	3	1.429	F (3, 24) = 1.012	P=0.4048
Speed	3	1.67	F (3, 24) = 1.183	P=0.3372
Condition	1	1.829	F (1, 8) = 0.592	P=0.4638
Residual	24	1.412		

Table 4.3 Two-way ANOVA of OMR evoked swimming distance

	DF	MS	F (DFn, DFd)	P value
Interaction	3	2850	F (3, 24) = 0.9722	0.4221
Speed	3	9358	F (3, 24) = 3.193	0.0417
Condition	1	5781	F (1, 8) = 0.4628	0.5155
Residual	24	2931		

4.3.3 The effects of subpallial dopaminergic neuron ablation on anxiety-like behaviours

It has been proposed that the dorsal subpallium is functionally equivalent to the extended amygdala and therefore mediates anxiety and fear-like behaviours (Perathoner et al., 2016, von Trotha et al., 2014, O'Connell and Hofmann, 2011). Zebrafish larvae exhibit multiple anxiety-like behaviours, including thigmotaxis; the avoidance of open fields; and an aversion to dark environments (Bai et al., 2016, Maximino et al., 2011, Maximino et al., 2010). Thigmotaxis is an evolutionarily conserved behaviour and is commonly used to assess anxiety (Simon et al., 1994). Examination of thigmotaxis behaviours in 5 dpf zebrafish of control (n_{fish} = 20) and ablated (n_{fish} = 11) groups. The behaviour was examined in an open field test in both light and dark conditions (see section 2.10 for methodology). Analysis of the swimming behaviour revealed that both groups exhibited a preference for the arena wall and dark conditions (Figure 4:9B). Moreover, in agreement with the literature (Schnorr et al., 2012), fish spend more time performing thigmotaxis in the dark than in the light (see Table 4.4 for two-way ANOVA, P < 0.0001). Finally, control and ablated zebrafish spent similar amounts of time performing thigmotaxis whilst in the illuminated arena or the darken arena (see Table 4.5 for Sidak multiple comparison). This finding suggests that zebrafish anxiety-like behaviours are not modulated by subpallial DAergic neurons.

Exposing larval zebrafish to anxiolytic stimuli can increase swimming distance and velocity (Liu et al., 2016, Peng et al., 2016). Whilst thigmotaxis was not affected by the loss of subpallial DAergic neurons, I wanted to assess the swimming behaviour when zebrafish were exhibiting thigmotaxis. To do this, locomotion was assessed as in section 4.3.1. Analysis of swimming velocity showed that the darkened environment caused zebrafish to swim at a higher velocity (Figure 4:9C, see Table 4.6 for two-way ANOVA, P < 0.0001). However, ablating subpallial DAergic neurons had no effect on swim velocity (see Table 4.7 for Sidak multiple comparison analysis). Analysis of the distance swam revealed that luminosity had no effect on cumulative distance swam over a 5-minute period (Figure 4:9D, see Table 4.8 for two-way ANOVA). Additionally, loss of subpallial

DAergic neurons did not affect swimming distance (see Table 4.9 for Sidak multiple comparison analysis).
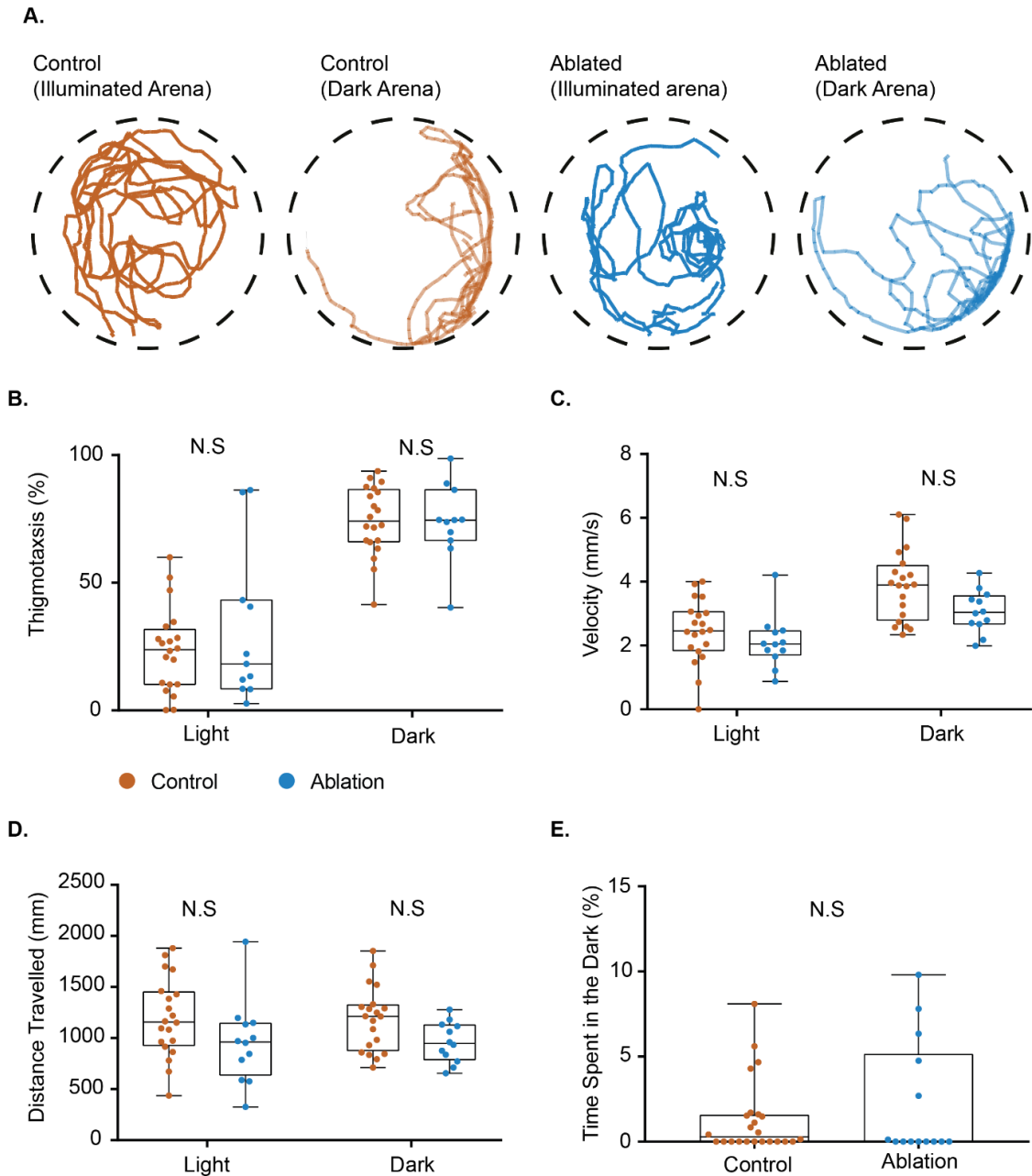
Figure 4:9 Thigmotaxis is not affected by the loss of subpallial DAergic neurons. A: Swimming trajectories of 5 dpf zebrafish in a 55mm diameter dish. Left to right; control illuminated arena, control dark arena, ablated illuminated arena and ablated dark arena. **B:** Box and whisker plot comparing the percentage of time spent performing thigmotaxis (swimming within 5mm of outer edge). **C:** Box and whisker plots comparing the swimming velocities of control and ablated fish during light and dark environments. **D:** Comparison of distance swam in light

and dark environments. **F:** Comparison of control and ablated fish performing place preference. N.S, no significant difference.

To further test the role of subpallial DAergic neurons in anxiety-like behaviours control and ablated fish were subjected to a place preference assay. Larval zebrafish exhibit preference for illuminated environments (Mathur et al., 2011). Here preference for darkened or well-lit areas of an arena was quantified. Subsequent analysis showed both control and ablated fish exhibited similar preferences for the illuminated side of the arena (control = 1.32 ± 2.16%, n_{fish} = 24, ablated = 2.25 ± 3.47%, n_{fish} = 14, p = 0.987, Mann-Whitney U, Figure 4:9E). Together, these findings show that subpallial DAergic neurons are unlikely to modulate anxiety-like responses.

Table 4.4 Two-way ANOVA analysis of thigmotaxis behaviour

	DF	MS	F (DFn, DFd)	P value
Interaction	1	231.8	F (1, 29) = 0.8604	0.3613
Luminosity	1	31167	F (1, 29) = 115.7	<0.0001
Condition	1	171..2	F (1, 29) = 0.4088	0.5276
Residual	29	269.4		

Table 4.5 Time performing thigmotaxis - Sidak multiple comparison

Control - Ablation	Diff. in mean	DF	P value
Light	-7.515	58	0.4888
Dark	0.5681	58	0.9958

Table 4.6 Two-way ANOVA analysis of swimming velocity during thigmotaxis

	DF	MS	F (DFn, DFd)	P value
Interaction	1	0.7993	F (1, 30) = 1.239	P=0.2745
Luminosity	1	21.45	F (1, 30) = 33.26	P<0.0001
Condition	1	4.779	F (1, 30) = 4.09	P=0.0521
Residual	30	0.645		

Table 4.7 Sidak analysis of swimming velocity during thigmotaxis

Control - Ablation	Diff. in mean	DF	P value
Light	0.3336	60	0.566
Dark	0.7953	60	0.051

Table 4.8 Two-way ANOVA analysis of the effect of luminosity on distance swam

	DF	MS	F (DFn, DFd)	P value
Interaction	1	779.4	F (1, 30) = 0.01052	P=0.9190
Luminosity	1	156.2	F (1, 30) = 0.002107	P=0.9637
Condition	1	824492	F (1, 30) = 5.224	P=0.0295
Residual	30	74115		

Table 4.9 Sidak analysis of the effect of luminosity on distance swam

Control - Ablation	Diff. in mean	DF	P value
Light	241.7	60	0.1101
Dark	227.2	60	0.1400

4.3.4 Effects of subpallial dopaminergic neuron ablation on foraging behaviours

Recent whole-brain activity mapping techniques have shown that neurons of the subpallium are activated in response to prey and DAergic drugs such as amphetamine (Randlett et al., 2015, von Trotha et al., 2014). This suggests that the subpallium may have a role in mediating reward and feeding behaviour. To determine if this was the case, I asked whether selectively ablating subpallial DAergic neurons affects foraging in larval fish. To do this, I examined responses of ablated fish to the presence of rotifers. Zebrafish exhibit foraging from 4 dpf, which is defined by complex locomotive behaviours with the integration of visual stimuli to pursue prey (Semmelhack et al., 2014, Nikolaou and Meyer, 2015, Muto and Kawakami, 2013). Larval zebrafish (5 dpf) were examined prior to experiments to determine if their mouths were close and not capable of feeding at this age. Zebrafish foraging behaviour is composed of several manoeuvres such as re-orientation towards prey (J-turn), prey tracking (eye convergence), an approach swim (striking) and capture event (Gahtan et al., 2005, Bianco et al., 2011a, Nikolaou and Meyer, 2015). Control zebrafish exhibited all components of foraging behaviours, including reorientation, an approach swim but failed to collide with prey (Figure 4:10A). These fish also initiated capture behaviour but were unable to complete this manoeuvre (bite; Figure 4:10B) as their mouths had not opened by this stage of development.
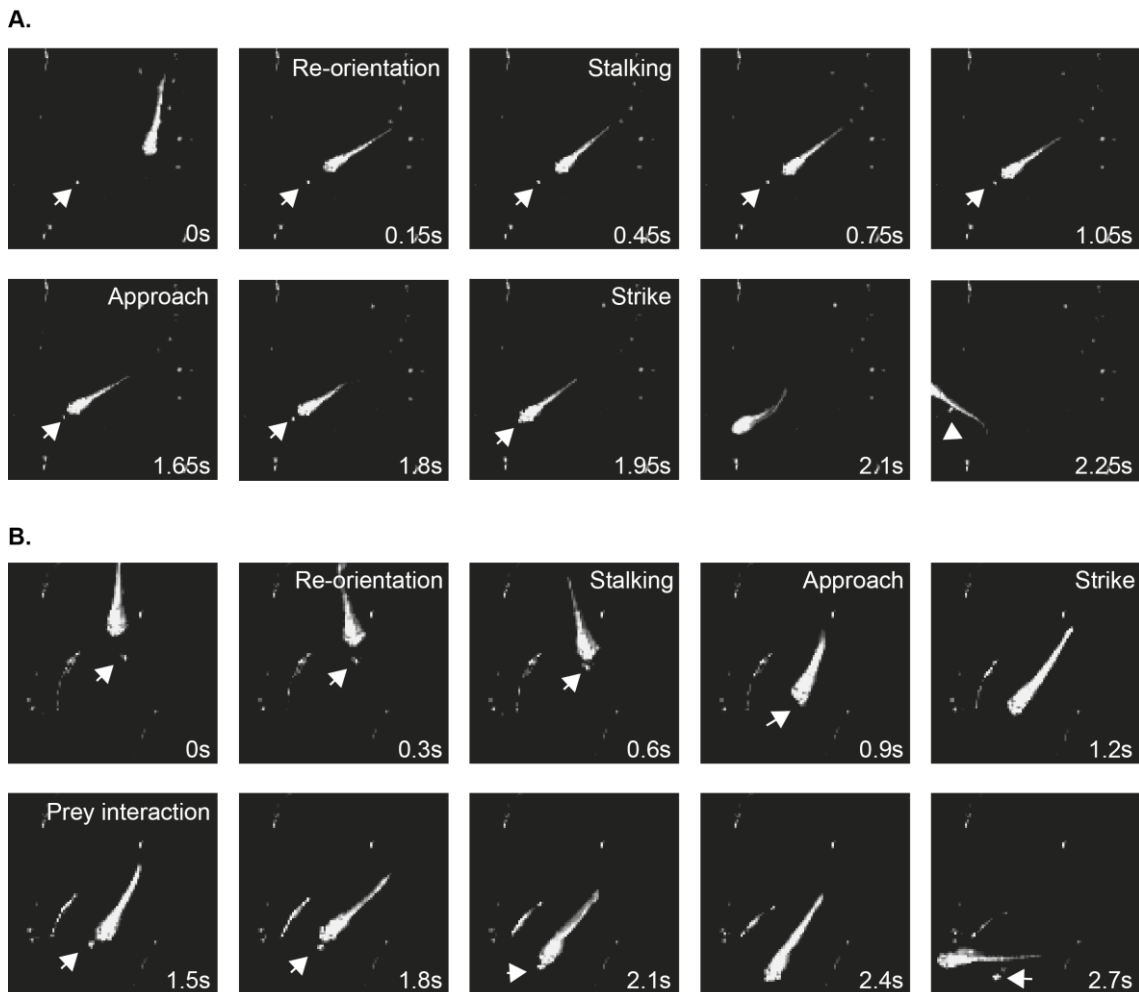
Figure 4:10 Examples of swimming manoeuvres during foraging at 5 dpf.
A-B: Image sequence of zebrafish performing foraging behaviours. **A:** Image sequence of a control zebrafish exhibiting a striking manoeuvre towards live prey. **B:** Consecutive images of a control zebrafish exhibiting 'prey capture' manoeuvres. Arrows denote the target prey.

Examination of foraging behaviour revealed that 77% of control fish exhibited foraging behaviours, whilst only 16% of ablated fish showed foraging behaviours (Chi-square test, 74.79, df = 1, z = 8.648, p = 0.0001, Figure 4:11a). Analysis of the striking manoeuvres showed that, when compared to controls, ablated fish exhibited a reduced strike rate (control = 0.20 ± 0.15 per minute, $n_{fish} = 24$, ablated = 0.11 ± 0.31 per minute, $n_{fish} = 19$, p = 0.0001, Mann-Whitney U, Figure 4:11B) and a reduced capture rate (control = 0.13 ± 0.13 per minute, $n_{fish} = 24$, ablated = 0.04 ± 0.11, $n_{fish} = 19$, p = 0.0023, Mann-Whitney U, Figure 4:11C). The capture probability (that is the number of capture events relative to the number of striking events) was also decreased in ablated fish (control = 0.55 ± 0.44, $n_{fish} = 24$,

ablated = 0.08 ± 0.19, n_{fish} = 19, p = 0.0001, Mann-Whitney U, Figure 4:11D). These findings suggest that selective loss of DAergic neurons in the subpallium perturbs foraging behaviours in larval zebrafish.
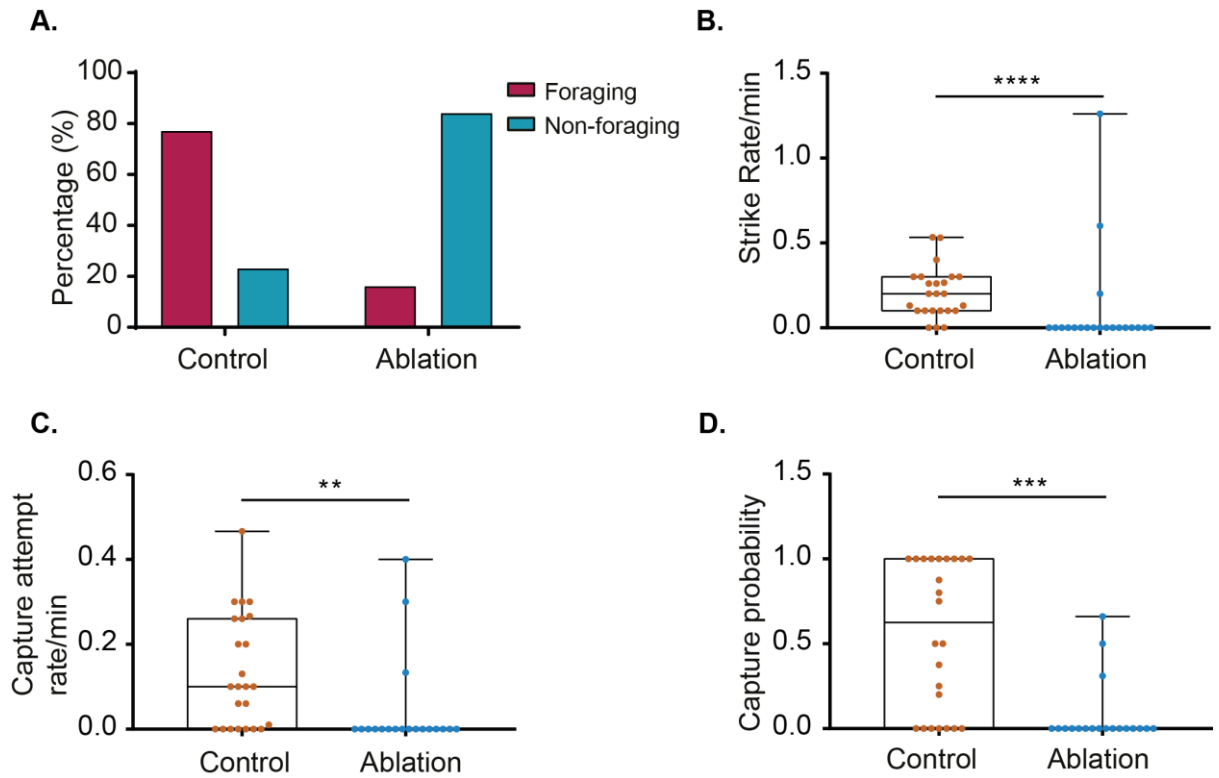
Figure 4:11 Loss of subpallial DAergic neurons reduces foraging behaviours. A: Bar chart illustrating the percentage of fish that exhibited foraging behaviour in control and ablated fish. **B:** Box and whisker plot comparing the strike rate of control and ablated fish. **C:** Box and whisker plot comparing the rate of attempted capture events. **D:** Comparison of the capture probability between control and ablated fish. ** = P < 0.005, *** = P < 0.0005, **** = P < 0.0001.

4.3.4.1 The effects of live prey on subpallial dopaminergic neuron activity

So far, these findings have revealed that lack of subpallial DAergic neurons negatively impact foraging behaviour, suggesting the activity of subpallial DAergic neurons may change in the presence of prey. Therefore, I examined the activity patterns of these cells in the presence and absence of prey using loose patch electrophysiology methods in awake but paralysed zebrafish.

On obtaining loose patch recordings from subpallial DAergic neurons, I observed periodic action potential discharges during control conditions (Figure 4:12A). On addition of rotifers to the recording chamber, action potential frequency increased significantly (control = 1.62 ± 1.36Hz, rotifers = 3.93 ± 1.78Hz, saline = 1.73 ± 0.66Hz, n_{fish} = 10, p = 0.0006, one-way ANOVA, Holm-Sidak's multiple comparison test, control vs rotifer p = 0.0003, rotifer vs saline p = 0.0082, control vs saline p = 0.8347, Figure 4:12B). This effect was reversed by subsequent removal of rotifers. These findings show that the subpallial DAergic neurons increase activity in response to prey and supports the hypothesis that subpallial DAergic neurons are involved in foraging behaviours.

A.

Control

10s

Rotifers

Wash

B.
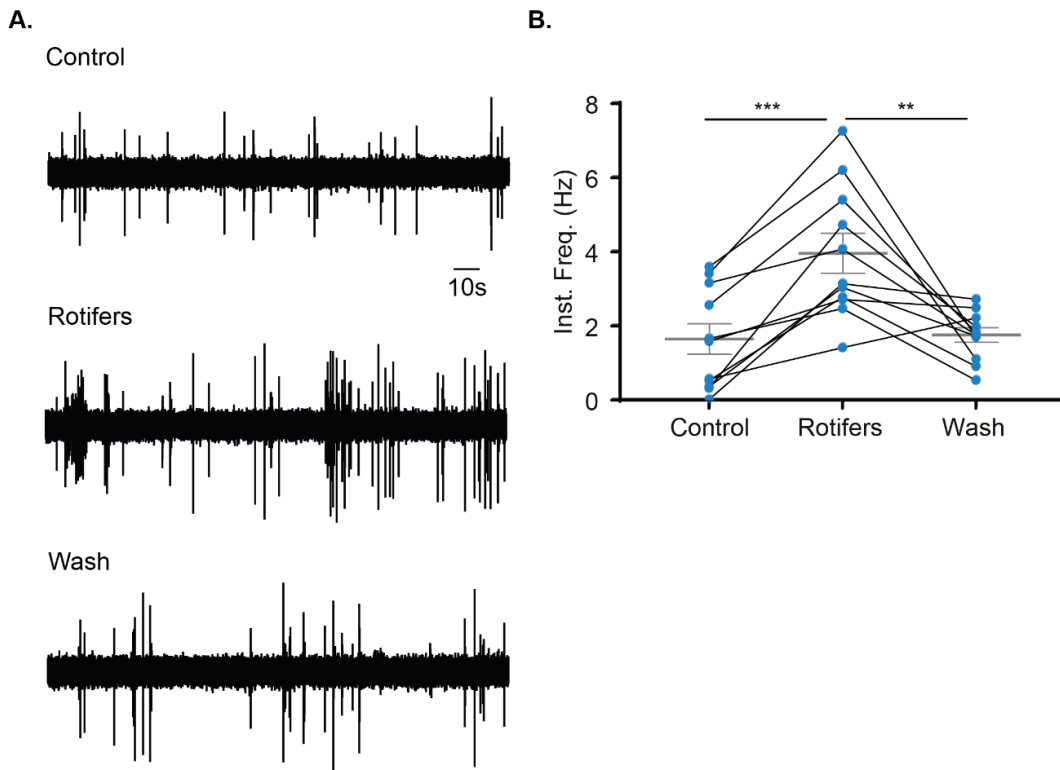
Figure 4:12 Exposure to live prey increases the firing activity of subpallial DAergic neurons. A: Extracellular action potential recordings of subpallial DAergic neurons at 5 dpf in control condition (upper trace), the presence of rotifers (middle trace) and during a saline wash condition (bottom trace). **B:** Paired-plot comparing the firing frequency of subpallial DAergic neurons during control, rotifer and saline wash conditions with mean and standard error superimposed. ** = $P < 0.005$, *** = $P < 0.0005$.

Thus far, my electrophysiological data suggest that subpallial DAergic neuron firing activity is increased by the presentation of prey. Next, I asked whether DA release can be detected in response to the exposure of rotifers using Fast-Scan Cyclic Voltammetry (FSCV). Studies have shown that DA can be detected in *ex vivo* zebrafish brains utilizing this approach (Jones et al., 2015, Shin et al., 2017). However, in vivo responses to prey presentation have not been investigated. To do this, a carbon fibre microelectrode was placed in the subpallium of awake yet paralysed fish. A voltage waveform optimised for the detection of DA was applied, and analyte release was measured for 2 minutes in control conditions, a further 4 minutes with rotifers and finally a saline wash for 4 minutes to remove the rotifers from the arena ($n_{fish} = 7$).
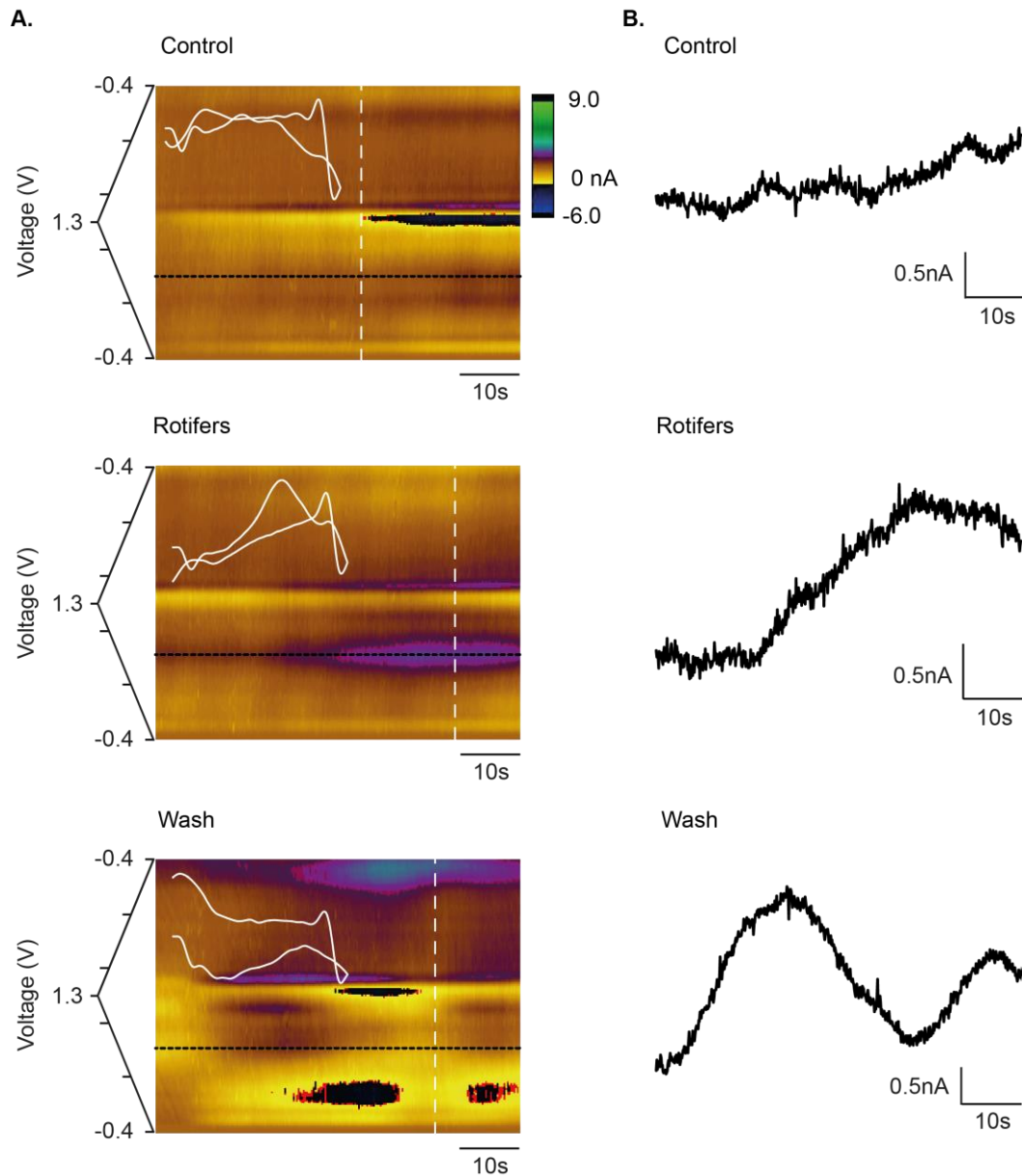
Figure 4:13 Rotifer exposure causes DA release in zebrafish subpallium. A-B: Colour plot and current vs. time plot from a single representative experiment of FSCV with carbon fibre placed in zebrafish subpallium at 5 dpf. **A:** Colour plot during control (upper trace), rotifer exposure (middle trace) and wash conditions (lower trace). The white trace shows a representative voltammogram during each condition. The dashed white line shows the position at which the voltammogram was taken. The dashed black line shows the position at which the current vs. time plots were taken. **B:** Current vs. time plot during control (upper trace), rotifer exposure (middle trace) and wash conditions (lower trace).

Using FSCV, DA release was not detected during control conditions (Figure 4:13A/B, upper panel). However, DA was detected with FSCV at approximately 0.6V, when exposed to rotifer (Figure 4:13A middle panel). On washout, the DA signal decreased to baseline (Figure 4:13A/B, lower panel). Comparison of the DA concentration before, during and after rotifer exposure revealed a significant increase in DA release when zebrafish are exposed to live prey (control= -11.82 ± 5.257 nM, rotifers = 293.6 ± 242.5 nM, wash = 81.11 ± 258.11 nM, n_{fish} = 7, p = 0.0207, Friedman test, Dunn's multiple comparison test, control vs rotifer p = 0.0485, rotifer vs wash p = 0.0485, control vs wash p = 0.9999, Figure 4:14A-C). These findings show that DA is released within subpallium when zebrafish are exposed to rotifers. Together, the FSCV data and loose patch experiments (Figure 4:12) suggests the presence of prey modulates the activity of subpallial DAergic neurons.
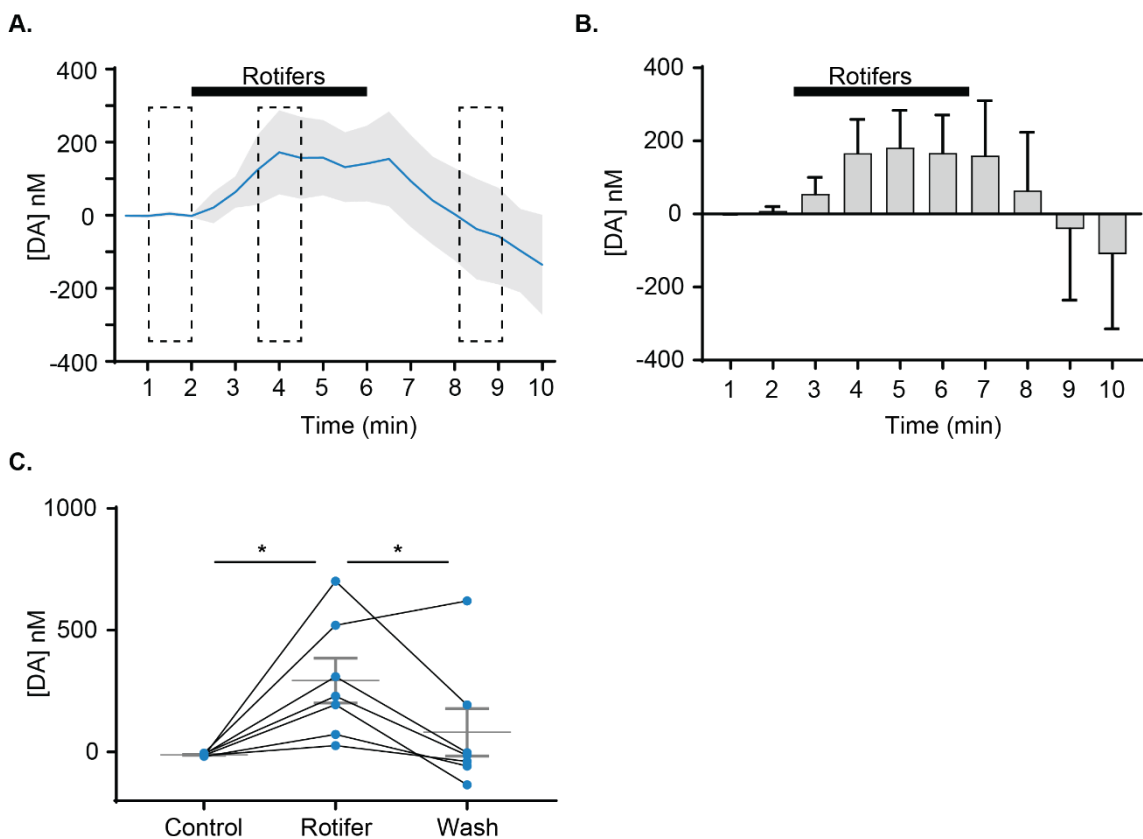
Figure 4:14 DA increases within the subpallium during exposure to live prey. A: Changes in DA concentration during control, rotifer exposure and wash conditions, the blue line represents mean, grey tone represents S.E.M. **B:** Bar chart illustrating mean DA concentration in 1-minute intervals. The bold line

represents the time during zebrafish are exposed to rotifers **C:** Paired plot comparing the DA concentration during control, rotifer exposure and wash conditions, concentrations were taken from **A**, represented by dashed lines with mean and standard error. * = P < 0.05.

4.3.4.2 Subpallial dopaminergic neuron activity of free-swimming fish during foraging

So far, I have shown that the subpallial DAergic neurons exhibit increased firing and that subpallial DA concentrations are elevated in the presence of prey. To confirm that these neurons are active during foraging, activated extracellular signal-regulated kinase (ERK) staining methods were used. Neuronal activity resulting in calcium influx activates the Ras-ERK signalling pathway, leading to the phosphorylation of ERK (Xia et al., 1996, Randlett et al., 2015). Therefore, pERK is a marker for neuronal activity that can be used to localise recently active neurons (Ji et al., 1999, Randlett et al., 2015). Here, free-swimming fish were maintained in either control conditions (saline only) or in the presence of prey (saline containing rotifers) for 1 hour. Thereafter, they were fixed and underwent standard anti-pERK staining (Randlett et al., 2015).

Control fish that were not exposed to rotifers displayed low levels of pERK staining in DAergic subpallial neurons (Figure 4:15B, left column). However, the percentage of subpallial DAergic neurons that expressed pERK was significantly increased in rotifer exposed fish (control = 11.11 ± 10.80%, n_{fish} = 10, Treatment = 47.22 ± 13.93%, n_{fish} = 8, p < 0.0001, Unpaired t test; Figure 4:15C). These findings support the premise that subpallial DAergic neurons are active in the presence of prey.
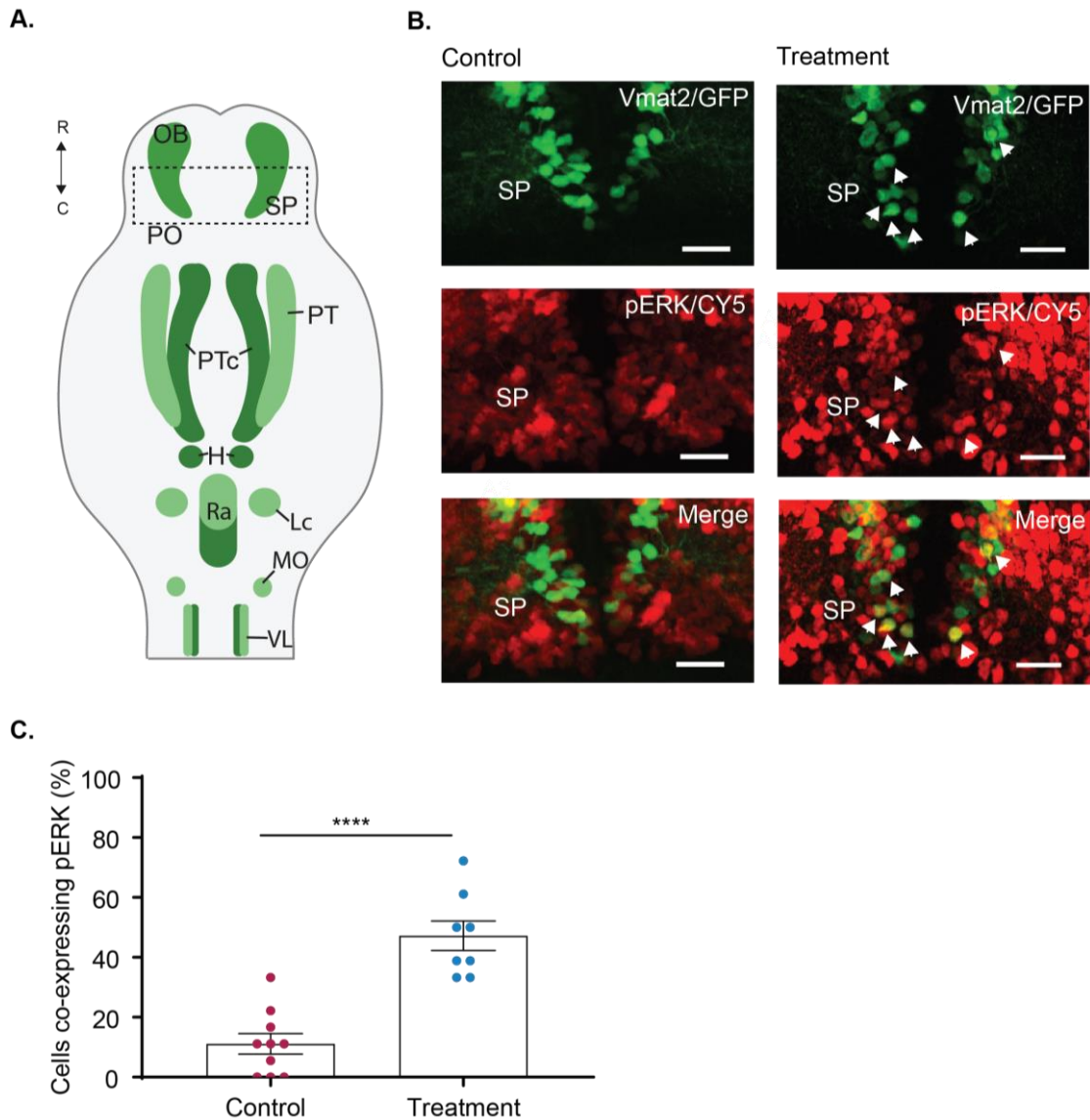
Figure 4:15 Subpallial DAergic neurons co-express pERK when exposed to live prey. A: Schematic overview of larval zebrafish brain (dorsal) showing the distribution of Vmat2 expression in ETvmat2:GFP fish. Dash line represents region of focus in confocal images. Orientation is indicated in panel (**A**); R = rostral and C = caudal. **B:** Z-stack images illustrating immunohistochemical staining for pERK positive neurons in the zebrafish subpallium in control (left column) and zebrafish exposed to rotifers (right column) and visualised by confocal microscopy. Left column: Vmat2/GFP expression (green). Middle column: Anti-pERK (red). Right column: merge of green and red channels. Scale bar = 20μm. **C:** Bar char comparing the percentage of subpallial DAergic neurons that co-express pERK in control and rotifer treatment conditions. Abbreviations; olfactory bulb (OB), subpallium (SP), preoptic (PO), posterior tuberculum (PTc), hypothalamus (H), pretectum (PT), locus coeruleus (LC), raphe nucleus (RA) and medulla oblangata (MO).****$P < 0.0001$.

4.3.4.3 Effects of subpallial dopaminergic neuron ablation on visual acuity

So far, I have found that subpallial DAergic neurons are active in the presence of prey and that ablation of these cells perturbs foraging behaviour. However, these effects could simply arise from impaired vision caused by ablation procedures. To address this, I first tested for the presence of the optokinetic response (OKR) in ablated fish. The OKR is a behaviour that is characterised by stereotyped eye movements in response to the presentation of moving objects (Cameron et al., 2013, Scheetz et al., 2018, Brockerhoff, 2006). The OKR is used as a behavioural screen designed to identify defects in the visual system and can examine the visual acuity of zebrafish (Brockerhoff, 2006). Typically a grating stimulus, alternating in direction is used to evoke the OKR (Roeser and Baier, 2003). To do this, I analysed the OKR of control and ablated zebrafish that are awake, yet immobile. Zebrafish were embedded in 3% methylcellulose and positioned in the upright position to ensure both left and right eyes were visible by the overhead camera. Zebrafish were acclimatised to the new environment for 5 minutes before being presented with the grating stimulus generated in open-source MATLAB suite described by Scheetz and colleagues (Scheetz et al., 2018).
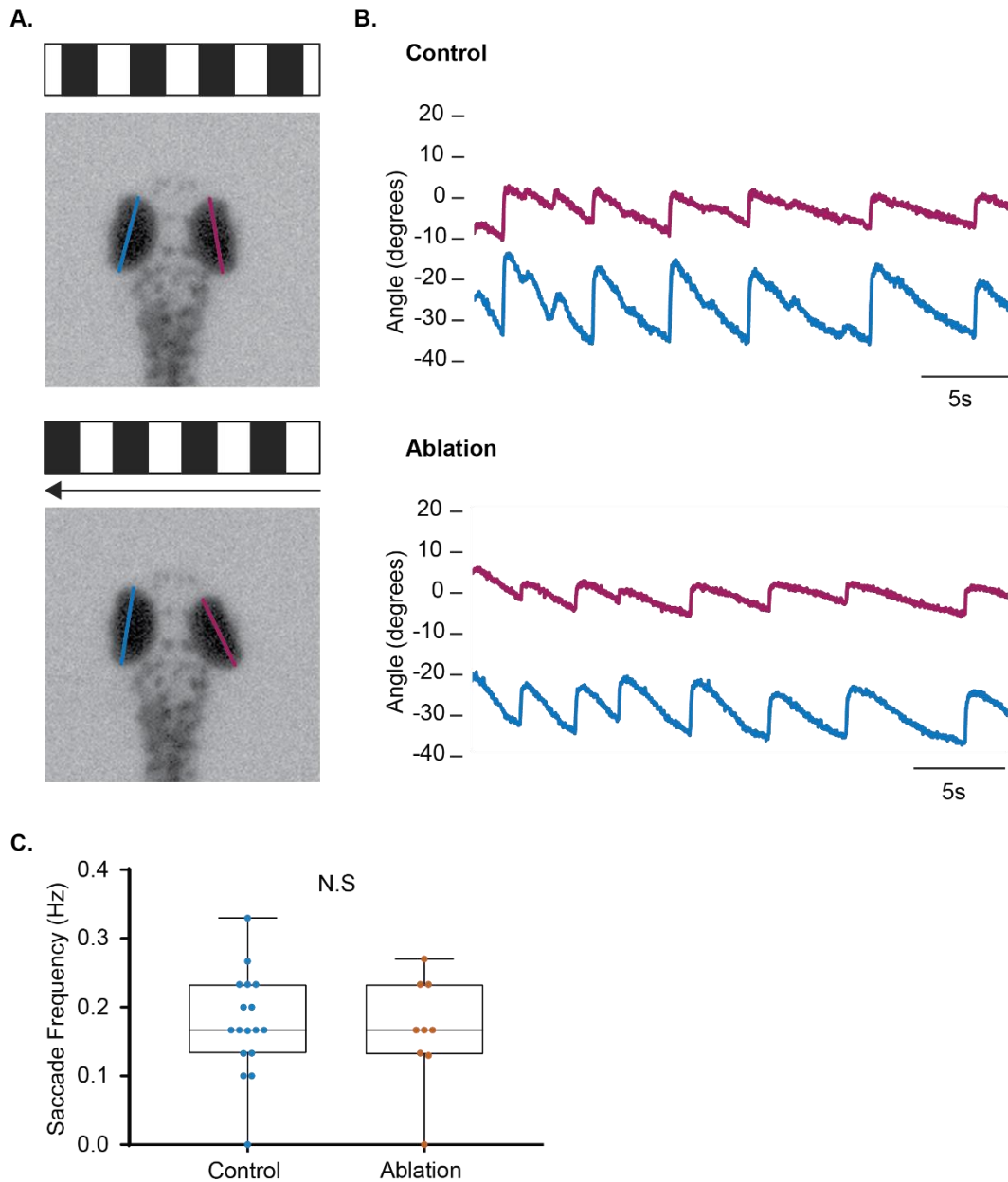
Figure 4:16 OKR is elicited by an anticlockwise grating stimulus. A: Images of initial eye position (upper panel) and the eye position at the end of a saccade and (lower panel) when shown an anticlockwise moving grating stimulus (shown with grating illustration). **B:** Ocular angle plotted against time shows the anticlockwise rotation of the eyes (left eye = blue and right eye = magenta) of control fish (upper panel) and ablated fish (lower panel). **C** Box and whisker plot comparing the saccade frequency of control and ablated fish in response to a leftward moving grating stimulus. N.S = Not Significant.
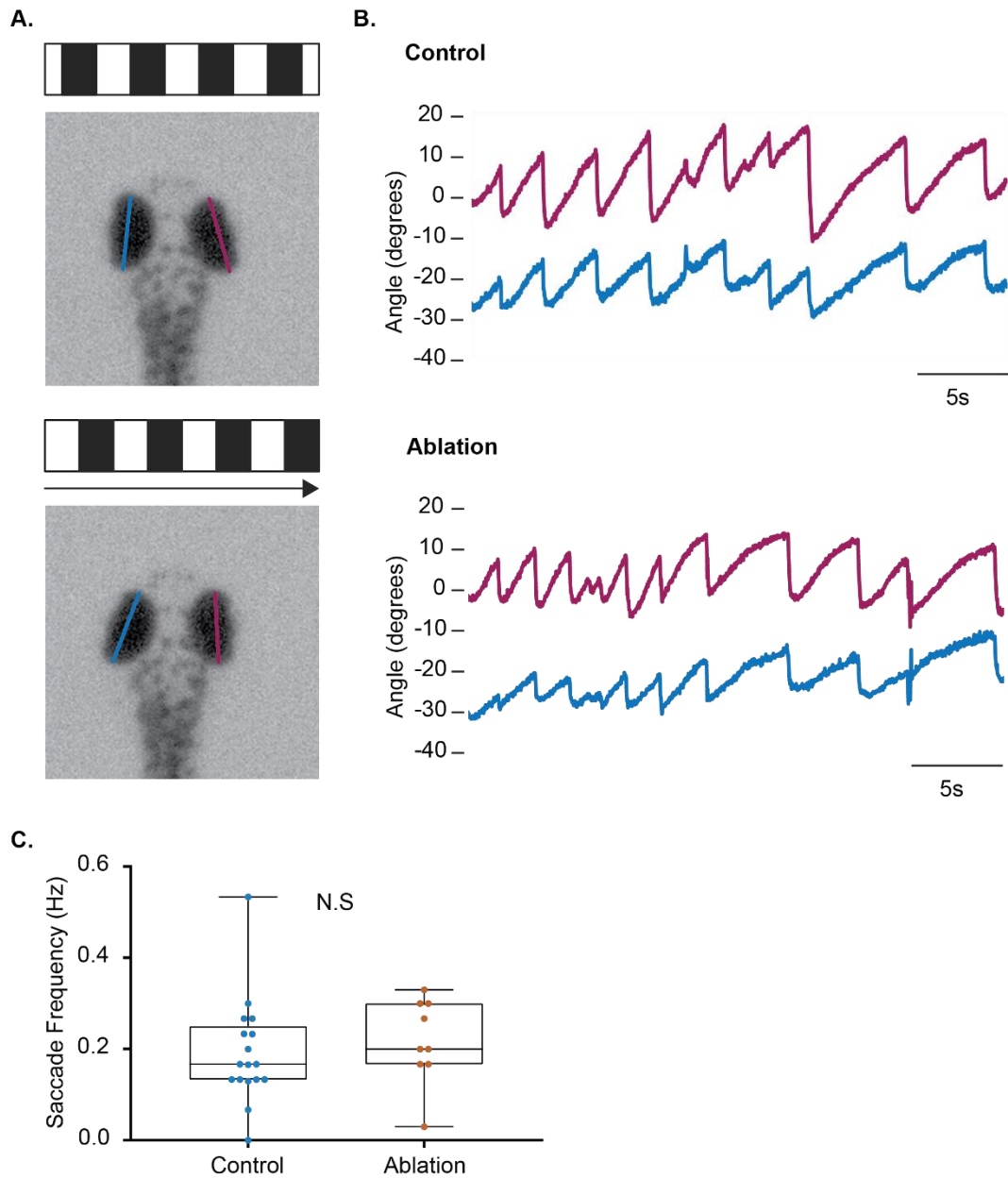
Figure 4:17 Selective loss of subpallial DAergic neurons does not affect the OKR of larval zebrafish. A: Images of initial eye position and the eye position at the end of a saccade (upper and lower panel, respectively), when shown a clockwise moving grating stimulus (shown with grating illustration). **B:** Ocular angle plotted against time show the clockwise rotation of the eyes (left eye = blue and right eye = magenta) of control fish (upper panel) and ablated fish (lower panel). **C:** Box and whisker plot comparing the saccade frequency of control and ablated fish in response to a rightward moving grating stimulus. N.S = not significant.

The OKR, which comprises saccadic movements (the smooth tracking of the object followed by resetting of eye position) could be elicited in both control and ablated fish when subjected to the grating stimulus (Figure 4:16A). The presentation of a leftward moving stimulus evoked the anticlockwise rotation of both eyes during the tracking phase of the OKR (Figure 4:16B). The saccade movement could be seen in both conditions (Figure 4:16B) and analysis showed similar saccade frequency between control and ablated fish (control = 0.18 ± 0.07 Hz, n_{fish} = 17, ablated = 0.16 ± 0.08 Hz, n_{fish} = 9, p = 0.5918, Unpaired t test, Figure 4:16C). The OKR could be evoked regardless of the direction of stimuli (Figure 4:17A, B). Similarly, a rightward moving stimuli evoked saccade movements and control and ablated fish had similar saccade frequencies (control = 0.19 ± 0.12 Hz, n_{fish} = 17, ablated = 0.20 ± 0.09 Hz, n_{fish} = 9, p = 0.3360, Mann-Whitney U, Figure 4:17C). In sum, these findings show that selective loss of subpallial DAergic does not affect the OKR which suggests that subpallial DAergic neurons are not required for visual acuity.

4.3.5 The effects of selective loss of subpallial dopaminergic neurons on prey tracking

Foraging is composed of a sequence of manoeuvres, including reorientations (j-turn), prey tracking, striking and capture (Budick and Malley, 2000, Henriques et al., 2019, Gahtan et al., 2005). Loss of subpallial DAergic neurons reduced the striking and capture behaviours; however, locomotion was not affected. Ablating subpallial DAergic neurons did not affect OKR in larval zebrafish, suggesting visual acuity was not affected by subpallial DA neuron ablation. I next asked whether ablating subpallial DAergic neurons perturbs prey tracking. To do this, I examined the eye movements of free-swimming zebrafish in the presence of rotifers.

Consistent with previous data, striking and capture manoeuvres were reduced in ablated fish. Nonetheless, eye convergence onto prey was observed in both control and ablated larvae (Figure 4:18A). Subsequent analysis of eye convergence duration during prey tracking revealed no difference between experimental conditions (control = 2.08 ± 1s, n_{fish} = 12, n_{events} = 70, ablated = 1.75 ± 0.79s, n_{fish} = 10, n_{events} = 31, p = 0.4491, Mann-Whitney U, Figure 4:18B). Similar to the findings by Bianco et al., (2011a), I found that the convergence angle of the eyes increased during prey tracking, knowns as binocular vision and this angle reduced after prey tracking events (Figure 4:18C, see Table 4.10 for Two-way ANOVA analysis). Analysis of the convergence angle before, during and after prey tracking showed no difference between control and ablated fish (see Table 4.11 for Sidak multiple comparisons analysis).

A.
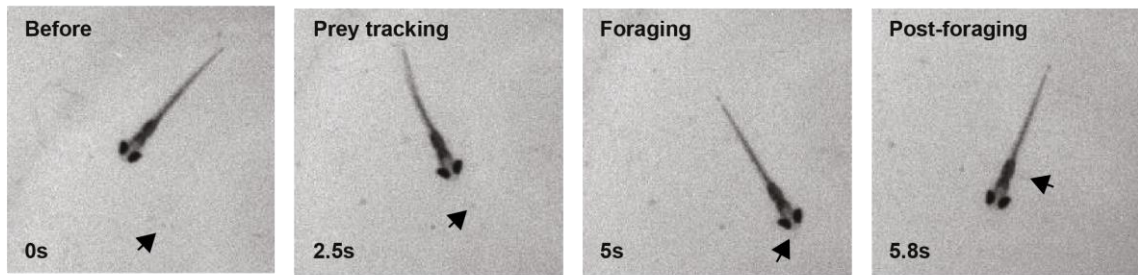
B.
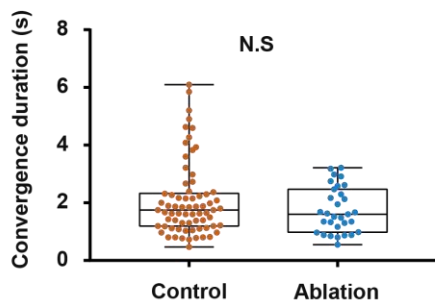
C.
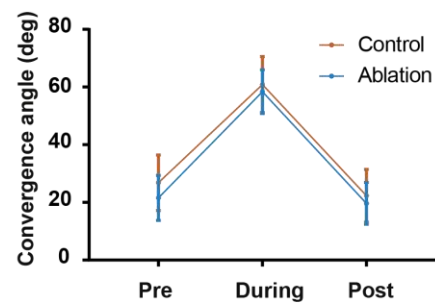
D.
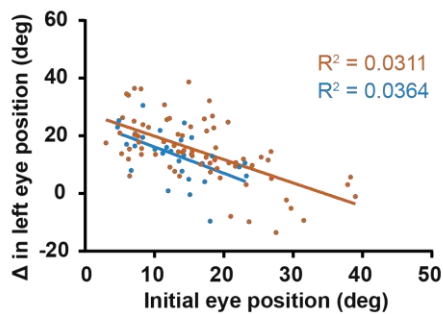
E.
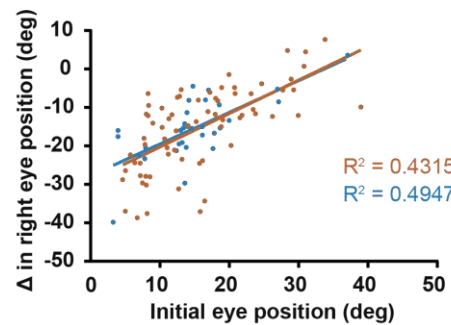
Figure 4:18 Selective loss of subpallial DAergic neurons does not affect prey tracking. A: Consecutive images showing eye movements of control zebrafish before foraging, during prey tracking, foraging and post-foraging. Arrow points to the target rotifer in the arena. **B:** Box and whisker plot comparing the duration of eye convergence throughout prey tracking and foraging. **C:** Line graph showing the convergence angle of both eye before, during and post prey tracking events for control and ablated fish. **D:** Change in left eye position during eye convergence plotted against initial eye position for control and ablated fish. **E:** Comparison of the change of the right eye position during eye convergence plotted against initial eye position for control and ablated fish.

I also examined eye rotations during prey tracking. With both eyes, a linear relationship with the initial location and the degree of eye rotation could be seen (Figure 4:18D/E). Larger clockwise (+ve) angular rotations were observed when the initial position of the left eye was not in binocular position (nasal position; Figure 4:18D). Linear regression analysis revealed there was no correlation, and

no difference between control and ablated fish when examining the rotation of the left during the initial stages of prey tracking (control R^2 = 0.037, n_{fish} = 12, n_{events} = 70, ablated R^2 = 0.031, n_{fish} = 10, n_{events} = 31, p = 0.1660, Figure 4:18D). Similar results were seen with right eye movements. When the initial position of the right eye was not in the binocular vision position, larger anticlockwise (-ve) angular rotations occurred to enter binocular vision conformation (Figure 4:18E). Linear regression analysis revealed correlation between the degree of eye rotation of the right eye, however there was no difference between control and ablated fish (control R^2 = 0.432, n_{fish} = 12, n_{events} = 70, ablated R^2 = 0.495, n_{fish} = 10, n_{events} = 31, p = 0.8370, Figure 4:18E). Together these results suggest that ablating subpallial DAergic neurons does not affect eye movements or convergent saccades and the ability to track prey. In sum, these findings suggest that subpallial DAergic neurons are not involved in prey tracking.

Table 4.10 Two-way ANOVA analysis of Eye Convergence

	DF	MS	F (DFn, DFd)	P value
Interaction	2	48.83	F (2, 192) = 0.7004	0.4976
Time	2	38281	F (2, 192) = 549.1	<0.0001
Condition	1	742.7	F (1, 96) = 7.372	0.0079
Residual	192	69.72		

Table 4.11 Sidak multiple comparison of Eye convergence

	Diff. in mean	DF	P value
Pre	5.214	288	0.0246
During	2.473	288	0.5040
Post.	2.66	288	0.4408

4.4   Discussion

In this chapter, I have examined the functional role of subpallial DAergic neurons locomotion, anxiety and foraging behaviours of larval zebrafish. The results presented in this chapter demonstrate three key findings. Firstly, loss of subpallial DAergic neurons has no effect on larval locomotor activity, visual acuity or anxiety-like behaviours. Secondly, loss of subpallial DAergic neurons is sufficient to perturb foraging behaviours in larval zebrafish and finally, subpallial DAergic neuron activity increases in response to prey.

4.4.1   The relationship between subpallial dopaminergic neurons and locomotion

I first sought to delineate the role of subpallial DAergic neurons in zebrafish behaviours, specifically behaviours that relate to mammalian striatum. The dorsal aspect of the striatum has functions relating to motor control, in which the basal ganglia receives DA input from the SNc, and in turn, modulates voluntary movement (Dudman and Krakauer, 2016). Selective laser ablation of subpallial DAergic neurons did not affect that motor output and beat glide swimming kinetics of free-swimming zebrafish.

If the subpallium is functionally homologous to the striatum that involves motor control, it can be assumed the subpallial DAergic neurons will perturb swimming behaviour. The function of SNc DAergic neurons to regulate the initiation of voluntary movements. In mammals the dorsal striatum receives DA input from the SNc, and DA transmission activates either D1-MSNs or D2-MSNs which has been shown to facilitate or inhibit movement, respectively. In Parkinson's disease, the DAergic neurons of the SNc are lost, and symptoms of this disease include reduced movement and rigidity. Additionally, exposure to MPTP, a neurotoxin that induces selective chemogenic ablation of the SNc DAergic neurons by oxidative stress, also elicits impaired motor output including reduced locomotion and rigidity (Langston, 2017). However, loss of subpallial DAergic neurons by laser ablation does not impair locomotion or the swimming kinetics of larval fish.

Similar locomotive impairment has been observed in zebrafish, studies have shown that exposing zebrafish to MPTP can cause loss of DAergic neurons clusters in the posterior tuberculum, and can induce locomotion deficits (Sallinen et al., 2010, Sallinen et al., 2009, Lam et al., 2005, Wen et al., 2008). A recent investigation showed selective loss of the DDNs, specifically DC2/4 by laser ablation could cause impaired locomotion (Jay et al., 2015). Patch-clamp recordings of DC2/4 revealed these neurons are active during fictive swimming episodes (Jay et al., 2015). The DC2/4 cluster possesses both ascending and descending projections providing DA input to the telencephalon and spinal cord, respectively (Tay et al., 2011, Jay et al., 2015). Early studies by Rink and Wullimann identified ascending DAergic projections from the DDNs and suggested they were equivalent to the SNc (Rink and Wullimann, 2004, Rink and Wullimann, 2002a, Rink and Wullimann, 2002b). Whilst DC2/4 have ascending projections to the subpallium, similar to that of the ascending projections of the SNc DAergic neurons, recent anatomical and functional studies have shown they equivalent to the A11 group (Tay et al., 2011, Koblinger et al., 2014b, Reinig et al., 2017). Loss of DC2/4 in zebrafish generates similar locomotion deficits observed in mammals, disruption to A11 DA transmission in the spinal cord can perturb locomotion in mammals, whilst optogenetic activation of the A11 DA neurons promotes locomotion (Pappas et al., 2008, Sharples et al., 2014, Koblinger et al., 2018).

In sum, ablating subpallial DAergic neurons, the primary source of DA input to the subpallium, the putative striatum, do not influence locomotion or swimming episodes. Therefore, the subpallial DAergic neurons do not appear to be functionally equivalent to SNc neurons.

4.4.2 The effects of selective loss of subpallial dopaminergic neurons on anxiety-like behaviours

Since genetic studies have suggested that the dorsal and postcommissural regions of the subpallium (Vs/Vp) is the putative extended amygdala (Perathoner et al., 2016, von Trotha et al., 2014), subpallial DAergic neurons could influence anxiety-like behaviours, similar to that of the mesolimbic pathway in mammals.

Ablating the subpallial DAergic neurons did not affect thigmotaxis or place preference in larval zebrafish, suggesting these neurons do not affect anxiety-like behaviours. If the subpallium is the extended amygdala and the subpallial DAergic neurons innervate this region, this raises the question as to whether subpallial DAergic neurons are functionally equivalent to the VTA neurons of that project to the amygdala. Anatomical studies suggest there are hodological similarities between subpallial DAergic neurons and the VTA neurons of mammals. Subpallial DAergic neurons innervate the putative amygdala in zebrafish, whilst subpopulations of VTA neurons innervate the amygdala in mammals (Lammel et al., 2014, Hasue and Shammah-Lagnado, 2002, Cho and Fudge, 2010, Tay et al., 2011). From this hodological data, we can infer that subpallial DAergic neurons innervate the putative amygdala, similar to amygdala projecting VTA neurons in mammals.

Functional studies have shown the mammalian amygdala is involved in a range of behaviours, including anxiety and fear response (Stamatakis et al., 2014, Fox et al., 2015, Shackman and Fox, 2016, Fox and Shackman, 2019, Newman, 1999, Trimble and Van Elst, 1999), and DA innervation has been shown to modulate these behaviours as well as activity in the amygdala (Gelowitz and Kokkinidis, 1999, de la Mora et al., 2010, Zarrindast et al., 2013). Loss of DAergic innervation to the BLA can cause anxiety-like behaviours (Zhang et al., 2017). Activation of the BLA induces anxiety-like behaviours and lesions to this region can attenuate anxiety-like behaviours (Siuda et al., 2016, Ranjbar et al., 2017). The BLA projects to the CeA and can subsequently modulate the CeA activity (Babaev et al., 2018). Optogenetic activation of BLA projections to the CeA reduces anxiety behaviours whilst inhibition of these projections promoted anxiety (Tye et al., 2011). The behavioural effects caused by the loss of subpallial DAergic neurons suggests these neurons are not involved in anxiety-like behaviours.

Nonetheless, ablating subpallial DAergic neurons in zebrafish did not mimic the behavioural effects of perturbed DA signalling in the extended amygdala of mammals. Non-selective DA receptor agonist can increase thigmotaxis behaviour in mice, therefore, increasing anxiety-like behaviours (Simon et al., 1994). Additionally, application of D_1 antagonist in the CeA attenuates anxiety-

like behaviours as well as freezing and startling in mammals (Lamont and Kokkinidis, 1998, Guarraci et al., 1999a, Guarraci et al., 1999b, Zarrindast et al., 2013). If blocking DA transmission can attenuate anxiety-like behaviours in mammals, then ablating subpallial DAergic neurons should attenuate anxiety-like behaviours in zebrafish. However, loss of subpallial DAergic neurons did not affect anxiety-like behaviours, suggesting these neurons do not modulate anxiety behaviours of zebrafish. To further investigate the role of subpallial DAergic neurons in anxiety, the application of anxiolytic drugs such as fluoxetine during scototaxis assay could be undertaken. Application of fluoxetine can reduce anxiety, subsequently zebrafish spend more time in a non-preferred environment (Egan et al., 2009, Kysil et al., 2017). Additionally, other paradigms can be used to investigate zebrafish anxiety such as the novel tank test, however, this paradigm is typically conducted in adult fish (Egan et al., 2009, Kysil et al., 2017).

4.4.3 The relationship of subpallial dopaminergic neurons activity and foraging behaviours

I next sought to delineate the role of subpallial DAergic neurons in foraging behaviours. Using electrophysiological recording, FSCV and pERK IHC, subpallial DAergic neurons increase in activity when exposed to live prey. Previous whole brain mapping of the zebrafish subpallium show this region is active during foraging (Randlett et al., 2015). Whilst this study didn't look directly at the activity of local DA neurons directly, I have shown they are active during foraging. The mammalian amygdala has been implicated in hunting behaviours, whole-brain mapping of rodent brains found the activity of the extended amygdala was associated with the predatory hunting (Comoli et al., 2005). Additionally, Han and colleagues examined the extended amygdala during hunting and foraging in rodents, and they found the activation of CeA during hunting/foraging for prey (live and artificial) and CeA activity can modulate the foraging locomotion and biting behaviour (Han et al., 2017).

There has been limited research into the relationship between DA transmission and the modulation of the amygdala role of predatory hunting in mammals; however, it has been shown that CeA circuits receive input relaying feeding-

related information and can positively modulate feeding behaviours (Douglass et al., 2017a). Additionally, activation of VTA DAergic neurons in rodents can increase feeding behaviours, and during feeding, DA levels increase within the CeA (Boekhoudt et al., 2017, Hajnal and Lenard, 1997). I observed similar results, exposing zebrafish to prey in conjunction with FSCV, DA release was detected in the zebrafish subpallium. Along with the extracellular recordings of the subpallial DAergic neurons, my work shows these neurons are activated when presented with prey. Since these neurons innervate the putative amygdala, it shows that the subpallial DAergic neurons are activated by the presentation and DA is release in the putative extended amygdala. Since similar observations were made in mammals regarding the VTA and CeA, it suggests the subpallial DAergic are homologous to the VTA neurons that innervate the amygdala.

Given the correlation between subpallial DAergic neuron activity and foraging, I next sought to examine whether disruption to DA signalling affected foraging. Ablating subpallial DAergic neurons perturbed foraging behaviours, and zebrafish were less likely to exhibit prey capture manoeuvres such as striking. Since subpallial DAergic neurons innervate the telencephalon, ablating these neurons could abolish DAergic innervation to the putative amygdala. There are limited studies into the role of DA in the modulation of amygdala and foraging in mammals; however, lesion to the CeA attenuated prey capture events (Han et al., 2017). Additionally, modulation of DA signalling in the amphibian CeA can alter prey capture events, injections of apomorphine, a D_1 and D_2 receptor agonist, attenuated prey capture behaviours in these animals (Glagow and Ewert, 1999, Lees, 1993). Whilst these experiments were conducted in different species, this work suggests DA and the amygdala influence prey capture behaviour. If the subpallium is functionally homologous to the extended amygdala, then subpallial DAergic neurons innervation modulates prey capture behaviour, and ablating these neurons perturbs this behaviour.

In mammals, lesions to the CeA disrupt signalling to the PAG in rodents and can attenuate foraging behaviours, including biting and pursuit locomotion (Han et al., 2017). The PAG is a critical output nucleus that has roles in hunting, aversion and defensive behaviours (Silva and McNaughton, 2019, Comoli et al., 2005). The PAG mediates behaviours via the mesencephalic locomotor region (MLR), a

region of the midbrain that initiates and controls movement via reticulospinal neurons (Franklin, 2019, Josset et al., 2018, Ryczko et al., 2016a). Lesions to the CeA-PAG-MLR pathway can reduce hunting behaviours, whilst optogenetic activation of the CeA-PAG-MLR pathway induces robust hunting behaviours in rodents (Han et al., 2017). In zebrafish, the PAG has been identified and is known as the griseum centrale (GC), which is located in the midbrain. The nMLF has been suggested to be homologous to the MLR in zebrafish (Severi et al., 2014, Naumann et al., 2016, Dunn et al., 2016b, Ryczko and Dubuc, 2013). A corresponding pathway exists between the zebrafish GC and nMLF (Olson et al., 2017, Robles et al., 2011, Kittelberger and Bass, 2013), and visual evoked prey capture behaviours are mediated by the nMLF (Gahtan et al., 2005). Therefore, the prey capture locomotion could be driven by the interaction of the GC and nMLF (Figure 4:19A). Since subpallial DAergic neurons do not innervate these structures, it is to be expected that these neurons do not affect locomotion directly. A study found neurites that innervated the tectum, including the GC, primarily originated from hypothalamic neurons, however, they found sparse labelling of neurons in the forebrain (Heap et al., 2018a). Unfortunately, the forebrain-GC pathway was not investigated to determine if these projections originate from the putative extended amygdala. If these neurons are located in the putative extended amygdala, then these neurons could be the amygdala-GC-nMLF and could be homologous to the mammalian CeA-PAG-MLR pathway (Figure 4:19). However, this pathway has not been investigated in zebrafish and further experiments are required to determine if this pathway is functionally equivalent to the CeA-PAG-MLR.

Rodent Brain
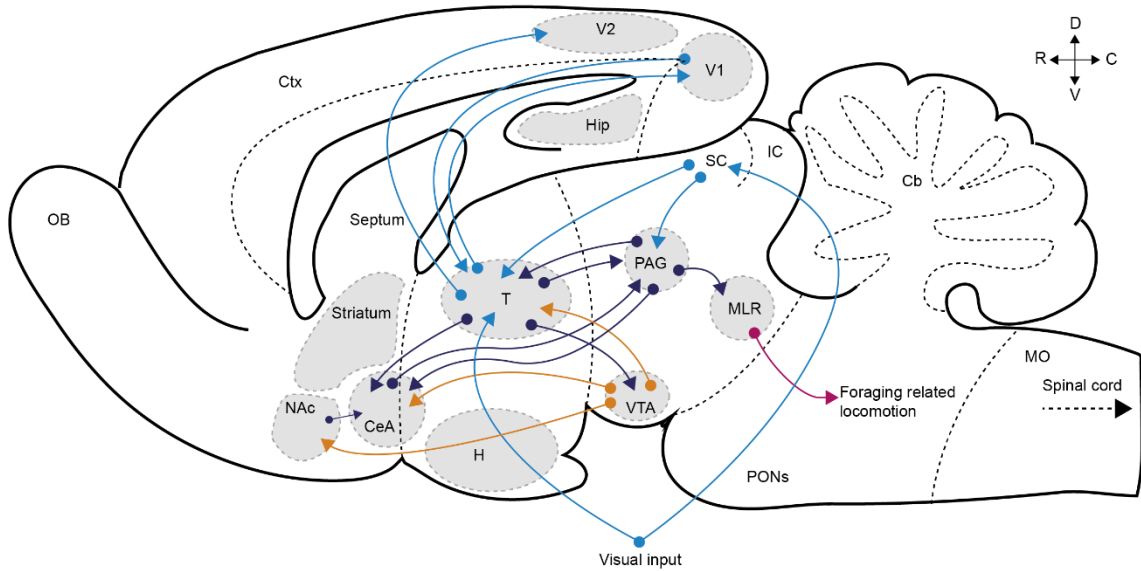
Zebrafish Brain
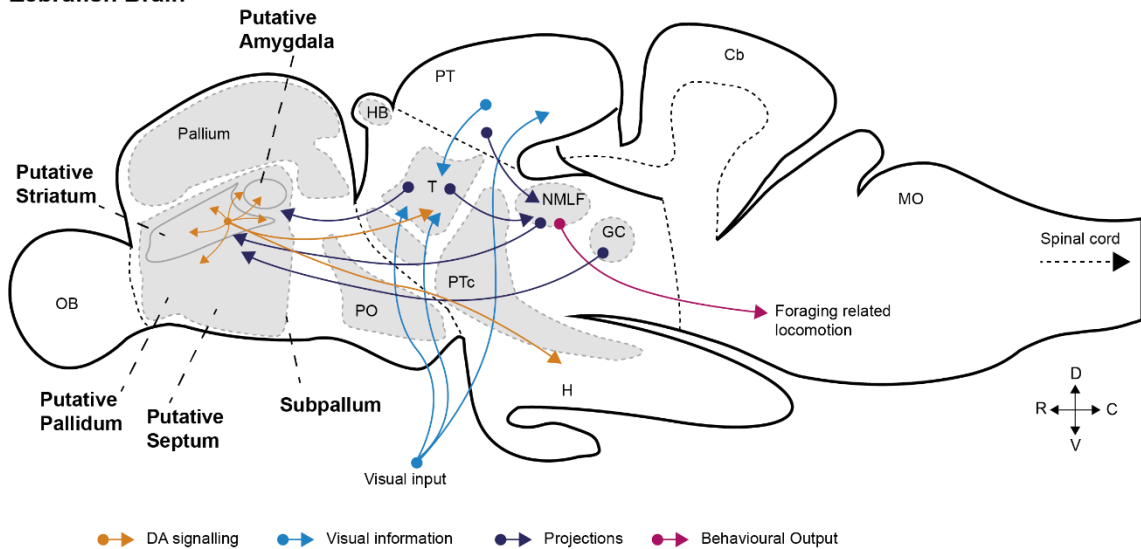
Figure 4:19 Comparison of rodent and zebrafish foraging related circuits. Schematic illustration of the sagittal cross-section of the rodent brain (upper illustration) and zebrafish brain (lower illustration). The flow of foraging related information across the brain of visual information (blue line), connections between nuclei (purple), DA transmission (orange) and locomotor output (magenta). Abbreviation: Cb; Cerebellum, CeA; Central nuclei of the amygdala, Ctx; Cortex, GC; griseum centrale, H; hypothalamus, Hb; habenular, Hip; Hippocampus, IC; Inferior Colliculus, MLR; Mesencephalic locomotor region, MO; Medulla, NAc; Nucleus accumbens, NMLF; nucleus of the medial longitudinal fasciculus, PAG; Periaqueductal grey, PO; preoptic region, PTc; posterior tuberculum, PT; pretectum, OB; olfactory bulb, SC; Superior Colliculus, T; Thalamus, VTA; ventral tegmental area, Adapted and derived from Mueller, (2012), Rink and Wullimann (2002) and Tay et al., (2011). (Mueller, 2012) (Mueller, 2012)

How then, does the loss of DA signalling perturb foraging in zebrafish? Ablating subpallial DAergic neurons reduced foraging behaviour, prey tracking was not affected along with locomotion. This suggests zebrafish recognise and track prey but are less likely to initiate capture or striking manoeuvres. A recent investigation found ablating the nucleus isthmi, a region in the zebrafish optic tectum had similar effects on prey capture behaviours to ablating subpallial DAergic neurons. Henriques and colleagues found that ablation of the nucleus isthmi resulted in failures in the ability to sustain prey capture sequences, these animals still exhibit prey capture manoeuvres and prey tracking (Henriques et al., 2019). The zebrafish optic tectum has been shown to recognise prey and drive hunting locomotion (Gahtan et al., 2005, Bianco and Engert, 2015, Bianco et al., 2011a, Henriques et al., 2019). Therefore, subpallial DAergic neurons do not appear to have a role in prey recognition, tracking and pursuit.

One explanation for the role of subpallial DAergic neurons is to modulate the putative amygdala to influence visually evoked prey capture behaviours is to affect motivation. Since DA is known to be involved in reward and motivation (Smith et al., 2013, Lee et al., 2006, Guarraci et al., 1999b), loss of subpallial DAergic neuron in zebrafish perturbs foraging by affecting reward or motivation-related circuits. However, loss of the subpallial DAergic neurons prior to an age when zebrafish are capable of feeding reduced zebrafish predatory hunting manoeuvres. This suggests subpallial DAergic neurons convey a motivational signal to pursue prey rather than reward since these zebrafish are not capable of feeding on a natural reward. Comoli and colleagues have suggested that the extended amygdala conveys motivational values which influence the motor output of predatory feeding (Comoli et al., 2005). Stimulation of D_1 receptor within the CeA can modulate the attention towards visual stimuli as well as motivation (Smith et al., 2015) supporting this argument. Additionally, it has been suggested that CeA conveys incentive motivation regarding prey and modulates the MLR via the PAG in mammals (Han et al., 2017, Robinson et al., 2014). Since these structures are conserved in zebrafish, subpallial DAergic neurons could be influencing visually evoked prey capture behaviour by providing motivational signals.

I conducted experiments in pre-feeding zebrafish and these animals are not able to experience the reward of food, another consideration is that, the subpallial DAergic neurons may be involved in motivation rather than reward. Since ablating subpallial DAergic neurons perturbed foraging in pre-feeding zebrafish, therefore, the motivation to pursue prey maybe perturbed by the loss of these neurons. Further studies are required to examine if subpallial DAergic neurons are involved in processing reward. This can be achieved by utilising conditioned place preference (CPP) paradigm (Mathur et al., 2011). Exposure to an addictive substance such as cocaine or amphetamine can change preference (Mathur et al., 2011, Brock et al., 2017). If subpallial DAergic neurons have a role in reward rather than motivation, ablating these neurons would affect CPP compared to control zebrafish.

Another explanation for the role of subpallial DAergic neurons in foraging, is that these neurons could modulate sensory integration and prey capture behaviours. Selective ablation of subpallial DAergic neurons perturbed prey capture behaviours without affecting locomotion, prey tracking or hunting initiation. A recent investigation found that ablating the nucleus isthmi of the zebrafish optic tectum had similar effects to prey capture behaviours to ablating subpallial DAergic neurons. (Henriques et al., 2019) found that ablation of the nucleus isthmi resulted in failures in the ability to sustain prey capture sequences. Both subpallial DAergic neurons and nucleus isthmi project to the thalamus (Tay et al., 2011, Henriques et al., 2019) and ablation of either group disrupts prey capture behaviours in similar ways. The thalamus integrates visual information from the ascending visual system and can influence behaviours (Heap et al., 2018b, Mueller, 2012). The thalamus projects to the subpallium as well as the optic tectum (Heap et al., 2018b, Mueller, 2012, Rink and Wullimann, 2004). Therefore, subpallial DAergic neurons may modulate prey capture circuits via a subpallium-thalamo-optic tectum loop and convey DA transmission relaying motivational, valence or decision-making signals (Figure 4:19). The VTA DAergic neurons project to the thalamus and can modulate sensory processing (Varela, 2014, Jacob and Nienborg, 2018). DA transmission can modulate the activity of the thalamus and subsequently modulate the visual evoked behaviours (Zhao et al., 2002, Varela, 2014). Since subpallial DAergic neurons project to the thalamus, it

suggests there is a conserved DA-thalamic pathway in zebrafish, similar to the VTA-thalamus (Figure 4:19A/B). However, further investigations are required to understand how DA modulates thalamus function in zebrafish and mammals.

In sum, subpallial DAergic neurons are activated by the visual stimulus when zebrafish are exposed to prey (Figure 4:20A). DA signalling from these neurons can modulate the putative amygdala/striatum, the thalamus and the hypothalamus (Figure 4:20A). Ablating subpallial DAergic neurons perturbs prey capture behaviour without affecting locomotion and prey tracking (Figure 4:20B). Loss of DA signalling to the thalamus (Figure 4:20B.1) could affect sensory processing of visual stimuli that influences the NMLF (Figure 4:20B.2) and reduces the pursuit of prey. Alternatively, Loss of DA signalling to the hypothalamus could affect motivational pursuit of prey (Figure 4:20B.3). Changes in activity of the hypothalamus can reduce the motivation to pursue prey by influencing the TeO (Figure 4:20B.4) and therefore perturb prey capture behaviour (Figure 4:20B.5). In mammals, disruption to the CeA-PAG-MLR pathway can attenuate prey capture behaviours. DA signalling from the VTA can influence CeA activity and subsequently affect prey capture behaviour by affecting motivational signals (Figure 4:19). If the subpallium of zebrafish is functionally equivalent to the extended amygdala, then subpallial DAergic neurons may be homologous to the VTA neurons and modulate these behaviours by influencing the motivational aspects of foraging.
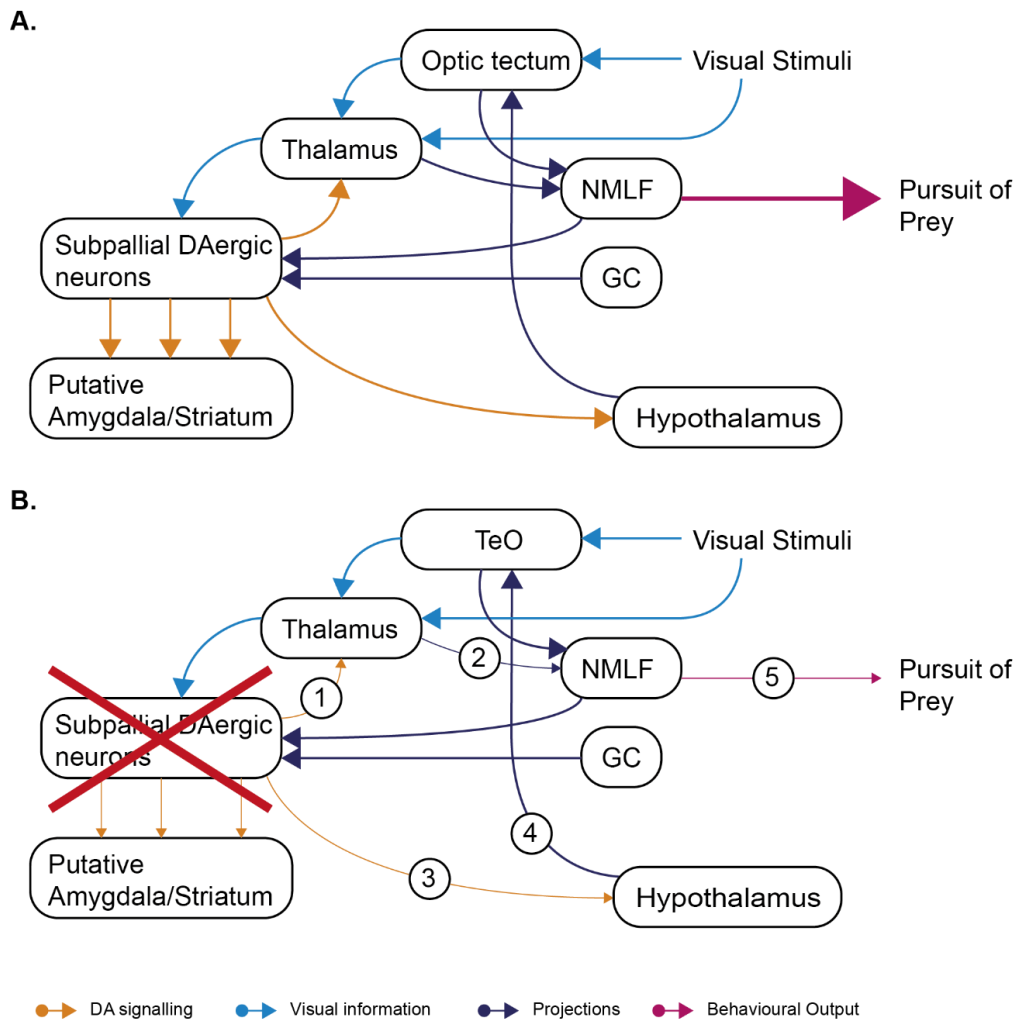
Figure 4:20 Schematic circuit of ascending visual system and the involvement of subpallial DAergic neurons. A - B: Schematic illustration of ascending visual system in zebrafish brain and the connectome of subpallial DAergic neurons. **A:** Visual information is relayed indirectly to the subpallial DAergic neurons by the thalamus. The thalamus receives input from the subpallial DAergic neurons to modulate the thalamus activity. Downstream signalling from the TeO and thalamus can influence motor output via the NMLF to pursue prey. **B:** Ablating subpallial DAergic neurons abolishes DA input to the putative amygdala/striatum, the thalamus (1) and the hypothalamus (3). Lack of DA signalling to the thalamus could affect sensory processing and change the thalamic influence of the NMLF (2) and subsequently perturbed the pursuit of prey (5). The lack of subpallial DAergic neurons reduces the DAergic input to the hypothalamus, which projects to the TeO and can influence prey capture behaviour. The flow of foraging related information across the brain of visual information (blue line), connections between nuclei (purple), DA transmission (orange) and locomotor output (magenta). Abbreviation: GC; griseum centrale, NMLF; nucleus of the medial longitudinal fasciculus, TeO; optic tectum, T; Thalamus, derived from Mueller, (2012), Rink and Wullimann (2002) and Tay et al., (2011).

4.4.4 Conclusion

In sum, the findings presented in this chapter suggest that subpallial DAergic neurons are active and release DA in the presence of live prey. Moreover, selective ablation of subpallial DAergic neurons significantly perturbed prey capture behaviours, reducing the probability of hunting-related locomotion without affecting prey tracking. Thus, the role of subpallial DAergic neurons may be to initiate or facilitate prey capture behaviours, possibly via provision of motivation signals to the extended amygdala.

.

CHAPTER

5

Delineating the Functional Role of Subpallial Dopaminergic Neurons in the Processing of Aversive Stimuli

5.1   Introduction

Startle behaviours are fast motor responses to sudden and intense stimuli which protect organisms from injury or predation. Startle behaviours can be seen in occur across several species ranging from humans to rodents and zebrafish (Koch, 1999). In mammals, startle behaviour can be evoked by acoustic, tactile and visual stimuli (Koch, 1999) and is driven by relatively simple circuits in the brainstem (Meloni and Davis, 1999, Lee et al., 1996). Studies have shown that startle reflexes can be modulated by fear-potentiated stimulation which is dependent on the amygdala (Zhao and Davis, 2004, Hitchcock and Davis, 1986). Moreover, DA transmission modulate startle reflexes in mammals (Meloni and Davis, 2000a).

Zebrafish startle behaviours are evoked by acoustic, touch, visual and olfactory stimuli and are characterised by series of high-velocity, highly stereotyped manoeuvres (Budick and Malley, 2000, Zeddies and Fay, 2005, Temizer et al., 2015). Several studies have shown that the subpallium, the putative striatum and extended amygdala, is activated by stimuli that elicit startle responses (Ganz et al., 2012, Perathoner et al., 2016, O'Connell and Hofmann, 2011, Randlett et al., 2015, Heap et al., 2018b, Vanwalleghem et al., 2017). This suggests the subpallium may be involved in the processing of aversive stimuli. The DAergic neurons of the zebrafish subpallium innervate the telencephalon, thalamus and hypothalamus (Tay et al., 2011) which have been shown to be activated by aversive stimuli (Randlett et al., 2015, Heap et al., 2018b, Vanwalleghem et al., 2017).Therefore, subpallial DAergic neurons could modulate these regions and the startle responses of zebrafish. However, to date, experiments have not addressed the involvement of subpallial DAergic neurons in startle behaviours.

In this chapter, I selectively ablate subpallial DAergic neurons so that their role in processing of aversive stimuli can be examined. Furthermore, I also ask how subpallial DAergic neuron firing is influenced by stimuli that evoke startle responses in zebrafish.

5.1.1 The mammalian fear and startle response

Fear is defined as defensive behavioural responses to threatening stimuli (Silva et al., 2016). The neural circuitry involved in detecting threatening stimuli include the sensory and association cortices which provide input into the lateral and central amygdala. In addition, inputs from the thalamus also to promote or decrease fear responses (Tovote et al., 2015). Startle behaviour is a fast-innate response to an unexpected intense stimulus (Koch, 1999). Silva and colleagues discussed three circuits (Figure 5:1) that mediate fear response in animals which include the detection, the integration and the output circuits (Silva et al., 2016). In mammals, these neural circuits elicit the escape behaviours via the PAG (Silva et al., 2016).
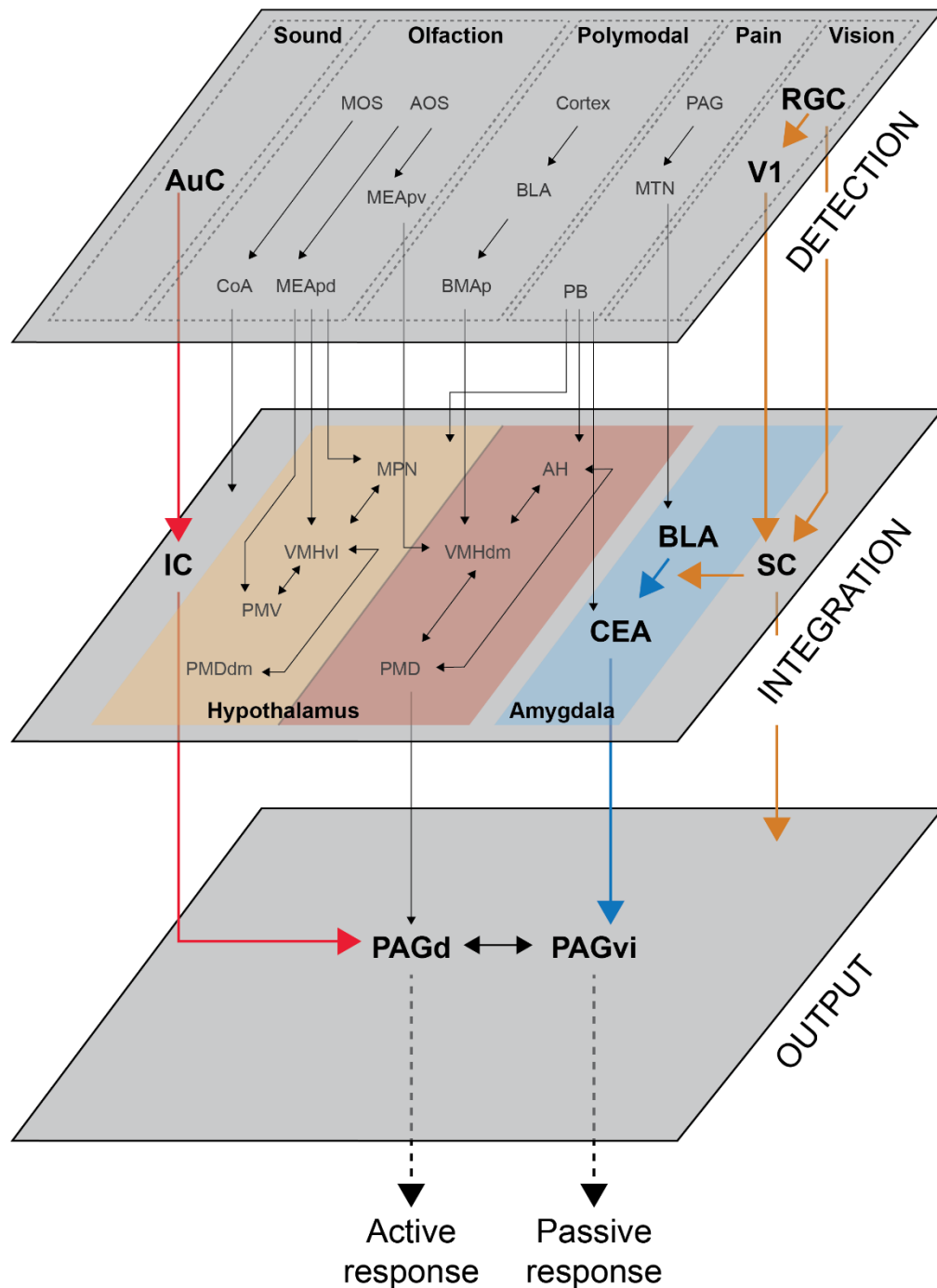
Figure 5:1 Schematic illustration of the neural circuits that mediate auditory and visual fear responses in mammals. Three units process fear, detection (upper panel), integration (middle panel) and an output unit (lower panel). Sensory information regarding a threat is collected via different sensory organs. Auditory stimuli (red line) are processed by the auditory cortex (AuC) and relayed to the inferior colliculus which projects to the dorsal region of the periaqueductal gray (PAGd). Whilst visual information (orange line) is relayed from retinal ganglion cells (RGC) directly to the superior colliculus (SC) and indirectly via the visual cortex (V1). Visual information is sent directly into the spinal cord to mediate a behavioural response or via the amygdala. Olfactory stimuli are processed by the main and accessory olfactory system (MOS and AOS,

respectively). Signals are relayed to the hypothalamus via the cortical amygdala (CoA) and medial amygdala (MEA). The fear circuit processes polymodal sensory information regarding a threat via the basolateral amygdala (BLA) and the basomedial amygdala (BMA), which integrates the information in the hypothalamic circuits. Pain is relayed via the PAG and midline thalamic nuclei (MTN) to the BLA, as well as the via the parabrachial nucleus (PB) to the CeA. The PAG receives information about multiple threats from the amygdala circuits (blue line) is the primary output for eliciting a behaviour. Redrawn from Silva et al., (2016).

5.1.1.1   The acoustic startle response in mammals

The acoustic startle reflex (ASR) is an innate defensive behavioural response to sudden, loud acoustic stimuli (Hormigo et al., 2018). The ASR has been studied in mammals, and the neural circuit that drives this behaviour is composed of the cochlear root neurons (CRNs), nucleus reticularis pontis caudalis (PnC) and motor neurons (Lee et al., 1996, Meloni and Davis, 2000b). Intense auditory stimuli is relayed to the ventrocaudal aspect of the PnC via the CRNs, which activate motor neurons via the reticulospinal network (Yeomans and Frankland, 1995, Gao et al., 2015). These neural circuits also integrate auditory information from the auditory cortex via the inferior colliculus (Chen et al., 2018).

DA transmission has been shown to modulate startle behaviour in mammals (Lewis and Gould, 2003, Meloni and Davis, 1999). The SNc projects directly to the PnC and indirectly to the pedunculopontine tegmental nucleus (PPTg) (Hormigo et al., 2018). The PnC is critical for the primary ASR, whilst the PPTg is involved in the regulation of motor output (Mori et al., 2016, Lee et al., 1996). Studies have shown that chemogenic ablation of SNc DAergic neurons affects the ASR kinetics, including response latency (Hormigo et al., 2018). This suggests that DA transmission from the SNc is involved in modulating the neural circuits that directly drive the ASR. Modulating DA transmission by the application of DA receptor agonists and antagonists also influence the ASR. The systematic application of D_1 receptor agonists can enhance the ASR amplitude (Meloni and Davis, 1999). However, deletion of the D_1 receptors revealed that D_1 KO mice have amplified ASR sensitivity (Halberstadt and Geyer, 2009). Together, this shows that either activation or disruption of D_1 receptor signalling in this region evokes similar behavioural responses.

Whilst the ASR is triggered by a relatively simple circuit that processes auditory information, it can be modulated/enhanced by the indirect pathway, in which the inferior colliculus receives input from the auditory cortex and influences the PAG to modulate reflexes (Winer et al., 2002, Winer et al., 1998) (Figure 5:1). Optogenetic activation of either the corticofugal neurons of the auditory cortex or inferior colliculus can initiate escape responses in rodents, whilst optogenetic inhibition has the opposite effect (Xiong et al., 2015). Additionally, optogenetic activation of inferior colliculus neurons projecting to the dorsal PAG can evoke escape behaviours (Xiong et al., 2015). The CeA modulates the ASR by indirectly innervating the PnC via the PAG, lesions to either the CeA or PAG block sensitisation of the ASR in footshock studies (Fendt et al., 1994). Additionally, lesions to the PAG can abolish the fear-potentiated startle reflex (Walker and Davis, 1997), suggesting the PAG is critical for indirect enhancement of the startle reflex. Interestingly, intra-amygdaloid infusions of D_1 antagonists can block the acquisition of fear-potentiated startle behaviours (Greba and Kokkinidis, 2000). Similarly, chemogenic lesions to the VTA blocked fear-potentiated startle responses (Borowski and Kokkinidis, 1996). Together, this suggests DA transmission to the amygdala can modify startle responses in mammals.

The ASR can be inhibited by prior exposure to weak stimuli, a phenomenon known as prepulse inhibition (PPI). Sensory input that mediates non-startling acoustic or visual stimuli is relayed to both inferior and superior colliculi. In turn, these structures activate the PPTg which then inhibits the PnC (Fendt et al., 2001). Since the PnC activates the reticulospinal system, inhibition of this structure via the PPTg results in the inhibition of the startle response, and lesions to the PPTg can reduce PPI without affecting startle amplitudes (Swerdlow and Geyer, 1993). DA transmission in the NAc has been shown to be a modulator of PPI (Zhang et al., 2000). The NAc innervates the PPTg directly and indirect via the ventral pallidum (Koch, 1999). Deficits in PPI can be induced by intra-accumbal infusion of DA agonist and rescued by the application of the DA receptor antagonist, haloperidol (Swerdlow et al., 2016, Swerdlow et al., 1994). In sum, DA signalling can modify startle behaviour by modulating PPI via the NAc or enhancing the ASR by fear-potentiated startling via the amygdaloid circuits.

5.1.1.2   Detection, processing and triggering the visually evoked startle response

Rodent escape behaviours are influenced by the contrast, speed and direction of looming stimuli (Yilmaz and Meister, 2013). Visual cues are detected by the retinal ganglion cells (RGCs), which are relayed directly to the superior colliculus and indirectly via the primary visual cortex (Figure 5:1). Visual information is relayed from RGCs to several structures, either directly to the superior colliculus or indirectly via projections to the dorsal lateral geniculate nucleus (LGN) of the thalamus, and subsequently to the primary visual cortex and superior colliculus (Ahmadlou et al., 2018, Yamasaki and Krauthamer, 1990). The visual cortex processes visual information to generate an image, whilst the superior colliculus is involved in sensorimotor integration and mediates reflexive approach and avoidance behaviours (Westby et al., 1990, Cohen and Castro-Alamancos, 2010). The superior colliculus receives input from visual nuclei including the ventral LGN and the visual cortex; as well as auditory centres such as the auditory cortex, inferior colliculus and lateral lemniscus (Cadusseau and Roger, 1985). In addition to these regions, the superior colliculus is innervated by the thalamus, hypothalamus and motor cortices (Cadusseau and Roger, 1985). There are three efferent pathways of the superior colliculus, known as the ascending and descending ipsilateral tectopontine-tectobulbar tracts and the contralateral descending or crossed tectospinal tract (Dean et al., 1988, Harting, 1977).

The superior colliculus receives a range of sensory and motor input and is critical for visually evoked startle/escape behaviours (Liu et al., 2011, Ito and Feldheim, 2018), and a subpopulation of neurons in the superior colliculus receives input from both visual and auditory cortices which drive escape behaviours in rodents (Zingg et al., 2017). Superior colliculus neurons exhibit speed tuning to looming stimuli (Zhao et al., 2014). Optogenetic inhibition of the superior colliculus modulates the visual cortex and pathways to the lateral posterior nucleus, influencing size tuning of these neurons (Ahmadlou et al., 2018). Moreover, a recent investigation revealed that the superior colliculus is necessary for the processing of visual stimuli and optogenetic activation of superior colliculus projections to the thalamus is sufficient to trigger behaviours similar to visually

evoked fear response (Wei et al., 2015). Inactivation of the cortical projections to the superior colliculus is sufficient to attenuate superior colliculus dependent visually evoked fear response (Liang et al., 2015). Therefore, the superior colliculus integrates sensory information and relays to other nuclei in the brain.

The amygdala is a major component for the processing of sensory information and eliciting fear responses (Martinez et al., 2011, Shackman and Fox, 2016, Fox and Shackman, 2019, Newman, 1999, Trimble and Van Elst, 1999, Fendt et al., 1994). The amygdala receives sensory information directly from the superior colliculus or indirectly via a non-canonical thalamic pathway (Wei et al., 2015). Activation of the superior colliculus – amygdala pathway can elicit escape behaviour in rodents, whilst lesions to the amygdala can abolish the visually-evoked escape responses (Shang et al., 2015, Wei et al., 2015). This suggests that visual information relating to threatening stimuli is relayed to the amygdala via the superior colliculus. Interestingly, lesions to the lateral posterior nucleus of the thalamus blocks colliculus – amygdala mediated behaviours while optogenetic activation of the thalamus mimics visually evoked fear responses (Wei et al., 2015). This shows that visual information is indirectly relayed to the amygdala via the thalamus. Yuan and colleagues have suggested a model of contextualising fear via thalamic relay of visual information to the cortex and superior colliculus which process and contextualise visual information and subsequently send this information to the amygdala which triggers fear responses (Yuan and Su, 2015). Taken together, these observations suggest that visual stimuli can trigger defensive or startle behaviour in mammals. Sensory information is relayed to the amygdala via the multiple pathways to elicit the appropriate behavioural response, and the amygdala is crucial for processing of threatening stimuli.

5.1.1.3 Integration of threat cues

Threatening cues are conveyed to downstream regions, including the hypothalamus and amygdala. The mammalian hypothalamus integrates sensory information regarding predatory threats and has been shown to be involved in mediating defensive behaviours: in rodents optogenetic activation of the ventromedial hypothalamic projections to the PAG induces freezing like

behaviours (Wang et al., 2015, Silva et al., 2016) while activation of the ventromedial hypothalamic projections to the anterior hypothalamic nucleus can induce avoidance behaviours in mammals (Wang et al., 2015).

The amygdaloid nuclei are critical for eliciting fear responses (Martinez et al., 2011, Shackman and Fox, 2016, Fox and Shackman, 2019, Newman, 1999, Trimble and Van Elst, 1999). The amygdala receives visual information via a thalamo-amygdalo-collicular feedback circuit (Marsh et al., 2002). Lesions to the amygdala can abolish escape responses to predator cues (Martinez et al., 2011), while lesions to the extended amygdala can abolish conditioned freezing behaviour (Nader et al., 2001, Zimmerman et al., 2007

). Visually evoked fear responses are processed by thalamo-amygdalo-collicular circuitry, information from the superior colliculus is relayed to the amygdala via the thalamus and lesions to the amygdala block visually evoked fear responses in rodents (Wei et al., 2015).

The mammalian amygdala and striatum receive DAergic input from the VTA and SNC (Gerfen and Surmeier, 2011, Lammel et al., 2011, Lammel et al., 2014, Hasue and Shammah-Lagnado, 2002). Nonetheless, the role of DA signalling and aversive stimuli is controversial. Historically, DAergic transmission in the NAc is associated with rewarding stimuli. Recent studies have shown the NAc projecting DAergic neurons from the VTA increase in activity in response to the presentation of aversive stimuli (Matsumoto and Hikosaka, 2009, Soares-Cunha et al., 2016a, Yoshimi et al., 2015, Schultz et al., 2017). Release of DA in the NAc shell increases when exposed to fear-evoking cues (Badrinarayan et al., 2012). The DAergic neurons of the ventral VTA are activated in response to aversive stimuli (Brischoux et al., 2009). DAergic neurons innervating the mPFC and NAc lateral shell increase in activity to aversion (Lammel et al., 2011). The NAc core and shell are composed of both D1 and D2-MSNs (Zahm, 1999). Excitation of D1-MSNs in the ventral NAc shell can elicit aversive behaviours, whilst activation of the dorsal NAc shell induced positive reinforcement of behaviours (Al-Hasani et al., 2015).

As mentioned previously, the amygdala is involved in the fear-potentiated startle reflexes (Fendt et al., 1994, Walker and Davis, 1997, Greba and Kokkinidis, 2000,

Borowski and Kokkinidis, 1996). Subpopulations of VTA DAergic neurons are excited when exposed visually aversive stimuli (Bromberg-Martin et al., 2010, Horvitz et al., 1997). Blocking DA signalling in the amygdala can attenuate fear-potentiated startle behaviour (Borowski and Kokkinidis, 1996, Greba and Kokkinidis, 2000, Greba et al., 2001, Lamont and Kokkinidis, 1998), and freezing and startling behaviours can be abolished by D_1 receptor antagonists (Lamont and Kokkinidis, 1998, Guarraci et al., 1999a, Guarraci et al., 1999b), while D_2 receptor agonism in the extended amygdala induces fear responses to threats (De Bundel et al., 2016). Interestingly, disruption to DA signalling to the CeA can attenuate the PPI, suggesting DA is involved in sensorimotor gating in the amygdala (Alsene et al., 2011). Together, this suggests DA signalling in the amygdala can modulate behavioural responses to threatening stimuli by influencing sensorimotor gating.

In sum, the amygdala receives visual and auditory input and is critical for processing threatening stimuli which. Activation of the superior and inferior colliculi is associated with the detection and processing of visual and auditory stimuli, respectively. These subcortical regions can modulate DA transmission to the amygdala and striatum which can modulate aversive behaviours in mammals.

5.1.1.4 Behavioural output of fear response

Threatening stimuli can elicit fear responses in animals; however, these responses can be highly variable. Some stimuli can elicit an innate fear response and directly trigger an avoidance behaviour such as flight or freezing. The PAG is found in the midbrain and co-ordinates behaviours by influencing sensory circuits and motor output (Koutsikou et al., 2015). Lesions to the PAG reduces both passive and active escape behaviours (Behbehani, 1995). In humans, startling stimuli can increase activity in the thalamo-PAG loop and the insular cortex (Lindner et al., 2015, Wu et al., 2014, Rinvik and Wiberg, 1990).

Reciprocal connections have been observed between the PAG and amygdala (Sun et al., 2019, Rizvi et al., 1991, Tupal and Faingold, 2012). The ventral PAG mediates passive escape responses, including freezing behaviour (Ullah et al., 2015), whilst the dorsal PAG mediates active escape behaviours such as flight

(Ullah et al., 2015). Stimulation of the dorsal PAG can evoke innate fear responses (Kim et al., 2013)and lesions to the amygdala blocks this PAG-mediated behaviour (Kim et al., 2013).

In sum, threatening stimuli are detected by multiple nuclei in the brain. These nuclei relay various forms of visual, auditory, olfactory and nociceptive information to critical neural circuits that convey threats. Structures including the amygdala, striatum and thalamus receive input regarding threats and these circuits determine if a stimulus is a threat and what the appropriate response is. DA has been shown to modulate these neural circuits and influence behavioural responses to aversive stimuli.

5.1.2   The zebrafish startle response

The zebrafish startle behaviour consists of a series of high-velocity manoeuvres (Figure 5:2) that allow this animal to escape predation and can be evoked by acoustic, touch, visual and olfactory stimuli (Budick and Malley, 2000, Zeddies and Fay, 2005, Temizer et al., 2015). Acoustic stimuli can evoke startle behaviours in zebrafish from 3 dpf, but a robust response can be observed from 4 dpf onwards (Roberts et al., 2011, Zeddies and Fay, 2005). Startle responses can also be evoked visually by looming stimuli (Temizer et al., 2015; Bhattacharyya et al., 2017).

Zebrafish exhibit a range of escape responses to evade threats; the most widely studied being the 'C-start'. This is composed of an initial tail bend, followed by a counter bend and subsequent escape swimming (Figure 5:2C) (Budick and Malley, 2000, Zeddies and Fay, 2005, Roberts et al., 2011). The initial bend of the body resembles a "C" shape and is driven by Mauthner cells of the reticulospinal system (Kalueff et al., 2013, Liu et al., 2012). Another startle response is known as an S-start (Kalueff et al., 2013, Liu et al., 2012). During an S-start, Mauthner cells are bilaterally activated and the latency between the ipsilateral and contralateral Mauthner cell to the stimulation drives which "S" shape body bend (Liu and Hale, 2017) (Figure 5:2D).

A.
Standard Turn

0s --→ 80ms

B.
O-bend

0s --→ 40ms

C.
C-start

0s ------------------------------→ 12ms

D.
S-start

0s ------------------------------→ 12ms
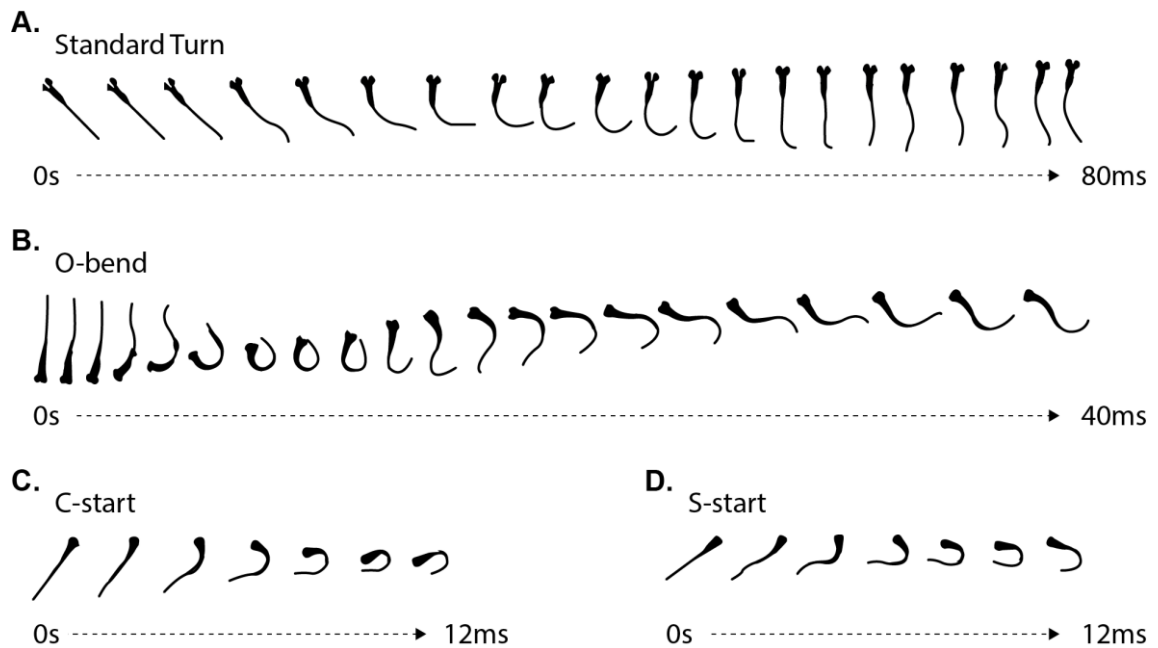
Figure 5:2 Swimming manoeuvres of larval zebrafish. A: Example of routine turn, illustrating small-angle bend and angular velocity over a long duration. **B:** Example escape response with 180º reorientation resembling "O" shape. **C:** Illustration of C-start escape response, high angular velocity and bend in body axis resembles "C" shape. **D:** Example of S-start escape response, and initial body bend resembles "S" shape characterised by rostral and caudal bends on opposing sides of the body. Adapted/redrawn from Liu et al., (2012), and Budick and Malley (2000).

5.1.2.1   Neural circuits of the zebrafish startle responses

The zebrafish startle response is primarily driven by hindbrain reticulospinal neurons (Hale et al., 2016) (Figure 5:3A). The hindbrain is divided into seven segments, with neurons within each segment possessing homologous morphology. The Mauthner cells are located within the 4th segment (Nakayama and Oda, 2004). In the 5th and 6th segment are Mauthner homologs called MiD2cm and MiD3cm (Nakayama and Oda, 2004). Mauthner cells and their homologs project contralaterally and descend into the spinal cord (Becker et al., 1997, Barry and Bennett, 1990, Hale et al., 2016) (Figure 5:3A). These reticulospinal cells receive auditory input from the cranial nerve VIII, and visual information from the optic tectum (Hale et al., 2016, Nakayama and Oda, 2004) and also receive mechanosensory information from Rohon-Beard neurons, sensory neurons found in dorsal spinal cord of larval zebrafish (Reyes et al., 2004, Palanca et al., 2013). Interestingly, Rohon-Beard neurons are embryonic

sensory neurons that undergo apoptosis and are only present in larval zebrafish (Reyes et al., 2004, Williams et al., 2000, Kanungo et al., 2009). The somatosensory function of Rohon-Beard neurons is replaced by the dorsal root ganglion (DRG) in older zebrafish (Williams et al., 2000, Honjo et al., 2011, McGraw et al., 2008). In addition to the DRG, the lateral line detects vibrations in water and sends tactile sensory information to the reticulospinal neurons (Olt et al., 2016a, Olt et al., 2016c, Olt et al., 2016b, Kohashi and Oda, 2008, Reyes et al., 2004).

Mauthner cells and their homologs are regulated by interneurons located in the hindbrain (Koyama et al., 2011, Hale et al., 2016) (Figure 5:3A). Mauthner cells are directly innervated by passive hyperpolarizing potential commissural (PHPcom) cells located in the rhombomere 4 of the hindbrain (Hale et al., 2016). PHPcom cells receive input from cranial nerve VIII and act as glycinergic inhibitory feed-forward neurons that inhibit Mauthner cells by hyperpolarisation (Koyama et al., 2011, Zottoli et al., 1987, Zottoli and Faber, 2000). Mauthner cells are also indirectly regulated by cranial relay neurons as part of a feedback loop (Koyama et al., 2011, Zottoli and Faber, 2000). Cranial relay neurons are excitatory, cholinergic neurons that are activated by Mauthner cells and synapse onto contralateral PHP neurons (PHPcol), providing inhibitory feedback (Koyama et al., 2011). The Mauthner cells are also regulated by contralateral spiral fiber neurons (SFNs), which are excitatory interneurons that directly innervate Mauthner cells (Koyama et al., 2011, Hale et al., 2016). Ablating SFNs largely abolishes Mauthner cell-dependent escape responses (Lacoste et al., 2015), suggesting they facilitate escape behaviour. Together, these interneurons regulate Mauthner cell activity to drive unilateral muscle activity during escape behaviour.

A.

B.
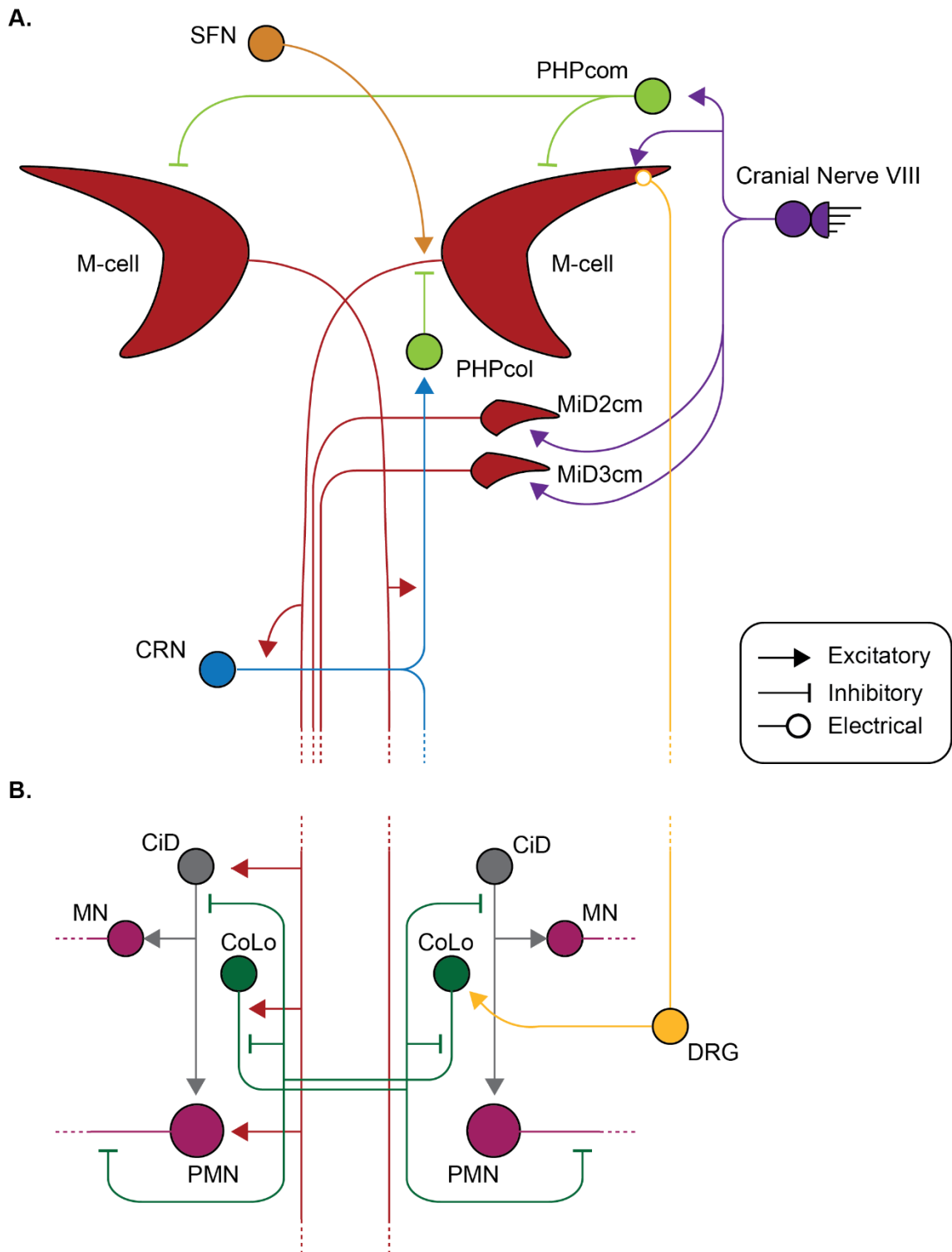
Figure 5:3 Schematic illustration of hindbrain and spinal cord circuitry for escape responses. A: Schematic illustration of the hindbrain circuitry that drives the Mauthner cell-dependent escape response. **B:** Illustration of the spinal cord circuity that drives Mauthner cell-dependent escape response. Abbreviations: SFN, Spiral fibre neurons; CRN, cranial relay neuron; DRG, dorsal root ganglion; PHPcol, passive hyperpolarizing potential collateral neuron; PHPcom, passive hyperpolarizing potential commissural neuron; PMN, primary motor neuron; MN,

motor neurons; CiD, Circumferential Descending; CoLo, Commissural local; M-cell, Mauthner Cell. Adapted from Hale et al., (2016).

Mauthner cells project to the contralateral spinal cord and provide glutamatergic excitation to circumferential descending (CiD) interneurons, commissural local (CoLo) interneurons and primary motor neurons (PMN; Figure 5:3B). CiDs are ipsilateral descending excitatory premotor interneurons that innervate both PMNs and secondary motor neurons (SMN) (Bhatt et al., 2007, McLean et al., 2007, McLean and Fetcho, 2009, Ritter et al., 2001). Ritter and colleagues suggest CiD activity may drive the initial bend of the escape response (Ritter et al., 2001). Furthermore, CoLo are inhibitory interneurons that project to the contralateral spinal cord and, when activated, inhibit contralateral PMNs and CiDs (Satou et al., 2009). Thus, stimulation of the Mauthner cells activates contralateral CiDs and CoLo, subsequently driving contralateral motor neuron activation, whilst simultaneously inhibiting cells of the ipsilateral spinal cord (Figure 5:3B). The resulting locomotion is a fast bend on the opposite side to the stimulated Mauthner cells.

Activation of Mauthner cells and their homologs drives escape behaviour in zebrafish (Kohashi and Oda, 2008, Troconis et al., 2017, Burgess and Granato, 2007a, Burgess and Granato, 2007b). Zebrafish C-starts are highly stereotyped (Budick and Malley, 2000) and comprise a characteristic tail bend (C-bend) followed by counter-bend that establishes the trajectory of the escape manoeuvre (Figure 5:2C). Mauthner cells and their homologs receive the same sensory information (visual, auditory and tactile), but differences in output to the spinal circuitry allow for an adaptive escape response (Nakayama and Oda, 2004). Auditory evoked C-starts have a bimodal distribution in the latency, bend angle, duration and angular velocity of the C-start (Burgess and Granato, 2007b). Based on these kinetics, zebrafish C-starts are divided into two categories, either short-latency C-start (SLC) and Long-latency C start (LLC) (Troconis et al., 2017, Burgess and Granato, 2007b). SLC response is driven by the Mauthner cells, whilst the LLC response is initiated the Mauthner cell homologs; MiD2cm and MiD3cm (Liu and Fetcho, 1999, Kohashi and Oda, 2008). It has been shown that C-start escape responses persist Mauthner cells are ablated. However, in this scenario, only LLC responses persist (Liu and Fetcho, 1999). This suggests that

Mauthner cells are required for SLC responses. By contrast, MiD2cm, and MiD3cm are active during LLC responses and ablating the Mauthners and their homologs attenuates both SLC and LLC responses (Kohashi and Oda, 2008). This suggests that LLCs are dependent of Mauthner cell homologs.

C-start escape responses have been shown to exhibit short term habituation (Roberts et al., 2011). SLC circuitry can exhibit habituation: exposing zebrafish to repetitive acoustic stimuli attenuates SLC responses and is associated with the suppression of Mauthner cells activity (Takahashi et al., 2017). However, the habituation of Mauthner cells has no effect on LLC responsiveness (Takahashi et al., 2017). A recent investigation has suggested the decision-making process to select the appropriate startle response is dynamic and dependent on previous experience as well as stimulus interpretation (Jain et al., 2018). Repetitive exposure to an acoustic stimulus can shift the bias from SLC to LLC response in larval fish (Jain et al., 2018). Therefore, examination of SLC – LLC in zebrafish can be used to study sensorimotor gating and decision-making behaviours.

The S-bend is another startle response displayed by zebrafish, characterised by the "S" shape bending of the body (Kalueff et al., 2013) (Figure 5:2D). Electrical stimulation of the tail of a zebrafish fish can elicit both S and C-start escape responses (Liu et al., 2012). During an S-start, Mauthner cells are bilaterally active, unlike a C-start during a touch evoked escape response (Liu and Hale, 2017). The proposed neural circuitry of S-start is that tail stimulation activates the lateral line, DRG, or Rohon-Beard cells which extend ascending projections to the Mauthner cells (Liu and Hale, 2017, Palanca et al., 2013) (Figure 5:3B). The DRG innervates the Mauthner cells via an electrical synapse (Sillar, 2009). Additionally, Rohon-Beard cells innervate CoLo directly, inhibiting muscle activity (Liu and Hale, 2017). Together, tail stimulation during an S-start bilaterally activates Mauthner cells and the unilateral activation of CoLos in the tail results in the S-shaped swimming manoeuvre. The latency between the ipsilateral and contralateral Mauthner cell spiking determines which hemisphere of the spinal cord is inhibited to block motor output (Liu and Hale, 2017).

5.1.2.2   Visually evoked escape response.

The study of zebrafish startle behaviours has revealed several neural circuits that integrate sensory information to drive escape behaviours. As mentioned earlier, Mauthner cells and their homologs receive auditory and mechanosensory information and innervate spinal cord interneurons and motor neurons to drive escape behaviour (Koyama et al., 2011) (Figure 5:4 – Pathway 1). Similarly, visually evoked startle behaviours are relayed by the same premotor output circuits as mechanosensory startle responses (Budick and Malley, 2000, Zeddies and Fay, 2005, Temizer et al., 2015, Dunn et al., 2016a). Mauthner cells receive input from the optic tectum (Zottoli et al., 1987), and visual input can activate reticulospinal neurons to generate escape responses to threatening stimuli (Canfield, 2006, Bhattacharyya et al., 2017) (Figure 5:4 – Pathway 2). Visual threat is calculated by the size and approach velocity of an object: large or fast-moving objects are processed by neural circuits as potential threats, whilst smaller objects, slower approaching objects are processed as potential prey (Preuss et al., 2014). Startle behaviour can be triggered by the presentation of a looming stimulus of ≥10° (Barker and Baier, 2015). Therefore, the visual system of zebrafish must distinguish between objects based on size and approach velocity and relay this information to the premotor system to elicit escape behaviour. Object size discrimination is dependent on the retinotectal circuits (Preuss et al., 2014), and lesions to these circuits can impair escape responses to looming stimuli (Temizer et al., 2015).

RGCs are activated by objects of a specific size (Levick, 1967, Olveczky et al., 2003). RGCs of various cyprinid fish can be segregated base on their object direction as well as size tuning (Damjanović et al., 2019), in which these neuron only activate when an object travels in a specific direction or is a particular size. The optic tectum, a structure equivalent to the mammalian superior colliculus, integrates visual information (May, 2006) to elicit avoidance and approach behaviours (Barker and Baier, 2015). The tectum can be segregated in areas based on the input from specific RGCs that relay size specific information generating a topographical map of object size across the optic tectum (Preuss et al., 2014, Helmbrecht et al., 2018). The superficial layers of the tectum are

selective to small stimuli whilst responses to larger stimuli occur deeper in the tectal neuropil (Preuss et al., 2014).

The neural circuits that process looming stimuli are the contralateral optic tectum to the retina that detected the stimulus (Figure 5:4 – Pathway 2) (Dunn et al., 2016a). The presentation of a looming stimuli can activate the AF6 and AF8 regions of the optic tectum (Temizer et al., 2015). Since the neurons optic tectum exhibit size and speed tuning, objects that could be interpreted as a threatening stimuli such as the approach velocity and angular size can trigger escape response in larval zebrafish (Temizer et al., 2015). This occurs by projections from the optic tectum to the Mauthner cell on the opposite side of the body, ipsilateral to the stimulus (Dunn et al., 2016a) (Figure 5:4 – Pathway 2).

Dunn and colleagues propose a multi-modal convergence pathway for sensory information that drives escape behaviour. Here, looming stimuli are detected by RGCs and information relating to size and velocity are processed in the contralateral optic tectum (Figure 5:4 – Pathway 3) (Dunn et al., 2016a). The alternative startle response is more variable since stimulation can elicit postsynaptic potentials in both ipsilateral and contralateral Mauthner cells and their homologues (Zottoli et al., 1987), however, the neural pathway has not been fully described (Korn and Faber, 2005) (Figure 5:4 – Pathway 3). Marquart and colleagues have suggested prepontine neurons could initiate Mauthner cell alternative escape behaviours, which generate delayed escape responses with a highly variable escape trajectory (Marquart et al., 2019). Similar to Dunn and colleagues, Marquart have shown these prepontine neurons integrate both acoustic and visual information and have suggested they allow for a dynamic and flexible escape response.
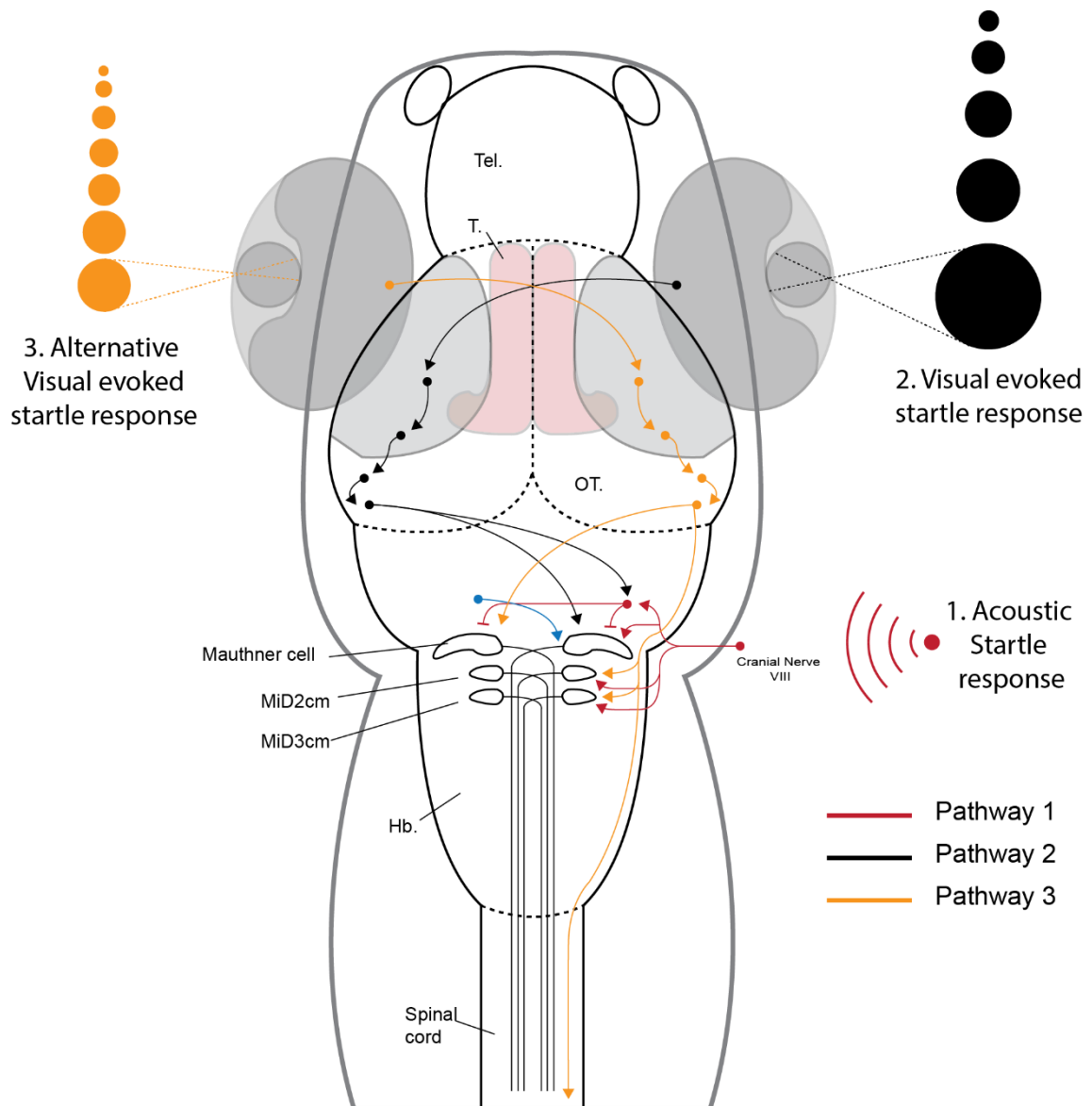
Figure 5:4 Proposed model for the flow of information to evoke startle behaviours in zebrafish. Schematic illustration of the hindbrain circuitry that drives the Mauthner cell-dependent escape response (pathway 1), the visual evoked startle response (pathway 2) and the alternative visually evoked escape behaviour (pathway 3). Adapted from Dunn et al., (2016) and Hale et al., (2016).

5.1.2.3 Ascending auditory and visual pathways

As mentioned earlier, Mauthner cells receive visual input via the optic tectum (Zottoli et al., 1987) as well as auditory and mechanosensory information from the otic capsule and lateral line (Eaton and Popper, 1995, Mirjany and Faber, 2011). However, sensory information, is also processed by forebrain structures

such as the thalamus (Randlett et al., 2015, Heap et al., 2018b, Vanwalleghem et al., 2017). In mammals the thalamus is a multi-nuclei structure that relays, modifies and filters sensory information across the brain (Mueller, 2012). The thalamus is a highly conserved structure across vertebrate including zebrafish (Lynn et al., 2015, Bandin et al., 2015, Schmitt and Halassa, 2017). Below, I will review the anatomical, genetic and functional studies of the ascending auditory and visual pathways in cyprinid fish, including zebrafish.

In zebrafish, the thalamus receives auditory and mechanosensory information (Mueller, 2012). Auditory information is relayed to the thalamus indirectly via the central nucleus of the torus semicircularis (TSc), a structure homologous to the IC in mammals (Mueller, 2012). The TSc receives auditory and mechanosensory input from the lateral line via the secondary octaval population (SOP), which is homologous to the mammalian superior olive (McCormick and Hernandez, 1996, McCormick, 1997). Both the TSc and SOP receive input via descending octaval nucleus (DON) and anterior octaval nucleus (AO) (Fame et al., 2006, Yamamoto et al., 2010b, Mueller, 2012) (Figure 5:5). A recent investigation using calcium imaging has shown the thalamus, along with the TSc and the octaval nuclei of larval zebrafish respond to auditory stimuli, suggesting the auditory pathways exist early in development (Vanwalleghem et al., 2017).

The cyprinid thalamus receives visual input from multiple areas including the optic tectum and direct input from the RGCs (Mueller, 2012, Henriques et al., 2019) (Figure 5:5). Additionally, information regarding looming stimuli has been shown to be relayed by the optic tectum to Mauthner cells, the hypothalamus and thalamus via different pathways (Yao et al., 2016, Mueller, 2012, Heap et al., 2018b). A recent investigation found that luminescence information is relayed via thalamo-tectal connections (Heap et al., 2018b). Selective ablation of these connections is sufficient to impair startle responses to the dark looming stimuli (Heap et al., 2018b), suggesting the thalamus is involved in the influencing responses to looming stimuli.

The thalamus is known to relay information to other brain regions, in cyprinids, it has been shown that this region processes auditory and visual information indirectly via the TSc and optic tectum, respectively (Mueller, 2012). The

thalamus projects to telencephalon, including the subpallium (Figure 5:5) (Rink and Wullimann, 2004, Rink and Wullimann, 2002a, Mueller, 2012). This suggests that the subpallium processes sensory information and studies have shown the pERK activity increases in the subpallium when zebrafish are exposed to auditory (Vanwalleghem et al., 2017), mechanosensory (Randlett et al., 2015) and visual stimuli (Heap et al., 2018b). Together, this suggests the subpallium is active in response to these stimuli and receives input from the ascending auditory and visual pathways, however, the role of the subpallium in processing auditory, mechanosensory and visual information has not been previously investigated. I have previously shown the subpallial DAergic neurons are active when presented with visual stimuli such as prey (see subsection 4.3.4).
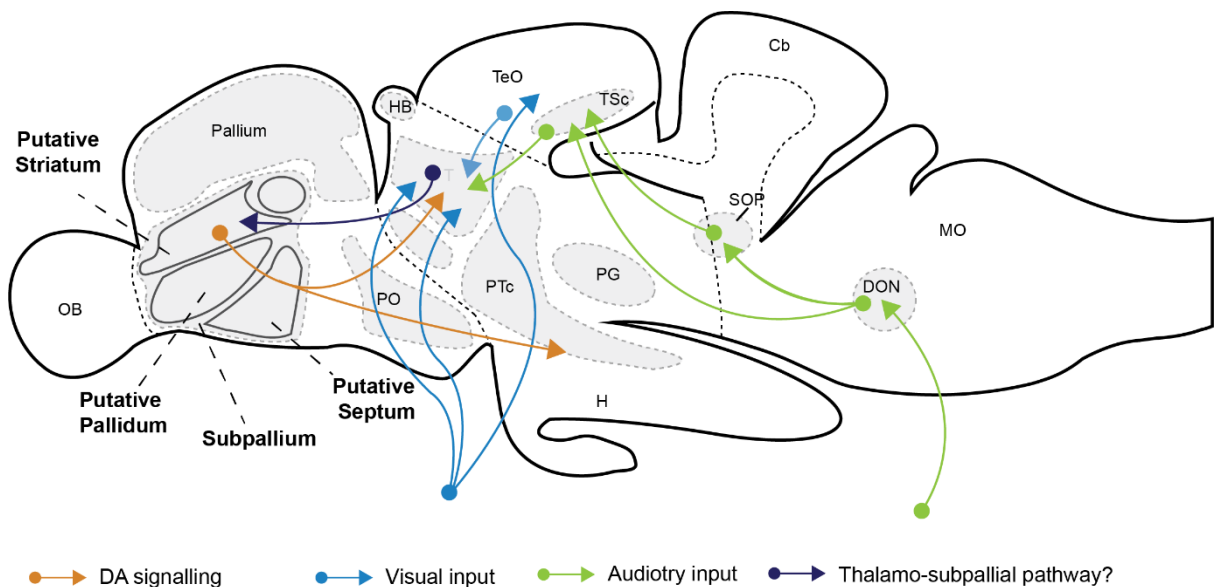
Figure 5:5 Ascending auditory and visual pathways in cyprinids. Schematic illustration of the sagittal cross-section of the zebrafish brain. Primary visual targets to the anterior thalamic nucleus (blue line) and the optic tectum (green) which is homologous to the mammalian superior colliculus. The dorsoposterior thalamic nucleus receives visual input from the TeO. The anterior thalamic nucleus projects to the subpallium/Vd providing visual information. The PG receives visual information from the Teo, which is relayed to the pallium. Abbreviation: A; anterior thalamic nucleus, CP; centroposterior thalamic nucleus, DP; dorsoposterior thalamic nucleus, Hb; habenular, Cb; Cerebellum, MO; Medulla, H; Hypothalamus, T; Thalamus, TeO; optic tectum, PO; preoptic region, PTc; posterior tuberculum, OB; olfactory bulb, Vd; dorsal, Vl; lateral, Vp; postcommissural, Vs; supracommissural, Vv; ventral zones of ventral telencephalon. Redrawn from Mueller, (2012).

5.1.2.4   Aminergic modulation of the zebrafish startle response

The study of DA transmission and the modulation of the zebrafish escape response is limited. TH-reactive projections have been observed close to dendrites of Mauthner cells and their homologues (McLean and Fetcho, 2004b). This suggests a potential interaction with DA input to the reticulospinal neurons. DA application can reduce repetitive firing of Mauthner cells (Curti and Pereda, 2010). A recent investigation found that exposing zebrafish to light flashes prior to acoustic stimulation can increase the chance of eliciting an acoustic-mediated C-start, a phenomenon which is driven by light-responsive DAergic neurons of the hypothalamus (Mu et al., 2012). Additionally, lesions to optic tectum can attenuate hypothalamic DAergic neuron responses to visual input (Yao et al., 2016). The acoustic-evoked startle response is modulated by D_1 receptor activity within the Mauthner cells, which enhances the signal to noise ratio of auditory signals (Mu et al., 2012). This shows DA transmission can modulate the activity of the reticulospinal neurons and subsequently the escape responses.

Whilst a recent study showed DA transmission could enhance startle behaviour, another study revealed a subpopulation of hypothalamic DAergic neurons positively regulate hindbrain inhibitory neurons during the presence of non-threatening stimuli, decreasing the probability of eliciting a visually evoked escape response (Yao et al., 2016, Mu et al., 2012). Thus, hypothalamic DAergic neurons activate inhibitory neurons that inhibit Mauthner cell activation. Together, these hypothalamic DAergic neurons both enhance and inhibit escape behaviour in zebrafish. An investigation into the role of other DAergic neurons and their influence of startle behaviour found chemogenic loss of DAergic of the pretectum and DDNs reduced spontaneous locomotion but did not affect visually evoked startle response (Stednitz et al., 2015). Together, this suggests specific groups of DAergic populations modulate startle behaviours by influencing the premotor system.

5.2   Aims and Objectives

The subpallium has been shown to be activated by mechanical, acoustic and visually aversive stimuli. However, the role of subpallial DAergic neurons in the processing of aversive stimuli has not been addressed. In mammals, the VTA has been shown to process aversive stimuli, and modulate the amygdala. Since it has been suggested the subpallial DAergic neurons are homologous to the midbrain DAergic neurons, if this is indeed the case, subpallial DAergic neurons could modulate aversive behaviours in zebrafish. I hypothesise that the subpallial DAergic neurons are activated by aversive stimuli and modulate startle behaviour. Using targeted laser ablation of subpallial DAergic neurons and behavioural paradigms, I examine the involvement of subpallial DAergic neurons in the acoustic evoked startle responses. Additionally I examined the role of subpallial DAergic neurons in visually evoked startle behaviours using looming stimuli that simulate an approaching virtual predator. Finally, I examined the firing activity of subpallial DAergic neurons when exposed to looming stimuli. The data presented in this chapter demonstrates that by 5 dpf, the subpallial DAergic neurons can selectively modulate long latency C-starts (LLC).

5.3   Results

5.3.1   Effects of selective loss of subpallial dopaminergic neurons on the acoustic startle response

Whole-brain mapping has revealed that the subpallium is active when zebrafish are exposed to aversive stimuli such as dish tapping (Randlett et al., 2015). Furthermore, a study found the subpallium was active in response to acoustic stimuli (Vanwalleghem et al., 2017). However, this study restrained the fish prior to acoustic stimulation, therefore, the escape response was not examined. Nonetheless, Vanwallenghem and colleagues presented zebrafish with acoustic stimuli (500Hz) that has been used to elicit robust escape responses in zebrafish (Zeddies and Fay, 2005, Troconis et al., 2017, Burgess and Granato, 2007b). Therefore, it could be assumed the subpallium activity in response to acoustic stimulation relates acoustically evoked escape responses, however, further experiments would be required to address this. Since regions of the subpallium are the putative striatum and extended amygdala (Mueller et al., 2008, Wullimann and Mueller, 2004, Perathoner et al., 2016, O'Connell and Hofmann, 2011), and these regions in mammals are known to process aversive stimuli and are modulated by DA signalling (Lamont and Kokkinidis, 1998, Guarraci et al., 1999a, Guarraci et al., 1999b), the subpallial DAergic neurons may be involved in acoustically evoked escape behaviour. Therefore, I aimed to determine if the subpallial DAergic neurons modulate aversive behaviours. Since auditory tone are another type of mechanosensory stimuli, I also examined acoustic startle responses to delineate the role of subpallial DAergic neurons in aversion.

There are multiple startle responses exhibited by zebrafish (section 5.1.2), as part of this study I focused on C-start escape behaviour. Figure 5:6A illustrates an acoustically evoked C-start in a 5 dpf zebrafish, which is composed of a C-bend (Figure 5:6B left panel), followed by a counter bend (Figure 5:6B right panel) and followed by escape swimming.
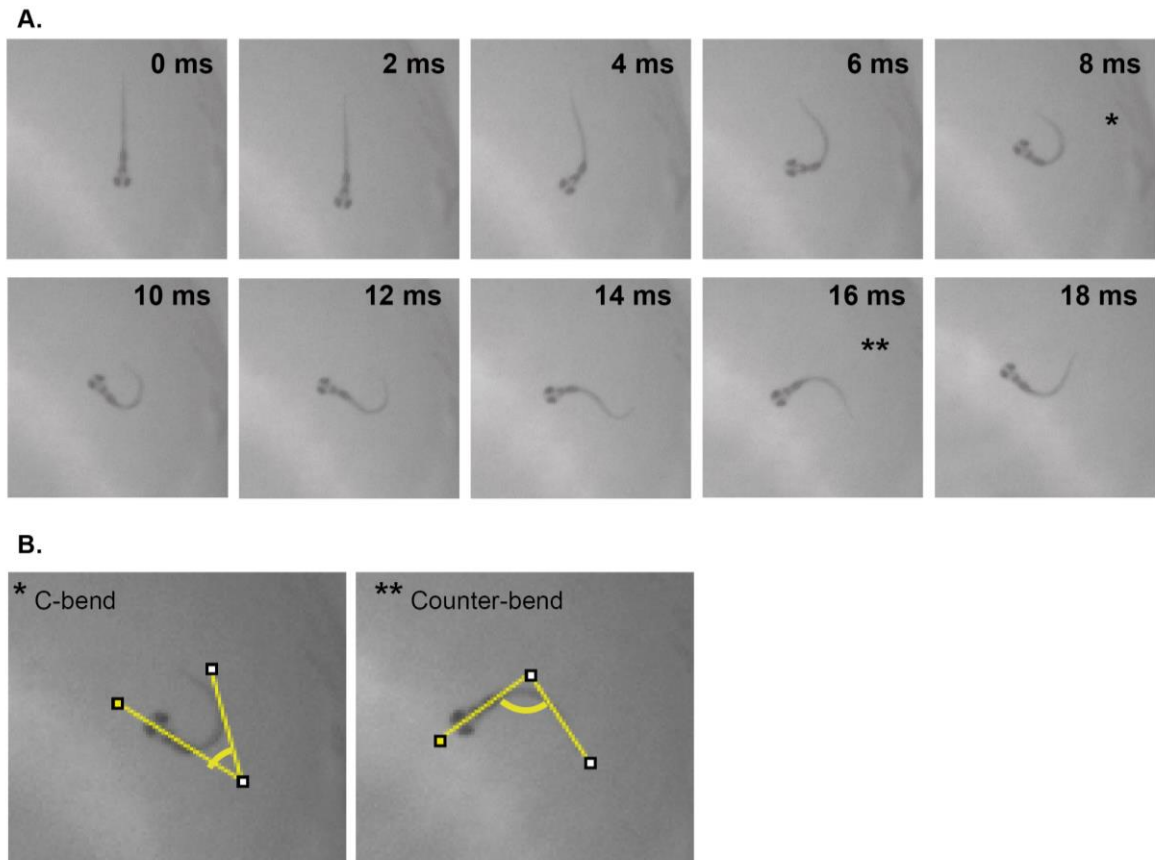
Figure 5:6 Example of acoustic startle response of larval zebrafish. A: Sequence of the acoustic startle response of 5 dpf zebrafish swimming trajectories of 5 dpf zebrafish, * = c-bend, ** = counter-bend. **B:** Example of c-bend (left panel) and counter-bend (right panel).

To determine the role of subpallial DAergic neurons in zebrafish startle behaviours, subpallial DAergic neurons were selectively ablated following procedures described in section 2.9. Subsequently, after recovery, these fish were exposed to a 500Hz acoustic pulse and C-start responses were analysed. When compared to non-ablated controls, ablated fish exhibited a shorter latency in evoked startle behaviours (control = 32.17 ± 37.29ms, $n_{fish} = 18$, $n_{events} = 40$, ablated = 11.1 ± 13.85ms, $n_{fish} = 13$, $n_{events} = 26$ p = 0.0001, Mann-Whitney U, Figure 5:7A). Examination of the startle response duration, measured from initial C-bend to the termination of escape swimming, revealed that ablation of subpallial DAergic neurons, resulted in shorter startle response durations (control = 0.156 ± 0.035s, $n_{fish} = 18$, $n_{events} = 40$, ablated = 0.120 ± 0.029s, $n_{fish} = 13$, $n_{events} = 26$, p = 0.0001, Unpaired t-test, Figure 5:7B). The velocity of the of startle

response did not differ between control and ablated fish (control = 22.55 ± 9.61mm/s, n_{fish} = 18, n_{events} = 40, ablated = 20.90 ± 9.36mm/s, n_{fish} = 13, n_{events} = 26, p = 0.4916, Unpaired t-test, Figure 5:7C). However, distance travelled during the startle response was reduced in ablated fish (control = 26.34 ± 8.71mm, n_{fish} = 18, n_{events} = 40, ablated = 20.76 ± 8.31mm, n_{fish} = 13, n_{events} = 26, p = 0.0155, Unpaired t-test, Figure 5:7D/E). Together, this suggests that fish lacking subpallial DAergic neurons have shorter response latency and a shorter-duration escape response.
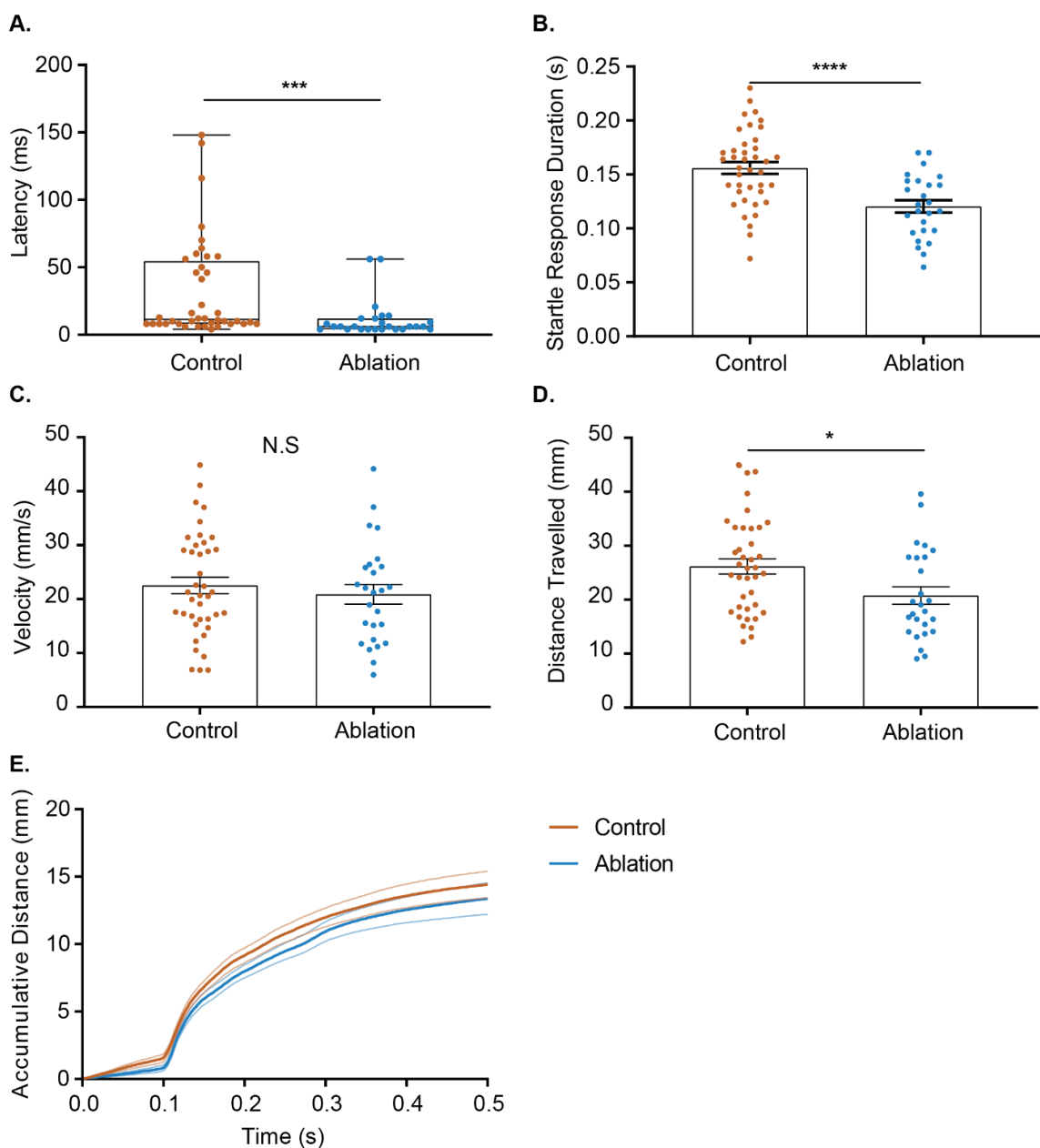
Figure 5:7 Acoustic startle behaviour kinetics are altered by the loss of subpallial DAergic neurons. A-E: Number of fish for each condition is control n_{fish} = 18, ablated n_{fish} = 13. **A:** Box and whisker plot comparing the latency of the acoustic startle response and duration of startle response **(B). C:** Comparison of the swimming velocity during the startle response. **D:** Box and whisker plot comparing the distance travelled from the initiation of the acoustic startle response. **E:** Cumulative distance travelled by control and ablated fish, the onset of stimulus at 0.1s. * = P < 0.05, *** = P < 0.0005, **** = P < 0.0001, N.S. = not significant.

Next, I sought to determine how kinematics of the escape response changes as a result of subpallial DA neuron ablation. Therefore, I analysed the kinetics of the C-bend and counter-bend components of the startle behaviour. The initial component of a C-start is a high-velocity bend in the body resembling a "C" (Kalueff 2013) (Figure 5:8A). Examination of the C-bend angle in both groups showed no difference (control = 42.25 ± 10.69⁰, n_{fish} = 18, n_{events} = 40, ablated = 42.46 ± 10.33⁰, n_{fish} = 13, n_{events} = 26, p = 0.9353, Unpaired t-test, Figure 5:8B). Subsequent analysis of the C-bend angular velocity also showed no change between the control and ablated groups (control = 12.63 ± 3.39⁰/ms-1, n_{fish} = 18, n_{events} = 40, ablated = 14.25 ± 3.72⁰/ms-1, n_{fish} = 13, n_{events} = 26, p = 0.072, Unpaired t-test, Figure 5:8C). The C-bend angular velocity had similar distribution in these groups (Figure 5:8D) suggesting the subpallial DAergic neurons do not modulate the motor response involved in generating the C-bend.
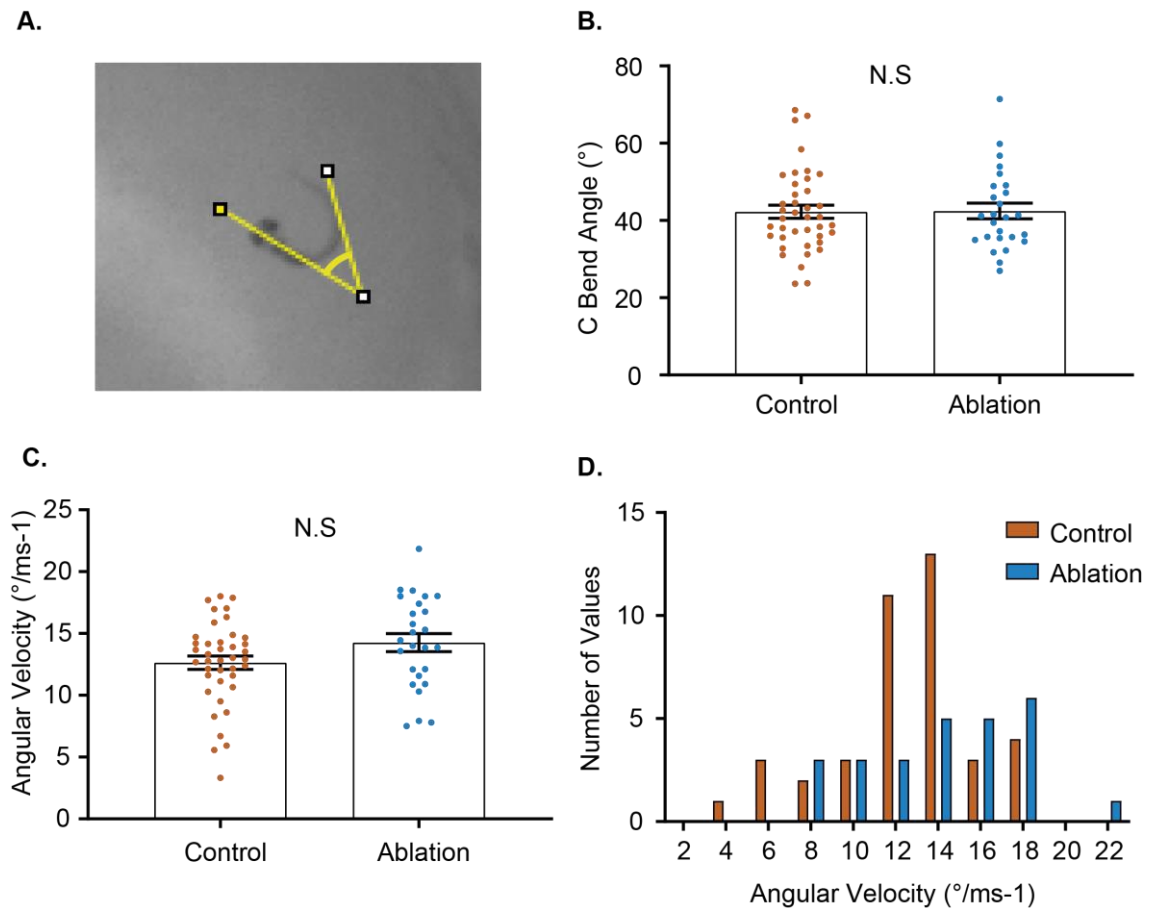
Figure 5:8 Selective loss of subpallial DAergic neurons does not affect the c-bend kinetics. A: Example of c-bend behaviour of 5 dpf fish and the method used to measure c-bend angle. **B:** Box plot comparing the c-bend angle at maximum flexion. **C:** Box plot comparing the angular velocity of the c-bend angle. **D:** Histogram depicting the distribution of the angular velocity of c-bends. N.S. = not significant.

Next, the counter-bend angle was measured in control and ablated fish (Figure 5:9A). This angle was larger in control than ablated fish (control = 115.4 ± 18.53°, n_{fish} = 18, n_{events} = 40, ablated = 98.93 ± 20.44°, n_{fish} = 13, n_{events} = 26, p = 0.0019, Mann-Whitney U, Figure 5:9B). Examination of the counter-bend angular velocity reveal that zebrafish lacking subpallial DAergic neurons exhibited counter-bends with greater angular velocity (control = 7.48 ± 3.99°/ms-1, n_{fish} = 18, n_{events} = 40, ablated = 9.99 ± 2.91/ms-1, n_{fish} = 13, n_{events} = 26, p = 0.0076, Unpaired t-test, Figure 5:9C). Analysis of the distribution of counter-bend angular velocity exhibited a shift in ablated fish, and these animals did not exhibit counter-bend responses with low angular velocities (Figure 5:9D). Together, this suggests that

subpallial DAergic neurons are involved in modulating the counter-bend component of the startle response.

A.

B.

C.

D.
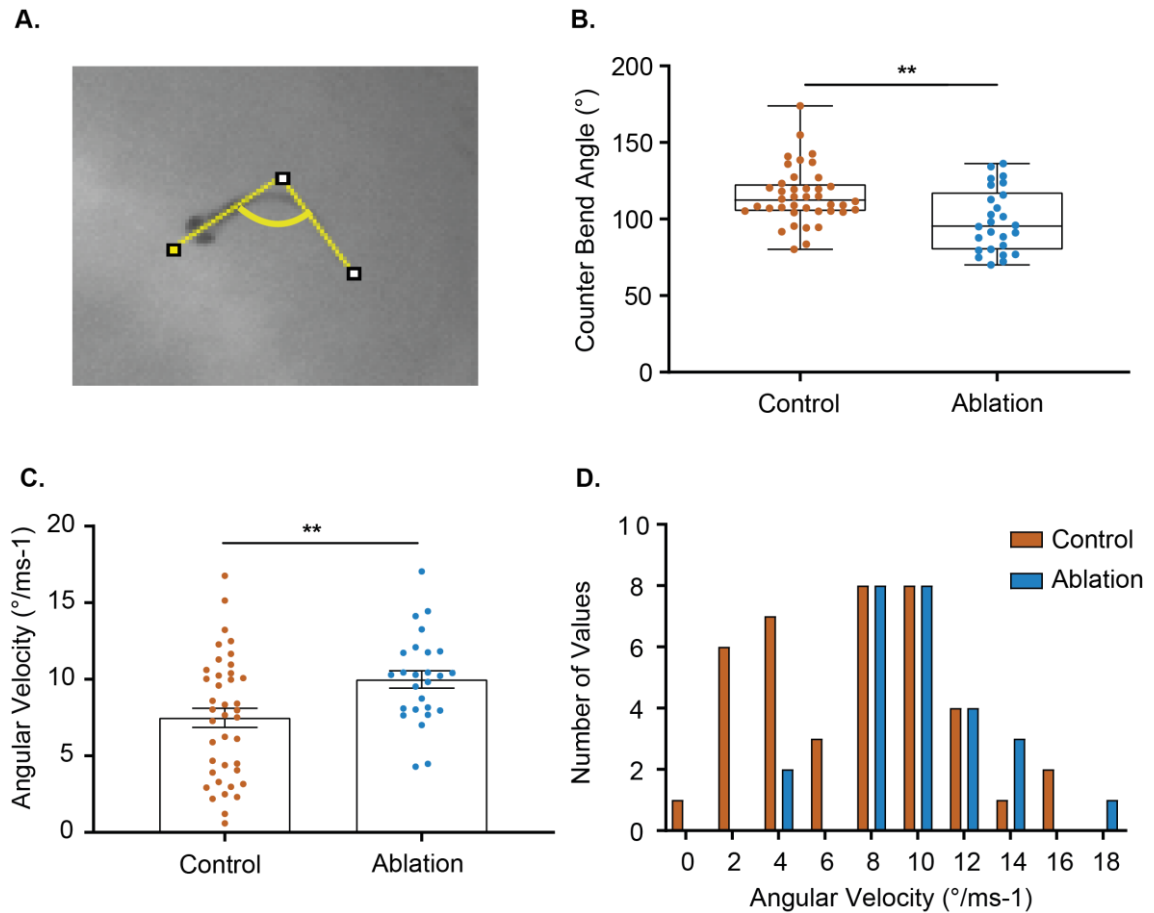
Figure 5:9 Selective loss of subpallial DAergic neurons alters the counter-bend response. A: Example of counter-bend response during startle behaviour and the method used to measure the c-bend angle. **B:** Box plot comparing the counter-bend angle at maximum flexion. **C:** Bar chart comparing the angular velocity of the counter-bend. **D:** Histogram showing the distribution of the angular velocity kinetic of the counter-bend. ** = P <0.005.

So far, I have shown that loss of subpallial DAergic neurons decreases the latency and duration of the acoustic startle response and also affects the kinetics of the counter-bend component of this manoeuvre. As mentioned previously, the C-start response can be divided into two categories, the Mauthner cell-driven SLC, and the Mauthner homolog dependent LLC. Acoustic-evoked SLC and LLC responses can be distinguished on the basis of response latency. Therefore startle responses were classified as SLC if they possess a latency ≤10ms and

LLC if they were $\geq$ 10ms (Burgess and Granato, 2007b, Troconis et al., 2017, Issa et al., 2011). I compared startle latency in ablated fish according to these criteria. The results revealed that 30.5% of control fish exhibited LLC responses whilst only 7.7% of ablated fish exhibited LLC responses (Chi-square test, 18.44, df = 1, z = 4.294, p < 0.0001, Figure 5:10A). This supports the initial hypothesis that loss of subpallial DAergic neurons is associated with a loss of LLC escape responses.

Along with latency, SLC and LLC response can be distinguished by the bimodal distribution of the C-bend response kinetics therefore examined parameters of C-bend responses in control and ablated fish. The C-bend angle of SLC responses shown no change in control or ablated fish (control = 43.55 ± 10.7°, n_{events} = 24, ablated = 41.32 ± 8.761°, n_{events} = 24, p = 0.4308, Unpaired t-test, Figure 5:10B). Similarly, the counter-bend angle of SLC was not affected by the loss of subpallial DAergic neurons (control = 107.5 ± 13.72°, n_{events}= 24, ablated = 101.8 ± 21.86°, n_{events} = 24, p = 0.2752, Unpaired t test, Figure 5:10C). This suggests that SLC kinetics are not affected by the loss of subpallial DAergic neurons.

There was a reduction in the number of LLC responses exhibited by ablated fish (n_{events} = 2). The angle of the LLC C-bend was increased in the ablated group (control = 40.31 ± 11.7°, n_{events} = 11, ablated = 54.33 ± 24.22°, n_{events} = 2, Figure 5:10D). Similarly, the LLC counter-bend angle was smaller in the ablated group (control = 135.6 ± 18.31°, n_{events} = 11, ablated = 84.22 ± 10.34°, n_{events} = 2, Figure 5:10E). However, the low number of data points of LLC responses in the ablated group meant that no statistical analysis could be conducted.
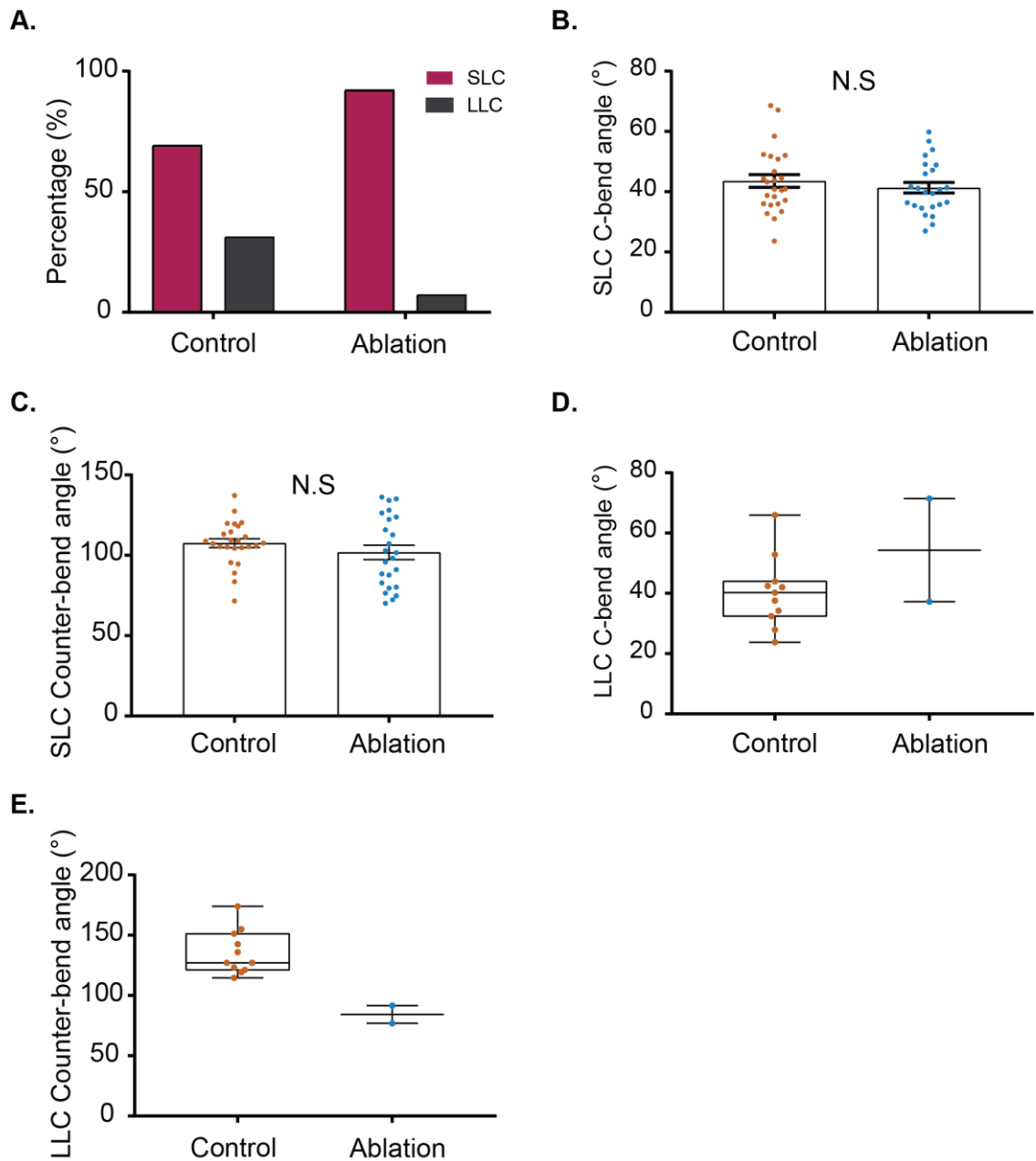
Figure 5:10 Ablating subpallial DAergic neurons reduces the presentation of LLC. A: Bar chart illustrating the percentage of SLC and LLC exhibited by control and ablated fish when exposed to an acoustic stimulus. **B:** Comparison Of the C-bend angle of SLC response **C:** Comparison of counter bend angle exhibit during SLC responses. **D:** Box plot comparing the C-bend angle of LLC response. **E:** Comparison of counter bend angle exhibited by LLC responses. N.S. = not significant.

5.3.2 Delineating the role of subpallial dopaminergic neurons in visually evoked startle response

So far, I have shown ablating subpallial DAergic neurons reduced the number of LLC responses evoked by acoustic stimuli. However, this experiment used a single tone to elicit a startle response and was not designed to evoke either SLC or LLC responses. Since SLC are evoked by high-intensity stimuli, and LLCs are elicited by low-intensity stimuli (Burgess and Granato, 2007b, Kohashi and Oda, 2008), presenting zebrafish with an acoustic stimulus that did not vary in intensity would not differentially elicit SLC and LLC. Therefore, I sought to determine if ablating subpallial DAergic neurons affected the proportion of LLC responses by presenting zebrafish looming stimuli of varying approach velocities to elicit visually evoked startle responses. The looming stimuli models an approaching object of constant velocity and can be used to delineate the relationship between approaching stimulus and onset of escape response. Therefore, zebrafish were exposed to looming stimuli that were projected onto an outer arena wall to elicit visually evoked startle behaviours (Figure 5:11). Simulated approach speed, the rate at which the looming stimulus expanded, was varied experimentally. Looming stimuli elicited visually-evoked startle responses in control and ablated fish. Examination of the response latency revealed an increase as stimulus approach velocity was decreased (Figure 5:12A, see Table 5.1 for two-way ANOVA, P > 0.0001). Control and ablated fish did not differ in response latency (see **Error! Reference source not found.** for Sidak multiple comparison analysis).

A.

B.

C.

Time (s)
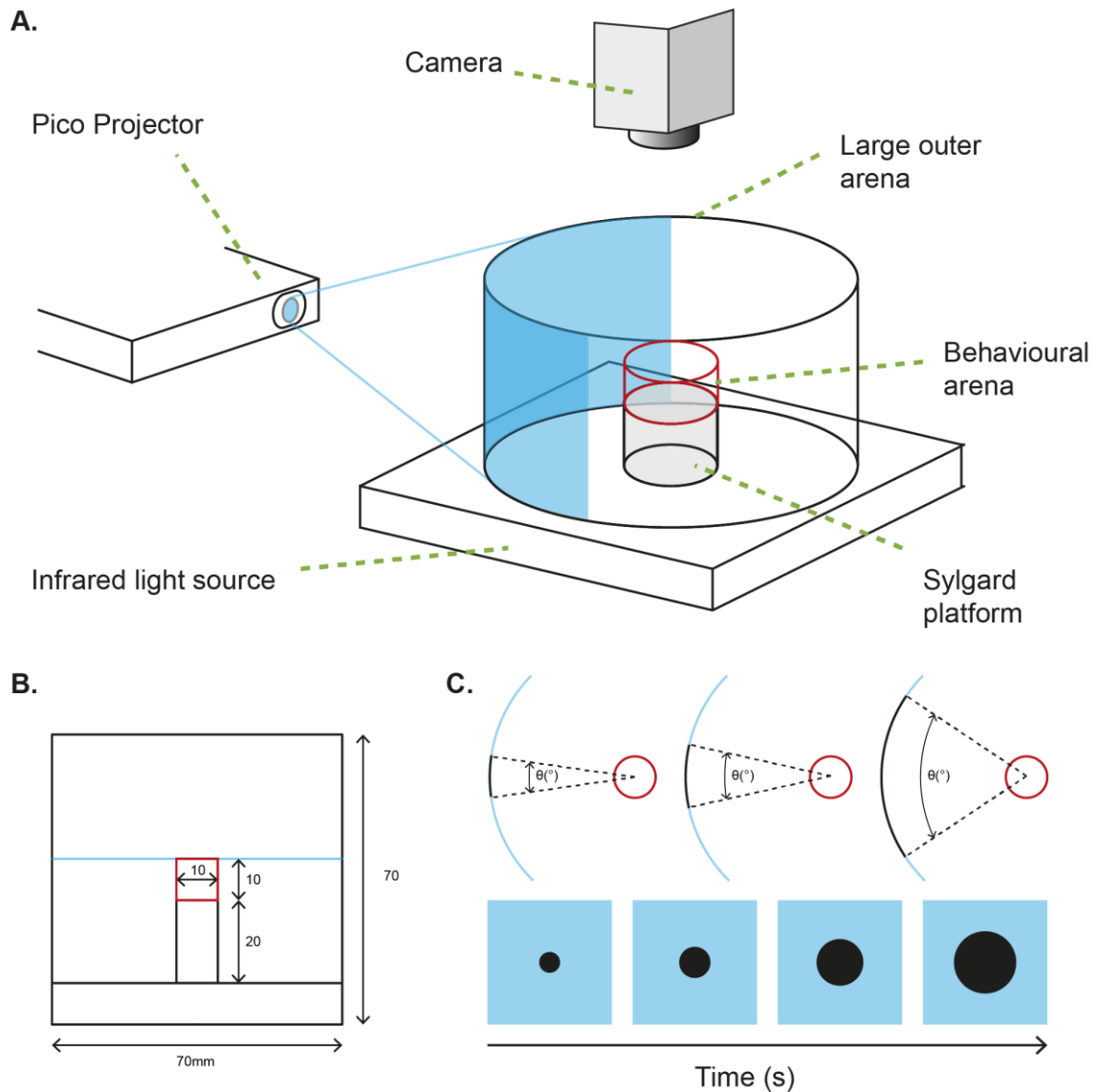
Figure 5:11 Virtual reality (free swimming) equipment schematic. A: Larval zebrafish at 5 dpf were placed in a behavioural arena (red outline) within a larger arena on top of an infrared light source with an overhead camera and a pico projector positioned 15cm away from outer dish wall. **B:** Lateral view schematic illustration of the behavioural arena (inner and outer) dimensions (all units in millimetre). Blue line represents water level. **C:** Representative illustration of approaching virtual stimuli (black circles) that expanded with an exponential velocity. The upper panel illustrates an aerial view of expanding stimuli against outer arena wall (dotted lines represent change in visual angle over time). The lower panel depicts the expanding stimulus presented to the zebrafish.

Previous studies found that visually evoked startle responses are triggered once an object reached an angular size threshold >10°, regardless of speed and direction (Temizer et al., 2015, Barker and Baier, 2015). Therefore, I sought to determine the critical object size needed to initiate startle responses. Subsequent analysis revealed that size of the looming stimulus the same, independent of speed (Figure 5:12B, see Table 5.2 for two-way ANOVA, P=0.3358). This is to be expected since zebrafish RGCs and neurons in the optic tectum exhibit size tuning and are capable of eliciting escape behaviour once a looming stimulus reaches the threshold of >10° (Barker and Baier, 2015, Dunn et al., 2016a). However, Bhattacharyya and colleagues found zebrafish responded when the object size reached ~ 35° (Bhattacharyya et al., 2017). Examination of the remaining time to collision, collision being the point when the object reaches a visual angle of 180° (Figure 5:12C), revealed that decreasing stimulus speed increased the time to collision (Figure 5:12D, see Table 5.3 for two-way ANOVA, P > 0.0001). Similar to latency, control and ablated fish did not differ in time to collision. Together, this shows that approaching stimuli of varying speed can change the response kinetics such as latency; however, the threshold of the object size to evoke a startle response remains the same regardless of stimulus speed.
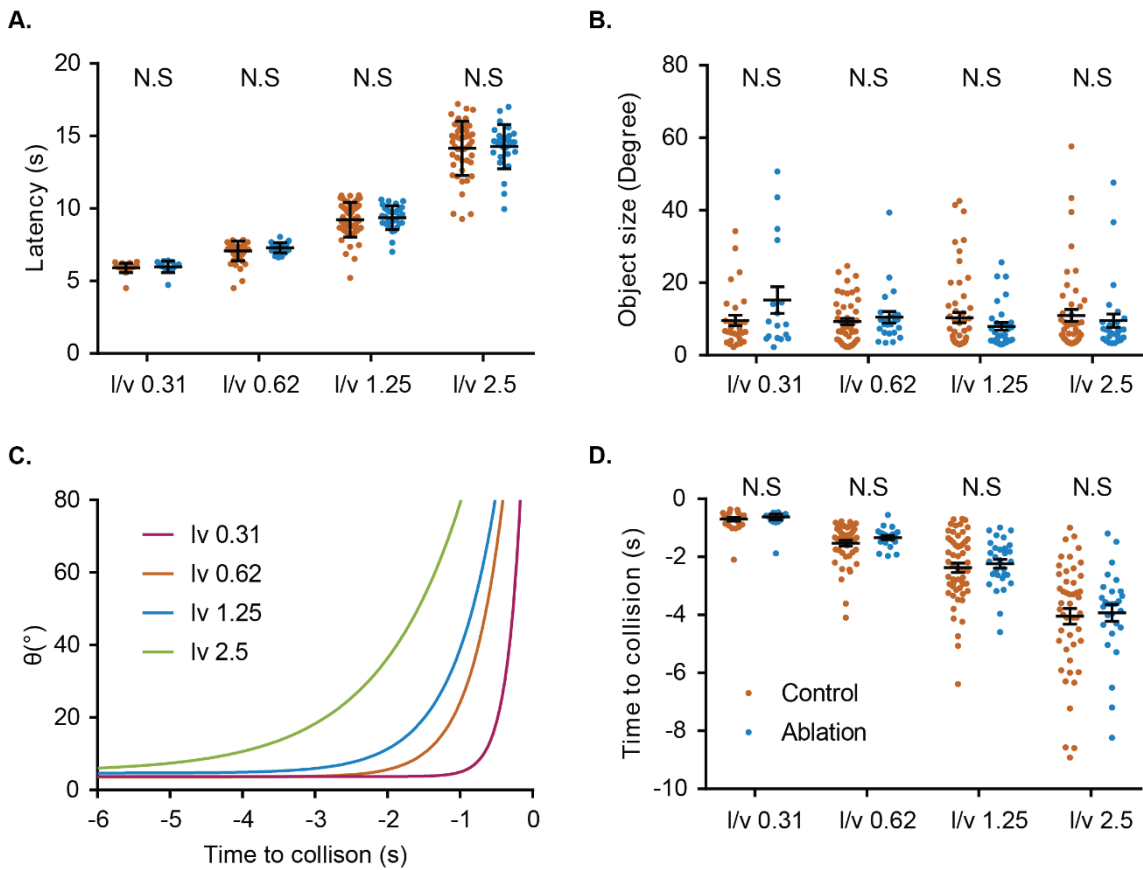
Figure 5:12 Visually evoked startle response kinetics are not affected by the loss of subpallial DAergic neurons. A: Latency of escape response from the presentation of the looming stimulus as a function of *l/v*. **B:** Angular size of looming stimulus at the onset of escape response as a function of *l/v*. **C:** Example of the change in the angular size of looming stimuli as it reaches collision. Time = 0 represents collision time, at which object reaches 180°, l = object's radius, v = approach speed. **D:** Time to collision at the onset of escape response as a function of *l/v*. N.S. = not significant.

Table 5.1 Two-way ANOVA analysis of the effect of looming stimuli on response latency

	DF	MS	F (DFn, DFd)	P value
Interaction	3	0.04651	$F_{(3, 272)} = 0.03544$	P=0.9910
Stimulus speed	3	809.6	$F_{(3, 272)} = 616.8$	P<0.0001****
Condition	1	1.144	$F_{(1, 272)} = 0.8719$	P=0.3513
Residual	272	1.313		

**** $P < 0.0001$

Table 5.2 Two-way ANOVA analysis of the looming stimuli size at the on point of startle response

	DF	MS	F (DFn, DFd)	P value
Interaction	3	173.3	F (3, 276) = 1.954	P=0.1212
Stimulus speed	3	100.6	F (3, 276) = 1.134	P=0.3358
Condition	1	34.71	F (1, 276) = 0.3913	P=0.5321
Residual	276	88.69		

Table 5.3 Two-way ANOVA analysis of the time to collision of looming stimuli triggered a startle response

	DF	MS	F (DFn, DFd)	P value
Interaction	3	0.03042	F (3, 271) = 0.0231	P=0.9952
Stimulus speed	3	119.5	F (3, 271) = 90.77	P<0.0001****
Condition	1	1.044	F (1, 271) = 0.7927	P=0.3741
Residual	271	1.316		

**** P < 0.0001

Previous studies have shown approach speed determines the type of escape response, with SLC being triggered by high approach velocities and LLC being evoked by low approach velocities (Burgess and Granato, 2007a, Burgess and Granato, 2007b, Kohashi and Oda, 2008, Temizer et al., 2015, Bhattacharyya et al., 2017). Since looming stimuli can elicit escape behaviour in both control and ablated fish, I sought to determine the effect of stimulus approach velocity on the probability of eliciting SLC or LLC responses. Examination of the effect of varying stimulus speed revealed the probability of triggering SLC was not influenced by velocity of approach (Figure 5:13A, see

Table 5.4 for two-way ANOVA, P = 0.0981). Similarly, ablating subpallial DAergic neurons had no effect on the probability of the SLC response.

Interestingly, stimulus speed did affect the probability of eliciting an LLC: decreasing the stimulus approach speed increased the probability of triggering an LLC (Figure 5:13B, see

Table 5.5 for two-way ANOVA, P = 0.0283). Selective ablation of subpallial DAergic neurons attenuated the presentation of LLCs compared to the control fish, and low intensity stimuli was able to elicit LLC in control but not ablated fish (see Table 5.6 for Sidak multiple comparison analysis). Together, this suggests that ablating the subpallial DAergic neurons is sufficient to reduce the LLC response. Since ablating subpallial DAergic neurons reduced the probability of eliciting LLC responses to stimuli with low approach velocities but the probability of SLC was not affected, I wanted to examine if the probability of freezing behaviour was affected by loss of subpallial DA signalling. Freezing behaviour is a fear response and is characterised by immobilisation to an aversive stimulus (Kalueff et al., 2013). Examination of the freezing behaviour revealed that decreasing stimulus speed reduces probability of freezing (Figure 5:13C, see Table 5.7 for two-way ANOVA, P=0.0548), consistent with the literature (Bhattacharyya et al., 2017). However, the comparison between control and ablated fish showed that loss of subpallial DAergic neurons increased the incidence of freezing behaviour in response to objects approaching at a velocity of l/v = 0.62 (see Table 5.8 for Sidak multiple comparison analysis). Finally, I aimed to determine if ablating subpallial DAergic neurons changed the probability of the looming stimulus failing to elicit a behavioural response such as freezing or startle response, as defined by C, S or O-bend. Analysis of the effect of stimulus approach velocity on the probability behavioural response revealed stimuli speed did not affect the probability of freezing, nor did neither did ablating subpallial DAergic neurons (Figure 5:13D, see Table 5.9 for two-way ANOVA, P=0.4910). Together, this shows that ablating subpallial DAergic neurons reduces the probability of LLC responses to looming stimuli with low approach velocity.
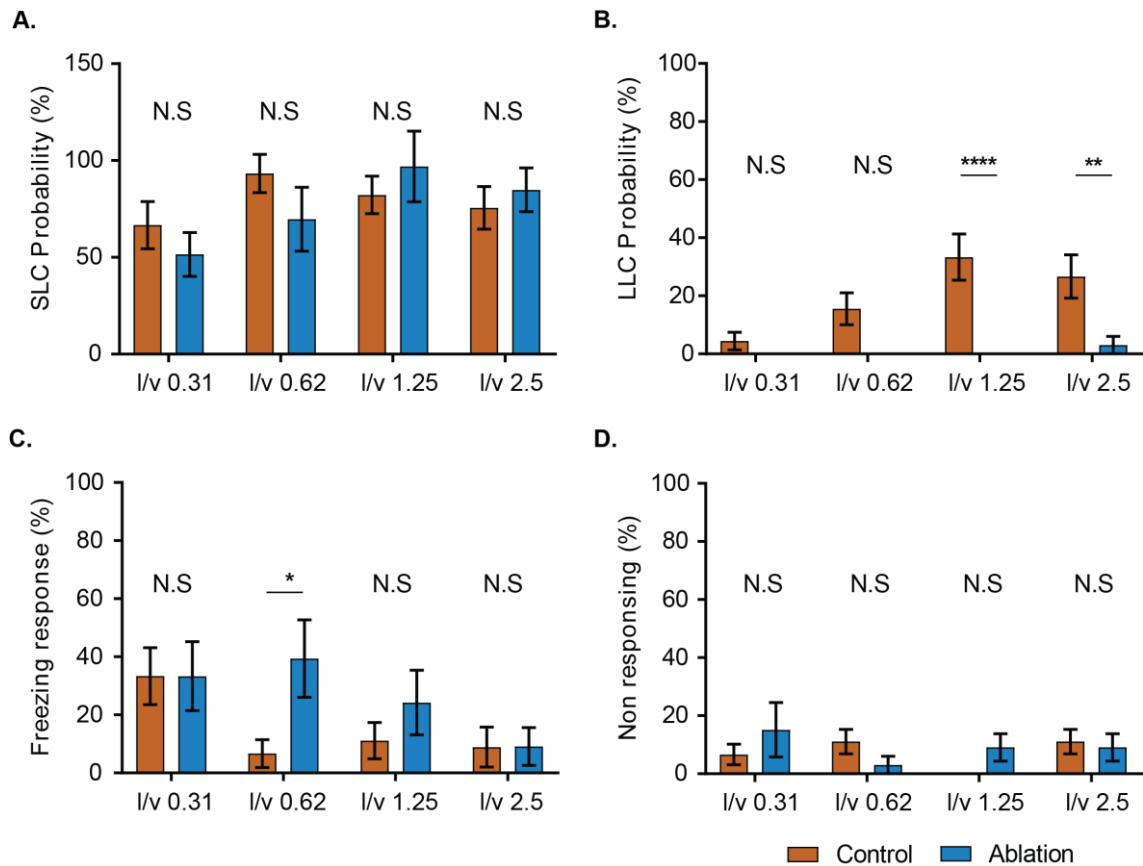
Figure 5:13 Selective loss of subpallial DAergic neurons reduces the probability of evoking an LLC. A: Probability of looming stimulus eliciting an SLC escape response as a function of *l/v*. **B:** Probability of looming stimulus triggering an LLC escape response as a function of *l/v*. **C:** Probability of looming stimuli eliciting freezing behaviour as a function of *l/v*. **D:** Probability of visual stimulus not evoking a change in behaviour as a function of *l/v*. * P = 0.05, ** P = 0.005, **** P <0.0001, N.S. = not significant.

Table 5.4 Two-way ANOVA analysis of the effect of looming stimuli on evoking an SLC response

	DF	MS	F (DFn, DFd)	P value
Interaction	3	2195	F (3, 96) = 1.101	P=0.3528
Stimulus speed	3	4303	F (3, 96) = 2.157	P=0.0981
Condition	1	345.1	F (1, 96) = 0.173	P=0.6784
Residual	96	1995		

Table 5.5 Two-way ANOVA analysis of the looming stimuli on evoking an LLC response

	DF	MS	F (DFn, DFd)	P value
Interaction	3	952.8	F (3, 96) = 2.675	P=0.0515
Stimulus speed	3	1124	F (3, 96) = 3.155	P=0.0283*
Condition	1	9399	F (1, 96) = 26.39	P<0.0001****
Residual	96	356.2		

* P < 0.05, **** P < 0.0001

Table 5.6 Sidak analysis of stimulus speed on the probability of evoking an LLC response

Control - Ablation	Diff. in mean	DF	P value
l/v 0.31	4.444	96	0.9606
l/v 0.62	15.56	96	0.1526
l/v 1.25	33.33	96	<0.0001****
l/v 2.5	23.64	96	0.0085***

*** P < 0.0005, **** P < 0.0001

Table 5.7 Two-way ANOVA analysis of the looming stimuli triggering freezing behaviour

	DF	MS	F (DFn, DFd)	P value
Interaction	3	1509	F (3, 96) = 1.504	P=0.2185
Stimulus speed	3	2634	F (3, 96) = 2.626	P=0.0548
Condition	1	3366	F (1, 96) = 3.356	P=0.0701
Residual	96	1003		

Table 5.8 Sidak analysis of stimulus speed and triggering freezing behaviour

Control - Ablation	Diff. in mean	DF	P value
l/v 0.31	6.061e-007	96	>0.9999
l/v 0.62	-32.73	96	0.0421*
l/v 1.25	-13.13	96	0.7584
l/v 2.5	-0.202	96	>0.9999

* P < 0.05

Table 5.9 Two-way ANOVA analysis of the looming stimuli on the not-triggering a startle response

	DF	MS	F (DFn, DFd)	P value
Interaction	3	444.3	F (3, 96) = 1.664	P=0.1798
Stimulus speed	3	216.4	F (3, 96) = 0.8106	P=0.4910
Condition	1	88.64	F (1, 96) = 0.332	P=0.5658
Residual	96	267		

Visually evoked escape responses generate highly structured manoeuvres to evade predators. Mauthner-dependent escape responses typically generate a ~180º change in orientation. However, slower stimuli generate more variable reorientations (Jain et al., 2018, Bhattacharyya et al., 2017). I therefore asked if ablating subpallial DAergic neurons affects reorientation of zebrafish during escape behaviour. Examination of initial bend angle when exposed to a front-looming stimulus (front; - 45º to 0 to + 45º; Figure 5.14A upper polar plots), revealed that both control and ablated fish exhibited 'perfect avoidance', in which zebrafish turn 180º away from the stimulus. Control and ablated fish displayed similar variability in the initial bend angle, regardless of approach speed (Levene's test, front: $N_{control, fast}$ = 8, $N_{ablation, fast}$ = 7, p = 0.666, $N_{control, slow}$ = 22, $N_{ablation, slow}$ = 9, p = 0.124, Figure 5:14B). Similarly, examination of the initial bend angle when exposed to a stimulus presented from behind (back, -135º to ±180º to +135º; Figure 5:14C) resulted in a turn of ~150º (Figure 5:14A lower polar plots). Additionally, control and ablated fish responded with similar variability in the initial bend angle, regardless of approach speed (Levene's test, back: $N_{control, fast}$ = 6, $N_{ablation, fast}$ = 2, p = 0.344, $N_{control, slow}$ = 13, $N_{ablation, slow}$ = 12, p = 0.850, Figure 5:14C). This suggests subpallial DAergic neurons do not affect the directionality of evasive responses when zebrafish are presented with looming stimuli that approach from the front or behind.
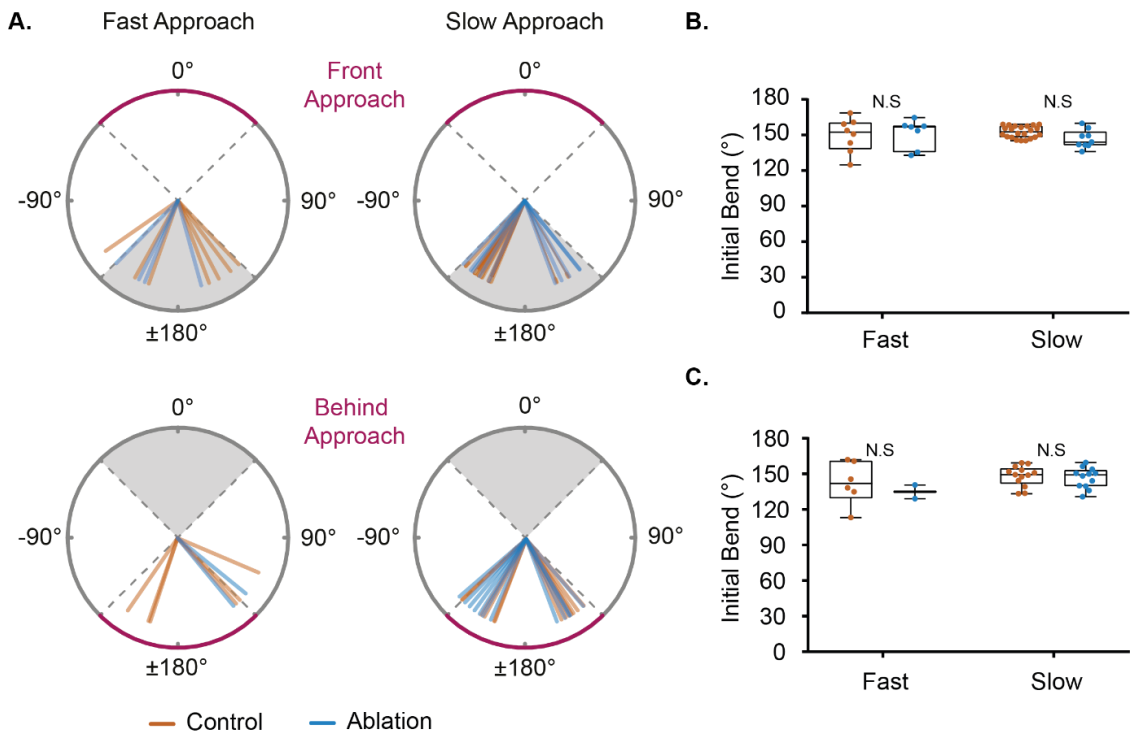
Figure 5:14 Control and ablated fish have similar orientation changes to visual stimuli. A: Top panel; direction of control and ablated zebrafish in response to a fast ($l/v = 0.31$) or slow ($l/v = 2.5$) approaching stimulus from the front of the zebrafish. Body midline axis represents 0°, approaching objects from the front were classified between -45° to +45°. Bottom panel; Direction of control and ablated zebrafish in response to a fast or slow approaching stimuli from behind the zebrafish. Body midline axis represents 0°, approaching objects from the front were classified between -135° to +135°. **B:** Box and whisker plot comparing the absolute initial bend angle of control and ablated fish in response to fast and stimuli when approached from the front. **C:** Box and whisker plot comparing the absolute initial bend angle of control and ablated fish in response to fast and stimuli when approached from behind. N.S. = not significant.

Examination of the effect of stimulus direction on the initial bend angle of zebrafish when exposed to a right-approaching stimulus (right; +45° to +135°; Figure 5:15A, upper polar plots) revealed control and ablated fish turned up to 180° from their original direction. Furthermore, control and ablated fish responded with similar variation in the initial bend angle when exposed to a fast stimulus, however, the slow stimulus elicited more variable swimming trajectories in ablated fish (Levene's test, right: $N_{control, fast} = 7$, $N_{ablation, fast} = 6$, $p = 0.730$, $N_{control, slow} = 27$, $N_{ablation, slow} = 10$, $p = 0.032$, Figure 5:15B). Examination of the visual stimuli when approaching from the left of the specimen (left -45° to -135°; Figure 5:15A, lower polar plots) showed zebrafish swam laterally in the opposite

direction to the stimuli. Similar changes in orientation were observed in response to fast approaching stimuli from the left (Levene's test, left: $N_{control, fast}$ = 9, $N_{ablation, fast}$ = 4, p = 0.100, $N_{control, slow}$ = 37, $N_{ablation, slow}$ = 29, p = 0.536, Figure 5:15C). With exception to slow looming stimuli approaching from the right, this suggests subpallial DAergic neurons do not affect the directionality of evasive response when zebrafish are presented with looming stimuli.
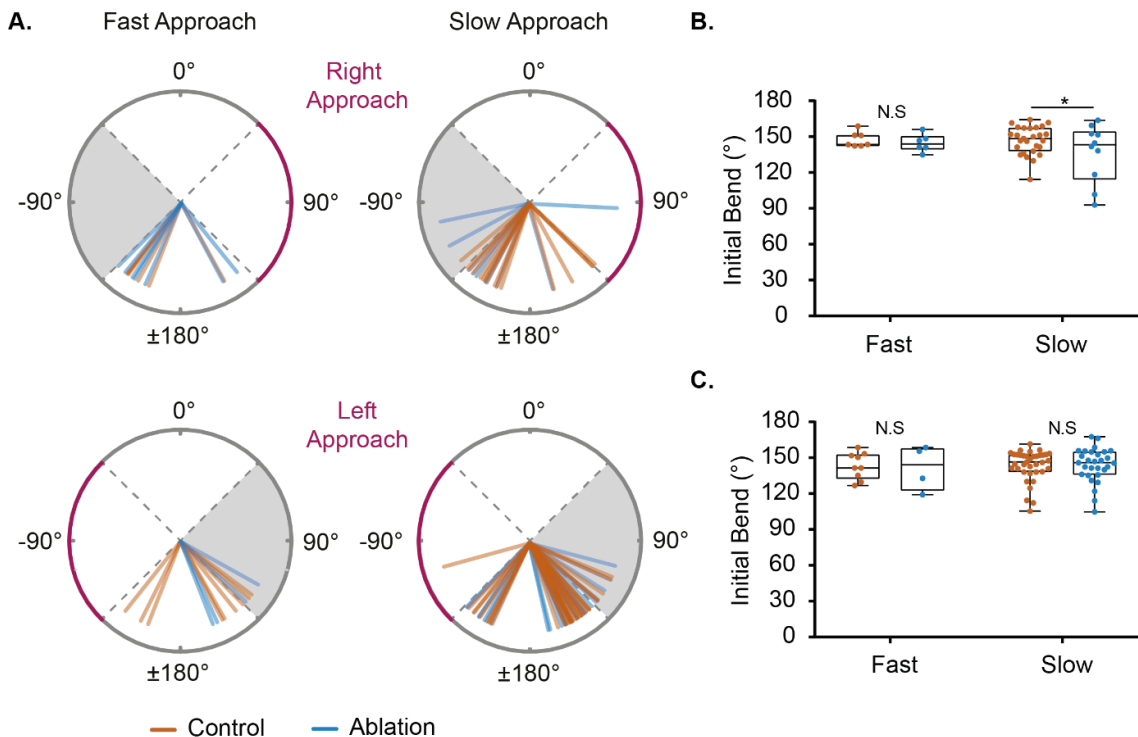
Figure 5:15 Laterally approaching visual stimuli triggers similar orientation responses in control and ablated fish. A: Top panel; the direction of control and ablated zebrafish in response to a fast or slow approaching stimuli from the right of the zebrafish. Body midline axis represents 0⁰, approaching objects from the right were classified between +45⁰ to +135⁰. Bottom panel; the direction of control and ablated zebrafish in response to a fast or slow approaching stimuli from left of the fish. Body midline axis represents 0⁰, approaching objects from the left were classified between -45⁰ to -135⁰ to the midline. **B:** Box and whisker plot comparing the absolute initial bend angle of control and ablated fish in response to fast and stimuli when approached from the right **C:** Box and whisker plot comparing the absolute initial bend angle of control and ablated fish in response to fast and stimuli when approached from left. * P < 0.05, N.S. = not significant.

Loss of subpallial DAergic neurons did not affect the variability in the direction of evasive responses. This contrasts with Bhattacharyya and colleagues who found that looming stimuli of slower approach velocity triggered an increase in the variation of the directionality of escape behaviours (Bhattacharyya et al., 2017). I did not observe an increase in variation when comparing stimuli of fast and slow approach velocities, however, I did not present looming stimuli with the same speeds, which could have an effect on the directionality of escape responses. Another explanation for this difference could arise from strain differences. Bhattacharyya and colleagues used short fin wild type fish whilst in this study I used long fin zebrafish. van den Bos and colleagues found that the startle behaviours of short fin and long fin zebrafish have different kinetics (van den Bos et al., 2017) and this could explain the differences between these experiments and previously published work.

In sum, loss of subpallial DAergic neurons reduces the probability of zebrafish eliciting LLC responses to threatening stimuli. Ablating subpallial DAergic neurons does not affect SLC startle kinetics, suggesting that Mauthner cells are not modulated by subpallial DAergic input. Since zebrafish lacking these neurons are less likely to elicit LLC responses, my findings suggest that these neurons modulate the probability of LLC responsiveness.

5.3.3 Activity of Subpallial dopaminergic neurons and looming stimuli

Since ablating subpallial DAergic neurons perturbs startling behaviour by attenuating the LLC response, I sought to examine the firing pattern of subpallial DAergic neurons when zebrafish are exposed to looming stimuli. In order to achieve this, a series of loose patch recordings were performed on awake but paralysed zebrafish at 5 dpf exposed to looming stimuli (Figure 5:16).
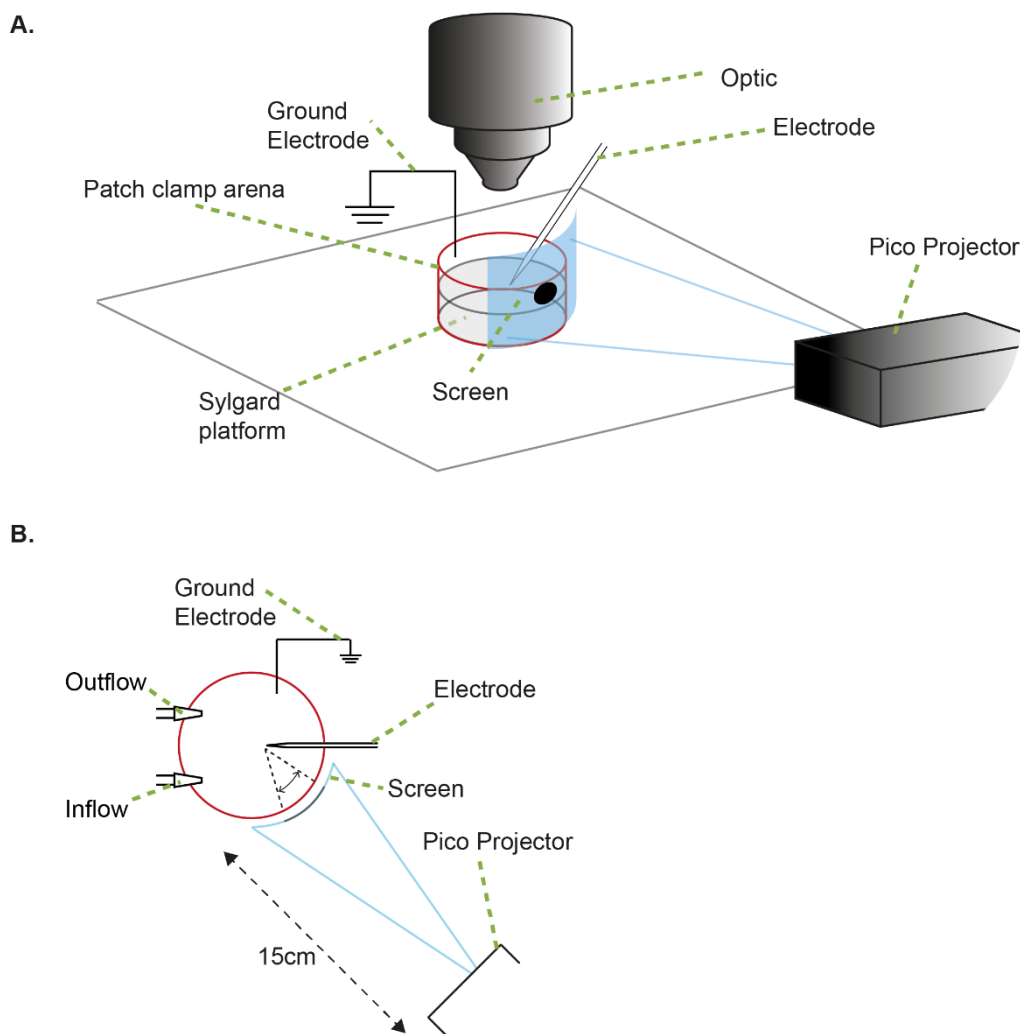
Figure 5:16 Virtual reality – physiological recording schematic. A: Paralysed yet awake larval zebrafish were placed in a patch arena (red outline) with a pico projector positioned 15cm away from dish wall, and looming stimuli were projected onto a screen surrounding the arena. **B:** Dorsal view schematic illustration of the patch-clamp dish with looming stimuli and equipment.

Firing activity was detected in subpallial DAergic neurons when exposed to fast-approaching looming stimuli (l/v = 0.31; Figure 5:17A/B), however, the firing frequency did not change (control = 1.38 ± 1.08Hz, looming = 0.89 ± 1.78Hz, post-stimulus = 1.89 ± 1.95Hz, n_{fish} = 6, n_{events} = 17, p = 0.1769, RM one-way ANOVA, Tukey's multiple comparison test, control vs looming p = 0.4083, looming vs post-stimulus p = 0.5980, control vs post-stimulus p = 0.2661, Figure 5:17C). This suggests subpallial DAergic neurons do not respond to stimuli with fast approach velocities.

Similarly, the firing activity of subpallial DAergic neurons did not change when exposed to looming stimuli with an intermediate approach velocity (l/v = 1.25; Figure 5:18A/B). The firing frequency did not differ between control, looming stimulus and post-stimulus conditions (control = 0.98 ± 1.64Hz, looming = 1.77 ± 2.28Hz, post-stimulus = 2.03 ± 2.71Hz, n_{fish} = 6, n_{events} = 17, p = 0.3968, Friedman test, Dunn's multiple comparison test control vs looming p = 0.6898, looming vs post-stimulus p = 0.7949, control vs post-stimulus p = 0.9999, Figure 5:18C).

Interestingly, when exposed to slow approaching stimuli (l/v = 2.5; Figure 5:19A/B), subpallial DAergic neuron firing changed significantly. When presented with the looming stimuli, firing frequency increased, an effect that was reversed on revival of stimuli (control = 0.96 ± 1.45Hz, looming = 3.89 ± 2.92Hz, post-stimulus = 1.98 ± 1.66Hz, n_{fish} = 6, n_{events} = 17, p < 0.0001, Friedman test, Dunn's multiple comparison test control vs looming p <0.0001, looming vs post-stimulus p = 0.0081, control vs post-stimulus p = 6898, Figure 5:19C). Together, this suggests subpallial DAergic neurons respond to looming stimuli with slow approach velocities.

A.

5s

B.

C.
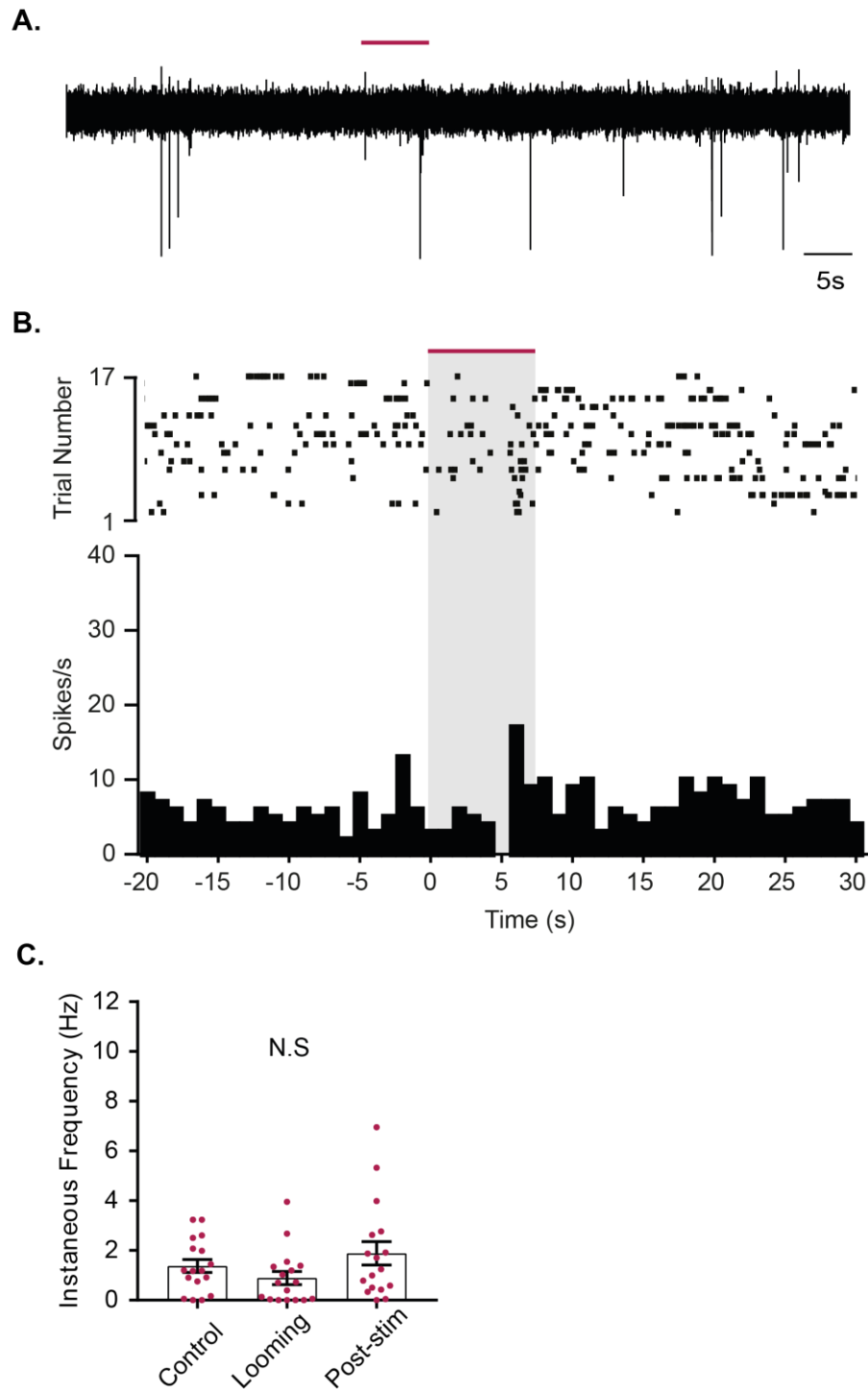
Figure 5:17 Firing activity of subpallial DAergic neurons does not change when exposed to fast approaching stimuli. A: Representative trace of subpallial DAergic neuron in response to looming stimuli (*I/v* 0.31). **B:** Raster plot and peri-stimulus time histogram (PSTH) of collective firing activity. **(A-B):** Magenta line represents the time at which the stimulus was present to zebrafish. **C:** Bar chart comparing firing frequencies during control, looming stimulus and post-stimulus. N.S. = not significant.

A.

5s

B.

C.
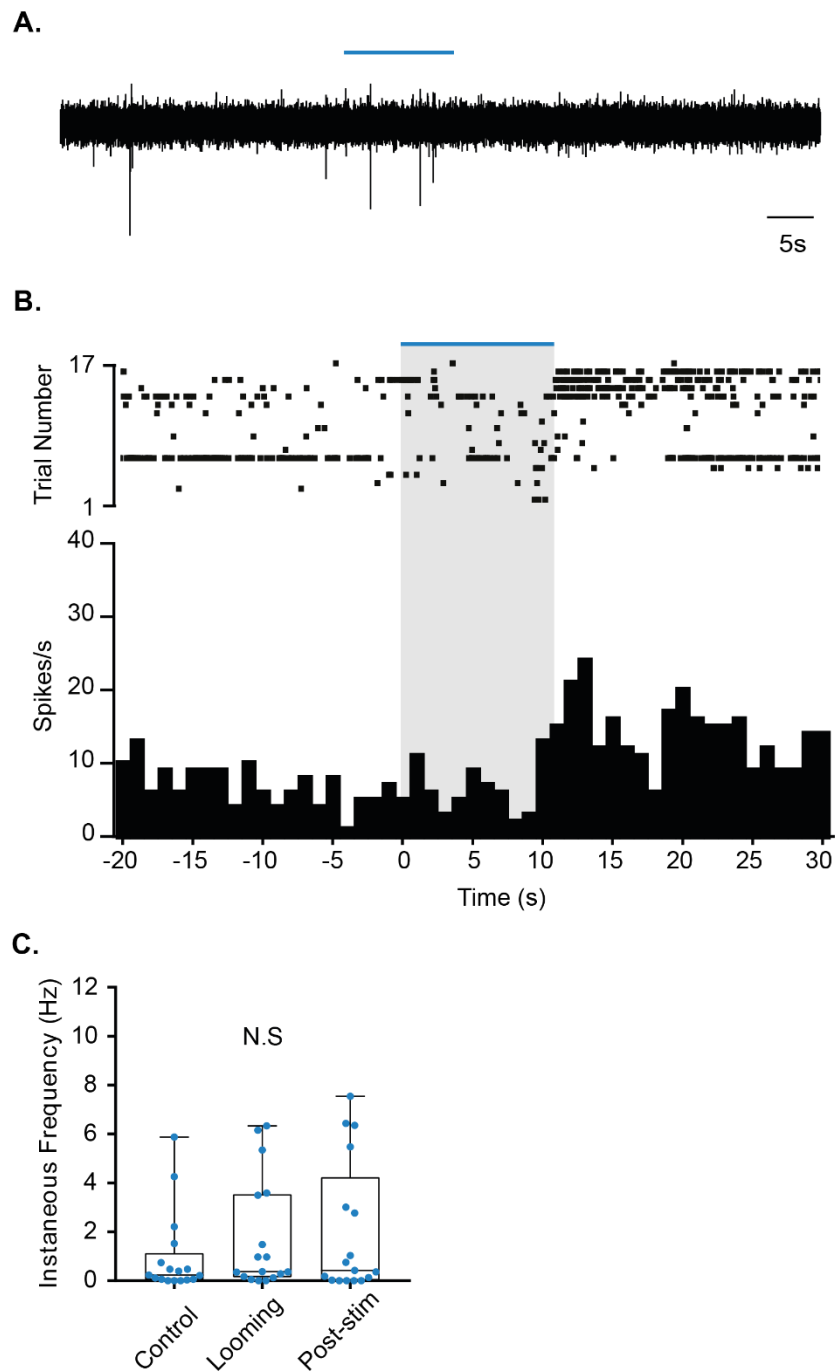
Figure 5:18 Firing activity of subpallial DAergic neurons in response to visually aversive stimuli. A: Representative recording of subpallial DAergic neuron firing activity when present with a looming stimulus (*l/v* 1.25), the blue line represents the time at which the stimulus was present to fish. **B:** Raster plot and PSTH summary of firing activity of subpallial DAergic neurons. **(A-B):** Blue line represents time at which the stimulus was presented to fish. **C:** Box and whisker plot comparing firing frequencies during control, looming stimulus (*l/v* 1.25), and post-stimulus. N.S = not significant.

A.

5s

B.

C.
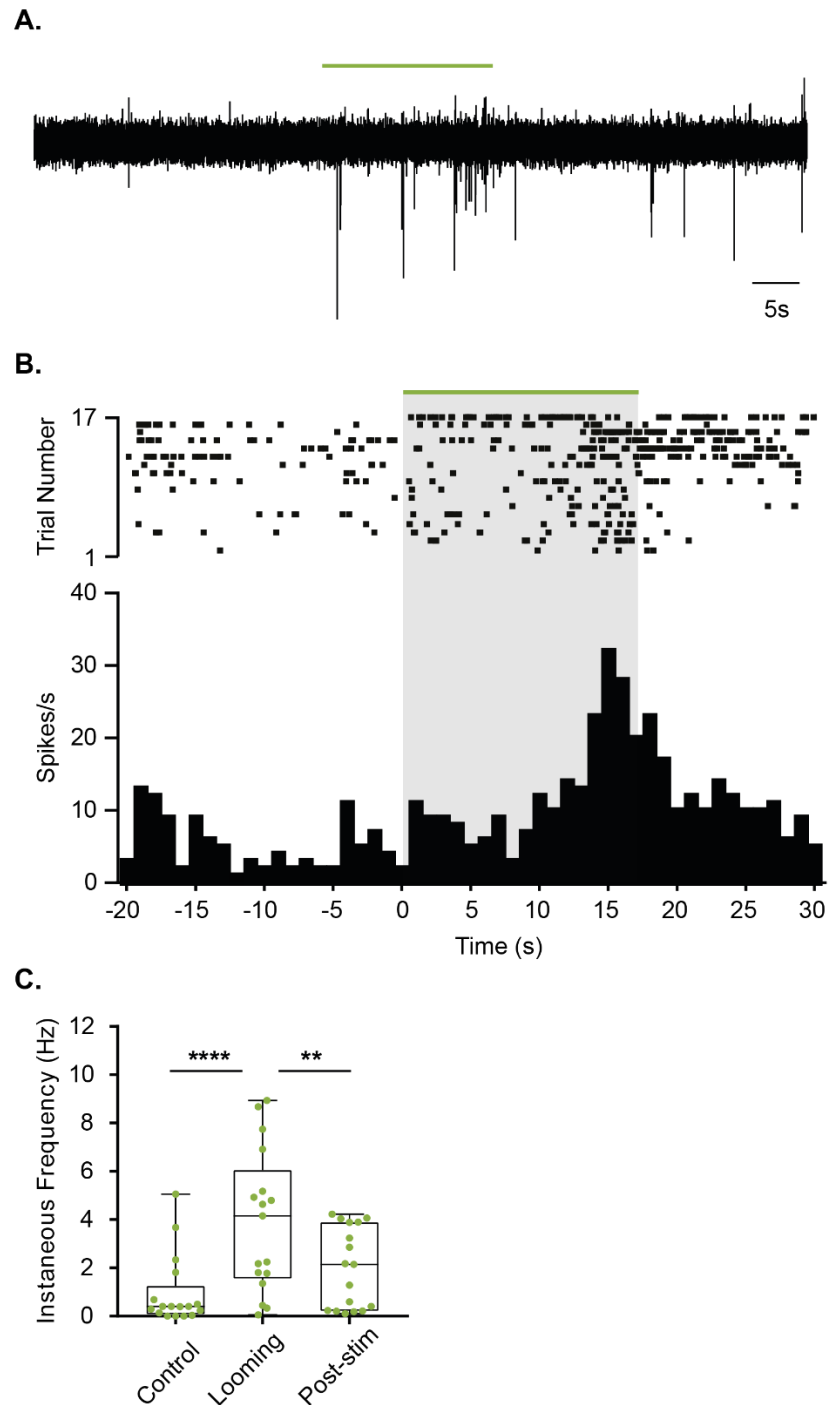
Figure 5:19 Firing activity of subpallial DAergic neurons increases when exposed to slow approaching virtual stimuli. A: Example recording of subpallial DAergic neuron as well as raster plot summary and PSTH (**B**) of collective firing patterns when exposed to stimuli with slow approach velocities (*l/v* 2.5). **(A-B):** Green line represents the time at which the stimulus was present to fish. **C:** Box and whisker plot comparing firing frequencies during control, looming stimulus (*l/v* 2.5), and post-stimulation. ** p = 0.005, **** p < 0.0001.

In sum, an examination of the startle responses suggests that ablating subpallial DAergic neurons reduces the occurrence of LLC responses to looming stimuli with a slow approach velocity. Bhattacharyya and colleagues found zebrafish are more likely to elicit an LLC escape response when presented with slow approaching loom stimuli (Bhattacharyya et al., 2017). Since ablating subpallial DAergic neurons reduces the probability of LLC response, this suggests that subpallial DAergic neurons facilitate the alternative escape behaviour in zebrafish, loose patch recordings revealed subpallial DAergic neurons increased firing frequency to specific looming stimuli. However, this response was restricted to stimuli with a slow approach velocity. Several studies using pERK IHC found that the subpallium is active when exposed to aversive acoustic stimuli, however, the role of subpallial DAergic neurons in this response was not addressed (Randlett et al., 2015, Vanwalleghem et al., 2017). Since subpallial DAergic neurons increase in activity in response to slow approaching looming stimuli, this suggests these neurons receive information about object kinetics.

5.4   Discussion

In this chapter, I have examined the role of subpallial DAergic neurons in modulation of zebrafish startle behaviours. The results presented in this chapter demonstrate three key findings: firstly, loss of subpallial DAergic neurons perturbs startle behaviours; secondly, ablation of these cells reduces the incidence of LLC responses and; finally, these neurons increase their activity to slow approaching looming stimuli.

5.4.1   The effects of subpallial dopaminergic neurons ablation on escape behaviour

Whole-brain activity mapping of the zebrafish revealed the subpallium is active when zebrafish are presented with aversive stimuli (Randlett et al., 2015, Vanwalleghem et al., 2017). I first sought to examine the effect of perturbed DAergic signalling on acoustic startle behaviours and found that ablating subpallial DAergic neurons reduces escape latency, decreases startle duration and distance swum. However, swimming velocity was not affected by the loss of subpallial DAergic neurons. Further analysis suggested selective ablation of subpallial DAergic neurons did not alter the kinetics of stereotypical C-bend manoeuvres; however, the counter-bend angular velocity increased in ablated fish. Since zebrafish C-start behaviours can be divided into SLC and LLC (Liu et al., 2012, Troconis et al., 2017), I analysed the proportion of these responses and found a specific reduction in LLCs in response to auditory stimuli. However, there were limitations to this experiment, since LLCs are more likely to be elicited at different auditory tone thresholds to the SLCs. This experiment used a single tone to elicit a startle response and was not designed to evoke either SLC and LLC responses. To investigate SLC and LLC response, I presented zebrafish with looming stimuli of varying approach speeds and found ablating subpallial DAergic neurons reduces the proportion of LLC responses when compared to control fish. Nonetheless, my findings indicate that subpallial DAergic neurons facilitate LLC responses to aversive stimuli.

By contrast, loss of subpallial DAergic neurons did not affect the incidence of SLCs in response to both acoustic and visual stimuli. This is to be expected since SLCs are driven by Mauthner cells, which generate fast escape reflexes through innervation of the contralateral spinal cord, triggering muscle contractions that mediate the high-velocity body bends (Bhatt et al., 2007, McLean et al., 2007, McLean and Fetcho, 2009, Liu and Fetcho, 1999, Kohashi and Oda, 2008). Mauthner cells receive auditory, mechanosensory and visual input from the cranial nerve, lateral line, Rohon-Beard neurons (depending on age) and the optic tectum (Canfield, 2006, Bhattacharyya et al., 2017, Zottoli et al., 1987, Palanca et al., 2013, Reyes et al., 2004, Hale et al., 2016, Nakayama and Oda, 2004, O'Malley et al., 1996). Previous work has shown that Mauthner cell are modulated by DA input (Curti and Pereda, 2010). Exposing zebrafish to a light flash prior to an acoustic stimuli increases the probability of evoking an acoustic-mediated C-start, an enhancement driven by light-responsive DAergic neurons in the hypothalamus (Mu et al., 2012). However, subpallial DAergic neurons do not innervate the Mauthner cells, subpallial DAergic neurons must be modulating escape behaviours by a polysynaptic pathway.

Selective loss of subpallial DAergic neurons reduced the probability of eliciting LLCs when exposed to auditory and visual stimuli, suggesting these neurons modulate the activity of cells that drive this response. The LLC is initiated by Mauthner cell homologs MiD2cm and MiD3cm (Liu and Fetcho, 1999, Kohashi and Oda, 2008). However, the sensorimotor pathways of LLCs are not fully understood. Nonetheless, it has been shown that the MiD2cm and MiD3cm are activated by auditory, mechanosensory and visual stimuli (Burgess and Granato, 2007b, Canfield, 2006, Nakayama and Oda, 2004) and are more likely to be evoked by low-intensity acoustic or slow approaching visual stimuli (Liu et al., 2012, Troconis et al., 2017, Bhattacharyya et al., 2017, Takahashi et al., 2017). Therefore, MiD2cm and MiD3cm appear to be selectively activated by less immediately threatening stimuli. As no TH reactivity is observed near to MiD2cm and MiD3cm, these neurons are unlikely to be directly modulated by DA input (McLean and Fetcho, 2004b).

How then, do subpallial DAergic neurons influence LLCs responses? Jain and colleagues suggest that the decision-making process to select an appropriate

response such as SLC vs LLC is a dynamic system that is dependent on previous experience and stimulus interpretation (Jain et al., 2018). SLC circuitry can exhibit habituation, an effect associated with the suppression of Mauthner cells activity, without affecting the LLC responsiveness (Takahashi et al., 2017). Repetitive exposure to acoustic stimuli can shift the bias from a SLC to LLC response in larval zebrafish (Jain et al., 2018). Ablating subpallial DAergic neurons decreases the LLC responsiveness, suggesting stimulus interpretation has changed as a result of this intervention. Marquart and colleagues found that prepontine neurons could initiate visually evoked escape behaviours, these responses were delayed and had a highly variable escape trajectory (Marquart et al., 2019). They also found that these prepontine neurons receive visual information from the optic tectum and do not project to the Mauthner cells. Subpallial DAergic neurons could modulate this parallel escape system by influencing the delay escape circuits described by Marquart.

In sum, ablating subpallial DAergic neurons reduces the probability of eliciting both acoustic and visually evoked LLCs, without affecting the SLC reflex. Since subpallial DAergic neurons do not directly innervate the reticulospinal neurons that drive escape behaviour, they are likely to modulate startle behaviours via polysynaptic pathways.

5.4.2   Delineating subpallial dopaminergic neurons firing patterns and looming stimuli.

I next sought to delineate the role of subpallial DAergic neurons in processing looming stimuli. During electrophysiological recordings, subpallial DAergic neurons only increased in activity when exposed to specific looming stimuli: firing frequency of these neurons increased when fish were exposed to the $l/v = 2.5$ stimuli (constant approach velocity = 4mm/s). In contrast, firing frequency was unaffected by looming stimuli with faster approach velocities ($l/v = 0.31$ and $l/v = 1.25$, 32 mm/s and 8mm/s, respectively). This suggests subpallial DAergic neurons response to slow approaching stimuli. There have been limited numbers of investigations into the functional role of the subpallium. They have found that the subpallium is active when exposed to aversive stimuli such as auditory,

mechanosensory stimuli and looming stimuli (Heap et al., 2018b, Vanwalleghem et al., 2017, Randlett et al., 2015). However, the activity of subpallial DAergic neurons in response to these stimuli was not investigated.

The examination of subpallial DAergic neuron sensory responses revealed an increase in activity when presented with looming stimuli of lower approach velocities. Heap and colleagues found that the telencephalon, thalamus, tectum and hindbrain respond to looming stimuli (Heap et al., 2018b). This study focused on thalamic and tectal, but not telencephalic, responses to looming stimuli. However, they suggested this region may process cognitive interpretation of threats. Therefore, the zebrafish subpallium may be equivalent to the mammalian amygdala and striatum. In mammals, DA transmission from the VTA to the NAc and amygdala increases in response to aversive stimuli (Badrinarayan et al., 2012, Brischoux et al., 2009, Lammel et al., 2011, Matsumoto and Hikosaka, 2009, Soares-Cunha et al., 2016a, Yoshimi et al., 2015, Schultz et al., 2017, Greba and Kokkinidis, 2000, Borowski and Kokkinidis, 1996). Blocking DA signalling in the amygdala can weaken fear-potentiated startle behaviours, as well as abolishing defensive behaviours (Lamont and Kokkinidis, 1998, Guarraci et al., 1999a, Guarraci et al., 1999b, Borowski and Kokkinidis, 1996, Greba and Kokkinidis, 2000, Greba et al., 2001). Furthermore, it has been shown that activation of D1-MSNs of the NAc shell can evoke aversive behaviours (Al-Hasani et al., 2015). Since slow approaching stimuli increase subpallial DAergic neuron activity, it could be hypothesised that these neurons have a similar role to VTA neurons, at least in the context of responding to aversive stimuli. Little is known in regard to the firing activity of VTA neurons responds to looming stimuli. Therefore, further understanding of the VTA, looming stimuli and visually evoked escape behaviours is required.

Ablating subpallial DAergic neurons attenuated LLC responses in fish presented with looming stimuli. This suggests that subpallial DAergic neurons influence the alternative escape response. In mammals, abolishing amygdaloid DA signalling can eliminate defensive behaviours (Lamont and Kokkinidis, 1998, Guarraci et al., 1999a, Guarraci et al., 1999b), suggesting a key role for defensive behaviour. As mentioned previously, subpallial DAergic neurons are the primary source of DA in the telencephalon hypothalamus (Tay et al., 2011). Ablating subpallial

DAergic neurons would reduce the DA transmission in the putative amygdala and I have shown that loss of these neurons perturbs escape behaviour in zebrafish. It suggests that loss of amygdaloid DA in zebrafish disrupts defensive behaviour, similar to findings in mammals. Therefore, these experiments support the hypothesis that the subpallial DAergic neurons are, at least in the context of threat detection, functionally equivalent to mammalian VTA neurons.

Since the loss of subpallial DAergic neurons reduces DA input to the putative striatum as well as perturbs escape responses, changes to zebrafish escape behaviour could be mediated via striatal structures. In mammals, DA signalling to the NAc has been shown to increases in response to aversive stimuli (Matsumoto and Hikosaka, 2009, Soares-Cunha et al., 2016a). It has been suggested that DA transmission in the NAc conveys motivational signals, regardless of rewarding or aversive nature of the stimuli (Matsumoto and Hikosaka, 2009, Matsumoto and Takada, 2013). Optogenetic manipulation of DA signalling in the NAc can increase or decrease progressive ratio task performance in rodents, an effect that is dependent on activation or inhibition of D2-MSNs (Soares-Cunha et al., 2016a). Additionally, a nonselective DA receptor antagonist was capable of decreasing response vigour in an effort-based choice task (Bailey et al., 2018). If subpallial DAergic neurons are involved in responding to aversive stimuli and ablating them decreases the probability of eliciting an alternative escape, this could be due to deficits in motivation or even attention. A recent investigation in rodents revealed DA transmission enhances the signal to noise ratio of aversive stimuli (Vander Weele et al., 2018). Therefore, subpallial DAergic neurons may modulate NAc activity and influence motivation and valence regarding threatening stimuli.

However, DA transmission has been shown to modulate decision making in many species (Filla et al., 2018, Rutledge et al., 2015). VTA neurons have been implicated in decision making and valence (Koob, 1996, Rogers, 2011). DA transmission in the striatum has been shown to define effort rather than the value aspect of decision making in rodents and dysfunction of DA signalling can generate deficits in motivation (Filla et al., 2018). Since ablating subpallial DAergic neurons reduced the probability of prey capture and LLC responses, my findings point towards deficits in decision making processes to predatory and prey stimuli.

5.4.3 Subpallial dopaminergic neurons and sensorimotor gating of threatening stimuli

If subpallial DAergic neurons respond to specific looming stimuli and loss of these neurons perturbs escape behaviours, what then, is the role of subpallial DAergic neurons in threat recognition? One possible explanation is that they modulate sensorimotor gating. The ascending auditory and visual pathways of teleosts converge in the thalamus, a structure that integrates, filters and relays motor and sensory information (Heap et al., 2018b, Mueller, 2012, Vanwalleghem et al., 2017). Subpallial DAergic neurons receive input from the thalamus but also project to the thalamus, suggesting a thalamo-subpallium loop that could modulate sensory processing. In mammals, the thalamus integrates sensory information and can influence escape behaviours (Tyll et al., 2011, Ewert et al., 2001). Studies have found VTA DAergic neurons innervate the thalamus and can modulate sensory processing in the thalamus (Varela, 2014, Jacob and Nienborg, 2018). It has been suggested that the VTA-thalamic pathways could modulate sensory processing of reward or threatening stimuli (Sanchez-Gonzalez et al., 2005). However, little is known of the function of the VTA-thalamus pathway (Groenewegen, 1988, Sanchez-Gonzalez et al., 2005, Papadopoulos and Parnavelas, 1990, Melchitzky et al., 2006). In zebrafish the thalamus responds to looming stimuli and lesions to this structure can attenuate startle behaviour (Heap et al., 2018b). Additionally, ablating subpallial DAergic neurons can attenuate LLC startle responses; therefore, these neurons could modulate the thalamus to influence escape behaviour. If subpallial DAergic neurons modulate the function of the thalamus, then further studies are required to delineate the role of DA modulation of thalamic activity. This can be addressed by using whole brain mapping techniques such as calcium imaging, which can be used to compare the activity of subpallial DAergic neurons and the thalamus. Furthermore, optogenetic tools can be used in conjunction to whole brain activity mapping to delineate the effects of optogenetic activation and inhibiton of subpallial DAergic neurons on the activity of the thalamus.

In addition to innervating the thalamus, the subpallial DAergic neurons innervate the putative amygdala, a structure involved in processing threatening stimuli. The

putative amygdala is innervated by the thalamus, a structure in which the ascending auditory and visual pathways of teleosts converge (Heap et al., 2018b, Mueller, 2012, Vanwalleghem et al., 2017). In mammals, there is a homologous pathway that connects the superior colliculus to the amygdala via the thalamus, a circuit known as the non-canonical thalamic pathway (Wei et al., 2015). Activation of this pathway can elicit escape behaviour in rodents, and its disruption abolishes fear responses to looming stimuli (Shang et al., 2015, Wei et al., 2015). The amygdala is critical for eliciting fear responses and lesions to this structure abolishes escape responses to predator cues (Martinez et al., 2011, Shackman and Fox, 2016, Fox and Shackman, 2019, Newman, 1999, Trimble and Van Elst, 1999). DA signalling has been studied extensively in the context of modulating amygdala-dependent aversive behaviour (Lamont and Kokkinidis, 1998, Guarraci et al., 1999a, Guarraci et al., 1999b, De Bundel et al., 2016). One study found that modulating DA transmission facilitates behaviours associated with threat recognition, and adaptive responses to deal with threatening stimuli (de la Mora et al., 2010).

Several studies have suggested the subpallium is involved in higher-order processing of sensory information and stimulus interpretation (Cheng et al., 2014, Heap et al., 2018b, Vanwalleghem et al., 2017). The subpallium has been shown to be active when presented with aversive acoustic, mechanosensory and visual stimuli. However, the role of subpallial DAergic neurons is not fully understood. Several studies have suggested LLC behavioural response is driven by threat assessment and influence by sensorimotor decision-making processes (Jain et al., 2018, Bhattacharyya et al., 2017). In this chapter, I found that ablating subpallial DAergic neurons reduced the probability of eliciting an LLC escape response. Additionally, I found subpallial DAergic neurons responded to looming stimuli with slow approach velocities. Together, this suggests these neurons respond to potentially threatening stimuli and influences decision-making processes behind threat assessment. To fully understand how subpallial DAergic neurons influence the decision-making processes, further studies are required to determine how DA signalling modulates the putative amygdala. For example, investigating the activity of the amygdala in response to social, attractive and aversive stimuli. This could be examined by the use of whole brain activity

mapping techniques can be used to compare the activity of subpallial DAergic neurons and the amygdala when zebrafish are exposed to social, rewarding or aversive stimuli. Furthermore, optogenetic tools can be used to inhibit subpallial DAergic neurons in conjunction with whole brain activity mapping to delineate the relationship on the amygdala as well as changes in behaviour.
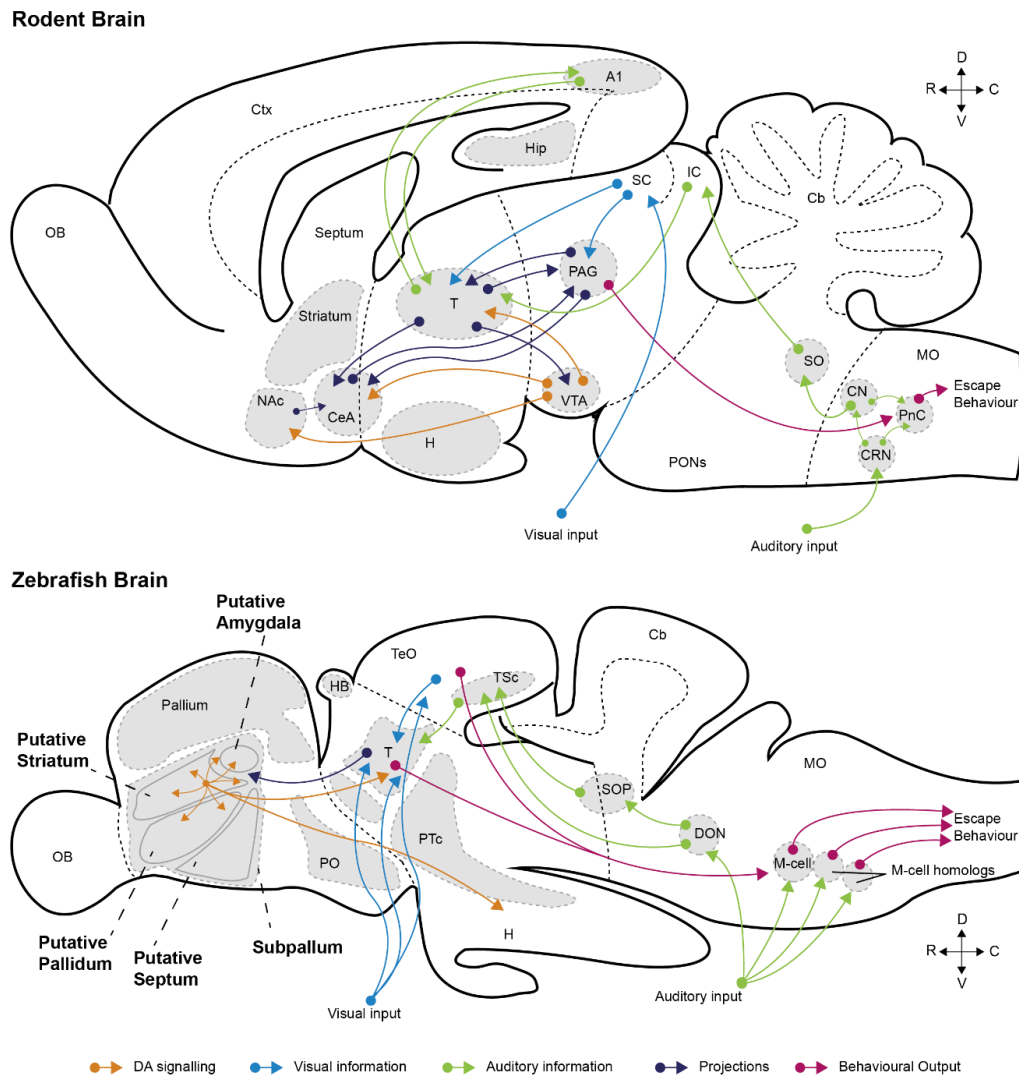
Figure 5:20 Comparison of rodent and zebrafish ascending auditory and visual circuits. Schematic illustration of the sagittal cross-section of the rodent brain (upper illustration) and zebrafish brain (lower illustration). The flow of foraging related information across the brain of visual information (blue line), connections between nuclei (purple), acoustic (green), DA transmission (orange) and locomotor output (magenta). Abbreviation: Cb; Cerebellum, CeA; Central nuclei of the amygdala, Ctx; Cortex, H; hypothalamus, Hb; habenular, Hip; Hippocampus, IC; Inferior Colliculus, MO; Medulla, NAc; Nucleus accumbens, NMLF; nucleus of the medial longitudinal fasciculus, PAG; Periaqueductal grey, PO; preoptic region, PTc; posterior tuberculum, PT; pretectum, OB; olfactory

bulb, SC; Superior Colliculus, T; Thalamus, VTA; ventral tegmental area, Adapted and derived from Mueller, (2012), Rink and Wullimann (2002) and Tay et al., (2011). (Mueller, 2012) (Mueller, 2012)

In sum, subpallial DAergic neurons are activated by the visual stimulus when zebrafish are exposed to looming stimuli (Figure 5:21A). These neurons receive sensory input from the thalamus which originates from ascending visual and auditory systems (Figure 5:21A). Subpallial DAergic neurons can influence startle behaviour by modulating sensory processing in the thalamus (Figure 5:21A). The thalamus processes sensory information. Ablating subpallial DAergic neurons perturbs LLC response to aversive stimuli (Figure 5:21B) whilst loss of DA signalling to the thalamus (Figure 5:21B.1) may affect sensory processing of aversive stimuli that is relayed to the Mauthner cells and their homologs (Figure 5:21B.2). Furthermore, loss of these DAergic neurons could affect the decision-making behaviour to respond to potential threats and reduces the probability of eliciting an LLC response (Figure 5:21).
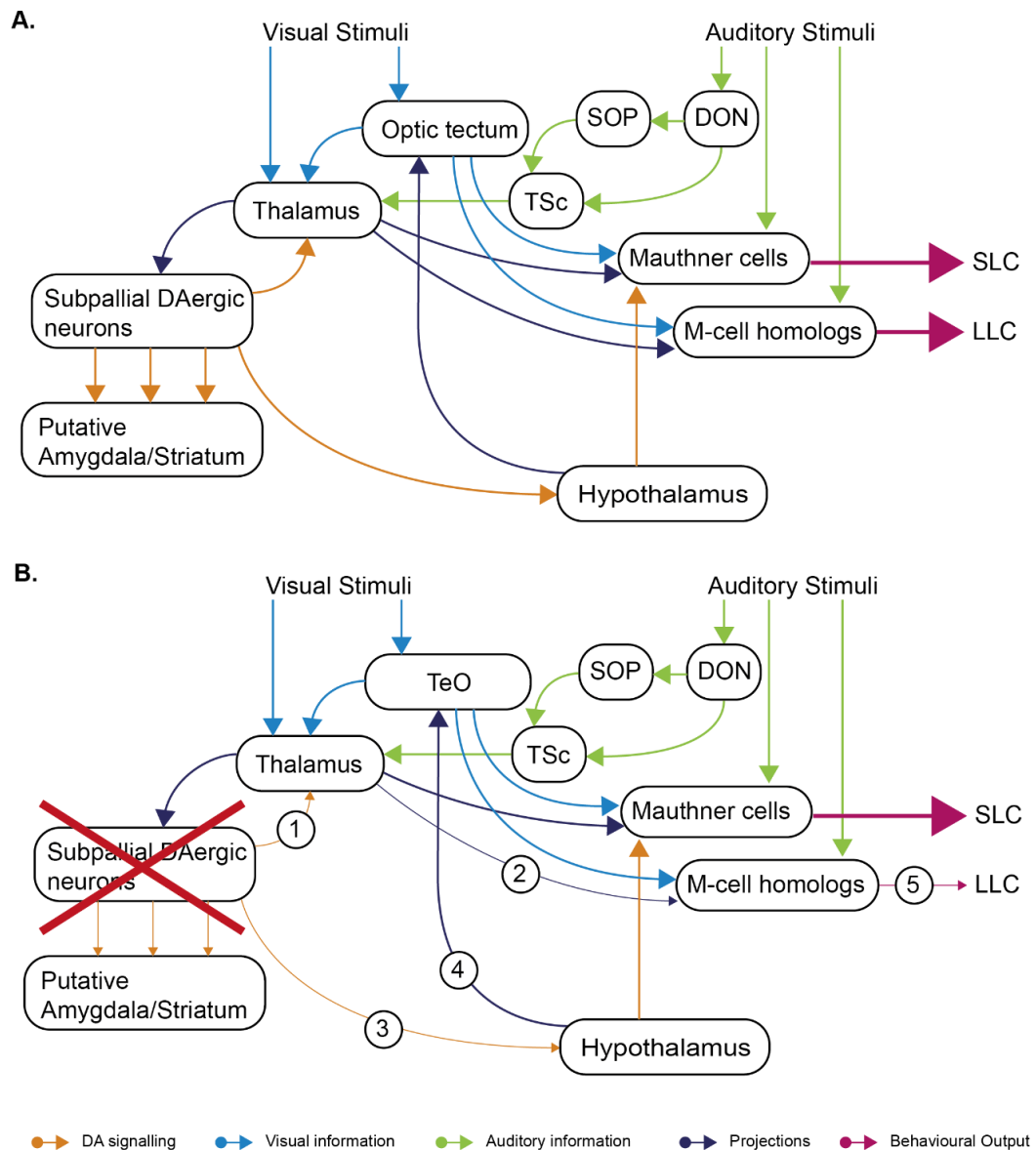
Figure 5:21 Schematic illustration of zebrafish sensory integration of startling stimuli. A - B: Schematic illustration of ascending visual system in zebrafish brain and the connectome of subpallial DAergic neurons. **A:** Visual information is relayed indirectly to the subpallial DAergic neurons by the thalamus. The thalamus receives input from the subpallial DAergic neurons to modulate the thalamus activity. Downstream signalling from the TeO and thalamus can influence motor output via the NMLF to pursue prey. **B:** Ablating subpallial DAergic neurons abolishes DA input to the putative amygdala/striatum, the thalamus (1) and the hypothalamus (3). Lack of DA signalling to the thalamus could affect sensory processing and change the thalamic influence of the NMLF (2) and subsequently perturbed the pursuit of prey (5). The lack of subpallial DAergic neurons reduces the DAergic input to the hypothalamus, which projects to the TeO and can influence prey capture behaviour. The flow of foraging related information across the brain of visual information (blue line), connections between nuclei (purple), DA transmission (orange) and locomotor output (magenta). Abbreviation: GC; griseum centrale, NMLF; nucleus of the medial

longitudinal fasciculus, TeO; optic tectum, T; Thalamus, derived from Mueller, (2012), Rink and Wullimann (2002) and Tay et al., (2011).

5.4.4   Conclusion

In sum, the findings presented in this chapter demonstrate the subpallial DAergic neurons are active when presented with threatening stimuli with a slow approach velocity. Selective ablation of the subpallial DAergic neurons was sufficient to perturb LLC responses to both acoustic and looming stimuli. Ablating these neurons affected the probability of LLC responses without disrupting swimming or startle kinetics. Loose patch recordings of subpallial DAergic neurons revealed that these cells increased their activity when exposed to looming stimuli with slow approach velocity; however, this was not observed with high velocity looming stimuli. This suggests subpallial DAergic neurons exhibit speed tuning. Therefore, subpallial DAergic neurons may respond to specific stimuli based on locomotive kinetics and influence behavioural response to aversive stimuli.

Discussion

Within this thesis, the physiology of subpallial DAergic neurons of larval zebrafish was characterised during the first 5 dpf. Furthermore, the role of subpallial DAergic neuron activity was examined to determine their involvement in zebrafish behaviour. In the first results chapter, the anatomical, morphological and physiological development of subpallial DAergic neurons was investigated. Whilst previous studies have already identified the morphology of subpallial DAergic neurons during early zebrafish development (Tay et al., 2011, McLean and Fetcho, 2004a) and mapped brain regions that innervate the subpallium (Rink and Wullimann, 2004, Rink and Wullimann, 2002a), the early development of the morphology, the physiological properties and afferent inputs to these cells have remained unknown.

Imaging of subpallial DAergic neurons revealed rapid morphological maturation during the first days of life. By 5 dpf, subpallial DAergic neurons arbourise extensively throughout the telencephalon, and a subpopulation of these neurons possess descending projections into the diencephalon. Previous investigations have observed these projections from 4 dpf, which innervate the thalamus and hypothalamus and estimate 50% of subpallial DAergic neurons possess these descending projections (Tay et al., 2011, McLean and Fetcho, 2004a). In mammals, VTA DAergic neurons have been observed to project to the thalamus and could modulate the activity of the thalamus and sensory processing (Varela, 2014). Sanchez-Gonzalez and colleagues have suggested that DA signalling could modulate thalamic relay regarding reward or threatening features of environmental stimuli (Sanchez-Gonzalez et al., 2005). However, relatively little is known about the function of VTA-thalamus signalling (Papadopoulos and Parnavelas, 1990, Groenewegen, 1988, Melchitzky et al., 2006, Sanchez-Gonzalez et al., 2005). The zebrafish thalamus is known to be activated by auditory and visual stimuli (Heap et al., 2018b, Vanwalleghem et al., 2017). If DA signalling to mammalian thalamus modulates thalamic activity, the subpallial DAergic neurons could modulate the activity of the zebrafish thalamus. However, further work is needed to determine the role of DA transmission in the thalamus.

Retrograde labelling studies revealed that by 3 to 5 dpf, inputs to subpallial DAergic neurons originate from brain regions that include the subpallium, preoptic, pretectum, posterior tuberculum and hindbrain regions. In adults, tracing

studies have shown that the subpallium receives local input from the olfactory bulb, pallium and subpallium as well as receiving input from the thalamus, posterior tuberculum and hindbrain areas including the raphe, LC, MO and premotor regions (Rink and Wullimann, 2004, Rink and Wullimann, 2002a). Similar afferent regions were identified in larval zebrafish when compared to previous work in adults; however, not all afferent nuclei were observed at larval stages. For example, studies found the subpallium receives both DAergic input from the posterior tuberculum and NAergic input from the Lc (Rink and Wullimann, 2001, Tay et al., 2011, McLean and Fetcho, 2004a), however, these projections were not observed in the neurobiotin retrograde labelling study in larval zebrafish, suggesting that at the stages studied here, DAergic neurons do not receive DA and NA input. Tay and colleagues found the ascending projections of DAergic neurons in the posterior tuberculum and the NAergic neurons of the LC superficially innervate the ventral aspect of the subpallium (Tay et al., 2011) whereas subpallial DAergic neurons are found in the dorsal aspect this region, which could account for the discrepancy in findings. Additionally, adult tracing studies found the subpallium receives input from the pallium and olfactory bulb (Rink and Wullimann, 2004, Rink and Wullimann, 2002a), however, at larval stages, pallial input was not observed. Therefore, innervation to these areas may occur during later developmental periods. Since tracing studies in larval and adult zebrafish found the subpallium and subpallial DAergic neurons are innervated by the thalamus and premotor network, they may receive input regarding sensory and motor information. Therefore, the function of subpallial DAergic neurons could be involved in the processing of sensorimotor signals.

I have shown that by 5 dpf, subpallial DAergic neurons arbourise locally and receive input from multiple regions. To determine when these cells become functionally integrated into the nervous system, I used electrophysiological methods. Whole-cell recordings of subpallial DAergic neurons revealed they receive both excitatory and inhibitory synaptic input from 3 dpf. At this time, these cells are also intrinsically excitable, becoming capable of generating robust trains of action potentials by 5 dpf. Importantly, subpallial DAergic neurons also display endogenous firing activity during loose patch recordings, suggesting they are an integrated part of the CNS by 5 dpf. Interestingly, the application of synaptic

231

blockers abolished the endogenous firing activity of subpallial DAergic neurons, demonstrating they do not exhibit autonomous firing. Autonomous firing is a physiological hallmark of many mammalian midbrain DAergic neurons, which is driven by voltage-dependent slow depolarisation oscillations (Grace and Bunney, 1984b, Grace and Onn, 1989, Tucker et al., 2012) and has been observed in the DAergic neurons of the olfactory bulb (Pignatelli et al., 2005). However, recent studies reveal variations in autonomous firing capability. Specifically, TIDA cells do not possess autonomous firing (Margolis et al., 2006, Lammel et al., 2008, Lyons et al., 2010, Lyons et al., 2012, Pignatelli et al., 2005). In zebrafish, DC2/4 group exhibit autonomous firing when synaptic transmission is blocked, (Jay et al., 2015). Together, this suggests autonomous firing is conserved across species, however, it is not conserved in all DAergic clusters. Autonomous firing patterns of DAergic neurons results in tonic DA release that maintains extracellular DA concentrations, generating a baseline for the proper functioning of target regions (Guzman et al., 2009, Albin et al., 1989, Grace, 2016). Loss of tonic firing has been implicated in changes in cognition, and attenuated tonic release is associated with enhanced phasic DA release in ADHD patients (Badgaiyan et al., 2015). One reason for this discrepancy is that subpallial DAergic neurons were investigated in early-stage zebrafish and autonomous firing may appear later in development. The use of physiological recording in older subpallial DAergic neurons would be able to determine if these neurons develop autonomous firing at later stages of life.

Traditional studies of the mammalian midbrain DAergic neurons suggested neurons possessed similar properties, however, recent studies have challenged the hypothesis of a conserved physiological 'signature' for DA neurons (Margolis et al., 2006, Lammel et al., 2008). I did not observe similar physiological properties in subpallial DAergic neurons, and I did not observe autonomous firing or identify an I_h current. I did not observe an I_h current in subpallial DAergic neurons, investigations into DC2/4 were unable to identify an I_h current (Jay, 2015). Therefore, this property is not conserved in zebrafish DAergic neurons. However, my studies were conducted in larval zebrafish, and these DAergic neurons may be still developing, and these properties may appear later in development. The use of electrophysiological techniques in older subpallial

DAergic neurons would be able to determine if these physiological features appear later in development.

In the second and third results chapters, I examined the functional relevance of subpallial DAergic neurons in early-stage zebrafish. Previous works have suggested that regions of the subpallium are the homologous striatum and extended amygdala (Ganz et al., 2012, Mueller et al., 2008, Wullimann and Mueller, 2004, Perathoner et al., 2016, O'Connell and Hofmann, 2011). Additionally, the subpallium has previously been shown to be active when zebrafish are exposed to rewarding stimuli (von Trotha et al., 2014, Randlett et al., 2015). However, the involvement of subpallial DAergic neurons during the exposure to rewarding stimuli has not been previously investigated. The work presented in chapter two used FSVC and IHC techniques to demonstrate that subpallial DAergic neurons are active when zebrafish are exposed to live prey. Moreover, laser ablation of subpallial DAergic abolished prey capture behaviours without affecting prey tracking or basal locomotion. This suggests that DA transmission from subpallial DAergic neurons is required for foraging behaviour.

Since loss of subpallial DAergic neurons did not affect locomotion, perturbation of foraging behaviour cannot be mediated by changes in swimming behaviour. This is to be expected, as a recent study has shown that motor activity during prey capture is controlled by the MeLc and MeLr of the nMLF reticulospinal neurons while visual evoked prey capture behaviour is mediated by the nMLF (Gahtan et al., 2005). These premotor neurons are modulated by visual input from the tectum to facilitate prey capture events (Nikolaou and Meyer, 2015, Gahtan et al., 2005, Muto and Kawakami, 2013, Tay et al., 2011). Since subpallial DAergic neurons do not innervate this region, ablating these neurons would not directly affect nMLF activity. However, the nMLF has been shown to receive DAergic input, suggesting this region is modulated by DA, though not from subpallial sources (McLean and Fetcho, 2004b).

Prey capture behaviour is composed of several manoeuvres, one of which is prey tracking. My studies revealed that loss of subpallial DAergic neurons has no effect on prey tracking. RGCs and neurons in the optic tectum have been shown to exhibit size, speed and direction tuning (Levick, 1967, Olveczky et al., 2003,

Damjanović et al., 2019, Bianco and Engert, 2015), which allows zebrafish to distinguish objects as prey or threat. Neurons of the optic tectum are segregated based on the object size they respond to, generating a topographical map of object size across this region (Preuss et al., 2014, Helmbrecht et al., 2018). The optic tectum integrates sensory information eliciting eye convergence via extraocular medial rectus motoneurons (Bianco and Engert, 2015).

In this study, selective ablation of subpallial DAergic neurons attenuated prey capture without affecting locomotion, prey tracking or initiation of hunting manoeuvres. A recent study found that ablation of the nucleus isthmi had similar effects on foraging, described as a failure to sustain prey capture sequences and resulting in aborted hunting attempts (Henriques et al., 2019). What then, is subpallial DAergic neuron signalling doing to the sensorimotor networks that drive prey capture behaviours? One explanation is that these cells may modulate thalamic activity thereby influencing integration of sensory information. In monkey, the thalamus receives DA input from multiple nuclei, including the VTA and SNc (Sanchez-Gonzalez et al., 2005). DA signalling can influence the activity of the thalamus, microinjections of D_1 and D_2 receptor antagonist in the thalamus reduced decisional impulsiveness and pursuit of a reward, as measured by an increase in omissions of lever presses (Wang et al., 2017). Disruption to DA signalling and DA transmission to the thalamus reduced motivation and attention to pursue reward in mammals (Winstanley et al., 2010, Wang et al., 2017). Since zebrafish subpallial DAergic neurons project to the thalamus and ablation of this pathway reduces the pursuit of prey the subpallial DAergic neurons could be involved in motivation, attention or decision-making processes related to acquisition of food, as they are in mammals.

Another possible explanation is that subpallial DAergic neurons influence pretecto-hypothalamic pathways. Using juxtacellular labelling techniques, I found subpallial DAergic neurons project to the hypothalamus, similar to the observations of (Tay et al., 2011). The pretecto-hypothalamic pathway is required for prey capture behaviours as ablation of this pathway abolishes this behaviour (Muto et al., 2017). Hypothalamic projections to the tectum can convey satiety, and fed zebrafish are less likely to pursue prey by reducing the activity of neurons that are tuned to small objects (Filosa et al., 2016). Since subpallial DAergic

neurons project to the hypothalamus, they could modulate the pretecto-hypothalamic loop and influence prey capture behaviour. In mammals, the extended amygdala and hypothalamus are also involved in predatory hunting behaviours (Comoli et al., 2005). Activation of the CeA can initiate hunting and lesions to this structure attenuates this behaviour (Han et al., 2017). Activation of the VTA and increased DA levels in the CeA can increase feeding behaviours (Hajnal and Lenard, 1997, Boekhoudt et al., 2017). Comoli and colleagues have suggested that the extended amygdala may convey motivation and influence motor output of predatory feeding (Comoli et al., 2005). Therefore, if the zebrafish subpallium is functionally equivalent to the extended amygdala, subpallial DAergic neurons may share a similar functional role to mammalian VTA neurons in regulation hunting behaviour via amygdala and hypothalamic circuits.

In the final results chapter, I examined the role of subpallial DAergic neurons in escape behaviour. As stated before, parts of the subpallium may be homologous to the extended amygdala. In mammals, the amygdala is known to be involved in processing fear and anxiety (Fox and Shackman, 2017, Ahrens et al., 2018, Jennings et al., 2013). Additionally, the subpallium is active when zebrafish are exposed to aversive stimuli (Randlett et al., 2015, Heap et al., 2018b, Vanwalleghem et al., 2017). However, it is unknown whether subpallial DAergic neurons are involved in this process. The work presented in chapter five demonstrates that selective loss of subpallial DAergic neurons perturbs startle behaviour, with zebrafish less likely to elicit LLC responses. Additionally, firing frequency of subpallial DAergic neurons increased when larvae were exposed to looming stimuli with slow, but not fast, approach speeds. This suggests that subpallial DAergic neurons may respond to aversive stimuli and modulate predator avoidance circuitry.

My data suggest that ablation of subpallial DAergic neurons selectively suppresses LLC escape responses in response to both visual and acoustic stimuli. However, bending manoeuvres or escape locomotion were not affected by the loss of subpallial DAergic neurons. Previous studies have shown the reticulospinal neurons including Mauthner, MiD2cm and MiD3cm neurons are critical for escape behaviours (Kohashi and Oda, 2008, Liu and Hale, 2017, Liu and Fetcho, 1999). Mauthner cells drive SLC responses, whilst the MiD2cm and

MiD3cm neurons elicit LLCs (Liu and Fetcho, 1999, Kohashi and Oda, 2008). Mauthner cells have been shown to receive DA input, however, MiD2cm and MiD3cm neurons do not appear to be directly innervated by DA neurons (McLean and Fetcho, 2004b). My data also suggests that subpallial DAergic neurons do not directly innervate reticulospinal networks. By contrast, Mauthner cells receive DA input, and this originates from the light-responsive hypothalamic DAergic neurons that have been shown to enhance acoustic-evoked SLC (Mu et al., 2012). Therefore, DA signalling to the Mauthner cells can modulate escape before, however, it is not through direct innervation from the subpallial DAergic neurons.

If subpallial DAergic neurons do not innervate reticulospinal neurons, how do these DAergic neurons modulate LLC responses? Investigations into the assessment of threats and behavioural responses to these stimuli reveals dynamic responses that ensure appropriate escape behaviour selection for a given threat (Jain et al., 2018). Recordings of subpallial DAergic neurons showed they respond to slow approaching looming stimuli. This suggests these cells receive information regarding object kinetics such as speed. The decision-making process involved in selection between SLC and LLC responses is greatly influenced by the threat, LLC responses are triggered by looming stimuli with lower approach velocities than SLC (Bhattacharyya et al., 2017, Barker and Baier, 2015, Temizer et al., 2015, Preuss et al., 2014). Since the activity of subpallial DAergic neurons increased in response to stimuli most likely to elicit LLC responses. Therefore, subpallial DAergic neurons could influence threat assessment and facilitate LLC behaviours.

Extracellular recordings of subpallial DAergic neurons when zebrafish were exposed to looming stimuli revealed that their activity only increased when exposed to slow approaching stimuli. The zebrafish thalamus has been shown to process visual information regarding looming stimuli and facilitate visually evoked escape behaviour (Heap et al., 2018b). In mammals, VTA DAergic neurons have been observed to project to the thalamus, and DA signalling can modulate sensory processing in the thalamus (Varela, 2014, Jacob and Nienborg, 2018). Sanchez-Gonzalez and colleagues have suggested that DA signalling could modulate thalamic relay regarding reward or threatening features of

environmental stimuli (Sanchez-Gonzalez et al., 2005). DA transmission in the thalamus has been shown to modulate the processing of visual stimuli in the thalamus (Albrecht et al., 1996). Several studies found that modulation of DA transmission in the thalamus can facilitate or inhibited visual induced spike activity which was dependent on visual stimulus size and contrast (Zhao et al., 2002, Zhao et al., 2001) These studies also found that thalamic DA signalling facilitated the activity in response to small stimuli (Zhao et al., 2002). Additionally, recent investigations have shown that DA transmission enhances the signal-to-noise ratio of aversive stimuli, thereby enhancing valence (Vander Weele et al., 2018). Subpallial DAergic neurons could have a similar role: as they respond to specific looming stimuli with slow approach speeds, they could enhance signal-to-noise ratio of information related to potential threats. Therefore, the DA signalling enhances the valence of potential threats by modulating activity in the telencephalon as well as sensory processing in the thalamus to facilitate LLC escape behaviours. This could be assessed by the use of optogenetic tools to drive the activity of subpallial DAergic neurons and determine if the proportion of LLC response is affected by subpallial DAergic neuron activity and if this activity modulates the activity of thalamic neurons.

Examining the role of subpallial DAergic neurons has revealed they respond to both attractive and aversive stimuli: activity in these cells neurons increases in response to both prey as and slow-approaching threats. Selective loss of subpallial DAergic neurons reduces the pursuit of prey and to respond to potential threats. DA neurons of the VTA have been shown to activate in response to both rewarding and aversive stimuli. Therefore, DA transmission may convey signals that relate to both rewarding and aversive stimuli which can include motivation, attention and valence (Wise, 2004, Nieoullon, 2002, Soares-Cunha et al., 2016b, Nieh et al., 2013).

If subpallial DAergic neurons are active in response to prey and looming stimuli, what is the role of subpallial DAergic neurons? One possible explanation for the role of subpallial DAergic neurons during prey capture and escape behaviours is they provide a mechanism of valence and influence decision making. In mammals, the thalamus integrates sensory information and can influence behavioural responses during prey capture and fear responses (Tyll et al., 2011,

Ewert et al., 2001). This structure receives input from both the amygdala and superior colliculus (homologous to the zebrafish optic tectum), and disruption to amygdala-thalamic or superior colliculus-thalamic circuits can disrupt the processing of aversive stimuli and escape behaviours in mammals. DA signalling has previously shown to enhance signal-to-noise ratio of aversive stimuli in fear response circuits and is a mechanism of valence processing (Vander Weele et al., 2018). In zebrafish and mammals, sensorimotor gating and decision-making circuits involve the tectum (Helmbrecht et al., 2018, Barker and Baier, 2015, Filosa et al., 2016, Huk and Shadlen, 2005, Kardamakis et al., 2015). Additionally, DA transmission has been shown to modulate these decision-making circuits in many species (Filla et al., 2018, Rutledge et al., 2015). VTA neurons have been implicated influencing decision making and valence (Koob, 1996, Rogers, 2011). DA transmission in the striatum has been shown to define effort rather than the value aspect of decision making in rodents and dysfunction of DA signalling can generate deficits in motivation (Filla et al., 2018). Since ablating subpallial DAergic neurons reduced probability of prey capture and LLC responses, suggests deficits in decision making processes to respond to stimuli.

In zebrafish, disruption to the thalamus-tectal pathways can perturb prey capture and visually evoked startle behaviour (Semmelhack et al., 2014, Mueller, 2012, Heap et al., 2018b). I found the subpallial DAergic neurons receive input from the pretectal region, and similar projections have been found in adult zebrafish, with the subpallium receiving input from the parvocellular superficial pretectal nucleus (PSp) of the thalamus (Rink and Wullimann, 2004, Rink and Wullimann, 2002a). The PSp in zebrafish is the equivalent to the lateral geniculate nucleus in the mammalian thalamus, which serves to relay visual information to the visual cortex (Semmelhack et al., 2014). Heap and colleagues found the subpallium and thalamus responds to looming stimuli, and luminescence information is relayed via thalamic pathways and can facilitate escape behaviour (Heap et al., 2018b). However, the role of thalamic– subpallial projections is not known. Additionally, my results suggest that subpallial DAergic neurons project to the thalamus. Taken together, this suggests a loop exist between the zebrafish subpallium and thalamus. To determine if this is indeed the case, whole-brain activity mapping techniques such as calcium imaging can be used to delineate how thalamus

activity is modulated by DA transmission by integrating optogenetic tools in which the activity of subpallial DAergic neurons can be directly modulated. Therefore, subpallial DAergic neurons can receive multi-sensory information via the thalamus. Subsequent DAergic signalling could convey valence and modulating decision making by influencing sensorimotor circuits at the thalamus and hypothalamus (Figure 6:1).
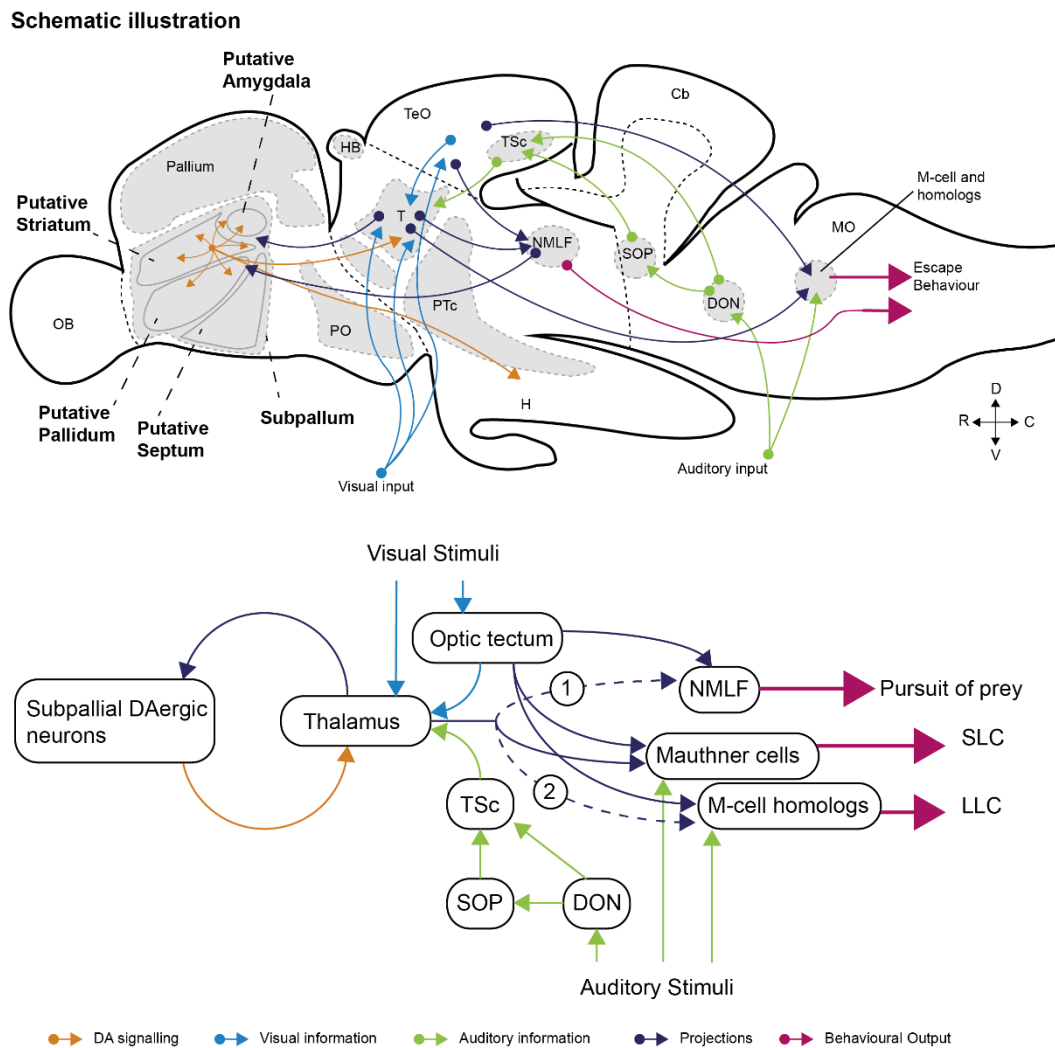
Figure 6:1 Hypothetical circuit for subpallial DAergic neurons signalling and sensorimotor gating and decision making. Schematic illustration of the sagittal cross-section of the zebrafish brain (upper) and flow chart of input and output circuits (lower). The flow of information across the brain, visual (blue line), auditory (green line) and thalamo-subpallial pathway (purple). DA transmission from the subpallium (orange) and proposed premotor input (magenta). The thalamus receives direct visual input and indirect sensory input from the TeO. Motor output is modulated by input from the thalamus, TeO and direct sensory information. Subpallial DAergic neurons receive input from the thalamus and are

relayed back to potential modulate decision making circuits. Influence the pursuit of prey (1) or to avoid potential threats (2). Abbreviation: PG; Preglomerular region, Hb; habenular, H; hypothalamus, Cb; Cerebellum, MO; Medulla, H; NMLF; nucleus of the medial longitudinal fasciculus, Hypothalamus, T; Thalamus, TeO; optic tectum, PO; preoptic region, PTc; posterior tuberculum, OB; olfactory bulb, DON; descending octaval nucleus , SOP; secondary octaval population, TSc; central nucleus of the torus semicircularis. Derived and adapted from Mueller, (2012), Rink and Wullimann (2002) and Tay et al., (2011).

Additionally, subpallial DAergic neurons innervate the subpallium extensively, and these neurons respond to both potential prey and predator (looming stimuli). In mammals, VTA neurons respond to both rewarding and aversive stimuli, which is relayed to the NAc and amygdala (Matsumoto and Hikosaka, 2009, Soares-Cunha et al., 2016a). These signals have been suggested to convey motivational signals irrespective of whether the stimulus is aversive or rewarding (Matsumoto and Hikosaka, 2009, Matsumoto and Takada, 2013). The subpallial DAergic neurons may correspond to the VTA neurons of mammals and modulate activity of the putative striatum and amygdala. However, the functional role of the presumptive zebrafish amygdala and striatum need to be further investigated. To address this, whole brain imaging techniques can be employed to analyse when the putative amygdala is active. The rodent amygdala is active when animals during fear, anxiety, reward, social, aggression and motivated behaviours, zebrafish can be presented with a range of stimuli to investigate what stimuli are processed by the putative amygdala. Since, several studies have shown that the subpallium is active when zebrafish are exposed to rewarding and threating stimuli as well as social stimuli(Randlett et al., 2015, von Trotha et al., 2014, Heap et al., 2018b, Vanwalleghem et al., 2017, Biechl et al., 2017). Functional studies could be conducted to determine the role of the putative amygdala. To address this, lesions to the amygdala can be used to determine how it is involved in learning, reward, cognition, and social behaviours. Furthermore, to understand how subpallial DAergic neurons affect the putative amygdala activity and function, pharmacological manipulation of DA signalling can be used to determine the role of DA in behaviour. Additionally, optogenetic activation and inhibition of subpallial DAergic neurons in conjunction with whole brain activity mapping and behaviour can be used to determine how the activity of these neurons affects the putative amygdala.

In sum, this thesis investigated the physiological properties of DA neurons within the subpallium and the functional role in zebrafish behaviour. The work presented in this thesis represents the first examination of the physiology and activity patterns of subpallial DAergic neurons during early development. Additionally, the work presented here demonstrates that disruption to subpallial DA signalling is sufficient to disrupt foraging and startle behaviours of free-swimming zebrafish. These findings will help inform future investigation into the role of DA signalling in valence and decision making.

References

ADINOFF, B. 2004. Neurobiologic processes in drug reward and addiction. *Harvard review of psychiatry,* 12**,** 305-320.

AHMADLOU, M., ZWEIFEL, L. S. & HEIMEL, J. A. 2018. Functional modulation of primary visual cortex by the superior colliculus in the mouse. *Nature Communications,* 9**,** 3895.

AHRENS, S., WU, M. V., FURLAN, A., HWANG, G. R., PAIK, R., LI, H., PENZO, M. A., TOLLKUHN, J. & LI, B. 2018. A Central Extended Amygdala Circuit That Modulates Anxiety. *The Journal of Neuroscience,* 38**,** 5567-5583.

AL-HASANI, R., MCCALL, J. G., SHIN, G., GOMEZ, A. M., SCHMITZ, G. P., BERNARDI, J. M., PYO, C. O., PARK, S. I., MARCINKIEWCZ, C. M., CROWLEY, N. A., KRASHES, M. J., LOWELL, B. B., KASH, T. L., ROGERS, J. A. & BRUCHAS, M. R. 2015. Distinct Subpopulations of Nucleus Accumbens Dynorphin Neurons Drive Aversion and Reward. *Neuron,* 87**,** 1063-77.

ALBIN, R. L., YOUNG, A. B. & PENNEY, J. B. 1989. The functional anatomy of basal ganglia disorders. *Trends in Neuroscience,* 12**,** 366-75.

ALBRECHT, D., QUASCHLING, U., ZIPPEL, U. & DAVIDOWA, H. 1996. Effects of dopamine on neurons of the lateral geniculate nucleus: an iontophoretic study. *Synapse,* 23**,** 70-8.

ALCAMI, P., FRANCONVILLE, R., LLANO, I. & MARTY, A. 2012. Measuring the firing rate of high-resistance neurons with cell-attached recording. *The Journal of Neuroscience,* 32**,** 3118-30.

ALSENE, K. M., RAJBHANDARI, A. K., RAMAKER, M. J. & BAKSHI, V. P. 2011. Discrete forebrain neuronal networks supporting noradrenergic regulation of sensorimotor gating. *Neuropsychopharmacology,* 36**,** 1003-1014.

AMBROGGI, F., ISHIKAWA, A., FIELDS, H. L. & NICOLA, S. M. 2008. Basolateral amygdala neurons facilitate reward-seeking behavior by exciting nucleus accumbens neurons. *Neuron,* 59**,** 648-61.

ANDEREGG, A., POULIN, J. F. & AWATRAMANI, R. 2015. Molecular heterogeneity of midbrain dopaminergic neurons--Moving toward single cell resolution. *FEBS letters,* 589**,** 3714-26.

ANDRZEJEWSKI, M. E. & RYALS, C. 2016. Dissociable hippocampal and amygdalar D1-like receptor contribution to discriminated Pavlovian conditioned approach learning. *Behavioral and Brain Sciences,* 299**,** 111-21.

ANGELO, K. & MARGRIE, T. W. 2011. Population diversity and function of hyperpolarization-activated current in olfactory bulb mitral cells. *Scientific Reports,* 1**,** 50.

ANZALONE, A., LIZARDI-ORTIZ, J. E., RAMOS, M., DE MEI, C., HOPF, F. W., IACCARINO, C., HALBOUT, B., JACOBSEN, J., KINOSHITA, C., WELTER, M., CARON, M. G., BONCI, A., SULZER, D. & BORRELLI, E. 2012. Dual control of dopamine synthesis and release by presynaptic and postsynaptic dopamine D2 receptors. *The Journal of Neuroscience,* 32**,** 9023-34.

BABAEV, O., PILETTI CHATAIN, C. & KRUEGER-BURG, D. 2018. Inhibition in the amygdala anxiety circuitry. *Experimental & molecular medicine,* 50**,** 18-18.

BADGAIYAN, R. D., SINHA, S., SAJJAD, M. & WACK, D. S. 2015. Attenuated Tonic and Enhanced Phasic Release of Dopamine in Attention Deficit Hyperactivity Disorder. *PLoS One,* 10**,** e0137326.

BADRINARAYAN, A., WESCOTT, S. A., VANDER WEELE, C. M., SAUNDERS, B. T., COUTURIER, B. E., MAREN, S. & ARAGONA, B. J. 2012. Aversive stimuli differentially modulate real-time dopamine transmission dynamics within the nucleus accumbens core and shell. *The Journal of Neuroscience,* 32**,** 15779-90.

BAI, Y., LIU, H., HUANG, B., WAGLE, M. & GUO, S. 2016. Identification of environmental stressors and validation of light preference as a measure of anxiety in larval zebrafish. *BMC Neuroscience,* 17**,** 63.

BAILEY, M. R., GOLDMAN, O., BELLO, E. P., CHOHAN, M. O., JEONG, N., WINIGER, V., CHUN, E., SCHIPANI, E., KALMBACH, A., CHEER, J. F., BALSAM, P. D. & SIMPSON, E. H. 2018. An Interaction between Serotonin Receptor Signaling and Dopamine Enhances Goal-Directed Vigor and Persistence in Mice. *The Journal of Neuroscience,* 38**,** 2149-2162.

BANDIN, S., MORONA, R. & GONZALEZ, A. 2015. Prepatterning and patterning of the thalamus along embryonic development of Xenopus laevis. *Frontiers in Neuroanatomy,* 9**,** 107.

BANKS, M. I., PEARCE, R. A. & SMITH, P. H. 1993. Hyperpolarization-activated cation current (Ih) in neurons of the medial nucleus of the trapezoid body: voltage-clamp analysis and enhancement by norepinephrine and cAMP suggest a modulatory mechanism in the auditory brain stem. *The Journal of Neurophysiology,* 70**,** 1420-32.

BARKER, ALISON J. & BAIER, H. 2015. Sensorimotor Decision Making in the Zebrafish Tectum. *Current Biology,* 25**,** 2804-2814.

BARRY, M. A. & BENNETT, M. V. 1990. Projections of giant fibers, a class of reticular interneurons, in the brain of the silver hatchetfish. *Brain, Behavior and Evolution,* 36**,** 391-400.

BEAN, B. P. 2007. The action potential in mammalian central neurons. *Nature Reviews Neuroscience,* 8**,** 451-65.

BEAULIEU, J. M. & GAINETDINOV, R. R. 2011. The physiology, signaling, and pharmacology of dopamine receptors. *Pharmacological Reviews,* 63**,** 182-217.

BECKER, T., WULLIMANN, M. F., BECKER, C. G., BERNHARDT, R. R. & SCHACHNER, M. 1997. Axonal regrowth after spinal cord transection in adult zebrafish. *The Journal of Comparative Neurology,* 377**,** 577-95.

BECKSTEAD, M. J., FORD, C. P., PHILLIPS, P. E. M. & WILLIAMS, J. T. 2007. Presynaptic regulation of dendrodendritic dopamine transmission. *European Journal of Neuroscience,* 26**,** 1479-1488.

BEELER, J. A., DAW, N., FRAZIER, C. R. & ZHUANG, X. 2010. Tonic dopamine modulates exploitation of reward learning. *Frontiers in Behavioral Neuroscience,* 4**,** 170.

BEHBEHANI, M. M. 1995. Functional characteristics of the midbrain periaqueductal gray. *Progress in Neurobiology,* 46**,** 575-605.

BEIER, K. T., STEINBERG, E. E., DELOACH, K. E., XIE, S., MIYAMICHI, K., SCHWARZ, L., GAO, X. J., KREMER, E. J., MALENKA, R. C. & LUO, L. 2015. Circuit Architecture of VTA Dopamine Neurons Revealed by Systematic Input-Output Mapping. *Cell,* 162**,** 622-634.

BEN-JONATHAN, N. & HNASKO, R. 2001. Dopamine as a prolactin (PRL) inhibitor. *Endocrinology Reviews,* 22**,** 724-63.

BENARROCH, E. E. 2015. The amygdala. *Functional organization and involvement in neurologic disorders,* 84**,** 313-324.

BENNINGER, F., BECK, H., WERNIG, M., TUCKER, K. L., BRUSTLE, O. & SCHEFFLER, B. 2003. Functional integration of embryonic stem cell-derived neurons in hippocampal slice cultures. *The Journal of Neuroscience,* 23**,** 7075-83.

BENSKEY, M., BEHROUZ, B., SUNRYD, J., PAPPAS, S. S., BAEK, S.-H., HUEBNER, M., LOOKINGLAND, K. J. & GOUDREAU, J. L. 2012. Recovery of hypothalamic tuberoinfundibular dopamine neurons from acute toxicant exposure is dependent upon protein synthesis and associated with an increase in parkin and ubiquitin carboxy-terminal hydrolase-L1 expression. *NeuroToxicology,* 33**,** 321-331.

BERGAMINI, G., SIGRIST, H., FERGER, B., SINGEWALD, N., SEIFRITZ, E. & PRYCE, C. R. 2016. Depletion of nucleus accumbens dopamine leads to impaired reward and aversion processing in mice: Relevance to motivation pathologies. *Neuropharmacology,* 109**,** 306-319.

BERKE, J. D. & HYMAN, S. E. 2000. Addiction, Dopamine, and the Molecular Mechanisms of Memory. *Neuron,* 25**,** 515-532.

BERRIDGE, K. C. & ROBINSON, T. E. 1998. What is the role of dopamine in reward: hedonic impact, reward learning, or incentive salience? *Brain Research Reviews,* 28**,** 309-69.

BEVAN, M. D. & WILSON, C. J. 1999. Mechanisms underlying spontaneous oscillation and rhythmic firing in rat subthalamic neurons. *The Journal of Neuroscience,* 19**,** 7617-28.

BHATT, D. H., MCLEAN, D. L., HALE, M. E. & FETCHO, J. R. 2007. Grading movement strength by changes in firing intensity versus recruitment of spinal interneurons. *Neuron,* 53**,** 91-102.

BHATTACHARYYA, K., MCLEAN, D. L. & MACIVER, M. A. 2017. Visual Threat Assessment and Reticulospinal Encoding of Calibrated Responses in Larval Zebrafish. *Current Biology,* 27**,** 2751-2762 e6.

BIANCO, I., KAMPFF, A. & ENGERT, F. 2011a. Prey Capture Behavior Evoked by Simple Visual Stimuli in Larval Zebrafish. *Frontiers in Systems Neuroscience,* 5.

BIANCO, ISAAC H. & ENGERT, F. 2015. Visuomotor Transformations Underlying Hunting Behavior in Zebrafish. *Current Biology,* 25**,** 831-846.

BIANCO, I. H., KAMPFF, A. R. & ENGERT, F. 2011b. Prey Capture Behavior Evoked by Simple Visual Stimuli in Larval Zebrafish. *Frontiers in Systems Neuroscience,* 5**,** 101.

BICANIC, I., HLADNIK, A. & PETANJEK, Z. 2017. A Quantitative Golgi Study of Dendritic Morphology in the Mice Striatal Medium Spiny Neurons. *Frontiers in Neuroanatomy,* 11**,** 37.

BIECHL, D., TIETJE, K., GERLACH, G. & WULLIMANN, M. F. 2016. Crypt cells are involved in kin recognition in larval zebrafish. *Scientific Reports,* 6**,** 24590.

BIECHL, D., TIETJE, K., RYU, S., GROTHE, B., GERLACH, G. & WULLIMANN, M. F. 2017. Identification of accessory olfactory system and medial amygdala in the zebrafish. *Scientific reports,* 7**,** 44295-44295.

BIESDORF, C., WANG, A. L., TOPIC, B., PETRI, D., MILANI, H., HUSTON, J. P. & DE SOUZA SILVA, M. A. 2015. Dopamine in the nucleus accumbens core, but not shell, increases during signaled food reward and decreases during delayed extinction. *Neurobiology of Learning and Memory,* 123**,** 125-39.

BIRD, A. D. & CUNTZ, H. 2019. Dissecting Sholl Analysis into Its Functional Components. *Cell Reports,* 27**,** 3081-3096.e5.

BJORKLUND, A. & DUNNETT, S. B. 2007. Dopamine neuron systems in the brain: an update. *Trends in Neuroscience,* 30**,** 194-202.

BLYTHE, S. N., ATHERTON, J. F. & BEVAN, M. D. 2007. Synaptic activation of dendritic AMPA and NMDA receptors generates transient high-frequency firing in substantia nigra dopamine neurons in vitro. *The Journal of Neurophysiology,* 97**,** 2837-50.

BLYTHE, S. N., WOKOSIN, D., ATHERTON, J. F. & BEVAN, M. D. 2009. Cellular mechanisms underlying burst firing in substantia nigra dopamine neurons. *The Journal of Neuroscience,* 29**,** 15531-41.

BOEHMLER, W., CARR, T., THISSE, C., THISSE, B., CANFIELD, V. A. & LEVENSON, R. 2007. D4 Dopamine receptor genes of zebrafish and effects of the antipsychotic clozapine on larval swimming behaviour. *Genes, Brain and Behavior,* 6**,** 155-66.

BOEHMLER, W., OBRECHT-PFLUMIO, S., CANFIELD, V., THISSE, C., THISSE, B. & LEVENSON, R. 2004. Evolution and expression of D2 and D3 dopamine receptor genes in zebrafish. *Developmental Dynamics,* 230**,** 481-93.

BOEKHOUDT, L., ROELOFS, T. J. M., DE JONG, J. W., DE LEEUW, A. E., LUIJENDIJK, M. C. M., WOLTERINK-DONSELAAR, I. G., VAN DER PLASSE, G. & ADAN, R. A. H. 2017. Does activation of midbrain dopamine neurons promote or reduce feeding? *International Journal of Obesity,* 41**,** 1131-1140.

BOROWSKI, T. B. & KOKKINIDIS, L. 1996. Contribution of ventral tegmental area dopamine neurons to expression of conditional fear: effects of electrical stimulation, excitotoxin lesions, and quinpirole infusion on potentiated startle in rats. *Behavioral Neuroscience,* 110**,** 1349-64.

BOSCHEN, S. L., WIETZIKOSKI, E. C., WINN, P. & DA CUNHA, C. 2011. The role of nucleus accumbens and dorsolateral striatal D2 receptors in active avoidance conditioning. *Neurobiology of Learning and Memory,* 96**,** 254-62.

BRETON, J. M., CHARBIT, A. R., SNYDER, B. J., FONG, P. T. K., DIAS, E. V., HIMMELS, P., LOCK, H. & MARGOLIS, E. B. 2019. Relative contributions and mapping of ventral tegmental area dopamine and GABA neurons by projection target in the rat. *The Journal of Comparative Neurology,* 527**,** 916-941.

BRISCHOUX, F., CHAKRABORTY, S., BRIERLEY, D. I. & UNGLESS, M. A. 2009. Phasic excitation of dopamine neurons in ventral VTA by noxious stimuli. *Proceedings of the National Academy of Sciences of the United States of America,* 106**,** 4894-9.

BROCK, A. J., GOODY, S. M. G., MEAD, A. N., SUDWARTS, A., PARKER, M. O. & BRENNAN, C. H. 2017. Assessing the Value of the Zebrafish Conditioned Place Preference Model for Predicting Human Abuse Potential. *Journal of Pharmacology and Experimental Therapeutics,* 363**,** 66-79.

BROCKERHOFF, S. E. 2006. Measuring the optokinetic response of zebrafish larvae. *Nature Protocols,* 1**,** 2448-51.

BROMBERG-MARTIN, E. S., MATSUMOTO, M. & HIKOSAKA, O. 2010. Dopamine in Motivational Control: Rewarding, Aversive, and Alerting. *Neuron,* 68**,** 815-834.

BROOKS, A. M. & BERNS, G. S. 2013. Aversive stimuli and loss in the mesocorticolimbic dopamine system. *Trends in Cognitive Sciences,* 17**,** 281-6.

BUDICK, S. A. & MALLEY, D. M. 2000. Locomotor repertoire of the larval zebrafish: swimming, turning and prey capture. *The Journal of Experimental Biology,* 203**,** 2565.

BUNNEY, B. S. & AGHAJANIAN, G. K. 1974. Electrophysiological effects of amphetamine on dopaminergic neurons. *Biochemical Pharmacology,* 23**,** 792-797.

BURGESS, H. A. & GRANATO, M. 2007a. Modulation of locomotor activity in larval zebrafish during light adaptation. *The Journal of Experimental Biology,* 210**,** 2526.

BURGESS, H. A. & GRANATO, M. 2007b. Sensorimotor Gating in Larval Zebrafish. *The Journal of Neuroscience,* 27**,** 4984-4994.

BURKE, D. A., ROTSTEIN, H. G. & ALVAREZ, V. A. 2017. Striatal Local Circuitry: A New Framework for Lateral Inhibition. *Neuron,* 96**,** 267-284.

BUSS, R. R. & DRAPEAU, P. 2001. Synaptic Drive to Motoneurons During Fictive Swimming in the Developing Zebrafish. *The Journal of Neurophysiology,* 86**,** 197.

CADET, J. L., JAYANTHI, S., MCCOY, M. T., BEAUVAIS, G. & CAI, N. S. 2010. Dopamine D1 receptors, regulation of gene expression in the brain, and neurodegeneration. *CNS & neurological disorders drug targets,* 9**,** 526-538.

CADUSSEAU, J. & ROGER, M. 1985. Afferent projections to the superior colliculus in the rat, with special attention to the deep layers. *J Hirnforsch,* 26**,** 667-81.

CAGNIARD, B., BALSAM, P. D., BRUNNER, D. & ZHUANG, X. 2006. Mice with chronically elevated dopamine exhibit enhanced motivation, but not learning, for a food reward. *Neuropsychopharmacology,* 31**,** 1362-70.

CAINE, S. B., NEGUS, S. S., MELLO, N. K., PATEL, S., BRISTOW, L., KULAGOWSKI, J., VALLONE, D., SAIARDI, A. & BORRELLI, E. 2002. Role of dopamine D2-like receptors in cocaine self-administration: studies with D2 receptor mutant mice and novel D2 receptor antagonists. *The Journal of Neuroscience,* 22**,** 2977-88.

CAINE, S. B., THOMSEN, M., GABRIEL, K. I., BERKOWITZ, J. S., GOLD, L. H., KOOB, G. F., TONEGAWA, S., ZHANG, J. & XU, M. 2007. Lack of self-administration of cocaine in dopamine D1 receptor knock-out mice. *The Journal of Neuroscience,* 27**,** 13140-50.

CALABRESI, P., PICCONI, B., TOZZI, A., GHIGLIERI, V. & DI FILIPPO, M. 2014. Direct and indirect pathways of basal ganglia: a critical reappraisal. *Nature Neuroscience,* 17**,** 1022-30.

CALHOON, G. G. & TYE, K. M. 2015. Resolving the neural circuits of anxiety. *Nature Neuroscience,* 18**,** 1394-404.

CAMERON, D. J., RASSAMDANA, F., TAM, P., DANG, K., YANEZ, C., GHAEMMAGHAMI, S. & DEHKORDI, M. I. 2013. The optokinetic response as a quantitative measure of visual acuity in zebrafish. *Journal of Visualized Experiments.*

CAMPEAU, S. & DAVIS, M. 1995. Involvement of the central nucleus and basolateral complex of the amygdala in fear conditioning measured with fear-potentiated startle in rats trained concurrently with auditory and visual conditioned stimuli. *The Journal of Neuroscience,* 15**,** 2301-11.

CANAVIER, C. C., EVANS, R. C., OSTER, A. M., PISSADAKI, E. K., DRION, G., KUZNETSOV, A. S. & GUTKIN, B. S. 2016. Implications of cellular models of dopamine neurons for disease. *The Journal of Neurophysiology,* 116**,** 2815-2830.

CANFIELD, J. G. 2006. Functional evidence for visuospatial coding in the Mauthner neuron. *Brain, Behavior and Evolution,* 67**,** 188-202.

CANNON, C. M., SCANNELL, C. A. & PALMITER, R. D. 2005. Mice lacking dopamine D1 receptors express normal lithium chloride-induced conditioned taste aversion for salt but not sucrose. *European Journal of Neuroscience,* 21**,** 2600-4.

CARBONE, C., COSTA, A., PROVENSI, G., MANNAIONI, G. & MASI, A. 2017. The Hyperpolarization-Activated Current Determines Synaptic Excitability, Calcium Activity and Specific Viability of Substantia Nigra Dopaminergic Neurons. *Frontiers in cellular neuroscience,* 11**,** 187-187.

CARBONI, E., SPIELEWOY, C., VACCA, C., NOSTEN-BERTRAND, M., GIROS, B. & DI CHIARA, G. 2001. Cocaine and amphetamine increase extracellular dopamine in the nucleus accumbens of mice lacking the dopamine transporter gene. *The Journal of Neuroscience,* 21**,** RC141: 1-4.

CARDINAL, R. N., PARKINSON, J. A., HALL, J. & EVERITT, B. J. 2002. Emotion and motivation: the role of the amygdala, ventral striatum, and prefrontal cortex. *Neuroscience & Biobehavioral Reviews,* 26**,** 321-52.

CARTER, A. G. & SABATINI, B. L. 2004. State-dependent calcium signaling in dendritic spines of striatal medium spiny neurons. *Neuron,* 44**,** 483-93.

CASTRO, D. C., COLE, S. L. & BERRIDGE, K. C. 2015. Lateral hypothalamus, nucleus accumbens, and ventral pallidum roles in eating and hunger: interactions between homeostatic and reward circuitry. *Frontiers in systems neuroscience,* 9**,** 90-90.

CHAISEHA, Y., YOUNGREN, O., AL-ZAILAIE, K. & EL HALAWANI, M. 2003. Expression of D1 and D2 dopamine receptors in the hypothalamus and pituitary during the turkey reproductive cycle: colocalization with vasoactive intestinal peptide. *Neuroendocrinology,* 77**,** 105-18.

CHAN, C. S., GUZMAN, J. N., ILIJIC, E., MERCER, J. N., RICK, C., TKATCH, T., MEREDITH, G. E. & SURMEIER, D. J. 2007. 'Rejuvenation' protects neurons in mouse models of Parkinson's disease. *Nature,* 447**,** 1081-6.

CHAND, A. N., GALLIANO, E., CHESTERS, R. A. & GRUBB, M. S. 2015. A distinct subtype of dopaminergic interneuron displays inverted structural

plasticity at the axon initial segment. *The Journal of Neuroscience,* 35**,** 1573-90.

CHANDRA, R., LENZ, J. D., GANCARZ, A. M., CHAUDHURY, D., SCHROEDER, G. L., HAN, M. H., CHEER, J. F., DIETZ, D. M. & LOBO, M. K. 2013. Optogenetic inhibition of D1R containing nucleus accumbens neurons alters cocaine-mediated regulation of Tiam1. *Frontiers in Molecular Neuroscience,* 6**,** 13.

CHEN, C., CHENG, M., ITO, T. & SONG, S. 2018. Neuronal Organization in the Inferior Colliculus Revisited with Cell-Type-Dependent Monosynaptic Tracing. *The Journal of Neuroscience,* 38**,** 3318-3332.

CHEN, W., NONG, Z., LI, Y., HUANG, J., CHEN, C. & HUANG, L. 2017. Role of Dopamine Signaling in Drug Addiction. *Current Topics in Medicinal Chemistry,* 17**,** 2440-2455.

CHENG, R.-K., JESUTHASAN, S. J. & PENNEY, T. B. 2014. Zebrafish forebrain and temporal conditioning. *Philosophical transactions of the Royal Society of London. Series B, Biological sciences,* 369**,** 20120462-20120462.

CHERGUI, K., CHARLETY, P. J., AKAOKA, H., SAUNIER, C. F., BRUNET, J. L., BUDA, M., SVENSSON, T. H. & CHOUVET, G. 1993. Tonic activation of NMDA receptors causes spontaneous burst discharge of rat midbrain dopamine neurons in vivo. *European Journal of Neuroscience,* 5**,** 137-44.

CHIENG, B. C., CHRISTIE, M. J. & OSBORNE, P. B. 2006. Characterization of neurons in the rat central nucleus of the amygdala: cellular physiology, morphology, and opioid sensitivity. *The Journal of Comparative Neurology,* 497**,** 910-27.

CHO, Y. T. & FUDGE, J. L. 2010. Heterogeneous dopamine populations project to specific subregions of the primate amygdala. *Neuroscience,* 165**,** 1501-18.

CHOI, E. Y., DING, S. L. & HABER, S. N. 2017. Combinatorial Inputs to the Ventral Striatum from the Temporal Cortex, Frontal Cortex, and Amygdala: Implications for Segmenting the Striatum. *eNeuro,* 4.

CHRISTIAN, D. T., ALEXANDER, N. J., DIAZ, M. R. & MCCOOL, B. A. 2013. Thalamic glutamatergic afferents into the rat basolateral amygdala exhibit increased presynaptic glutamate function following withdrawal from chronic intermittent ethanol. *Neuropharmacology,* 65**,** 134-142.

CHUNG, S. J., LEE, J. J., HAM, J. H., YE, B. S., LEE, P. H. & SOHN, Y. H. 2016. Striatal Dopamine Depletion Patterns and Early Non-Motor Burden in Parkinsons Disease. *PLoS One,* 11**,** e0161316.

CLARK, M. & BRACCI, E. 2018. Dichotomous Dopaminergic Control of Ventral Pallidum Neurons. *Frontiers in cellular neuroscience,* 12**,** 260-260.

COHEN, J. D. & CASTRO-ALAMANCOS, M. A. 2010. Neural correlates of active avoidance behavior in superior colliculus. *The Journal of Neuroscience,* 30**,** 8502-11.

COLE, S. L., ROBINSON, M. J. F. & BERRIDGE, K. C. 2018. Optogenetic self-stimulation in the nucleus accumbens: D1 reward versus D2 ambivalence. *PLoS One,* 13**,** e0207694.

COMOLI, E., RIBEIRO-BARBOSA, E. R., NEGRAO, N., GOTO, M. & CANTERAS, N. S. 2005. Functional mapping of the prosencephalic systems involved in organizing predatory behavior in rats. *Neuroscience,* 130**,** 1055-67.

CORNET, C., DI DONATO, V. & TERRIENTE, J. 2018. Combining Zebrafish and CRISPR/Cas9: Toward a More Efficient Drug Discovery Pipeline. *Frontiers in Pharmacology,* 9**,** 703.

COSTA, K. M. 2014. The effects of aging on substantia nigra dopamine neurons. *The Journal of Neuroscience,* 34**,** 15133-4.

CRAIG, A. M., BLACKSTONE, C. D., HUGANIR, R. L. & BANKER, G. 1994. Selective clustering of glutamate and gamma-aminobutyric acid receptors opposite terminals releasing the corresponding neurotransmitters. *Proceedings of the National Academy of Sciences of the United States of America,* 91**,** 12373-7.

CRUZ, H. G., IVANOVA, T., LUNN, M. L., STOFFEL, M., SLESINGER, P. A. & LUSCHER, C. 2004. Bi-directional effects of GABA(B) receptor agonists on the mesolimbic dopamine system. *Nature Neuroscience,* 7**,** 153-9.

CURTI, S. & PEREDA, A. E. 2010. Functional specializations of primary auditory afferents on the Mauthner cells: interactions between membrane and synaptic properties. *Journal of physiology, Paris,* 104**,** 203-214.

DALLEY, J. W., MAR, A. C., ECONOMIDOU, D. & ROBBINS, T. W. 2008. Neurobehavioral mechanisms of impulsivity: fronto-striatal systems and functional neurochemistry. *Pharmacology Biochemistry and Behavior,* 90**,** 250-60.

DAMJANOVIĆ, I., MAXIMOV, P. V., ALIPER, A. T., ZAICHIKOVA, A. A., GAČIĆ, Z. & MAXIMOVA, E. M. 2019. Putative targets of direction-selective retinal ganglion cells in the tectum opticum of cyprinid fish. *Brain Research,* 1708**,** 20-26.

DANJO, T., YOSHIMI, K., FUNABIKI, K., YAWATA, S. & NAKANISHI, S. 2014. Aversive behavior induced by optogenetic inactivation of ventral tegmental area dopamine neurons is mediated by dopamine D2 receptors in the nucleus accumbens. *Proceedings of the National Academy of Sciences of the United States of America,* 111**,** 6455-60.

DAUBNER, S. C., LE, T. & WANG, S. 2011. Tyrosine hydroxylase and regulation of dopamine synthesis. *Archives of Biochemistry and Biophysics,* 508**,** 1-12.

DAUER, W. & PRZEDBORSKI, S. 2003. Parkinson's Disease: Mechanisms and Models. *Neuron,* 39**,** 889-909.

DAVIS, M. & WHALEN, P. J. 2000. The amygdala: vigilance and emotion. *Molecular Psychiatry,* 6**,** 13.

DE BUNDEL, D., ZUSSY, C., ESPALLERGUES, J., GERFEN, C. R., GIRAULT, J. A. & VALJENT, E. 2016. Dopamine D2 receptors gate generalization of conditioned threat responses through mTORC1 signaling in the extended amygdala. *Molecular Psychiatry* 21**,** 1545-1553.

DE JONG, J. W., AFJEI, S. A., POLLAK DOROCIC, I., PECK, J. R., LIU, C., KIM, C. K., TIAN, L., DEISSEROTH, K. & LAMMEL, S. 2019. A Neural Circuit Mechanism for Encoding Aversive Stimuli in the Mesolimbic Dopamine System. *Neuron,* 101**,** 133-151 e7.

DE JONG, J. W., ROELOFS, T. J., MOL, F. M., HILLEN, A. E., MEIJBOOM, K. E., LUIJENDIJK, M. C., VAN DER EERDEN, H. A., GARNER, K. M., VANDERSCHUREN, L. J. & ADAN, R. A. 2015. Reducing Ventral Tegmental Dopamine D2 Receptor Expression Selectively Boosts Incentive Motivation. *Neuropsychopharmacology,* 40**,** 2085-95.

DE LA MORA, M. P., GALLEGOS-CARI, A., ARIZMENDI-GARCIA, Y., MARCELLINO, D. & FUXE, K. 2010. Role of dopamine receptor mechanisms in the amygdaloid modulation of fear and anxiety: Structural and functional analysis. *Progress in Neurobiology,* 90**,** 198-216.

DE MEI, C., RAMOS, M., IITAKA, C. & BORRELLI, E. 2009. Getting specialized: presynaptic and postsynaptic dopamine D2 receptors. *Current Opinion in Pharmacology,* 9**,** 53-8.

DE OLIVEIRA, A. R., REIMER, A. E., REIS, F. M. & BRANDAO, M. L. 2017. Dopamine D2-like receptors modulate freezing response, but not the activation of HPA axis, during the expression of conditioned fear. *Experimental Brain Research,* 235**,** 429-436.

DE SOUZA CAETANO, K. A., DE OLIVEIRA, A. R. & BRANDAO, M. L. 2013. Dopamine D2 receptors modulate the expression of contextual conditioned fear: role of the ventral tegmental area and the basolateral amygdala. *Behavioural Pharmacology,* 24**,** 264-74.

DEACON, T. W., PAKZABAN, P. & ISACSON, O. 1994. The lateral ganglionic eminence is the origin of cells committed to striatal phenotypes: neural transplantation and developmental evidence. *Brain Research* 668**,** 211-9.

DEAN, P., REDGRAVE, P. & MITCHELL, I. J. 1988. Chapter 3: Organisation of efferent projections from superior colliculus to brainstem in rat: evidence for functional output channels. *In:* HICKS, T. P. & BENEDEK, G. (eds.) *Progress in Brain Research.* Elsevier.

DEISTER, C. A., TEAGARDEN, M. A., WILSON, C. J. & PALADINI, C. A. 2009. An Intrinsic Neuronal Oscillator Underlies Dopaminergic Neuron Bursting. *The Journal of Neuroscience,* 29**,** 15888-15897.

DEMARIA, J. E., NAGY, G. M., LERANT, A. A., FEKETE, M. I., LEVENSON, C. W. & FREEMAN, M. E. 2000. Dopamine transporters participate in the physiological regulation of prolactin. *Endocrinology,* 141**,** 366-74.

DESERNO, L., SCHLAGENHAUF, F. & HEINZ, A. 2016. Striatal dopamine, reward, and decision making in schizophrenia. *Dialogues Clin Neurosci,* 18**,** 77-89.

DIAS, V., JUNN, E. & MOURADIAN, M. M. 2013. The role of oxidative stress in Parkinson's disease. *Journal of Parkinson's disease,* 3**,** 461-491.

DIFIGLIA, M. 1987. Synaptic organization of cholinergic neurons in the monkey neostriatum. *The Journal of Comparative Neurology,* 255**,** 245-58.

DOUGLASS, A. M., KUCUKDERELI, H., PONSERRE, M., MARKOVIC, M., GRÜNDEMANN, J., STROBEL, C., ALCALA MORALES, P. L., CONZELMANN, K.-K., LÜTHI, A. & KLEIN, R. 2017a. Central amygdala circuits modulate food consumption through a positive-valence mechanism. *Nature Neuroscience,* 20**,** 1384.

DOUGLASS, A. M., KUCUKDERELI, H., PONSERRE, M., MARKOVIC, M., GRUNDEMANN, J., STROBEL, C., ALCALA MORALES, P. L., CONZELMANN, K. K., LUTHI, A. & KLEIN, R. 2017b. Central amygdala circuits modulate food consumption through a positive-valence mechanism. *Nature Neuroscience,* 20**,** 1384-1394.

DREHER, J. C., MEYER-LINDENBERG, A., KOHN, P. & BERMAN, K. F. 2008. Age-related changes in midbrain dopaminergic regulation of the human reward system. *Proceedings of the National Academy of Sciences of the United States of America,* 105**,** 15106-11.

DUBOIS, D. W., PARRISH, A. R., TRZECIAKOWSKI, J. P. & FRYE, G. D. 2004. Binge ethanol exposure delays development of GABAergic miniature postsynaptic currents in septal neurons. *Developmental brain research,* 152**,** 199-212.

DUDMAN, J. T. & KRAKAUER, J. W. 2016. The basal ganglia: from motor commands to the control of vigor. *Current Opinion in Neurobiology,* 37**,** 158-166.

DUNN, TIMOTHY W., GEBHARDT, C., NAUMANN, EVA A., RIEGLER, C., AHRENS, MISHA B., ENGERT, F. & DEL BENE, F. 2016a. Neural Circuits Underlying Visually Evoked Escapes in Larval Zebrafish. *Neuron,* 89**,** 613-628.

DUNN, T. W., MU, Y., NARAYAN, S., RANDLETT, O., NAUMANN, E. A., YANG, C. T., SCHIER, A. F., FREEMAN, J., ENGERT, F. & AHRENS, M. B. 2016b. Brain-wide mapping of neural activity controlling zebrafish exploratory locomotion. *Elife,* 5**,** e12741.

DUVARCI, S. & PARE, D. 2014. Amygdala microcircuits controlling learned fear. *Neuron,* 82**,** 966-980.

EATON, R. C. & POPPER, A. N. 1995. The octavolateralis system and Mauthner cell: interactions and questions. *Brain, Behavior and Evolution,* 46**,** 124-30.

EGAN, R. J., BERGNER, C. L., HART, P. C., CACHAT, J. M., CANAVELLO, P. R., ELEGANTE, M. F., ELKHAYAT, S. I., BARTELS, B. K., TIEN, A. K., TIEN, D. H., MOHNOT, S., BEESON, E., GLASGOW, E., AMRI, H., ZUKOWSKA, Z. & KALUEFF, A. V. 2009. Understanding behavioral and physiological phenotypes of stress and anxiety in zebrafish. *Behavioural Brain Research,* 205**,** 38-44.

EIDEN, L. E. & WEIHE, E. 2011. VMAT2: a dynamic regulator of brain monoaminergic neuronal function interacting with drugs of abuse. *Annals of the New York Academy of Sciences,* 1216**,** 86-98.

ELSWORTH, J. D. & ROTH, R. H. 1997. Dopamine synthesis, uptake, metabolism, and receptors: relevance to gene therapy of Parkinson's disease. *Experimental Neurology,* 144**,** 4-9.

ERICSSON, J., SILBERBERG, G., ROBERTSON, B., WIKSTROM, M. A. & GRILLNER, S. 2011. Striatal cellular properties conserved from lampreys to mammals. *The Journal of Physiology,* 589**,** 2979-92.

ERICSSON, J., STEPHENSON-JONES, M., KARDAMAKIS, A., ROBERTSON, B., SILBERBERG, G. & GRILLNER, S. 2013a. Evolutionarily conserved differences in pallial and thalamic short-term synaptic plasticity in striatum. *The Journal of Physiology,* 591**,** 859-74.

ERICSSON, J., STEPHENSON-JONES, M., PEREZ-FERNANDEZ, J., ROBERTSON, B., SILBERBERG, G. & GRILLNER, S. 2013b. Dopamine differentially modulates the excitability of striatal neurons of the direct and indirect pathways in lamprey. *The Journal of Neuroscience,* 33**,** 8045-54.

EVANS, R. & KHALIQ, Z. 2015. T-type calcium channels trigger a hyperpolarization induced afterdepolarization in substantia nigra dopamine neurons. *BMC Neuroscience,* 16**,** P123.

EVANS, R. C., MANIAR, Y. M. & BLACKWELL, K. T. 2013. Dynamic modulation of spike timing-dependent calcium influx during corticostriatal upstates. *The Journal of Neurophysiology,* 110**,** 1631-45.

EVERITT, B. J., PARKINSON, J. A., OLMSTEAD, M. C., ARROYO, M., ROBLEDO, P. & ROBBINS, T. W. 1999. Associative processes in addiction and reward. The role of amygdala-ventral striatal subsystems. *Annals of the New York Academy of Sciences,* 877**,** 412-38.

EWERT, J. P., BUXBAUM-CONRADI, H., DREISVOGT, F., GLAGOW, M., MERKEL-HARFF, C., RÖTTGEN, A., SCHÜRG-PFEIFFER, E. & SCHWIPPERT, W. W. 2001. Neural modulation of visuomotor functions underlying prey-catching behaviour in anurans: perception, attention, motor performance, learning. *Comparative Biochemistry and Physiology Part A: Molecular & Integrative Physiology,* 128**,** 417-460.

FADOK, J. P., MARKOVIC, M., TOVOTE, P. & LÜTHI, A. 2018. New perspectives on central amygdala function. *Current Opinion in Neurobiology,* 49**,** 141-147.

FALLON, J. H. & MOORE, R. Y. 1978. Catecholamine innervation of the basal forebrain. IV. Topography of the dopamine projection to the basal forebrain and neostriatum. *The Journal of Comparative Neurology,* 180**,** 545-80.

FAME, R. M., BRAJON, C. & GHYSEN, A. 2006. Second-order projection from the posterior lateral line in the early zebrafish brain. *Neural Development,* 1**,** 4-4.

FASANO, C., KORTLEVEN, C. & TRUDEAU, L. E. 2010. Chronic activation of the D2 autoreceptor inhibits both glutamate and dopamine synapse formation and alters the intrinsic properties of mesencephalic dopamine neurons in vitro. *European Journal of Neuroscience,* 32**,** 1433-41.

FAVUZZI, E. & RICO, B. 2018. Molecular diversity underlying cortical excitatory and inhibitory synapse development. *Current Opinion in Neurobiology,* 53**,** 8-15.

FELIX, R. A. & MAGNUSSON, A. K. 2016. Development of excitatory synaptic transmission to the superior paraolivary and lateral superior olivary nuclei optimizes differential decoding strategies. *Neuroscience,* 334**,** 1-12.

FENDT, M., KOCH, M. & SCHNITZLER, H.-U. 1994. Lesions of the central gray block the sensitization of the acoustic startle response in rats. *Brain Research,* 661**,** 163-173.

FENDT, M., LI, L. & YEOMANS, J. S. 2001. Brain stem circuits mediating prepulse inhibition of the startle reflex. *Psychopharmacology (Berl),* 156**,** 216-24.

FENU, S., BASSAREO, V. & DI CHIARA, G. 2001. A role for dopamine D1 receptors of the nucleus accumbens shell in conditioned taste aversion learning. *The Journal of Neuroscience,* 21**,** 6897-904.

FENU, S. & DI CHIARA, G. 2003. Facilitation of conditioned taste aversion learning by systemic amphetamine: role of nucleus accumbens shell dopamine D1 receptors. *European Journal of Neuroscience,* 18**,** 2025-30.

FIELD, T. M., SHIN, M., STUCKY, C. S., LOOMIS, J. & JOHNSON, M. A. 2018. Electrochemical Measurement of Dopamine Release and Uptake in Zebrafish Following Treatment with Carboplatin. *Chemphyschem,* 19**,** 1192-1196.

FILIPPI, A., MAHLER, J., SCHWEITZER, J. & DRIEVER, W. 2010. Expression of the paralogous tyrosine hydroxylase encoding genes th1 and th2 reveals the full complement of dopaminergic and noradrenergic neurons in zebrafish larval and juvenile brain. *The Journal of Comparative Neurology,* 518**,** 423-38.

FILLA, I., BAILEY, M. R., SCHIPANI, E., WINIGER, V., MEZIAS, C., BALSAM, P. D. & SIMPSON, E. H. 2018. Striatal dopamine D2 receptors regulate effort but not value-based decision making and alter the dopaminergic encoding of cost. *Neuropsychopharmacology,* 43**,** 2180-2189.

FILOSA, A., BARKER, A. J., DAL MASCHIO, M. & BAIER, H. 2016. Feeding State Modulates Behavioral Choice and Processing of Prey Stimuli in the Zebrafish Tectum. *Neuron,* 90**,** 596-608.

FIORENTINI, C., SAVOIA, P., BONO, F., TALLARICO, P. & MISSALE, C. 2015. The D3 dopamine receptor: From structural interactions to function. *European Neuropsychopharmacology,* 25**,** 1462-1469.

FLANIGAN, M. & LECLAIR, K. 2017. Shared Motivational Functions of Ventral Striatum D1 and D2 Medium Spiny Neurons. *The Journal of Neuroscience,* 37**,** 6177-6179.

FLORESCO, S. B. 2015. The nucleus accumbens: an interface between cognition, emotion, and action. *Annual Review of Psychology,* 66**,** 25-52.

FLORESCO, S. B. & TSE, M. T. 2007. Dopaminergic regulation of inhibitory and excitatory transmission in the basolateral amygdala-prefrontal cortical pathway. *The Journal of Neuroscience,* 27**,** 2045-57.

FOLGUEIRA, M., BAYLEY, P., NAVRATILOVA, P., BECKER, T. S., WILSON, S. W. & CLARKE, J. D. 2012. Morphogenesis underlying the development of the everted teleost telencephalon. *Neural Development,* 7**,** 32.

FORD, C. P. 2014. The role of D2-autoreceptors in regulating dopamine neuron activity and transmission. *Neuroscience,* 282**,** 13-22.

FOX, A. S., OLER, J. A., TROMP DO, P. M., FUDGE, J. L. & KALIN, N. H. 2015. Extending the amygdala in theories of threat processing. *Trends in Neuroscience,* 38**,** 319-29.

FOX, A. S. & SHACKMAN, A. J. 2017. The central extended amygdala in fear and anxiety: Closing the gap between mechanistic and neuroimaging research. *Neuroscience Letters.*

FOX, A. S. & SHACKMAN, A. J. 2019. The central extended amygdala in fear and anxiety: Closing the gap between mechanistic and neuroimaging research. *Neuroscience Letters,* 693**,** 58-67.

FRANKLIN, T. B. 2019. Recent Advancements Surrounding the Role of the Periaqueductal Gray in Predators and Prey. *Frontiers in behavioral neuroscience,* 13**,** 60-60.

FREEDMAN, L. J. & CASSELL, M. D. 1994. Distribution of dopaminergic fibers in the central division of the extended amygdala of the rat. *Brain Research* 633**,** 243-52.

FREEZE, B. S., KRAVITZ, A. V., HAMMACK, N., BERKE, J. D. & KREITZER, A. C. 2013. Control of basal ganglia output by direct and indirect pathway projection neurons. *The Journal of Neuroscience,* 33**,** 18531-9.

FU, Y., YUAN, Y., HALLIDAY, G., RUSZNAK, Z., WATSON, C. & PAXINOS, G. 2012. A cytoarchitectonic and chemoarchitectonic analysis of the dopamine cell groups in the substantia nigra, ventral tegmental area, and retrorubral field in the mouse. *Brain Structure and Function,* 217**,** 591-612.

FUDGE, J. L. & HABER, S. N. 2000. The central nucleus of the amygdala projection to dopamine subpopulations in primates. *Neuroscience,* 97**,** 479-94.

FUNAHASHI, M., MITOH, Y., KOHJITANI, A. & MATSUO, R. 2003. Role of the hyperpolarization-activated cation current (Ih) in pacemaker activity in

area postrema neurons of rat brain slices. *The Journal of physiology,* 552**,** 135-148.

GABBIANI, F., KRAPP, H. G. & LAURENT, G. 1999. Computation of object approach by a wide-field, motion-sensitive neuron. *The Journal of Neuroscience,* 19**,** 1122-41.

GABEL, L. A. & NISENBAUM, E. S. 1998. Biophysical characterization and functional consequences of a slowly inactivating potassium current in neostriatal neurons. *The Journal of Neurophysiology,* 79**,** 1989-2002.

GAGNON, D., PETRYSZYN, S., SANCHEZ, M. G., BORIES, C., BEAULIEU, J. M., DE KONINCK, Y., PARENT, A. & PARENT, M. 2017. Striatal Neurons Expressing D(1) and D(2) Receptors are Morphologically Distinct and Differently Affected by Dopamine Denervation in Mice. *Scientific Reports,* 7**,** 41432-41432.

GAHTAN, E., TANGER, P. & BAIER, H. 2005. Visual Prey Capture in Larval Zebrafish Is Controlled by Identified Reticulospinal Neurons Downstream of the Tectum. *The Journal of Neuroscience,* 25**,** 9294-9303.

GALARRAGA, E., VILCHIS, C., TKATCH, T., SALGADO, H., TECUAPETLA, F., PEREZ-ROSELLO, T., PEREZ-GARCI, E., HERNANDEZ-ECHEAGARAY, E., SURMEIER, D. J. & BARGAS, J. 2007. Somatostatinergic modulation of firing pattern and calcium-activated potassium currents in medium spiny neostriatal neurons. *Neuroscience,* 146**,** 537-54.

GALLAGHER, M. & CHIBA, A. A. 1996. The amygdala and emotion. *Current Opinion in Neurobiology,* 6**,** 221-7.

GALLO, E. F., MESZAROS, J., SHERMAN, J. D., CHOHAN, M. O., TEBOUL, E., CHOI, C. S., MOORE, H., JAVITCH, J. A. & KELLENDONK, C. 2018. Accumbens dopamine D2 receptors increase motivation by decreasing inhibitory transmission to the ventral pallidum. *Nature Communications,* 9**,** 1086.

GAMBARDELLA, C., PIGNATELLI, A. & BELLUZZI, O. 2012. The h-current in the substantia Nigra pars compacta neurons: a re-examination. *PLoS One,* 7**,** e52329.

GANGAROSSA, G., ESPALLERGUES, J., MAILLY, P., DE BUNDEL, D., DE KERCHOVE D'EXAERDE, A., HERVE, D., GIRAULT, J. A., VALJENT, E. & KRIEGER, P. 2013. Spatial distribution of D1R- and D2R-expressing medium-sized spiny neurons differs along the rostro-caudal axis of the mouse dorsal striatum. *Frontiers in Neural Circuits,* 7**,** 124.

GANTZ, S. C., FORD, C. P., MORIKAWA, H. & WILLIAMS, J. T. 2018. The Evolving Understanding of Dopamine Neurons in the Substantia Nigra and Ventral Tegmental Area. *Annual Review of Physiology,* 80**,** 219-241.

GANZ, J., KASLIN, J., FREUDENREICH, D., MACHATE, A., GEFFARTH, M. & BRAND, M. 2012. Subdivisions of the adult zebrafish subpallium by molecular marker analysis. *The Journal of Comparative Neurology,* 520**,** 633-55.

GANZ, J., KROEHNE, V., FREUDENREICH, D., MACHATE, A., GEFFARTH, M., BRAASCH, I., KASLIN, J. & BRAND, M. 2015. Subdivisions of the adult zebrafish pallium based on molecular marker analysis. *F1000Research,* 3**,** 308-308.

GAO, B. X. & ZISKIND-CONHAIM, L. 1998. Development of ionic currents underlying changes in action potential waveforms in rat spinal motoneurons. *The Journal of Neurophysiology,* 80**,** 3047-61.

GAO, P. P., ZHANG, J. W., FAN, S. J., SANES, D. H. & WU, E. X. 2015. Auditory midbrain processing is differentially modulated by auditory and visual cortices: An auditory fMRI study. *Neuroimage,* 123**,** 22-32.

GARCIA-LOPEZ, M., ABELLAN, A., LEGAZ, I., RUBENSTEIN, J. L., PUELLES, L. & MEDINA, L. 2008. Histogenetic compartments of the mouse centromedial and extended amygdala based on gene expression patterns during development. *The Journal of Comparative Neurology,* 506**,** 46-74.

GELOWITZ, D. L. & KOKKINIDIS, L. 1999. Enhanced amygdala kindling after electrical stimulation of the ventral tegmental area: implications for fear and anxiety. *The Journal of Neuroscience,* 19**,** RC41.

GERFEN, C. R. 1988. Synaptic organization of the striatum. *Journal of Electron Microscopy Technique,* 10**,** 265-81.

GERFEN, C. R., ENGBER, T. M., MAHAN, L. C., SUSEL, Z., CHASE, T. N., MONSMA, F. J., JR. & SIBLEY, D. R. 1990. D1 and D2 dopamine receptor-regulated gene expression of striatonigral and striatopallidal neurons. *Science,* 250**,** 1429-32.

GERFEN, C. R. & SURMEIER, D. J. 2011. Modulation of striatal projection systems by dopamine. *Annual Review of Neuroscience,* 34**,** 441-66.

GERTLER, T. S., CHAN, C. S. & SURMEIER, D. J. 2008. Dichotomous anatomical properties of adult striatal medium spiny neurons. *The Journal of Neuroscience,* 28**,** 10814-24.

GIROS, B., EL MESTIKAWY, S., GODINOT, N., ZHENG, K., HAN, H., YANG-FENG, T. & CARON, M. G. 1992. Cloning, pharmacological characterization, and chromosome assignment of the human dopamine transporter. *Molecular Pharmacology,* 42**,** 383-90.

GLAGOW, M. & EWERT, J. 1999. Apomorphine alters prey-catching patterns in the common toad: behavioral experiments and (14)C-2-deoxyglucose brain mapping studies. *Brain, Behavior and Evolution,* 54**,** 223-42.

GOBERT, A., RIVET, J. M., AUDINOT, V., CISTARELLI, L., SPEDDING, M., VIAN, J., PEGLION, J. L. & MILLAN, M. J. 1995. Functional correlates of dopamine D3 receptor activation in the rat in vivo and their modulation by the selective antagonist, (+)-S 14297: II. Both D2 and "silent" D3 autoreceptors control synthesis and release in mesolimbic, mesocortical and nigrostriatal pathways. *Journal of Pharmacology and Experimental Therapeutics,* 275**,** 899-913.

GOLDMAN-RAKIC, P. S. 1992. Dopamine-mediated mechanisms of the prefrontal cortex. *Seminars in Neuroscience,* 4**,** 149-159.

GONG, W., NEILL, D. B., LYNN, M. & JUSTICE, J. B., JR. 1999. Dopamine D1/D2 agonists injected into nucleus accumbens and ventral pallidum differentially affect locomotor activity depending on site. *Neuroscience,* 93**,** 1349-58.

GONZALEZ-FORERO, D. & ALVAREZ, F. J. 2005. Differential postnatal maturation of GABAA, glycine receptor, and mixed synaptic currents in Renshaw cells and ventral spinal interneurons. *The Journal of Neuroscience,* 25**,** 2010-23.

GONZALEZ, A. M., WALTHER, D., PAZOS, A. & UHL, G. R. 1994. Synaptic vesicular monoamine transporter expression: distribution and pharmacologic profile. *Molecular Brain Research,* 22**,** 219-26.

GOZZI, A., JAIN, A., GIOVANNELLI, A., BERTOLLINI, C., CRESTAN, V., SCHWARZ, A. J., TSETSENIS, T., RAGOZZINO, D., GROSS, C. T. & BIFONE, A. 2010. A neural switch for active and passive fear. *Neuron,* 67**,** 656-66.

GRACE, A. A. 2016. Dysregulation of the dopamine system in the pathophysiology of schizophrenia and depression. *Nature Reviews Neuroscience,* 17**,** 524-32.

GRACE, A. A. & BUNNEY, B. S. 1984a. The control of firing pattern in nigral dopamine neurons: burst firing. *The Journal of Neuroscience,* 4**,** 2877-90.

GRACE, A. A. & BUNNEY, B. S. 1984b. The control of firing pattern in nigral dopamine neurons: single spike firing. *The Journal of Neuroscience,* 4**,** 2866-76.

GRACE, A. A. & ONN, S. P. 1989. Morphology and electrophysiological properties of immunocytochemically identified rat dopamine neurons recorded in vitro. *The Journal of Neuroscience,* 9**,** 3463-81.

GRAHN, J. A., PARKINSON, J. A. & OWEN, A. M. 2008. The cognitive functions of the caudate nucleus. *Progress in Neurobiology,* 86**,** 141-55.

GRAY, T. S. & MAGNUSON, D. J. 1992. Peptide immunoreactive neurons in the amygdala and the bed nucleus of the stria terminalis project to the midbrain central gray in the rat. *Peptides,* 13**,** 451-60.

GRAYBIEL, A. M. 1990. Neurotransmitters and neuromodulators in the basal ganglia. *Trends in Neuroscience,* 13**,** 244-54.

GREALISH, S., MATTSSON, B., DRAXLER, P. & BJORKLUND, A. 2010. Characterisation of behavioural and neurodegenerative changes induced by intranigral 6-hydroxydopamine lesions in a mouse model of Parkinson's disease. *European Journal of Neuroscience,* 31**,** 2266-78.

GREBA, Q., GIFKINS, A. & KOKKINIDIS, L. 2001. Inhibition of amygdaloid dopamine D2 receptors impairs emotional learning measured with fear-potentiated startle. *Brain Research* 899**,** 218-26.

GREBA, Q. & KOKKINIDIS, L. 2000. Peripheral and intraamygdalar administration of the dopamine D1 receptor antagonist SCH 23390 blocks fear-potentiated startle but not shock reactivity or the shock sensitization of acoustic startle. *Behavioral Neuroscience,* 114**,** 262-72.

GRILLNER, S., ROBERTSON, B. & STEPHENSON-JONES, M. 2013. The evolutionary origin of the vertebrate basal ganglia and its role in action selection. *The Journal of physiology,* 591**,** 5425-5431.

GROENEWEGEN, H. J. 1988. Organization of the afferent connections of the mediodorsal thalamic nucleus in the rat, related to the mediodorsal-prefrontal topography. *Neuroscience,* 24**,** 379-431.

GROVES, P. M., WILSON, C. J., YOUNG, S. J. & REBEC, G. V. 1975. Self-inhibition by dopaminergic neurons. *Science,* 190**,** 522-8.

GUARRACI, F. A., FROHARDT, R. J., FALLS, W. A. & KAPP, B. S. 2000. The effects of intra-amygdaloid infusions of a D2 dopamine receptor antagonist on Pavlovian fear conditioning. *Behavioral Neuroscience,* 114**,** 647-51.

GUARRACI, F. A., FROHARDT, R. J. & KAPP, B. S. 1999a. Amygdaloid D1 dopamine receptor involvement in Pavlovian fear conditioning. *Brain Research* 827**,** 28-40.

GUARRACI, F. A., FROHARDT, R. J., YOUNG, S. L. & KAPP, B. S. 1999b. A functional role for dopamine transmission in the amygdala during conditioned fear. *Annals of the New York Academy of Sciences,* 877**,** 732-6.

GUILLOT, T. S. & MILLER, G. W. 2009. Protective actions of the vesicular monoamine transporter 2 (VMAT2) in monoaminergic neurons. *Molecular Neurobiology,* 39**,** 149-70.

GUREVICH, E. V. & JOYCE, J. N. 1999. Distribution of dopamine D3 receptor expressing neurons in the human forebrain: comparison with D2 receptor expressing neurons. *Neuropsychopharmacology,* 20**,** 60-80.

GUZMAN, J. N., SANCHEZ-PADILLA, J., CHAN, C. S. & SURMEIER, D. J. 2009. Robust pacemaking in substantia nigra dopaminergic neurons. *The Journal of Neuroscience,* 29**,** 11011-9.

GUZMAN, J. N., SANCHEZ-PADILLA, J., WOKOSIN, D., KONDAPALLI, J., ILIJIC, E., SCHUMACKER, P. T. & SURMEIER, D. J. 2010. Oxidant stress evoked by pacemaking in dopaminergic neurons is attenuated by DJ-1. *Nature,* 468**,** 696-700.

HAJNAL, A. & LENARD, L. 1997. Feeding-related dopamine in the amygdala of freely moving rats. *Neuroreport,* 8**,** 2817-20.

HALBERSTADT, A. L. & GEYER, M. A. 2009. Habituation and sensitization of acoustic startle: opposite influences of dopamine D1 and D2-family receptors. *Neurobiology of Learning and Memory,* 92**,** 243-8.

HALE, M. E., KATZ, H. R., PEEK, M. Y. & FREMONT, R. T. 2016. Neural circuits that drive startle behavior, with a focus on the Mauthner cells and spiral fiber neurons of fishes. *Journal of Neurogenetics,* 30**,** 89-100.

HALL, Z. W. & SANES, J. R. 1993. Synaptic structure and development: The neuromuscular junction. *Cell,* 72**,** 99-121.

HAMID, A. A., PETTIBONE, J. R., MABROUK, O. S., HETRICK, V. L., SCHMIDT, R., VANDER WEELE, C. M., KENNEDY, R. T., ARAGONA, B. J. & BERKE, J. D. 2016. Mesolimbic dopamine signals the value of work. *Nature Neuroscience,* 19**,** 117-26.

HAN, W., TELLEZ, L. A., RANGEL, M. J., JR., MOTTA, S. C., ZHANG, X., PEREZ, I. O., CANTERAS, N. S., SHAMMAH-LAGNADO, S. J., VAN DEN POL, A. N. & DE ARAUJO, I. E. 2017. Integrated Control of Predatory Hunting by the Central Nucleus of the Amygdala. *Cell,* 168**,** 311-324.e18.

HARTING, J. K. 1977. Descending pathways from the superior collicullus: an autoradiographic analysis in the rhesus monkey (Macaca mulatta). *The Journal of Comparative Neurology,* 173**,** 583-612.

HASUE, R. H. & SHAMMAH-LAGNADO, S. J. 2002. Origin of the dopaminergic innervation of the central extended amygdala and accumbens shell: a combined retrograde tracing and immunohistochemical study in the rat. *The Journal of Comparative Neurology,* 454**,** 15-33.

HE, C., CHEN, F., LI, B. & HU, Z. 2014. Neurophysiology of HCN channels: from cellular functions to multiple regulations. *Progress in Neurobiology,* 112**,** 1-23.

HEAP, L. A., VANWALLEGHEM, G. C., THOMPSON, A. W., FAVRE-BULLE, I., RUBINSZTEIN-DUNLOP, H. & SCOTT, E. K. 2018a. Hypothalamic Projections to the Optic Tectum in Larval Zebrafish. *Frontiers in neuroanatomy,* 11**,** 135-135.

HEAP, L. A. L., VANWALLEGHEM, G., THOMPSON, A. W., FAVRE-BULLE, I. A. & SCOTT, E. K. 2018b. Luminance Changes Drive Directional Startle through a Thalamic Pathway. *Neuron,* 99**,** 293-301.e4.

HEATH, F. C., JURKUS, R., BAST, T., PEZZE, M. A., LEE, J. L., VOIGT, J. P. & STEVENSON, C. W. 2015. Dopamine D1-like receptor signalling in the hippocampus and amygdala modulates the acquisition of contextual fear conditioning. *Psychopharmacology (Berl),* 232**,** 2619-29.

HEEKEREN, H. R., WARTENBURGER, I., MARSCHNER, A., MELL, T., VILLRINGER, A. & REISCHIES, F. M. 2007. Role of ventral striatum in reward-based decision making. *Neuroreport,* 18**,** 951-5.

HELMBRECHT, T. O., DAL MASCHIO, M., DONOVAN, J. C., KOUTSOULI, S. & BAIER, H. 2018. Topography of a Visuomotor Transformation. *Neuron,* 100**,** 1429-1445.e4.

HENRIQUES, P. M., RAHMAN, N., JACKSON, S. E. & BIANCO, I. H. 2019. Nucleus Isthmi Is Required to Sustain Target Pursuit during Visually Guided Prey-Catching. *Current Biology,* 29**,** 1771-1786.e5.

HERNANDEZ-LOPEZ, S., TKATCH, T., PEREZ-GARCI, E., GALARRAGA, E., BARGAS, J., HAMM, H. & SURMEIER, D. J. 2000. D2 dopamine receptors in striatal medium spiny neurons reduce L-type Ca^{2+} currents and excitability via a novel PLC[beta]1-IP3-calcineurin-signaling cascade. *The Journal of Neuroscience,* 20**,** 8987-95.

HERRMANN, M. J., BOEHME, S., BECKER, M. P., TUPAK, S. V., GUHN, A., SCHMIDT, B., BRINKMANN, L. & STRAUBE, T. 2016. Phasic and sustained brain responses in the amygdala and the bed nucleus of the stria terminalis during threat anticipation. *Human Brain Mapping,* 37**,** 1091-102.

HIKIDA, T., KIMURA, K., WADA, N., FUNABIKI, K. & NAKANISHI, S. 2010. Distinct roles of synaptic transmission in direct and indirect striatal pathways to reward and aversive behavior. *Neuron,* 66**,** 896-907.

HIKIDA, T., YAWATA, S., YAMAGUCHI, T., DANJO, T., SASAOKA, T., WANG, Y. & NAKANISHI, S. 2013. Pathway-specific modulation of nucleus accumbens in reward and aversive behavior via selective transmitter receptors. *Proceedings of the National Academy of Sciences of the United States of America,* 110**,** 342-7.

HIMI, T., CAO, M. & MORI, N. 1995. Reduced expression of the molecular markers of dopaminergic neuronal atrophy in the aging rat brain. *The Journals of Gerontology Series A Biological Sciences,* 50**,** B193-200.

HITCHCOCK, J. & DAVIS, M. 1986. Lesions of the amygdala, but not of the cerebellum or red nucleus, block conditioned fear as measured with the potentiated startle paradigm. *Behavioral Neuroscience,* 100**,** 11-22.

HITCHCOCK, J. M. & DAVIS, M. 1987. Fear-potentiated startle using an auditory conditioned stimulus: effect of lesions of the amygdala. *Physiology & Behavior,* 39**,** 403-8.

HITZEMANN, R., HITZEMANN, B., RIVERA, S., GATLEY, J., THANOS, P., SHOU, L. L. & WILLIAMS, R. W. 2003. Dopamine D2 receptor binding, Drd2 expression and the number of dopamine neurons in the BXD recombinant inbred series: genetic relationships to alcohol and other drug associated phenotypes. *Alcoholism: Clinical and Experimental Research,* 27**,** 1-11.

HOLLAND, P. C., HAN, J. S. & GALLAGHER, M. 2000. Lesions of the amygdala central nucleus alter performance on a selective attention task. *The Journal of Neuroscience,* 20**,** 6701-6.

HOLZSCHUH, J., BARRALLO-GIMENO, A., ETTL, A. K., DURR, K., KNAPIK, E. W. & DRIEVER, W. 2003. Noradrenergic neurons in the zebrafish hindbrain are induced by retinoic acid and require tfap2a for expression of the neurotransmitter phenotype. *Development,* 130**,** 5741-54.

HOLZSCHUH, J., RYU, S., ABERGER, F. & DRIEVER, W. 2001. Dopamine transporter expression distinguishes dopaminergic neurons from other catecholaminergic neurons in the developing zebrafish embryo. *Mechanisms of Development,* 101**,** 237-43.

HONJO, Y., PAYNE, L. & EISEN, J. S. 2011. Somatosensory mechanisms in zebrafish lacking dorsal root ganglia. *Journal of anatomy,* 218**,** 271-276.

HORMIGO, S., LOPEZ, D. E., CARDOSO, A., ZAPATA, G., SEPULVEDA, J. & CASTELLANO, O. 2018. Direct and indirect nigrofugal projections to the nucleus reticularis pontis caudalis mediate in the motor execution of the acoustic startle reflex. *Brain Structure and Function,* 223**,** 2733-2751.

HORVITZ, J. C. 2000. Mesolimbocortical and nigrostriatal dopamine responses to salient non-reward events. *Neuroscience,* 96**,** 651-656.

HORVITZ, J. C., STEWART, T. & JACOBS, B. L. 1997. Burst activity of ventral tegmental dopamine neurons is elicited by sensory stimuli in the awake cat. *Brain Research* 759**,** 251-8.

HOWE, K., CLARK, M. D., TORROJA, C. F., TORRANCE, J., BERTHELOT, C., MUFFATO, M., COLLINS, J. E., HUMPHRAY, S., MCLAREN, K., MATTHEWS, L., MCLAREN, S., SEALY, I., CACCAMO, M., CHURCHER, C., SCOTT, C., BARRETT, J. C., KOCH, R., RAUCH, G.-J., WHITE, S., CHOW, W., KILIAN, B., QUINTAIS, L. T., GUERRA-ASSUNÇÃO, J. A., ZHOU, Y., GU, Y., YEN, J., VOGEL, J.-H., EYRE, T., REDMOND, S., BANERJEE, R., CHI, J., FU, B., LANGLEY, E., MAGUIRE, S. F., LAIRD, G. K., LLOYD, D., KENYON, E., DONALDSON, S., SEHRA, H., ALMEIDA-KING, J., LOVELAND, J., TREVANION, S., JONES, M., QUAIL, M., WILLEY, D., HUNT, A., BURTON, J., SIMS, S., MCLAY, K., PLUMB, B., DAVIS, J., CLEE, C., OLIVER, K., CLARK, R., RIDDLE, C., ELLIOTT, D., THREADGOLD, G., HARDEN, G., WARE, D., BEGUM, S., MORTIMORE, B., KERRY, G., HEATH, P., PHILLIMORE, B., TRACEY, A., CORBY, N., DUNN, M., JOHNSON, C., WOOD, J., CLARK, S., PELAN, S., GRIFFITHS, G., SMITH, M., GLITHERO, R., HOWDEN, P., BARKER, N., LLOYD, C., STEVENS, C., HARLEY, J., HOLT, K., PANAGIOTIDIS, G., LOVELL, J., BEASLEY, H., HENDERSON, C., GORDON, D., AUGER, K., WRIGHT, D., COLLINS, J., RAISEN, C., DYER, L., LEUNG, K., ROBERTSON, L., AMBRIDGE, K., LEONGAMORNLERT, D., MCGUIRE, S., GILDERTHORP, R., GRIFFITHS, C., MANTHRAVADI, D., NICHOL, S., BARKER, G., et al. 2013. The zebrafish reference genome sequence and its relationship to the human genome. *Nature,* 496**,** 498.

HUK, A. C. & SHADLEN, M. N. 2005. Neural activity in macaque parietal cortex reflects temporal integration of visual motion signals during perceptual decision making. *The Journal of Neuroscience,* 25**,** 10420-36.

HURD, Y. L., MCGREGOR, A. & PONTEN, M. 1997. In vivo amygdala dopamine levels modulate cocaine self-administration behaviour in the rat: D1

dopamine receptor involvement. *European Journal of Neuroscience,* 9**,** 2541-8.

HYLAND, B. I., REYNOLDS, J. N., HAY, J., PERK, C. G. & MILLER, R. 2002. Firing modes of midbrain dopamine cells in the freely moving rat. *Neuroscience,* 114**,** 475-92.

IKEMOTO, K., NAGATSU, I., NISHIMURA, A., NISHI, K. & ARAI, R. 1998. Do all of human midbrain tyrosine hydroxylase neurons synthesize dopamine? *Brain Research* 805**,** 255-8.

IKEMOTO, S. 2007. Dopamine reward circuitry: two projection systems from the ventral midbrain to the nucleus accumbens-olfactory tubercle complex. *Brain Research Reviews,* 56**,** 27-78.

ISSA, F. A., O'BRIEN, G., KETTUNEN, P., SAGASTI, A., GLANZMAN, D. L. & PAPAZIAN, D. M. 2011. Neural circuit activity in freely behaving zebrafish (Danio rerio). *The Journal of Experimental Biology,* 214**,** 1028-1038.

ISSIDORIDES, M. R., HAVAKI, S., ARVANITIS, D. L. & CHRYSANTHOU-PITEROU, M. 2004. Noradrenaline storage function of species-specific protein bodies, markers of monoamine neurons in human locus coeruleus demonstrated by dopamine-beta-hydroxylase immunogold localization. *Progress in Neuro-Psychopharmacology & Biological Psychiatry,* 28**,** 829-47.

ITO, S. & FELDHEIM, D. A. 2018. The Mouse Superior Colliculus: An Emerging Model for Studying Circuit Formation and Function. *Frontiers in Neural Circuits,* 12**,** 10.

JABER, M., ROBINSON, S. W., MISSALE, C. & CARON, M. G. 1996. Dopamine receptors and brain function. *Neuropharmacology,* 35**,** 1503-19.

JACOB, S. N. & NIENBORG, H. 2018. Monoaminergic Neuromodulation of Sensory Processing. *Frontiers in neural circuits,* 12**,** 51-51.

JAIN, R. A., WOLMAN, M. A., MARSDEN, K. C., NELSON, J. C., SHOENHARD, H., ECHEVERRY, F. A., SZI, C., BELL, H., SKINNER, J., COBBS, E. N., SAWADA, K., ZAMORA, A. D., PEREDA, A. E. & GRANATO, M. 2018. A Forward Genetic Screen in Zebrafish Identifies the G-Protein-Coupled Receptor CaSR as a Modulator of Sensorimotor Decision Making. *Current Biology,* 28**,** 1357-1369.e5.

JANAK, P. H. & TYE, K. M. 2015. From circuits to behaviour in the amygdala. *Nature,* 517**,** 284-92.

JANG, H. J., CHO, K. H., PARK, S. W., KIM, M. J., YOON, S. H. & RHIE, D. J. 2010. The development of phasic and tonic inhibition in the rat visual cortex. *The Korean Journal of Physiology & Pharmacology,* 14**,** 399-405.

JAY, M. 2015. *Neuromodulation of spinal networks in embryonic and larval zebrafish.* PhD Thesis University of Leicester.

JAY, M., DE FAVERI, F. & MCDEARMID, J. R. 2015. Firing dynamics and modulatory actions of supraspinal dopaminergic neurons during zebrafish locomotor behavior. *Current Biology,* 25**,** 435-44.

JENNI, N. L., LARKIN, J. D. & FLORESCO, S. B. 2017. Prefrontal Dopamine D1 and D2 Receptors Regulate Dissociable Aspects of Decision Making via Distinct Ventral Striatal and Amygdalar Circuits. *The Journal of Neuroscience,* 37**,** 6200-6213.

JENNINGS, J. H., SPARTA, D. R., STAMATAKIS, A. M., UNG, R. L., PLEIL, K. E., KASH, T. L. & STUBER, G. D. 2013. Distinct extended amygdala circuits for divergent motivational states. *Nature,* 496**,** 224-8.

JENSEN, J., MCINTOSH, A. R., CRAWLEY, A. P., MIKULIS, D. J., REMINGTON, G. & KAPUR, S. 2003. Direct activation of the ventral striatum in anticipation of aversive stimuli. *Neuron,* 40**,** 1251-7.

JI, R. R., BABA, H., BRENNER, G. J. & WOOLF, C. J. 1999. Nociceptive-specific activation of ERK in spinal neurons contributes to pain hypersensitivity. *Nature Neuroscience,* 2**,** 1114-9.

JOHNSON, P. L., MOLOSH, A., FITZ, S. D., ARENDT, D., DEEHAN, G. A., FEDERICI, L. M., BERNABE, C., ENGLEMAN, E. A., RODD, Z. A., LOWRY, C. A. & SHEKHAR, A. 2015. Pharmacological depletion of serotonin in the basolateral amygdala complex reduces anxiety and disrupts fear conditioning. *Pharmacology Biochemistry and Behavior,* 138**,** 174-9.

JONES, L., MCCUTCHEON, J., YOUNG, A. & NORTON, W. 2015. Neurochemical measurements in the zebrafish brain. *Frontiers in Behavioral Neuroscience,* 9.

JOSSET, N., ROUSSEL, M., LEMIEUX, M., LAFRANCE-ZOUBGA, D., RASTQAR, A. & BRETZNER, F. 2018. Distinct Contributions of Mesencephalic Locomotor Region Nuclei to Locomotor Control in the Freely Behaving Mouse. *Current Biology,* 28**,** 884-901.e3.

KALUEFF, A. V., GEBHARDT, M., STEWART, A. M., CACHAT, J. M., BRIMMER, M., CHAWLA, J. S., CRADDOCK, C., KYZAR, E. J., ROTH, A., LANDSMAN, S., GAIKWAD, S., ROBINSON, K., BAATRUP, E., TIERNEY, K., SHAMCHUK, A., NORTON, W., MILLER, N., NICOLSON, T., BRAUBACH, O., GILMAN, C. P., PITTMAN, J., ROSEMBERG, D. B., GERLAI, R., ECHEVARRIA, D., LAMB, E., NEUHAUSS, S. C. F., WENG, W., BALLY-CUIF, L. & SCHNEIDER, H. 2013. Towards a Comprehensive Catalog of Zebrafish Behavior 1.0 and Beyond. *Zebrafish,* 10**,** 70-86.

KANUNGO, J., ZHENG, Y.-L., MISHRA, B. & PANT, H. C. 2009. Zebrafish Rohon-Beard neuron development: cdk5 in the midst. *Neurochemical research,* 34**,** 1129-1137.

KARDAMAKIS, A. A., SAITOH, K. & GRILLNER, S. 2015. Tectal microcircuit generating visual selection commands on gaze-controlling neurons. *Proceedings of the National Academy of Sciences of the United States of America,* 112**,** E1956-65.

KASLIN, J. & PANULA, P. 2001. Comparative anatomy of the histaminergic and other aminergic systems in zebrafish (Danio rerio). *The Journal of Comparative Neurology,* 440**,** 342-377.

KAUFLING, J., GIRARD, D., MAITRE, M., LESTE-LASSERRE, T. & GEORGES, F. 2017. Species-specific diversity in the anatomical and physiological organisation of the BNST-VTA pathway. *European Journal of Neuroscience,* 45**,** 1230-1240.

KEBABIAN, J. W. & CALNE, D. B. 1979. Multiple receptors for dopamine. *Nature,* 277**,** 93-6.

KEIFLIN, R. & JANAK, P. H. 2015. Dopamine Prediction Errors in Reward Learning and Addiction: From Theory to Neural Circuitry. *Neuron,* 88**,** 247-63.

KELLY, M. A., RUBINSTEIN, M., PHILLIPS, T. J., LESSOV, C. N., BURKHART-KASCH, S., ZHANG, G., BUNZOW, J. R., FANG, Y., GERHARDT, G. A., GRANDY, D. K. & LOW, M. J. 1998. Locomotor activity in D2 dopamine receptor-deficient mice is determined by gene dosage, genetic background, and developmental adaptations. *The Journal of Neuroscience,* 18**,** 3470-9.

KHALIQ, Z. M. & BEAN, B. P. 2008. Dynamic, nonlinear feedback regulation of slow pacemaking by A-type potassium current in ventral tegmental area neurons. *The Journal of Neuroscience,* 28**,** 10905-17.

KHALIQ, Z. M. & BEAN, B. P. 2010. Pacemaking in dopaminergic ventral tegmental area neurons: depolarizing drive from background and voltage-dependent sodium conductances. *The Journal of Neuroscience,* 30**,** 7401-13.

KIEHN, O. & EKEN, T. 1998. Functional role of plateau potentials in vertebrate motor neurons. *Current Opinion in Neurobiology,* 8**,** 746-752.

KIM, B., YOON, S., NAKAJIMA, R., LEE, H. J., LIM, H. J., LEE, Y. K., CHOI, J. S., YOON, B. J., AUGUSTINE, G. J. & BAIK, J. H. 2018. Dopamine D2 receptor-mediated circuit from the central amygdala to the bed nucleus of the stria terminalis regulates impulsive behavior. *Proceedings of the National Academy of Sciences of the United States of America,* 115**,** E10730-E10739.

KIM, E. J., HOROVITZ, O., PELLMAN, B. A., TAN, L. M., LI, Q., RICHTER-LEVIN, G. & KIM, J. J. 2013. Dorsal periaqueductal gray-amygdala pathway conveys both innate and learned fear responses in rats. *Proceedings of the National Academy of Sciences of the United States of America,* 110**,** 14795-800.

KIMM, T., KHALIQ, Z. M. & BEAN, B. P. 2015. Differential Regulation of Action Potential Shape and Burst-Frequency Firing by BK and Kv2 Channels in Substantia Nigra Dopaminergic Neurons. *The Journal of Neuroscience,* 35**,** 16404-17.

KIMMEL, C. B., BALLARD, W. W., KIMMEL, S. R., ULLMANN, B. & SCHILLING, T. F. 1995. Stages of embryonic development of the zebrafish. *Developmental Dynamics,* 203**,** 253-310.

KIMURA, M., KATO, M. & SHIMAZAKI, H. 1990. Physiological properties of projection neurons in the monkey striatum to the globus pallidus. *Experimental Brain Research,* 82**,** 672-6.

KITAI, S. T. & SURMEIER, D. J. 1993. Cholinergic and dopaminergic modulation of potassium conductances in neostriatal neurons. *Advances in Neurology,* 60**,** 40-52.

KITTELBERGER, J. M. & BASS, A. H. 2013. Vocal-motor and auditory connectivity of the midbrain periaqueductal gray in a teleost fish. *The Journal of Comparative Neurology,* 521**,** 791-812.

KOBLINGER, K., FUZESI, T., EJDRYGIEWICZ, J., KRAJACIC, A., BAINS, J. S. & WHELAN, P. J. 2014a. Characterization of A11 neurons projecting to the spinal cord of mice. *PLoS One,* 9**,** e109636.

KOBLINGER, K., FÜZESI, T., EJDRYGIEWICZ, J., KRAJACIC, A., BAINS, J. S. & WHELAN, P. J. 2014b. Characterization of A11 neurons projecting to the spinal cord of mice. *PloS one,* 9**,** e109636-e109636.

KOBLINGER, K., JEAN-XAVIER, C., SHARMA, S., FUZESI, T., YOUNG, L., EATON, S. E. A., KWOK, C. H. T., BAINS, J. S. & WHELAN, P. J. 2018.

Optogenetic Activation of A11 Region Increases Motor Activity. *Frontiers in Neural Circuits,* 12**,** 86.

KOCH, M. 1999. The neurobiology of startle. *Progress in Neurobiology,* 59**,** 107-28.

KOHASHI, T. & ODA, Y. 2008. Initiation of Mauthner- or Non-Mauthner-Mediated Fast Escape Evoked by Different Modes of Sensory Input. *The Journal of Neuroscience,* 28**,** 10641-10653.

KOOB, G. F. 1992. Drugs of abuse: anatomy, pharmacology and function of reward pathways. *Trends in Pharmacological Sciences* 13**,** 177-84.

KOOB, G. F. 1996. Hedonic valence, dopamine and motivation. *Molecular Psychiatry,* 1**,** 186-9.

KOOB, G. F. 2003. Neuroadaptive mechanisms of addiction: studies on the extended amygdala. *European Neuropsychopharmacology,* 13**,** 442-52.

KORN, H. & FABER, D. S. 2005. The Mauthner cell half a century later: a neurobiological model for decision-making? *Neuron,* 47**,** 13-28.

KOUTSIKOU, S., WATSON, T. C., CROOK, J. J., LEITH, J. L., LAWRENSON, C. L., APPS, R. & LUMB, B. M. 2015. The Periaqueductal Gray Orchestrates Sensory and Motor Circuits at Multiple Levels of the Neuraxis. *The Journal of Neuroscience,* 35**,** 14132-47.

KOYAMA, M., KINKHABWALA, A., SATOU, C., HIGASHIJIMA, S. & FETCHO, J. 2011. Mapping a sensory-motor network onto a structural and functional ground plan in the hindbrain. *Proceedings of the National Academy of Sciences of the United States of America,* 108**,** 1170-5.

KRACK, P., HARIZ, M. I., BAUNEZ, C., GURIDI, J. & OBESO, J. A. 2010. Deep brain stimulation: from neurology to psychiatry? *Trends in Neuroscience,* 33**,** 474-84.

KRASHIA, P., MARTINI, A., NOBILI, A., AVERSA, D., D'AMELIO, M., BERRETTA, N., GUATTEO, E. & MERCURI, N. B. 2017. On the properties of identified dopaminergic neurons in the mouse substantia nigra and ventral tegmental area. *European Journal of Neuroscience,* 45**,** 92-105.

KRAVITZ, A. V., FREEZE, B. S., PARKER, P. R. L., KAY, K., THWIN, M. T., DEISSEROTH, K. & KREITZER, A. C. 2010. Regulation of parkinsonian motor behaviours by optogenetic control of basal ganglia circuitry. *Nature,* 466**,** 622-626.

KRAVITZ, A. V., TYE, L. D. & KREITZER, A. C. 2012. Distinct roles for direct and indirect pathway striatal neurons in reinforcement. *Nature Neuroscience,* 15**,** 816-8.

KREITZER, A. C. & MALENKA, R. C. 2008. Striatal Plasticity and Basal Ganglia Circuit Function. *Neuron,* 60**,** 543-554.

KUHLMAN, S. J., LU, J., LAZARUS, M. S. & HUANG, Z. J. 2010. Maturation of GABAergic inhibition promotes strengthening of temporally coherent inputs among convergent pathways. *PLoS Computational Biology,* 6**,** e1000797.

KUMER, S. C. & VRANA, K. E. 1996. Intricate regulation of tyrosine hydroxylase activity and gene expression. *Journal of Neurochemistry,* 67**,** 443-62.

KUPCHIK, Y. M. & KALIVAS, P. W. 2017. The Direct and Indirect Pathways of the Nucleus Accumbens are not What You Think. *Neuropsychopharmacology,* 42**,** 369-370.

KYSIL, E. V., MESHALKINA, D. A., FRICK, E. E., ECHEVARRIA, D. J., ROSEMBERG, D. B., MAXIMINO, C., LIMA, M. G., ABREU, M. S., GIACOMINI, A. C., BARCELLOS, L. J. G., SONG, C. & KALUEFF, A. V. 2017. Comparative Analyses of Zebrafish Anxiety-Like Behavior Using Conflict-Based Novelty Tests. *Zebrafish,* 14**,** 197-208.

LACEY, M. G., MERCURI, N. B. & NORTH, R. A. 1987. Dopamine acts on D2 receptors to increase potassium conductance in neurones of the rat substantia nigra zona compacta. *The Journal of Physiology,* 392**,** 397-416.

LACOSTE, A. M. B., SCHOPPIK, D., ROBSON, D. N., HAESEMEYER, M., PORTUGUES, R., LI, J. M., RANDLETT, O., WEE, C. L., ENGERT, F. & SCHIER, A. F. 2015. A convergent and essential interneuron pathway for Mauthner-cell-mediated escapes. *Current Biology,* 25**,** 1526-1534.

LALIVE, A. L., MUNOZ, M. B., BELLONE, C., SLESINGER, P. A., LUSCHER, C. & TAN, K. R. 2014. Firing modes of dopamine neurons drive bidirectional GIRK channel plasticity. *The Journal of Neuroscience,* 34**,** 5107-14.

LAM, C. S., KORZH, V. & STRAHLE, U. 2005. Zebrafish embryos are susceptible to the dopaminergic neurotoxin MPTP. *European Journal of Neuroscience,* 21**,** 1758-62.

LAMBERT, A. M., BONKOWSKY, J. L. & MASINO, M. A. 2012. The conserved dopaminergic diencephalospinal tract mediates vertebrate locomotor development in zebrafish larvae. *The Journal of Neuroscience,* 32**,** 13488-500.

LAMMEL, S., HETZEL, A., HACKEL, O., JONES, I., LISS, B. & ROEPER, J. 2008. Unique properties of mesoprefrontal neurons within a dual mesocorticolimbic dopamine system. *Neuron,* 57**,** 760-73.

LAMMEL, S., ION, D. I., ROEPER, J. & MALENKA, R. C. 2011. Projection-specific modulation of dopamine neuron synapses by aversive and rewarding stimuli. *Neuron,* 70**,** 855-62.

LAMMEL, S., LIM, B. K. & MALENKA, R. C. 2014. Reward and aversion in a heterogeneous midbrain dopamine system. *Neuropharmacology,* 76 Pt B**,** 351-9.

LAMONT, E. W. & KOKKINIDIS, L. 1998. Infusion of the dopamine D1 receptor antagonist SCH 23390 into the amygdala blocks fear expression in a potentiated startle paradigm. *Brain Research* 795**,** 128-36.

LANCIEGO, J. L., LUQUIN, N. & OBESO, J. A. 2012. Functional neuroanatomy of the basal ganglia. *Cold Spring Harbor perspectives in medicine,* 2**,** a009621.

LANGSTON, J. W. 2017. The MPTP Story. *Journal of Parkinson's disease,* 7**,** S11-S19.

LARKIN, J. D., JENNI, N. L. & FLORESCO, S. B. 2016. Modulation of risk/reward decision making by dopaminergic transmission within the basolateral amygdala. *Psychopharmacology (Berl),* 233**,** 121-36.

LASZLO, K., PECZELY, L., KOVACS, A., ZAGORACZ, O., OLLMANN, T., KERTES, E., KALLAI, V., CSETENYI, B., KARADI, Z. & LENARD, L. 2018. The role of intraamygdaloid neurotensin and dopamine interaction in conditioned place preference. *Behavioral and Brain Sciences,* 344**,** 85-90.

LE MOINE, C. & BLOCH, B. 1995. D1 and D2 dopamine receptor gene expression in the rat striatum: sensitive cRNA probes demonstrate prominent segregation of D1 and D2 mRNAs in distinct neuronal

populations of the dorsal and ventral striatum. *The Journal of Comparative Neurology,* 355**,** 418-26.

LEBOW, M. A. & CHEN, A. 2016. Overshadowed by the amygdala: the bed nucleus of the stria terminalis emerges as key to psychiatric disorders. *Molecular Psychiatry,* 21**,** 450-63.

LEDOUX, J. 2007. The amygdala. *Current Biology,* 17**,** R868-74.

LEE, H. J., YOUN, J. M., O, M. J., GALLAGHER, M. & HOLLAND, P. C. 2006. Role of substantia nigra-amygdala connections in surprise-induced enhancement of attention. *The Journal of Neuroscience,* 26**,** 6077-81.

LEE, Y., LOPEZ, D. E., MELONI, E. G. & DAVIS, M. 1996. A primary acoustic startle pathway: obligatory role of cochlear root neurons and the nucleus reticularis pontis caudalis. *The Journal of Neuroscience,* 16**,** 3775-89.

LEES, A. J. 1993. Dopamine agonists in Parkinson's disease: a look at apomorphine. *Fundamental & Clinical Pharmacology,* 7**,** 121-8.

LENARD, L., OLLMANN, T., LASZLO, K., KOVACS, A., GALOSI, R., KALLAI, V., ATTILA, T., KERTES, E., ZAGORACZ, O., KARADI, Z. & PECZELY, L. 2017. Role of D2 dopamine receptors of the ventral pallidum in inhibitory avoidance learning. *Behavioral and Brain Sciences,* 321**,** 99-105.

LENKA, N., LU, Z. J., SASSE, P., HESCHELER, J. & FLEISCHMANN, B. K. 2002. Quantitation and functional characterization of neural cells derived from ES cells using nestin enhancer-mediated targeting in vitro. *Journal of Cell Science & Therapy,* 115**,** 1471-85.

LERANT, A., HERMAN, M. E. & FREEMAN, M. E. 1996. Dopaminergic neurons of periventricular and arcuate nuclei of pseudopregnant rats: semicircadian rhythm in Fos-related antigens immunoreactivities and in dopamine concentration. *Endocrinology,* 137**,** 3621-8.

LEVEY, A. I., HERSCH, S. M., RYE, D. B., SUNAHARA, R. K., NIZNIK, H. B., KITT, C. A., PRICE, D. L., MAGGIO, R., BRANN, M. R. & CILIAX, B. J. 1993. Localization of D1 and D2 dopamine receptors in brain with subtype-specific antibodies. *Proceedings of the National Academy of Sciences of the United States of America,* 90**,** 8861-5.

LEVICK, W. R. 1967. Receptive fields and trigger features of ganglion cells in the visual streak of the rabbits retina. *The Journal of Physiology,* 188**,** 285-307.

LEWIS, M. C. & GOULD, T. J. 2003. Nicotine and ethanol enhancements of acoustic startle reflex are mediated in part by dopamine in C57BL/6J mice. *Pharmacology Biochemistry and Behavior,* 76**,** 179-86.

LI, Y., ZUO, Y., YU, P., PING, X. & CUI, C. 2015. Role of basolateral amygdala dopamine D2 receptors in impulsive choice in acute cocaine-treated rats. *Behavioral and Brain Sciences,* 287**,** 187-95.

LIANG, F., XIONG, X. R., ZINGG, B., JI, X. Y., ZHANG, L. I. & TAO, H. W. 2015. Sensory Cortical Control of a Visually Induced Arrest Behavior via Corticotectal Projections. *Neuron,* 86**,** 755-67.

LIAO, R.-M. 2008. Development of conditioned place preference induced by intra-accumbens infusion of amphetamine is attenuated by co-infusion of dopamine D1 and D2 receptor antagonists. *Pharmacology Biochemistry and Behavior,* 89**,** 367-373.

LIM, A., KANG, U. & MCGEHEE, D. 2014. Striatal cholinergic interneuron regulation and circuit effect. *Frontiers in synaptic neuroscience,* 6**,** 22.

LINDNER, K., NEUBERT, J., PFANNMOLLER, J., LOTZE, M., HAMM, A. O. & WENDT, J. 2015. Fear-potentiated startle processing in humans: Parallel fMRI and orbicularis EMG assessment during cue conditioning and extinction. *International Journal of Psychophysiology,* 98**,** 535-45.

LISS, B., FRANZ, O., SEWING, S., BRUNS, R., NEUHOFF, H. & ROEPER, J. 2001. Tuning pacemaker frequency of individual dopaminergic neurons by Kv4.3L and KChip3.1 transcription. *The EMBO journal,* 20**,** 5715-5724.

LIU, K. S. & FETCHO, J. R. 1999. Laser Ablations Reveal Functional Relationships of Segmental Hindbrain Neurons in Zebrafish. *Neuron,* 23**,** 325-335.

LIU, X., LIN, J., ZHANG, Y., PENG, X., GUO, N. & LI, Q. 2016. Effects of diphenylhydantoin on locomotion and thigmotaxis of larval zebrafish. *Neurotoxicology and Teratology,* 53**,** 41-7.

LIU, Y.-C., BAILEY, I. & HALE, M. E. 2012. Alternative startle motor patterns and behaviors in the larval zebrafish (Danio rerio). *Journal of Comparative Physiology A,* 198**,** 11-24.

LIU, Y., DORE, J. & CHEN, X. 2007. Calcium influx through L-type channels generates protein kinase M to induce burst firing of dopamine cells in the rat ventral tegmental area. ***J Biol Chem***, 282**,** 8594-603.

LIU, Y. C. & HALE, M. E. 2017. Local Spinal Cord Circuits and Bilateral Mauthner Cell Activity Function Together to Drive Alternative Startle Behaviors. *Current Biology,* 27**,** 697-704.

LIU, Y. J., WANG, Q. & LI, B. 2011. Neuronal responses to looming objects in the superior colliculus of the cat. *Brain, Behavior and Evolution,* 77**,** 193-205.

LOBO, M. K., COVINGTON, H. E., CHAUDHURY, D., FRIEDMAN, A. K., SUN, H., DAMEZ-WERNO, D., DIETZ, D. M., ZAMAN, S., KOO, J. W., KENNEDY, P. J., MOUZON, E., MOGRI, M., NEVE, R. L., DEISSEROTH, K., HAN, M.-H. & NESTLER, E. J. 2010. Cell Type–Specific Loss of BDNF Signaling Mimics Optogenetic Control of Cocaine Reward. *Science,* 330**,** 385-390.

LOBO, M. K. & NESTLER, E. J. 2011. The striatal balancing act in drug addiction: distinct roles of direct and indirect pathway medium spiny neurons. *Frontiers in neuroanatomy,* 5**,** 41-41.

LOTHARIUS, J. & BRUNDIN, P. 2002. Pathogenesis of parkinson's disease: dopamine, vesicles and α-synuclein. *Nature Reviews Neuroscience,* 3**,** 932.

LUO, S. X. & HUANG, E. J. 2016. Dopaminergic Neurons and Brain Reward Pathways: From Neurogenesis to Circuit Assembly. *The American journal of pathology,* 186**,** 478-488.

LUSCHER, C. & MALENKA, R. C. 2011. Drug-evoked synaptic plasticity in addiction: from molecular changes to circuit remodeling. *Neuron,* 69**,** 650-63.

LYNN, A. M., SCHNEIDER, D. A. & BRUCE, L. L. 2015. Development of the Avian Dorsal Thalamus: Patterns and Gradients of Neurogenesis. *Brain, Behavior and Evolution,* 86**,** 94-109.

LYONS, D. J., HELLYSAZ, A. & BROBERGER, C. 2012. Prolactin Regulates Tuberoinfundibular Dopamine Neuron Discharge Pattern: Novel Feedback Control Mechanisms in the Lactotrophic Axis. *The Journal of Neuroscience,* 32**,** 8074-8083.

LYONS, D. J., HORJALES-ARAUJO, E. & BROBERGER, C. 2010. Synchronized Network Oscillations in Rat Tuberoinfundibular Dopamine Neurons: Switch to Tonic Discharge by Thyrotropin-Releasing Hormone. *Neuron,* 65**,** 217-229.

MACCAFERRI, G. & MCBAIN, C. J. 1996. The hyperpolarization-activated current (Ih) and its contribution to pacemaker activity in rat CA1 hippocampal stratum oriens-alveus interneurones. *The Journal of Physiology,* 497 (Pt 1)**,** 119-30.

MAGRINELLI, F., PICELLI, A., TOCCO, P., FEDERICO, A., RONCARI, L., SMANIA, N., ZANETTE, G. & TAMBURIN, S. 2016. Pathophysiology of Motor Dysfunction in Parkinson's Disease as the Rationale for Drug Treatment and Rehabilitation. *Parkinsons Disease,* 2016**,** 9832839.

MAHAPATRA, A. 2010. Overeating, obesity, and dopamine receptors. *ACS Chemical Neuroscience,* 1**,** 346-347.

MAHLER, J., FILIPPI, A. & DRIEVER, W. 2010. DeltaA/DeltaD regulate multiple and temporally distinct phases of notch signaling during dopaminergic neurogenesis in zebrafish. *The Journal of Neuroscience,* 30**,** 16621-35.

MALDONADO, R., SAIARDI, A., VALVERDE, O., SAMAD, T. A., ROQUES, B. P. & BORRELLI, E. 1997. Absence of opiate rewarding effects in mice lacking dopamine D2 receptors. *Nature,* 388**,** 586-9.

MARGOLIS, E. B., LOCK, H., HJELMSTAD, G. O. & FIELDS, H. L. 2006. The ventral tegmental area revisited: is there an electrophysiological marker for dopaminergic neurons? *The Journal of Physiology,* 577**,** 907-24.

MARGOLIS, E. B., MITCHELL, J. M., ISHIKAWA, J., HJELMSTAD, G. O. & FIELDS, H. L. 2008. Midbrain dopamine neurons: projection target determines action potential duration and dopamine D(2) receptor inhibition. *The Journal of Neuroscience,* 28**,** 8908-13.

MARINO, R. A. & LEVY, R. 2019. Differential effects of D1 and D2 dopamine agonists on memory, motivation, learning and response time in non-human primates. *European Journal of Neuroscience,* 49**,** 199-214.

MARQUART, G. D., TABOR, K. M., BERGERON, S. A., BRIGGMAN, K. L. & BURGESS, H. A. 2019. Prepontine non-giant neurons drive flexible escape behavior in zebrafish. *PLOS Biology,* 17**,** e3000480.

MARSH, R. A., FUZESSERY, Z. M., GROSE, C. D. & WENSTRUP, J. J. 2002. Projection to the inferior colliculus from the basal nucleus of the amygdala. *The Journal of Neuroscience,* 22**,** 10449-60.

MARTI, J., SANTA-CRUZ, M. C., MOLINA, V., SERRA, R., BAYER, S. A., GHETTI, B. & HERVAS, J. P. 2009. Regional differences in the vulnerability of substantia nigra dopaminergic neurons in weaver mice. *Acta Neurobiologiae Experimentalis,* 69**,** 198-206.

MARTINEZ, R. C., CARVALHO-NETTO, E. F., RIBEIRO-BARBOSA, E. R., BALDO, M. V. & CANTERAS, N. S. 2011. Amygdalar roles during exposure to a live predator and to a predator-associated context. *Neuroscience,* 172**,** 314-28.

MATHESON, T., ROGERS, S. M. & KRAPP, H. G. 2004. Plasticity in the visual system is correlated with a change in lifestyle of solitarious and gregarious locusts. *The Journal of Neurophysiology,* 91**,** 1-12.

MATHUR, P., LAU, B. & GUO, S. 2011. Conditioned place preference behavior in zebrafish. *Nature Protocols,* 6**,** 338-45.

MATSUI, H. 2017. Dopamine system, cerebellum, and nucleus ruber in fish and mammals. *Development, Growth & Differentiation,* 59**,** 219-227.

MATSUMOTO, M. 2015. Dopamine signals and physiological origin of cognitive dysfunction in Parkinson's disease. *Movement Disorders,* 30**,** 472-83.

MATSUMOTO, M. & HIKOSAKA, O. 2009. Two types of dopamine neuron distinctly convey positive and negative motivational signals. *Nature,* 459**,** 837-41.

MATSUMOTO, M. & TAKADA, M. 2013. Distinct representations of cognitive and motivational signals in midbrain dopamine neurons. *Neuron,* 79**,** 1011-24.

MAXIMINO, C., DA SILVA, A. W. B., GOUVEIA, A. & HERCULANO, A. M. 2011. Pharmacological analysis of zebrafish (Danio rerio) scototaxis. *Progress in Neuro-Psychopharmacology and Biological Psychiatry,* 35**,** 624-631.

MAXIMINO, C., DE BRITO, T. M., COLMANETTI, R., PONTES, A. A. A., DE CASTRO, H. M., DE LACERDA, R. I. T., MORATO, S. & GOUVEIA, A. 2010. Parametric analyses of anxiety in zebrafish scototaxis. *Behavioural Brain Research,* 210**,** 1-7.

MAY, P. J. 2006. The mammalian superior colliculus: laminar structure and connections. *Progress in Brain Research,* 151**,** 321-78.

MCCALL, J. G., SIUDA, E. R., BHATTI, D. L., LAWSON, L. A., MCELLIGOTT, Z. A., STUBER, G. D. & BRUCHAS, M. R. 2017. Locus coeruleus to basolateral amygdala noradrenergic projections promote anxiety-like behavior. *Elife,* 6.

MCCALL, N. M., MARRON FERNANDEZ DE VELASCO, E. & WICKMAN, K. 2019. GIRK Channel Activity in Dopamine Neurons of the Ventral Tegmental Area Bidirectionally Regulates Behavioral Sensitivity to Cocaine. *The Journal of Neuroscience,* 39**,** 3600-3610.

MCCORMICK, C. A. 1997. Organization and connections of octaval and lateral line centers in the medulla of a clupeid, Dorosoma cepedianum. *Hear Research,* 110**,** 39-60.

MCCORMICK, C. A. & HERNANDEZ, D. V. 1996. Connections of octaval and lateral line nuclei of the medulla in the goldfish, including the cytoarchitecture of the secondary octaval population in goldfish and catfish. *Brain, Behavior and Evolution,* 47**,** 113-37.

MCDONALD, A. J. 1991. Topographical organization of amygdaloid projections to the caudatoputamen, nucleus accumbens, and related striatal-like areas of the rat brain. *Neuroscience,* 44**,** 15-33.

MCGINNIS, M. M., SICILIANO, C. A. & JONES, S. R. 2016. Dopamine D3 autoreceptor inhibition enhances cocaine potency at the dopamine transporter. *Journal of Neurochemistry,* 138**,** 821-9.

MCGRAW, H. F., NECHIPORUK, A. & RAIBLE, D. W. 2008. Zebrafish dorsal root ganglia neural precursor cells adopt a glial fate in the absence of neurogenin1. *The Journal of Neuroscience,* 28**,** 12558-12569.

MCHUGH, P. C. & BUCKLEY, D. A. 2015. The structure and function of the dopamine transporter and its role in CNS diseases. *Vitam Horm,* 98**,** 339-69.

MCLEAN, D. L., FAN, J., HIGASHIJIMA, S., HALE, M. E. & FETCHO, J. R. 2007. A topographic map of recruitment in spinal cord. *Nature,* 446**,** 71-5.

MCLEAN, D. L. & FETCHO, J. R. 2004a. Ontogeny and innervation patterns of dopaminergic, noradrenergic, and serotonergic neurons in larval zebrafish. *The Journal of Comparative Neurology,* 480**,** 38-56.

MCLEAN, D. L. & FETCHO, J. R. 2004b. Relationship of tyrosine hydroxylase and serotonin immunoreactivity to sensorimotor circuitry in larval zebrafish. *The Journal of Comparative Neurology,* 480**,** 57-71.

MCLEAN, D. L. & FETCHO, J. R. 2009. Spinal interneurons differentiate sequentially from those driving the fastest swimming movements in larval zebrafish to those driving the slowest ones. *The Journal of Neuroscience,* 29**,** 13566-13577.

MEFFERT, H., PENNER, E., VANTIEGHEM, M. R., SYPHER, I., LESHIN, J. & BLAIR, R. J. R. 2018. The role of ventral striatum in reward-based attentional bias. *Brain Research* 1689**,** 89-97.

MEISER, J., WEINDL, D. & HILLER, K. 2013. Complexity of dopamine metabolism. *Cell communication and signaling : CCS,* 11**,** 34-34.

MEISTER, B. & ELDE, R. 1993. Dopamine transporter mRNA in neurons of the rat hypothalamus. *Neuroendocrinology,* 58**,** 388-95.

MELCHITZKY, D. S., ERICKSON, S. L. & LEWIS, D. A. 2006. Dopamine innervation of the monkey mediodorsal thalamus: Location of projection neurons and ultrastructural characteristics of axon terminals. *Neuroscience,* 143**,** 1021-1030.

MELONI, E. G. & DAVIS, M. 1999. Enhancement of the acoustic startle response in rats by the dopamine D1 receptor agonist SKF 82958. *Psychopharmacology (Berl),* 144**,** 373-80.

MELONI, E. G. & DAVIS, M. 2000a. Enhancement of the acoustic startle response by dopamine agonists after 6-hydroxydopamine lesions of the substantia nigra pars compacta: corresponding changes in c-Fos expression in the caudate-putamen. *Brain Research* 879**,** 93-104.

MELONI, E. G. & DAVIS, M. 2000b. GABA in the deep layers of the superior Colliculus/Mesencephalic reticular formation mediates the enhancement of startle by the dopamine D1 receptor agonist SKF 82958 in rats. *The Journal of Neuroscience,* 20**,** 5374-81.

MERCURI, N. B., BONCI, A., CALABRESI, P., STRATTA, F., STEFANI, A. & BERNARDI, G. 1994. Effects of dihydropyridine calcium antagonists on rat midbrain dopaminergic neurones. *British Journal of Pharmacology* 113**,** 831-8.

MERCURI, N. B., SAIARDI, A., BONCI, A., PICETTI, R., CALABRESI, P., BERNARDI, G. & BORRELLI, E. 1997. Loss of autoreceptor function in dopaminergic neurons from dopamine D2 receptor deficient mice. *Neuroscience,* 79**,** 323-7.

MERICKEL, A., ROSANDICH, P., PETER, D. & EDWARDS, R. H. 1995. Identification of residues involved in substrate recognition by a vesicular monoamine transporter. *Journal of Biological Chemistry,* 270**,** 25798-804.

MIKHAILOVA, M. A., BASS, C. E., GRINEVICH, V. P., CHAPPELL, A. M., DEAL, A. L., BONIN, K. D., WEINER, J. L., GAINETDINOV, R. R. & BUDYGIN, E. A. 2016. Optogenetically-induced tonic dopamine release from VTA-nucleus accumbens projections inhibits reward consummatory behaviors. *Neuroscience,* 333**,** 54-64.

MILLER, E. K., FREEDMAN, D. J. & WALLIS, J. D. 2002. The prefrontal cortex: categories, concepts and cognition. *Philosophical transactions of the Royal Society of London. Series B, Biological sciences,* 357**,** 1123-36.

MINAMI, S., SATOYOSHI, H., IDE, S., INOUE, T., YOSHIOKA, M. & MINAMI, M. 2017. Suppression of reward-induced dopamine release in the nucleus

accumbens in animal models of depression: Differential responses to drug treatment. *Neuroscience Letters,* 650**,** 72-76.

MIRJANY, M. & FABER, D. S. 2011. Characteristics of the anterior lateral line nerve input to the Mauthner cell. *The Journal of Experimental Biology,* 214**,** 3368-77.

MISSALE, C., NASH, S. R., ROBINSON, S. W., JABER, M. & CARON, M. G. 1998. Dopamine receptors: from structure to function. *Physiological Reviews,* 78**,** 189-225.

MOGA, M. M., WEIS, R. P. & MOORE, R. Y. 1995. Efferent projections of the paraventricular thalamic nucleus in the rat. *The Journal of Comparative Neurology,* 359**,** 221-38.

MORALES, M. & MARGOLIS, E. B. 2017. Ventral tegmental area: cellular heterogeneity, connectivity and behaviour. *Nature Reviews Neuroscience,* 18**,** 73-85.

MOREIRA, C. M., MASSON, S., CARVALHO, M. C. & BRANDAO, M. L. 2007. Exploratory behaviour of rats in the elevated plus-maze is differentially sensitive to inactivation of the basolateral and central amygdaloid nuclei. *Brain Research Bulletin,* 71**,** 466-74.

MORERA-HERRERAS, T., MIGUELEZ, C., ARISTIETA, A., RUIZ-ORTEGA, J. Á. & UGEDO, L. 2012. Endocannabinoid Modulation of Dopaminergic Motor Circuits. *Frontiers in Pharmacology,* 3.

MORI, F., OKADA, K.-I., NOMURA, T. & KOBAYASHI, Y. 2016. The Pedunculopontine Tegmental Nucleus as a Motor and Cognitive Interface between the Cerebellum and Basal Ganglia. *Frontiers in neuroanatomy,* 10**,** 109-109.

MORIKAWA, H. & PALADINI, C. A. 2011. Dynamic regulation of midbrain dopamine neuron activity: intrinsic, synaptic, and plasticity mechanisms. *Neuroscience,* 198**,** 95-111.

MU, Y., LI, X.-Q., ZHANG, B. & DU, J.-L. 2012. Visual Input Modulates Audiomotor Function via Hypothalamic Dopaminergic Neurons through a Cooperative Mechanism. *Neuron,* 75**,** 688-699.

MUELLER, T. 2012. What is the Thalamus in Zebrafish? *Frontiers in Neuroscience,* 6**,** 64.

MUELLER, T., DONG, Z., BERBEROGLU, M. A. & GUO, S. 2011. The Dorsal Pallium in Zebrafish, Danio rerio (Cyprinidae, Teleostei). *Brain research,* 1381**,** 95-105.

MUELLER, T., WULLIMANN, M. F. & GUO, S. 2008. Early teleostean basal ganglia development visualized by zebrafish Dlx2a, Lhx6, Lhx7, Tbr2 (eomesa), and GAD67 gene expression. *The Journal of Comparative Neurology,* 507**,** 1245-57.

MULLER, J. F., MASCAGNI, F. & MCDONALD, A. J. 2009. Dopaminergic innervation of pyramidal cells in the rat basolateral amygdala. *Brain Structure and Function,* 213**,** 275-88.

MURER, M. G., DZIEWCZAPOLSKI, G., SALIN, P., VILA, M., TSENG, K. Y., RUBERG, M., RUBINSTEIN, M., KELLY, M. A., GRANDY, D. K., LOW, M. J., HIRSCH, E., RAISMAN-VOZARI, R. & GERSHANIK, O. 2000. The indirect basal ganglia pathway in dopamine D2 receptor-deficient mice. *Neuroscience,* 99**,** 643-650.

MUTO, A. & KAWAKAMI, K. 2013. Prey capture in zebrafish larvae serves as a model to study cognitive functions. *Frontiers in Neural Circuits,* 7.

MUTO, A., LAL, P., AILANI, D., ABE, G., ITOH, M. & KAWAKAMI, K. 2017. Activation of the hypothalamic feeding centre upon visual prey detection. *Nature Communications,* 8**,** 15029.

NADER, K., MAJIDISHAD, P., AMORAPANTH, P. & LEDOUX, J. E. 2001. Damage to the lateral and central, but not other, amygdaloid nuclei prevents the acquisition of auditory fear conditioning. *Learning & Memory,* 8**,** 156-63.

NAKANISHI, S., HIKIDA, T. & YAWATA, S. 2014. Distinct dopaminergic control of the direct and indirect pathways in reward-based and avoidance learning behaviors. *Neuroscience,* 282**,** 49-59.

NAKAYAMA, H. & ODA, Y. 2004. Common sensory inputs and differential excitability of segmentally homologous reticulospinal neurons in the hindbrain. *The Journal of Neuroscience,* 24**,** 3199-209.

NATSUBORI, A., TSUTSUI-KIMURA, I., NISHIDA, H., BOUCHEKIOUA, Y., SEKIYA, H., UCHIGASHIMA, M., WATANABE, M., DE KERCHOVE D'EXAERDE, A., MIMURA, M., TAKATA, N. & TANAKA, K. F. 2017. Ventrolateral Striatal Medium Spiny Neurons Positively Regulate Food-Incentive, Goal-Directed Behavior Independently of D1 and D2 Selectivity. *The Journal of Neuroscience,* 37**,** 2723-2733.

NAUMANN, E. A., FITZGERALD, J. E., DUNN, T. W., RIHEL, J., SOMPOLINSKY, H. & ENGERT, F. 2016. From Whole-Brain Data to Functional Circuit Models: The Zebrafish Optomotor Response. *Cell,* 167**,** 947-960.e20.

NEUHAUSS, S. C., BIEHLMAIER, O., SEELIGER, M. W., DAS, T., KOHLER, K., HARRIS, W. A. & BAIER, H. 1999. Genetic disorders of vision revealed by a behavioral screen of 400 essential loci in zebrafish. *The Journal of Neuroscience,* 19**,** 8603-15.

NEUHOFF, H., NEU, A., LISS, B. & ROEPER, J. 2002. I(h) channels contribute to the different functional properties of identified dopaminergic subpopulations in the midbrain. *The Journal of Neuroscience,* 22**,** 1290-302.

NEWMAN, S. W. 1999. The medial extended amygdala in male reproductive behavior. A node in the mammalian social behavior network. *Annals of the New York Academy of Sciences,* 877**,** 242-57.

NG, K. H., POLLOCK, M. W., URBANCZYK, P. J. & SANGHA, S. 2018. Altering D1 receptor activity in the basolateral amygdala impairs fear suppression during a safety cue. *Neurobiology of Learning and Memory,* 147**,** 26-34.

NICOLA, S. M., SURMEIER, J. & MALENKA, R. C. 2000. Dopaminergic modulation of neuronal excitability in the striatum and nucleus accumbens. *Annual Review of Neuroscience,* 23**,** 185-215.

NIEH, E. H., KIM, S. Y., NAMBURI, P. & TYE, K. M. 2013. Optogenetic dissection of neural circuits underlying emotional valence and motivated behaviors. *Brain Research* 1511**,** 73-92.

NIEOULLON, A. 2002. Dopamine and the regulation of cognition and attention. *Progress in Neurobiology,* 67**,** 53-83.

NIKOLAOU, N. & MEYER, MARTIN P. 2015. Neurobiology: Imaging Prey Capture Circuits in Zebrafish. *Current Biology,* 25**,** R273-R275.

NIRENBERG, M. J., CHAN, J., LIU, Y., EDWARDS, R. H. & PICKEL, V. M. 1996a. Ultrastructural localization of the vesicular monoamine transporter-2 in midbrain dopaminergic neurons: potential sites for somatodendritic

storage and release of dopamine. *The Journal of Neuroscience,* 16**,** 4135-45.

NIRENBERG, M. J., VAUGHAN, R. A., UHL, G. R., KUHAR, M. J. & PICKEL, V. M. 1996b. The dopamine transporter is localized to dendritic and axonal plasma membranes of nigrostriatal dopaminergic neurons. *The Journal of Neuroscience,* 16**,** 436-47.

NISENBAUM, E. S. & WILSON, C. J. 1995. Potassium currents responsible for inward and outward rectification in rat neostriatal spiny projection neurons. *The Journal of Neuroscience,* 15**,** 4449-63.

NISENBAUM, E. S., XU, Z. C. & WILSON, C. J. 1994. Contribution of a slowly inactivating potassium current to the transition to firing of neostriatal spiny projection neurons. *The Journal of Neurophysiology,* 71**,** 1174-89.

NIV, Y., DAW, N. D., JOEL, D. & DAYAN, P. 2007. Tonic dopamine: opportunity costs and the control of response vigor. *Psychopharmacology (Berl),* 191**,** 507-20.

NORTHCUTT, R. G. 2006. Connections of the lateral and medial divisions of the goldfish telencephalic pallium. *The Journal of Comparative Neurology,* 494**,** 903-43.

O'CONNELL, L. A. & HOFMANN, H. A. 2011. The vertebrate mesolimbic reward system and social behavior network: a comparative synthesis. *The Journal of Comparative Neurology,* 519**,** 3599-639.

O'MALLEY, D. M., KAO, Y. H. & FETCHO, J. R. 1996. Imaging the functional organization of zebrafish hindbrain segments during escape behaviors. *Neuron,* 17**,** 1145-55.

OKAMOTO, T., HARNETT, M. T. & MORIKAWA, H. 2006. Hyperpolarization-activated cation current (Ih) is an ethanol target in midbrain dopamine neurons of mice. *The Journal of Neurophysiology,* 95**,** 619-626.

OLSON, I., SURYANARAYANA, S. M., ROBERTSON, B. & GRILLNER, S. 2017. Griseum centrale, a homologue of the periaqueductal gray in the lamprey. *IBRO Reports,* 2**,** 24-30.

OLSON, P. A., TKATCH, T., HERNANDEZ-LOPEZ, S., ULRICH, S., ILIJIC, E., MUGNAINI, E., ZHANG, H., BEZPROZVANNY, I. & SURMEIER, D. J. 2005. G-protein-coupled receptor modulation of striatal CaV1.3 L-type Ca2+ channels is dependent on a Shank-binding domain. *The Journal of Neuroscience,* 25**,** 1050-62.

OLSSON, M., BJORKLUND, A. & CAMPBELL, K. 1998. Early specification of striatal projection neurons and interneuronal subtypes in the lateral and medial ganglionic eminence. *Neuroscience,* 84**,** 867-76.

OLT, J., ALLEN, C. E. & MARCOTTI, W. 2016a. In vivo physiological recording from the lateral line of juvenile zebrafish. *The Journal of Physiology,* 594**,** 5427-38.

OLT, J., ORDOOBADI, A. J., MARCOTTI, W. & TRAPANI, J. G. 2016b. Chapter 11 - Physiological recordings from the zebrafish lateral line. *In:* DETRICH, H. W., WESTERFIELD, M. & ZON, L. I. (eds.) *Methods in Cell Biology.* Academic Press.

OLT, J., ORDOOBADI, A. J., MARCOTTI, W. & TRAPANI, J. G. 2016c. Physiological recordings from the zebrafish lateral line. *Methods in Cell Biology,* 133**,** 253-79.

OLVECZKY, B. P., BACCUS, S. A. & MEISTER, M. 2003. Segregation of object and background motion in the retina. *Nature,* 423**,** 401-8.

OSORIO, J., MUELLER, T., RETAUX, S., VERNIER, P. & WULLIMANN, M. F. 2010. Phylotypic expression of the bHLH genes Neurogenin2, Neurod, and Mash1 in the mouse embryonic forebrain. *The Journal of Comparative Neurology,* 518**,** 851-71.

OVERTON, P. & CLARK, D. 1992. Iontophoretically administered drugs acting at the N-methyl-D-aspartate receptor modulate burst firing in A9 dopamine neurons in the rat. *Synapse,* 10**,** 131-40.

OVERTON, P. G. & CLARK, D. 1997. Burst firing in midbrain dopaminergic neurons. *Brain Research Reviews,* 25**,** 312-34.

PALADINI, C. A. & ROEPER, J. 2014. Generating bursts (and pauses) in the dopamine midbrain neurons. *Neuroscience,* 282**,** 109-121.

PALANCA, A. M. S., LEE, S.-L., YEE, L. E., JOE-WONG, C., TRINH, L. A., HIROYASU, E., HUSAIN, M., FRASER, S. E., PELLEGRINI, M. & SAGASTI, A. 2013. New transgenic reporters identify somatosensory neuron subtypes in larval zebrafish. *Developmental neurobiology,* 73**,** 152-167.

PALMITER, R. D. 2008. Dopamine signaling in the dorsal striatum is essential for motivated behaviors: lessons from dopamine-deficient mice. *Annals of the New York Academy of Sciences,* 1129**,** 35-46.

PANULA, P., CHEN, Y. C., PRIYADARSHINI, M., KUDO, H., SEMENOVA, S., SUNDVIK, M. & SALLINEN, V. 2010. The comparative neuroanatomy and neurochemistry of zebrafish CNS systems of relevance to human neuropsychiatric diseases. *Neurobiology of Disease,* 40**,** 46-57.

PAPADOPOULOS, G. C. & PARNAVELAS, J. G. 1990. Distribution and synaptic organization of dopaminergic axons in the lateral geniculate nucleus of the rat. *The Journal of Comparative Neurology,* 294**,** 356-61.

PAPE, H. C. 1996. Queer current and pacemaker: the hyperpolarization-activated cation current in neurons. *Annual Review of Physiology,* 58**,** 299-327.

PAPPAS, S. S., BEHROUZ, B., JANIS, K. L., GOUDREAU, J. L. & LOOKINGLAND, K. J. 2008. Lack of D2 receptor mediated regulation of dopamine synthesis in A11 diencephalospinal neurons in male and female mice. *Brain Research* 1214**,** 1-10.

PARDO-GARCIA, T. R., GARCIA-KELLER, C., PENALOZA, T., RICHIE, C. T., PICKEL, J., HOPE, B. T., HARVEY, B. K., KALIVAS, P. W. & HEINSBROEK, J. A. 2019. Ventral Pallidum Is the Primary Target for Accumbens D1 Projections Driving Cocaine Seeking. *The Journal of Neuroscience,* 39**,** 2041-2051.

PARKER, J. G., ZWEIFEL, L. S., CLARK, J. J., EVANS, S. B., PHILLIPS, P. E. & PALMITER, R. D. 2010. Absence of NMDA receptors in dopamine neurons attenuates dopamine release but not conditioned approach during Pavlovian conditioning. *Proceedings of the National Academy of Sciences of the United States of America,* 107**,** 13491-6.

PARKER, M., BROCK, A., WALTON, R. & BRENNAN, C. 2013. The role of zebrafish (Danio rerio) in dissecting the genetics and neural circuits of executive function. *Frontiers in Neural Circuits,* 7.

PECZELY, L., OLLMANN, T., LASZLO, K., KOVACS, A., GALOSI, R., SZABO, A., KARADI, Z. & LENARD, L. 2014. Role of D1 dopamine receptors of the ventral pallidum in inhibitory avoidance learning. *Behavioral and Brain Sciences,* 270**,** 131-6.

PENG, X., LIN, J., ZHU, Y., LIU, X., ZHANG, Y., JI, Y., YANG, X., ZHANG, Y., GUO, N. & LI, Q. 2016. Anxiety-related behavioral responses of pentylenetetrazole-treated zebrafish larvae to light-dark transitions. *Pharmacology Biochemistry and Behavior,* 145**,** 55-65.

PERATHONER, S., CORDERO-MALDONADO, M. L. & CRAWFORD, A. D. 2016. Potential of zebrafish as a model for exploring the role of the amygdala in emotional memory and motivational behavior. *Journal of Neuroscience Research,* 94**,** 445-62.

PEREZ-FERNANDEZ, J., KARDAMAKIS, A. A., SUZUKI, D. G., ROBERTSON, B. & GRILLNER, S. 2017. Direct Dopaminergic Projections from the SNc Modulate Visuomotor Transformation in the Lamprey Tectum. *Neuron,* 96**,** 910-924 e5.

PEREZ-FERNANDEZ, J., STEPHENSON-JONES, M., SURYANARAYANA, S. M., ROBERTSON, B. & GRILLNER, S. 2014. Evolutionarily conserved organization of the dopaminergic system in lamprey: SNc/VTA afferent and efferent connectivity and D2 receptor expression. *The Journal of Comparative Neurology,* 522**,** 3775-94.

PEREZ DE LA MORA, M., GALLEGOS-CARI, A., CRESPO-RAMIREZ, M., MARCELLINO, D., HANSSON, A. C. & FUXE, K. 2012. Distribution of dopamine D(2)-like receptors in the rat amygdala and their role in the modulation of unconditioned fear and anxiety. *Neuroscience,* 201**,** 252-66.

PEREZ DE LA MORA, M., JACOBSEN, K. X., CRESPO-RAMIREZ, M., FLORES-GRACIA, C. & FUXE, K. 2008. Wiring and volume transmission in rat amygdala. Implications for fear and anxiety. *Neurochemical research,* 33**,** 1618-33.

PETROVICH, G. D., CANTERAS, N. S. & SWANSON, L. W. 2001. Combinatorial amygdalar inputs to hippocampal domains and hypothalamic behavior systems. *Brain Research Reviews,* 38**,** 247-289.

PHILIPPART, F., DESTREEL, G., MERINO-SEPULVEDA, P., HENNY, P., ENGEL, D. & SEUTIN, V. 2016. Differential Somatic Ca2+ Channel Profile in Midbrain Dopaminergic Neurons. *The Journal of Neuroscience,* 36**,** 7234-45.

PHILLIPS, P. E. & STAMFORD, J. A. 2000. Differential recruitment of N-, P- and Q-type voltage-operated calcium channels in striatal dopamine release evoked by 'regular' and 'burst' firing. *Brain Research* 884**,** 139-46.

PIGNATELLI, A., BORIN, M., FOGLI ISEPPE, A., GAMBARDELLA, C. & BELLUZZI, O. 2013. The h-current in periglomerular dopaminergic neurons of the mouse olfactory bulb. *PLoS One,* 8**,** e56571.

PIGNATELLI, A., KOBAYASHI, K., OKANO, H. & BELLUZZI, O. 2005. Functional properties of dopaminergic neurones in the mouse olfactory bulb. *The Journal of Physiology,* 564**,** 501-514.

PLENZ, D. & WICKENS, J. R. 2016. Chapter 6 - The Striatal Skeleton: Medium Spiny Projection Neurons and Their Lateral Connections. *In:* STEINER, H. & TSENG, K. Y. (eds.) *Handbook of Behavioral Neuroscience.* Elsevier.

POMBAL, M. A., EL MANIRA, A. & GRILLNER, S. 1997a. Afferents of the lamprey striatum with special reference to the dopaminergic system: a combined tracing and immunohistochemical study. *The Journal of Comparative Neurology,* 386**,** 71-91.

POMBAL, M. A., EL MANIRA, A. & GRILLNER, S. 1997b. Organization of the lamprey striatum - transmitters and projections. *Brain Research* 766**,** 249-54.

PORTAVELLA, M., VARGAS, J. P., TORRES, B. & SALAS, C. 2002. The effects of telencephalic pallial lesions on spatial, temporal, and emotional learning in goldfish. *Brain Research Bulletin,* 57**,** 397-9.

PORTUGUES, R. & ENGERT, F. 2011. Adaptive Locomotor Behavior in Larval Zebrafish. *Frontiers in Systems Neuroscience,* 5.

PREUSS, STEPHANIE J., TRIVEDI, CHINTAN A., VOM BERG-MAURER, COLETTE M., RYU, S. & BOLLMANN, JOHANN H. 2014. Classification of Object Size in Retinotectal Microcircuits. *Current Biology,* 24**,** 2376-2385.

PUTZIER, I., KULLMANN, P. H., HORN, J. P. & LEVITAN, E. S. 2009. Cav1.3 channel voltage dependence, not Ca2+ selectivity, drives pacemaker activity and amplifies bursts in nigral dopamine neurons. *The Journal of Neuroscience,* 29**,** 15414-9.

RANDLETT, O., WEE, C. L., NAUMANN, E. A., NNAEMEKA, O., SCHOPPIK, D., FITZGERALD, J. E., PORTUGUES, R., LACOSTE, A. M., RIEGLER, C., ENGERT, F. & SCHIER, A. F. 2015. Whole-brain activity mapping onto a zebrafish brain atlas. *Nature Methods,* 12**,** 1039-46.

RANI, M. & KANUNGO, M. S. 2006. Expression of D2 dopamine receptor in the mouse brain. *Biochem Biophys Res Commun,* 344**,** 981-6.

RANJBAR, H., RADAHMADI, M., REISI, P. & ALAEI, H. 2017. Effects of electrical lesion of basolateral amygdala nucleus on rat anxiety-like behaviour under acute, sub-chronic, and chronic stresses. *Clinical and Experimental Pharmacology and Physiology,* 44**,** 470-479.

REBOLLEDO-SOLLEIRO, D., ARAIZA, L. F. O., BROCCOLI, L., HANSSON, A. C., ROCHA-ARRIETA, L. L., AGUILAR-ROBLERO, R., CRESPO-RAMIREZ, M., FUXE, K. & PEREZ DE LA MORA, M. 2016. Dopamine D1 receptor activity is involved in the increased anxiety levels observed in STZ-induced diabetes in rats. *Behavioral and Brain Sciences,* 313**,** 293-301.

REINIG, S., DRIEVER, W. & ARRENBERG, A. B. 2017. The Descending Diencephalic Dopamine System Is Tuned to Sensory Stimuli. *Current Biology,* 27**,** 318-333.

REN, G., LI, S., ZHONG, H. & LIN, S. 2013. Zebrafish tyrosine hydroxylase 2 gene encodes tryptophan hydroxylase. *Journal of Biological Chemistry,* 288**,** 22451-9.

REN, K., GUO, B., DAI, C., YAO, H., SUN, T., LIU, X., BAI, Z., WANG, W. & WU, S. 2017. Striatal Distribution and Cytoarchitecture of Dopamine Receptor Subtype 1 and 2: Evidence from Double-Labeling Transgenic Mice. *Frontiers in neural circuits,* 11**,** 57-57.

RENAUD, L. P. 1981. A neurophysiological approach to the identification, connections and pharmacology of the hypothalamic tuberoinfundibular system. *Neuroendocrinology,* 33**,** 186-91.

REVAY, R., VAUGHAN, R., GRANT, S. & KUHAR, M. J. 1996. Dopamine transporter immunohistochemistry in median eminence, amygdala, and other areas of the rat brain. *Synapse,* 22**,** 93-9.

REYES, R., HAENDEL, M., GRANT, D., MELANCON, E. & EISEN, J. S. 2004. Slow degeneration of zebrafish Rohon-Beard neurons during programmed cell death. *Developmental Dynamics,* 229**,** 30-41.

REYES, S., COTTAM, V., KIRIK, D., DOUBLE, K. L. & HALLIDAY, G. M. 2013. Variability in neuronal expression of dopamine receptors and transporters in the substantia nigra. *Movement Disorders,* 28**,** 1351-9.

REYNOLDS, J. N., HYLAND, B. I. & WICKENS, J. R. 2001. A cellular mechanism of reward-related learning. *Nature,* 413**,** 67-70.

RIFKIN, R. A., HUYGHE, D., LI, X., PARAKALA, M., AISENBERG, E., MOSS, S. J. & SLESINGER, P. A. 2018. GIRK currents in VTA dopamine neurons control the sensitivity of mice to cocaine-induced locomotor sensitization. *Proceedings of the National Academy of Sciences of the United States of America,* 115**,** E9479-E9488.

RINK, E. & WULLIMANN, M. F. 2001. The teleostean (zebrafish) dopaminergic system ascending to the subpallium (striatum) is located in the basal diencephalon (posterior tuberculum). *Brain Research* 889**,** 316-30.

RINK, E. & WULLIMANN, M. F. 2002a. Connections of the ventral telencephalon and tyrosine hydroxylase distribution in the zebrafish brain (Danio rerio) lead to identification of an ascending dopaminergic system in a teleost. *Brain Research Bulletin,* 57**,** 385-387.

RINK, E. & WULLIMANN, M. F. 2002b. Development of the catecholaminergic system in the early zebrafish brain: an immunohistochemical study. *Developmental brain research,* 137**,** 89-100.

RINK, E. & WULLIMANN, M. F. 2004. Connections of the ventral telencephalon (subpallium) in the zebrafish (Danio rerio). *Brain Research* 1011**,** 206-20.

RINVIK, E. & WIBERG, M. 1990. Demonstration of a reciprocal connection between the periaqueductal gray matter and the reticular nucleus of the thalamus. *Anatomy and embryology,* 181**,** 577-84.

RITTER, D. A., BHATT, D. H. & FETCHO, J. R. 2001. In vivo imaging of zebrafish reveals differences in the spinal networks for escape and swimming movements. *The Journal of Neuroscience,* 21**,** 8956-65.

RIZVI, T. A., ENNIS, M., BEHBEHANI, M. M. & SHIPLEY, M. T. 1991. Connections between the central nucleus of the amygdala and the midbrain periaqueductal gray: topography and reciprocity. *The Journal of Comparative Neurology,* 303**,** 121-31.

ROBERTS, A. C., BILL, B. R. & GLANZMAN, D. L. 2013. Learning and memory in zebrafish larvae. *Frontiers in Neural Circuits,* 7**,** 126.

ROBERTS, A. C., REICHL, J., SONG, M. Y., DEARINGER, A. D., MORIDZADEH, N., LU, E. D., PEARCE, K., ESDIN, J. & GLANZMAN, D. L. 2011. Habituation of the C-Start Response in Larval Zebrafish Exhibits Several Distinct Phases and Sensitivity to NMDA Receptor Blockade. *PLOS ONE,* 6**,** e29132.

ROBERTSON, B., AUCLAIR, F., MENARD, A., GRILLNER, S. & DUBUC, R. 2007. GABA distribution in lamprey is phylogenetically conserved. *The Journal of Comparative Neurology,* 503**,** 47-63.

ROBERTSON, B., HUERTA-OCAMPO, I., ERICSSON, J., STEPHENSON-JONES, M., PEREZ-FERNANDEZ, J., BOLAM, J. P., DIAZ-HEIJTZ, R. & GRILLNER, S. 2012. The dopamine D2 receptor gene in lamprey, its expression in the striatum and cellular effects of D2 receptor activation. *PLoS One,* 7**,** e35642.

ROBERTSON, B., KARDAMAKIS, A., CAPANTINI, L., PEREZ-FERNANDEZ, J., SURYANARAYANA, S. M., WALLEN, P., STEPHENSON-JONES, M. & GRILLNER, S. 2014. The lamprey blueprint of the mammalian nervous system. *Progress in Brain Research,* 212**,** 337-49.

ROBERTSON, C. L., ISHIBASHI, K., MANDELKERN, M. A., BROWN, A. K., GHAHREMANI, D. G., SABB, F., BILDER, R., CANNON, T., BORG, J. & LONDON, E. D. 2015. Striatal D1- and D2-type dopamine receptors are linked to motor response inhibition in human subjects. *The Journal of Neuroscience,* 35**,** 5990-7.

ROBINSON, M. J., WARLOW, S. M. & BERRIDGE, K. C. 2014. Optogenetic excitation of central amygdala amplifies and narrows incentive motivation to pursue one reward above another. *The Journal of Neuroscience,* 34**,** 16567-80.

ROBLES, E., SMITH, S. J. & BAIER, H. 2011. Characterization of genetically targeted neuron types in the zebrafish optic tectum. *Frontiers in Neural Circuits,* 5**,** 1.

ROESER, T. & BAIER, H. 2003. Visuomotor behaviors in larval zebrafish after GFP-guided laser ablation of the optic tectum. *The Journal of Neuroscience,* 23**,** 3726-34.

ROGERS, R. D. 2011. The roles of dopamine and serotonin in decision making: evidence from pharmacological experiments in humans. *Neuropsychopharmacology,* 36**,** 114-132.

ROOT, D. H., MELENDEZ, R. I., ZABORSZKY, L. & NAPIER, T. C. 2015. The ventral pallidum: Subregion-specific functional anatomy and roles in motivated behaviors. *Progress in Neurobiology,* 130**,** 29-70.

ROSENKRANZ, J. A. & GRACE, A. A. 1999. Modulation of basolateral amygdala neuronal firing and afferent drive by dopamine receptor activation in vivo. *The Journal of Neuroscience,* 19**,** 11027-39.

RUTLEDGE, R. B., SKANDALI, N., DAYAN, P. & DOLAN, R. J. 2015. Dopaminergic Modulation of Decision Making and Subjective Well-Being. *The Journal of Neuroscience,* 35**,** 9811-22.

RYCZKO, D., AUCLAIR, F., CABELGUEN, J.-M. & DUBUC, R. 2016a. The mesencephalic locomotor region sends a bilateral glutamatergic drive to hindbrain reticulospinal neurons in a tetrapod. *The Journal of Comparative Neurology,* 524**,** 1361-1383.

RYCZKO, D., CONE, J. J., ALPERT, M. H., GOETZ, L., AUCLAIR, F., DUBE, C., PARENT, M., ROITMAN, M. F., ALFORD, S. & DUBUC, R. 2016b. A descending dopamine pathway conserved from basal vertebrates to mammals. *Proceedings of the National Academy of Sciences of the United States of America,* 113**,** E2440-9.

RYCZKO, D. & DUBUC, R. 2013. The multifunctional mesencephalic locomotor region. *Current Pharmaceutical Design,* 19**,** 4448-70.

SADDORIS, M. P., CACCIAPAGLIA, F., WIGHTMAN, R. M. & CARELLI, R. M. 2015. Differential Dopamine Release Dynamics in the Nucleus Accumbens Core and Shell Reveal Complementary Signals for Error Prediction and Incentive Motivation. *The Journal of Neuroscience,* 35**,** 11572-82.

SAH, P., FABER, E. S., LOPEZ DE ARMENTIA, M. & POWER, J. 2003. The amygdaloid complex: anatomy and physiology. *Physiological Reviews,* 83**,** 803-34.

SAINT-AMANT, L. & DRAPEAU, P. 1998. Time course of the development of motor behaviors in the zebrafish embryo. *Journal of Neurobiology,* 37**,** 622-32.

SALAMONE, J. D. & CORREA, M. 2012. The mysterious motivational functions of mesolimbic dopamine. *Neuron,* 76**,** 470-485.

SALLINEN, V., KOLEHMAINEN, J., PRIYADARSHINI, M., TOLEIKYTE, G., CHEN, Y. C. & PANULA, P. 2010. Dopaminergic cell damage and vulnerability to MPTP in Pink1 knockdown zebrafish. *Neurobiology of Disease,* 40**,** 93-101.

SALLINEN, V., TORKKO, V., SUNDVIK, M., REENILA, I., KHRUSTALYOV, D., KASLIN, J. & PANULA, P. 2009. MPTP and MPP+ target specific aminergic cell populations in larval zebrafish. *Journal of Neurochemistry,* 108**,** 719-31.

SANCHEZ-GONZALEZ, M. A., GARCIA-CABEZAS, M. A., RICO, B. & CAVADA, C. 2005. The primate thalamus is a key target for brain dopamine. *The Journal of Neuroscience,* 25**,** 6076-83.

SATOU, C., KIMURA, Y., KOHASHI, T., HORIKAWA, K., TAKEDA, H., ODA, Y. & HIGASHIJIMA, S. 2009. Functional role of a specialized class of spinal commissural inhibitory neurons during fast escapes in zebrafish. *The Journal of Neuroscience,* 29**,** 6780-93.

SAUTER, A. M., LEW, J. Y., BABA, Y. & GOLDSTEIN, M. 1977. Effect of phenylethanolamine N-methyltransferase and dopamine-β-hydroxylase inhibition on epinephrine levels in the brain. *Life Sciences,* 21**,** 261-266.

SCHEETZ, S. D., SHAO, E., ZHOU, Y., CARIO, C. L., BAI, Q. & BURTON, E. A. 2018. An open-source method to analyze optokinetic reflex responses in larval zebrafish. *Journal of Neuroscience Methods,* 293**,** 329-337.

SCHMITT, L. I. & HALASSA, M. M. 2017. Interrogating the mouse thalamus to correct human neurodevelopmental disorders. *Molecular Psychiatry,* 22**,** 183-191.

SCHNORR, S. J., STEENBERGEN, P. J., RICHARDSON, M. K. & CHAMPAGNE, D. L. 2012. Measuring thigmotaxis in larval zebrafish. *Behavioral and Brain Sciences,* 228**,** 367-74.

SCHULTZ, W. 1998. Predictive reward signal of dopamine neurons. *The Journal of Neurophysiology,* 80**,** 1-27.

SCHULTZ, W. 2016. Dopamine reward prediction-error signalling: a two-component response. *Nature Reviews Neuroscience,* 17**,** 183-95.

SCHULTZ, W., STAUFFER, W. R. & LAK, A. 2017. The phasic dopamine signal maturing: from reward via behavioural activation to formal economic utility. *Current Opinion in Neurobiology,* 43**,** 139-148.

SCHWEITZER, J. & DRIEVER, W. 2009. Development of the dopamine systems in zebrafish. *Adv Exp Med Biol,* 651**,** 1-14.

SCHWEITZER, J., LOHR, H., FILIPPI, A. & DRIEVER, W. 2012. Dopaminergic and noradrenergic circuit development in zebrafish. *Developmental Neurobiology,* 72**,** 256-68.

SEE, R. E., FUCHS, R. A., LEDFORD, C. C. & MCLAUGHLIN, J. 2003. Drug addiction, relapse, and the amygdala. *Annals of the New York Academy of Sciences,* 985**,** 294-307.

SEMMELHACK, J. L., DONOVAN, J. C., THIELE, T. R., KUEHN, E., LAURELL, E. & BAIER, H. 2014. A dedicated visual pathway for prey detection in larval zebrafish. *Elife,* 3.

SEUTIN, V., MASSOTTE, L., RENETTE, M. F. & DRESSE, A. 2001. Evidence for a modulatory role of Ih on the firing of a subgroup of midbrain dopamine neurons. *Neuroreport,* 12**,** 255-8.

SEVERI, K. E., PORTUGUES, R., MARQUES, J. C., O'MALLEY, D. M., ORGER, M. B. & ENGERT, F. 2014. Neural control and modulation of swimming speed in the larval zebrafish. *Neuron,* 83**,** 692-707.

SHACKMAN, A. J. & FOX, A. S. 2016. Contributions of the Central Extended Amygdala to Fear and Anxiety. *The Journal of Neuroscience,* 36**,** 8050-63.

SHANG, C., LIU, Z., CHEN, Z., SHI, Y., WANG, Q., LIU, S., LI, D. & CAO, P. 2015. BRAIN CIRCUITS. A parvalbumin-positive excitatory visual pathway to trigger fear responses in mice. *Science,* 348**,** 1472-7.

SHARP, B. M. 2017. Basolateral amygdala and stress-induced hyperexcitability affect motivated behaviors and addiction. *Transl Psychiatry,* 7**,** e1194.

SHARPLES, S. A., KOBLINGER, K., HUMPHREYS, J. M. & WHELAN, P. J. 2014. Dopamine: a parallel pathway for the modulation of spinal locomotor networks. *Frontiers in Neural Circuits,* 8**,** 55.

SHEPARD, P. D. & STUMP, D. 1999. Nifedipine blocks apamin-induced bursting activity in nigral dopamine-containing neurons. *Brain Research* 817**,** 104-9.

SHI, Y. W., FAN, B. F., XUE, L., WEN, J. L. & ZHAO, H. 2017. Regulation of Fear Extinction in the Basolateral Amygdala by Dopamine D2 Receptors Accompanied by Altered GluR1, GluR1-Ser845 and NR2B Levels. *Frontiers in Behavioral Neuroscience,* 11**,** 116.

SHIN, M., FIELD, T. M., STUCKY, C. S., FURGURSON, M. N. & JOHNSON, M. A. 2017. Ex Vivo Measurement of Electrically Evoked Dopamine Release in Zebrafish Whole Brain. *ACS Chemical Neuroscience,* 8**,** 1880-1888.

SHMOEL, N., RABIEH, N., OJOVAN, S. M., EREZ, H., MAYDAN, E. & SPIRA, M. E. 2016. Multisite electrophysiological recordings by self-assembled loose-patch-like junctions between cultured hippocampal neurons and mushroom-shaped microelectrodes. *Scientific Reports,* 6**,** 27110.

SICILIANO, C. A. & JONES, S. R. 2017. Cocaine Potency at the Dopamine Transporter Tracks Discrete Motivational States During Cocaine Self-Administration. *Neuropsychopharmacology,* 42**,** 1893-1904.

SIDHU, A. & NIZNIK, H. B. 2000. Coupling of dopamine receptor subtypes to multiple and diverse G proteins. *International Journal of Developmental Neuroscience,* 18**,** 669-77.

SILLAR, K. T. 2009. Mauthner cells. *Current Biology,* 19**,** R353-R355.

SILLIVAN, S. E. & KONRADI, C. 2011. Expression and function of dopamine receptors in the developing medial frontal cortex and striatum of the rat. *Neuroscience,* 199**,** 501-514.

SILVA, B. A., GROSS, C. T. & GRAFF, J. 2016. The neural circuits of innate fear: detection, integration, action, and memorization. *Learning & Memory,* 23**,** 544-55.

SILVA, C. & MCNAUGHTON, N. 2019. Are periaqueductal gray and dorsal raphe the foundation of appetitive and aversive control? A comprehensive review. *Progress in Neurobiology,* 177**,** 33-72.

SIMON, P., DUPUIS, R. & COSTENTIN, J. 1994. Thigmotaxis as an index of anxiety in mice. Influence of dopaminergic transmissions. *Behavioral and Brain Sciences,* 61**,** 59-64.

SIUDA, E. R., AL-HASANI, R., MCCALL, J. G., BHATTI, D. L. & BRUCHAS, M. R. 2016. Chemogenetic and Optogenetic Activation of Galphas Signaling in the Basolateral Amygdala Induces Acute and Social Anxiety-Like States. *Neuropsychopharmacology,* 41**,** 2011-23.

SMEETS, W. J. & GONZALEZ, A. 2000. Catecholamine systems in the brain of vertebrates: new perspectives through a comparative approach. *Brain Research Reviews,* 33**,** 308-79.

SMITH, E. S., FABIAN, P., ROSENTHAL, A., KADDOUR-DJEBBAR, A. & LEE, H. J. 2015. The roles of central amygdala D1 and D2 receptors on attentional performance in a five-choice task. *Behavioral Neuroscience,* 129**,** 564-75.

SMITH, E. S., GEISSLER, S. A., SCHALLERT, T. & LEE, H. J. 2013. The role of central amygdala dopamine in disengagement behavior. *Behavioral Neuroscience,* 127**,** 164-74.

SMITH, K. S., TINDELL, A. J., ALDRIDGE, J. W. & BERRIDGE, K. C. 2009. Ventral pallidum roles in reward and motivation. *Behavioral and Brain Sciences,* 196**,** 155-67.

SMITS, S. M., VON OERTHEL, L., HOEKSTRA, E. J., BURBACH, J. P. & SMIDT, M. P. 2013. Molecular marker differences relate to developmental position and subsets of mesodiencephalic dopaminergic neurons. *PLoS One,* 8**,** e76037.

SOARES-CUNHA, C., COIMBRA, B., DAVID-PEREIRA, A., BORGES, S., PINTO, L., COSTA, P., SOUSA, N. & RODRIGUES, A. J. 2016a. Activation of D2 dopamine receptor-expressing neurons in the nucleus accumbens increases motivation. *Nature Communications,* 7**,** 11829.

SOARES-CUNHA, C., COIMBRA, B., DOMINGUES, A. V., VASCONCELOS, N., SOUSA, N. & RODRIGUES, A. J. 2018. Nucleus Accumbens Microcircuit Underlying D2-MSN-Driven Increase in Motivation. *eNeuro,* 5.

SOARES-CUNHA, C., COIMBRA, B., SOUSA, N. & RODRIGUES, A. J. 2016b. Reappraising striatal D1- and D2-neurons in reward and aversion. *Neuroscience & Biobehavioral Reviews,* 68**,** 370-386.

SOARES-CUNHA, C., DE VASCONCELOS, N. A. P., COIMBRA, B., DOMINGUES, A. V., SILVA, J. M., LOUREIRO-CAMPOS, E., GASPAR, R., SOTIROPOULOS, I., SOUSA, N. & RODRIGUES, A. J. 2019. Nucleus accumbens medium spiny neurons subtypes signal both reward and aversion. *Molecular Psychiatry*.

SPAMPANATO, J., POLEPALLI, J. & SAH, P. 2011. Interneurons in the basolateral amygdala. *Neuropharmacology,* 60**,** 765-73.

SPANO, P. F., GOVONI, S. & TRABUCCHI, M. 1978. Studies on the pharmacological properties of dopamine receptors in various areas of the central nervous system. *Advances in Biochemistry and Psychopharmacology,* 19**,** 155-65.

STAGKOURAKIS, S., DUNEVALL, J., TALEAT, Z., EWING, A. G. & BROBERGER, C. 2019. Dopamine release dynamics in the tuberoinfundibular dopamine system. *The Journal of Neuroscience*.

STAGKOURAKIS, S., KIM, H., LYONS, DAVID J. & BROBERGER, C. 2016. Dopamine Autoreceptor Regulation of a Hypothalamic Dopaminergic Network. *Cell Reports,* 15**,** 735-747.

STAGKOURAKIS, S., PEREZ, C. T., HELLYSAZ, A., AMMARI, R. & BROBERGER, C. 2018. Network oscillation rules imposed by species-specific electrical coupling. *Elife,* 7.

STAMATAKIS, A. M., SPARTA, D. R., JENNINGS, J. H., MCELLIGOTT, Z. A., DECOT, H. & STUBER, G. D. 2014. Amygdala and bed nucleus of the stria terminalis circuitry: Implications for addiction-related behaviors. *Neuropharmacology,* 76 Pt B**,** 320-8.

STEDNITZ, S. J., FRESHNER, B., SHELTON, S., SHEN, T., BLACK, D. & GAHTAN, E. 2015. Selective toxicity of L-DOPA to dopamine transporter-expressing neurons and locomotor behavior in zebrafish larvae. *Neurotoxicology and Teratology,* 52**,** 51-6.

STEPHENSON-JONES, M., ERICSSON, J., ROBERTSON, B. & GRILLNER, S. 2012. Evolution of the basal ganglia: dual-output pathways conserved throughout vertebrate phylogeny. *The Journal of Comparative Neurology,* 520**,** 2957-73.

STEPHENSON-JONES, M., SAMUELSSON, E., ERICSSON, J., ROBERTSON, B. & GRILLNER, S. 2011. Evolutionary conservation of the basal ganglia as a common vertebrate mechanism for action selection. *Current Biology,* 21**,** 1081-91.

STEVENSON, C. W. & GRATTON, A. 2003. Basolateral amygdala modulation of the nucleus accumbens dopamine response to stress: role of the medial prefrontal cortex. *European Journal of Neuroscience,* 17**,** 1287-95.

STICE, E. & DAGHER, A. 2010. Genetic variation in dopaminergic reward in humans. *Forum Nutrition,* 63**,** 176-85.

STRANGE, P. G. 1990. Role of the mesostriatal dopamine pathway. *Trends in Neuroscience,* 13**,** 93-5.

STRAUB, C., SAULNIER, J. L., BEGUE, A., FENG, D. D., HUANG, K. W. & SABATINI, B. L. 2016. Principles of Synaptic Organization of GABAergic Interneurons in the Striatum. *Neuron,* 92**,** 84-92.

STRUBING, C., AHNERT-HILGER, G., SHAN, J., WIEDENMANN, B., HESCHELER, J. & WOBUS, A. M. 1995. Differentiation of pluripotent embryonic stem cells into the neuronal lineage in vitro gives rise to mature inhibitory and excitatory neurons. *Mechanisms of Development,* 53**,** 275-87.

SUDHOF, T. C. 2012. Calcium control of neurotransmitter release. *Cold Spring Harbor perspectives in biology,* 4**,** a011353.

SUDHOF, T. C. 2018. Towards an Understanding of Synapse Formation. *Neuron,* 100**,** 276-293.

SULZER, D. 2011. How Addictive Drugs Disrupt Presynaptic Dopamine Neurotransmission. *Neuron,* 69**,** 628-649.

SUN, N., YI, H. & CASSELL, M. D. 1994. Evidence for a GABAergic interface between cortical afferents and brainstem projection neurons in the rat central extended amygdala. *The Journal of Comparative Neurology,* 340**,** 43-64.

SUN, Y., BLANCO-CENTURION, C., ZOU, B., BENDELL, E., SHIROMANI, P. J. & LIU, M. 2019. Amygdala GABA Neurons Project To vlPAG And mPFC. *IBRO Reports,* 6**,** 132-136.

SUNDVIK, M. & PANULA, P. 2012. Organization of the histaminergic system in adult zebrafish (Danio rerio) brain: neuron number, location, and cotransmitters. *The Journal of Comparative Neurology,* 520**,** 3827-45.

SURMEIER, D. J., BARGAS, J., HEMMINGS, H. C., JR., NAIRN, A. C. & GREENGARD, P. 1995. Modulation of calcium currents by a D1 dopaminergic protein kinase/phosphatase cascade in rat neostriatal neurons. *Neuron,* 14**,** 385-97.

SURMEIER, D. J., DING, J., DAY, M., WANG, Z. & SHEN, W. 2007. D1 and D2 dopamine-receptor modulation of striatal glutamatergic signaling in striatal medium spiny neurons. *Trends in Neuroscience,* 30**,** 228-35.

SURMEIER, D. J. & KITAI, S. T. 1993. D1 and D2 dopamine receptor modulation of sodium and potassium currents in rat neostriatal neurons. *Progress in Brain Research,* 99**,** 309-24.

SURMEIER, D. J. & KITAI, S. T. 1997. State-dependent regulation of neuronal excitability by dopamine. *Nihon Shinkei Seishin Yakurigaku Zasshi,* 17**,** 105-10.

SURMEIER, D. J., OBESO, J. A. & HALLIDAY, G. M. 2017. Selective neuronal vulnerability in Parkinson disease. *Nature reviews. Neuroscience,* 18**,** 101-113.

SURMEIER, D. J., STEFANI, A., FOEHRING, R. C. & KITAI, S. T. 1991. Developmental regulation of a slowly-inactivating potassium conductance in rat neostriatal neurons. *Neuroscience Letters,* 122**,** 41-6.

SUTOR, B. & LUHMANN, H. J. 1995. Development of excitatory and inhibitory postsynaptic potentials in the rat neocortex. *Perspectives on Developmental Neurobiology,* 2**,** 409-19.

SVEINBJORNSDOTTIR, S. 2016. The clinical symptoms of Parkinson's disease. *Journal of Neurochemistry,* 139 Suppl 1**,** 318-324.

SWERDLOW, N. R., BRAFF, D. L. & GEYER, M. A. 2016. Sensorimotor gating of the startle reflex: what we said 25 years ago, what has happened since then, and what comes next. *Journal of Psychopharmacology,* 30**,** 1072-1081.

SWERDLOW, N. R., BRAFF, D. L., TAAID, N. & GEYER, M. A. 1994. Assessing the validity of an animal model of deficient sensorimotor gating in schizophrenic patients. *Archives Of General Psychiatry,* 51**,** 139-54.

SWERDLOW, N. R. & GEYER, M. A. 1993. Prepulse inhibition of acoustic startle in rats after lesions of the pedunculopontine tegmental nucleus. *Behavioral Neuroscience,* 107**,** 104-17.

TAKAHASHI, M., INOUE, M., TANIMOTO, M., KOHASHI, T. & ODA, Y. 2017. Short-term desensitization of fast escape behavior associated with suppression of Mauthner cell activity in larval zebrafish. *Neuroscience Research,* 121**,** 29-36.

TAPIA, M., BAUDOT, P., FORMISANO-TREZINY, C., DUFOUR, M. A., TEMPORAL, S., LASSERRE, M., MARQUEZE-POUEY, B., GABERT, J., KOBAYASHI, K. & GOAILLARD, J. M. 2018. Neurotransmitter identity and electrophysiological phenotype are genetically coupled in midbrain dopaminergic neurons. *Scientific Reports,* 8**,** 13637.

TAY, T. L., RONNEBERGER, O., RYU, S., NITSCHKE, R. & DRIEVER, W. 2011. Comprehensive catecholaminergic projectome analysis reveals single-neuron integration of zebrafish ascending and descending dopaminergic systems. *Nature Communications,* 2**,** 171.

TEMIZER, I., DONOVAN, J. C., BAIER, H. & SEMMELHACK, J. L. 2015. A Visual Pathway for Looming-Evoked Escape in Larval Zebrafish. *Current Biology,* 25**,** 1823-34.

TEPPER, J. M., KOÓS, T., IBANEZ-SANDOVAL, O., TECUAPETLA, F., FAUST, T. W. & ASSOUS, M. 2018. Heterogeneity and Diversity of Striatal GABAergic Interneurons: Update 2018. *Frontiers in Neuroanatomy,* 12.

THIBAULT, D., LOUSTALOT, F., FORTIN, G. M., BOURQUE, M.-J. & TRUDEAU, L.-É. 2013. Evaluation of D1 and D2 dopamine receptor segregation in the developing striatum using BAC transgenic mice. *PloS one,* 8, e67219-e67219.

THIEL, K. J., WENZEL, J. M., PENTKOWSKI, N. S., HOBBS, R. J., ALLEWEIRELDT, A. T. & NEISEWANDER, J. L. 2010. Stimulation of dopamine D2/D3 but not D1 receptors in the central amygdala decreases cocaine-seeking behavior. *Behavioral and Brain Sciences,* 214, 386-94.

THOMPSON, R. H., MENARD, A., POMBAL, M. & GRILLNER, S. 2008. Forebrain dopamine depletion impairs motor behavior in lamprey. *European Journal of Neuroscience,* 27, 1452-60.

TIMMERMAN, W., DEINUM, M. E., WESTERINK, B. H. & SCHUILING, G. A. 1995. Lack of evidence for dopamine autoreceptors in the mediobasal hypothalamus: a microdialysis study in awake rats. *Neuroscience Letters,* 195, 113-6.

TONG, H. & MCDEARMID, J. R. 2012. Pacemaker and plateau potentials shape output of a developing locomotor network. *Current Biology,* 22, 2285-93.

TORRISI, S., GORKA, A. X., GONZALEZ-CASTILLO, J., O'CONNELL, K., BALDERSTON, N., GRILLON, C. & ERNST, M. 2018. Extended amygdala connectivity changes during sustained shock anticipation. *Transl Psychiatry,* 8, 33.

TOVOTE, P., FADOK, J. P. & LUTHI, A. 2015. Neuronal circuits for fear and anxiety. *Nature Reviews Neuroscience,* 16, 317-31.

TRIFILIEFF, P. & MARTINEZ, D. 2014. Imaging addiction: D2 receptors and dopamine signaling in the striatum as biomarkers for impulsivity. *Neuropharmacology,* 76 Pt B, 498-509.

TRIMBLE, M. R. & VAN ELST, L. T. 1999. On some clinical implications of the ventral striatum and the extended amygdala. Investigations of aggression. *Annals of the New York Academy of Sciences,* 877, 638-44.

TROCONIS, E. L., ORDOOBADI, A. J., SOMMERS, T. F., AZIZ-BOSE, R., CARTER, A. R. & TRAPANI, J. G. 2017. Intensity-dependent timing and precision of startle response latency in larval zebrafish. *The Journal of Physiology,* 595, 265-282.

TSUTSUI-KIMURA, I., NATSUBORI, A., MORI, M., KOBAYASHI, K., DREW, M. R., DE KERCHOVE D'EXAERDE, A., MIMURA, M. & TANAKA, K. F. 2017a. Distinct Roles of Ventromedial versus Ventrolateral Striatal Medium Spiny Neurons in Reward-Oriented Behavior. *Current Biology,* 27, 3042-3048 e4.

TSUTSUI-KIMURA, I., TAKIUE, H., YOSHIDA, K., XU, M., YANO, R., OHTA, H., NISHIDA, H., BOUCHEKIOUA, Y., OKANO, H., UCHIGASHIMA, M., WATANABE, M., TAKATA, N., DREW, M. R., SANO, H., MIMURA, M. & TANAKA, K. F. 2017b. Dysfunction of ventrolateral striatal dopamine receptor type 2-expressing medium spiny neurons impairs instrumental motivation. *Nature Communications,* 8, 14304.

TUCKER, K. R., HUERTAS, M. A., HORN, J. P., CANAVIER, C. C. & LEVITAN, E. S. 2012. Pacemaker rate and depolarization block in nigral dopamine

neurons: a somatic sodium channel balancing act. *The Journal of Neuroscience,* 32**,** 14519-31.

TUPAL, S. & FAINGOLD, C. L. 2012. The amygdala to periaqueductal gray pathway: plastic changes induced by audiogenic kindling and reversal by gabapentin. *Brain Research* 1475**,** 71-9.

TYE, K. M., PRAKASH, R., KIM, S. Y., FENNO, L. E., GROSENICK, L., ZARABI, H., THOMPSON, K. R., GRADINARU, V., RAMAKRISHNAN, C. & DEISSEROTH, K. 2011. Amygdala circuitry mediating reversible and bidirectional control of anxiety. *Nature,* 471**,** 358-62.

TYLL, S., BUDINGER, E. & NOESSELT, T. 2011. Thalamic influences on multisensory integration. *Communicative & integrative biology,* 4**,** 378-381.

UCHIMURA, N., CHERUBINI, E. & NORTH, R. A. 1989. Inward rectification in rat nucleus accumbens neurons. *The Journal of Neurophysiology,* 62**,** 1280-6.

ULLAH, F., DOS ANJOS-GARCIA, T., DOS SANTOS, I. R., BIAGIONI, A. F. & COIMBRA, N. C. 2015. Relevance of dorsomedial hypothalamus, dorsomedial division of the ventromedial hypothalamus and the dorsal periaqueductal gray matter in the organization of freezing or oriented and non-oriented escape emotional behaviors. *Behavioral and Brain Sciences,* 293**,** 143-52.

VAN DEN BOS, R., MES, W., GALLIGANI, P., HEIL, A., ZETHOF, J., FLIK, G. & GORISSEN, M. 2017. Further characterisation of differences between TL and AB zebrafish (Danio rerio): Gene expression, physiology and behaviour at day 5 of the larval stage. *PloS one,* 12**,** e0175420-e0175420.

VANDER WEELE, C. M., SICILIANO, C. A., MATTHEWS, G. A., NAMBURI, P., IZADMEHR, E. M., ESPINEL, I. C., NIEH, E. H., SCHUT, E. H. S., PADILLA-COREANO, N., BURGOS-ROBLES, A., CHANG, C. J., KIMCHI, E. Y., BEYELER, A., WICHMANN, R., WILDES, C. P. & TYE, K. M. 2018. Dopamine enhances signal-to-noise ratio in cortical-brainstem encoding of aversive stimuli. *Nature,* 563**,** 397-401.

VANWALLEGHEM, G., HEAP, L. A. & SCOTT, E. K. 2017. A profile of auditory-responsive neurons in the larval zebrafish brain. *The Journal of Comparative Neurology,* 525**,** 3031-3043.

VARELA, C. 2014. Thalamic neuromodulation and its implications for executive networks. *Frontiers in neural circuits,* 8**,** 69-69.

VEINANTE, P. & FREUND-MERCIER, M.-J. 1998. Intrinsic and extrinsic connections of the rat central extended amygdala: an in vivo electrophysiological study of the central amygdaloid nucleus. *Brain Research,* 794**,** 188-198.

VOGT WEISENHORN, D. M., GIESERT, F. & WURST, W. 2016. Diversity matters - heterogeneity of dopaminergic neurons in the ventral mesencephalon and its relation to Parkinson's Disease. *The Journal of Neurochemistry,* 139 Suppl 1**,** 8-26.

VON TROTHA, J. W., VERNIER, P. & BALLY-CUIF, L. 2014. Emotions and motivated behavior converge on an amygdala-like structure in the zebrafish. *European Journal of Neuroscience,* 40**,** 3302-15.

WALKER, D. L. & DAVIS, M. 1997. Involvement of the dorsal periaqueductal gray in the loss of fear-potentiated startle accompanying high footshock training. *Behavioral Neuroscience,* 111**,** 692-702.

WANG, L., CHEN, I. Z. & LIN, D. 2015. Collateral pathways from the ventromedial hypothalamus mediate defensive behaviors. *Neuron,* 85**,** 1344-58.

WANG, Z., LIANG, S., YU, S., XIE, T., WANG, B., WANG, J., LI, Y., SHAN, B. & CUI, C. 2017. Distinct Roles of Dopamine Receptors in the Lateral Thalamus in a Rat Model of Decisional Impulsivity. *Neuroscience Bulletin,* 33**,** 413-422.

WARACZYNSKI, M. 2016. Toward a systems-oriented approach to the role of the extended amygdala in adaptive responding. *Neuroscience & Biobehavioral Reviews,* 68**,** 177-194.

WARACZYNSKI, M. A. 2006. The central extended amygdala network as a proposed circuit underlying reward valuation. *Neuroscience & Biobehavioral Reviews,* 30**,** 472-496.

WASSALL, R. D., TERAMOTO, N. & CUNNANE, T. C. 2009. Noradrenaline. *In:* SQUIRE, L. R. (ed.) *Encyclopedia of Neuroscience.* Oxford: Academic Press.

WEI, P., LIU, N., ZHANG, Z., LIU, X., TANG, Y., HE, X., WU, B., ZHOU, Z., LIU, Y., LI, J., ZHANG, Y., ZHOU, X., XU, L., CHEN, L., BI, G., HU, X., XU, F. & WANG, L. 2015. Processing of visually evoked innate fear by a non-canonical thalamic pathway. *Nature Communications,* 6**,** 6756.

WELTER, M., VALLONE, D., SAMAD, T. A., MEZIANE, H., USIELLO, A. & BORRELLI, E. 2007. Absence of dopamine D2 receptors unmasks an inhibitory control over the brain circuitries activated by cocaine. *Proceedings of the National Academy of Sciences of the United States of America,* 104**,** 6840-5.

WEN, L., WEI, W., GU, W., HUANG, P., REN, X., ZHANG, Z., ZHU, Z., LIN, S. & ZHANG, B. 2008. Visualization of monoaminergic neurons and neurotoxicity of MPTP in live transgenic zebrafish. *Developmental Biology (New York, N.Y.: 1985),* 314**,** 84-92.

WESTBY, G. W., KEAY, K. A., REDGRAVE, P., DEAN, P. & BANNISTER, M. 1990. Output pathways from the rat superior colliculus mediating approach and avoidance have different sensory properties. *Experimental Brain Research,* 81**,** 626-38.

WESTERFIELD, M. 2000. *A guide for the laboratory use of zebrafish Danio (Brachydanio) rerio,* Eugene, University of Oregon Press.

WIETZIKOSKI, E. C., BOSCHEN, S. L., MIYOSHI, E., BORTOLANZA, M., DOS SANTOS, L. M., FRANK, M., BRANDAO, M. L., WINN, P. & DA CUNHA, C. 2012. Roles of D1-like dopamine receptors in the nucleus accumbens and dorsolateral striatum in conditioned avoidance responses. *Psychopharmacology (Berl),* 219**,** 159-69.

WILLIAMS, J. A., BARRIOS, A., GATCHALIAN, C., RUBIN, L., WILSON, S. W. & HOLDER, N. 2000. Programmed cell death in zebrafish rohon beard neurons is influenced by TrkC1/NT-3 signaling. *Developmental Biology,* 226**,** 220-30.

WILSON, C. J. & KAWAGUCHI, Y. 1996. The origins of two-state spontaneous membrane potential fluctuations of neostriatal spiny neurons. *The Journal of Neuroscience,* 16**,** 2397-410.

WINER, J. A., CHERNOCK, M. L., LARUE, D. T. & CHEUNG, S. W. 2002. Descending projections to the inferior colliculus from the posterior thalamus and the auditory cortex in rat, cat, and monkey. *Hear Research,* 168**,** 181-95.

WINER, J. A., LARUE, D. T., DIEHL, J. J. & HEFTI, B. J. 1998. Auditory cortical projections to the cat inferior colliculus. *The Journal of Comparative Neurology,* 400**,** 147-74.

WINSTANLEY, C. A., ZEEB, F. D., BEDARD, A., FU, K., LAI, B., STEELE, C. & WONG, A. C. 2010. Dopaminergic modulation of the orbitofrontal cortex affects attention, motivation and impulsive responding in rats performing the five-choice serial reaction time task. *Behavioural Brain Research,* 210**,** 263-272.

WISE, R. A. 2004. Dopamine, learning and motivation. *Nature Reviews Neuroscience,* 5**,** 483-94.

WOLF, M. E. & ROTH, R. H. 1990. Autoreceptor regulation of dopamine synthesis. *Annals of the New York Academy of Sciences,* 604**,** 323-43.

WU, D., WANG, S., STEIN, J. F., AZIZ, T. Z. & GREEN, A. L. 2014. Reciprocal interactions between the human thalamus and periaqueductal gray may be important for pain perception. *Experimental Brain Research,* 232**,** 527-34.

WULLIMANN, M. F. 2009. Secondary neurogenesis and telencephalic organization in zebrafish and mice: a brief review. *Integrative Zoology,* 4**,** 123-33.

WULLIMANN, M. F. & MUELLER, T. 2004. Teleostean and mammalian forebrains contrasted: Evidence from genes to behavior. *The Journal of Comparative Neurology,* 475**,** 143-62.

WULLIMANN, M. F. & RINK, E. 2002. The teleostean forebrain: a comparative and developmental view based on early proliferation, Pax6 activity and catecholaminergic organization. *Brain Research Bulletin,* 57**,** 363-370.

XIA, Z., DUDEK, H., MIRANTI, C. K. & GREENBERG, M. E. 1996. Calcium influx via the NMDA receptor induces immediate early gene transcription by a MAP kinase/ERK-dependent mechanism. *The Journal of Neuroscience,* 16**,** 5425-36.

XIANG, L., SZEBENI, K., SZEBENI, A., KLIMEK, V., STOCKMEIER, C. A., KAROLEWICZ, B., KALBFLEISCH, J. & ORDWAY, G. A. 2008. Dopamine receptor gene expression in human amygdaloid nuclei: elevated D4 receptor mRNA in major depression. *Brain Research,* 1207**,** 214-24.

XIONG, X. R., LIANG, F., ZINGG, B., JI, X. Y., IBRAHIM, L. A., TAO, H. W. & ZHANG, L. I. 2015. Auditory cortex controls sound-driven innate defense behaviour through corticofugal projections to inferior colliculus. *Nature Communications,* 6**,** 7224.

YAMAMOTO, K., RUUSKANEN, J. O., WULLIMANN, M. F. & VERNIER, P. 2010a. Two tyrosine hydroxylase genes in vertebrates New dopaminergic territories revealed in the zebrafish brain. *Molecular and Cellular Neuroscience,* 43**,** 394-402.

YAMAMOTO, N., KATO, T., OKADA, Y. & SOMIYA, H. 2010b. Somatosensory nucleus in the torus semicircularis of cyprinid teleosts. *The Journal of Comparative Neurology,* 518**,** 2475-502.

YAMAMOTO, R., AHMED, N., ITO, T., GUNGOR, N. Z. & PARE, D. 2018. Optogenetic Study of Anterior BNST and Basomedial Amygdala Projections to the Ventromedial Hypothalamus. *eNeuro,* 5.

YAMASAKI, D. S. & KRAUTHAMER, G. M. 1990. Somatosensory neurons projecting from the superior colliculus to the intralaminar thalamus in the rat. *Brain Research Bulletin,* 523**,** 188-94.

YANG, Y. & WANG, J.-Z. 2017. From Structure to Behavior in Basolateral Amygdala-Hippocampus Circuits. *Frontiers in neural circuits,* 11**,** 86-86.

YAO, Y., LI, X., ZHANG, B., YIN, C., LIU, Y., CHEN, W., ZENG, S. & DU, J. 2016. Visual Cue-Discriminative Dopaminergic Control of Visuomotor Transformation and Behavior Selection. *Neuron,* 89**,** 598-612.

YASUI, Y., BREDER, C. D., SAPER, C. B. & CECHETTO, D. F. 1991. Autonomic responses and efferent pathways from the insular cortex in the rat. *The Journal of Comparative Neurology,* 303**,** 355-74.

YEOMANS, J. S. & FRANKLAND, P. W. 1995. The acoustic startle reflex: neurons and connections. *Brain Research Reviews,* 21**,** 301-314.

YILMAZ, M. & MEISTER, M. 2013. Rapid innate defensive responses of mice to looming visual stimuli. *Current Biology,* 23**,** 2011-2015.

YOSHIMI, K., KUMADA, S., WEITEMIER, A., JO, T. & INOUE, M. 2015. Reward-Induced Phasic Dopamine Release in the Monkey Ventral Striatum and Putamen. *PLoS One,* 10**,** e0130443.

YOUNG, W. S., 3RD, BONNER, T. I. & BRANN, M. R. 1986. Mesencephalic dopamine neurons regulate the expression of neuropeptide mRNAs in the rat forebrain. *Proceedings of the National Academy of Sciences of the United States of America,* 83**,** 9827-31.

YUAN, T. F. & SU, H. 2015. Fear learning through the two visual systems, a commentary on: "A parvalbumin-positive excitatory visual pathway to trigger fear responses in mice". *Frontiers in Neural Circuits,* 9**,** 56.

ZAHM, D. S. 1999. Functional-anatomical implications of the nucleus accumbens core and shell subterritories. *Annals of the New York Academy of Sciences,* 877**,** 113-28.

ZARRINDAST, M. R., ESLAHI, N., REZAYOF, A., ROSTAMI, P. & ZAHMATKESH, M. 2013. Modulation of ventral tegmental area dopamine receptors inhibit nicotine-induced anxiogenic-like behavior in the central amygdala. *Progress in Neuro-Psychopharmacology & Biological Psychiatry,* 41**,** 11-7.

ZEDDIES, D. G. & FAY, R. R. 2005. Development of the acoustically evoked behavioral response in zebrafish to pure tones. *The Journal of Experimental Biology,* 208**,** 1363-1372.

ZHANG, J., FORKSTAM, C., ENGEL, J. A. & SVENSSON, L. 2000. Role of dopamine in prepulse inhibition of acoustic startle. *Psychopharmacology (Berl),* 149**,** 181-8.

ZHANG, L., LIU, Y. & CHEN, X. 2005. Carbachol induces burst firing of dopamine cells in the ventral tegmental area by promoting calcium entry through L-type channels in the rat. *The Journal of Physiology,* 568**,** 469-81.

ZHANG, T., CHEN, T., CHEN, P., ZHANG, B., HONG, J. & CHEN, L. 2017. MPTP-Induced Dopamine Depletion in Basolateral Amygdala via Decrease of D2R Activation Suppresses GABAA Receptors Expression and LTD Induction Leading to Anxiety-Like Behaviors. *Frontiers in Molecular Neuroscience,* 10**,** 247.

ZHANG, X. & VAN DEN POL, A. N. 2015. Dopamine/Tyrosine Hydroxylase Neurons of the Hypothalamic Arcuate Nucleus Release GABA, Communicate with Dopaminergic and Other Arcuate Neurons, and Respond to Dynorphin, Met-Enkephalin, and Oxytocin. *The Journal of Neuroscience,* 35**,** 14966-82.

ZHAO, X., LIU, M. & CANG, J. 2014. Visual cortex modulates the magnitude but not the selectivity of looming-evoked responses in the superior colliculus of awake mice. *Neuron,* 84**,** 202-213.

ZHAO, Y., KERSCHER, N., EYSEL, U. & FUNKE, K. 2001. Changes of contrast gain in cat dorsal lateral geniculate nucleus by dopamine receptor agonists. *Neuroreport,* 12**,** 2939-45.

ZHAO, Y., KERSCHER, N., EYSEL, U. & FUNKE, K. 2002. D1 and D2 receptor-mediated dopaminergic modulation of visual responses in cat dorsal lateral geniculate nucleus. *The Journal of Physiology,* 539**,** 223-238.

ZHAO, Z. & DAVIS, M. 2004. Fear-potentiated startle in rats is mediated by neurons in the deep layers of the superior colliculus/deep mesencephalic nucleus of the rostral midbrain through the glutamate non-NMDA receptors. *The Journal of Neuroscience,* 24**,** 10326-34.

ZHU, Y., WIENECKE, C. F., NACHTRAB, G. & CHEN, X. 2016. A thalamic input to the nucleus accumbens mediates opiate dependence. *Nature,* 530**,** 219-22.

ZIMMERMAN, J. M., RABINAK, C. A., MCLACHLAN, I. G. & MAREN, S. 2007

The central nucleus of the amygdala is essential for acquiring and expressing conditional fear after overtraining. *Learning & Memory,* 14**,** 634-644.

ZINGG, B., CHOU, X. L., ZHANG, Z. G., MESIK, L., LIANG, F., TAO, H. W. & ZHANG, L. I. 2017. AAV-Mediated Anterograde Transsynaptic Tagging: Mapping Corticocollicular Input-Defined Neural Pathways for Defense Behaviors. *Neuron,* 93**,** 33-47.

ZOTTOLI, S. J. & FABER, D. S. 2000. ■ Review : The Mauthner Cell: What Has it Taught us? *Neuroscientist,* 6**,** 26-38.

ZOTTOLI, S. J., HORDES, A. R. & FABER, D. S. 1987. Localization of optic tectal input to the ventral dendrite of the goldfish Mauthner cell. *Brain Research,* 401**,** 113-121.

ZWEIFEL, L. S., PARKER, J. G., LOBB, C. J., RAINWATER, A., WALL, V. Z., FADOK, J. P., DARVAS, M., KIM, M. J., MIZUMORI, S. J., PALADINI, C. A., PHILLIPS, P. E. & PALMITER, R. D. 2009. Disruption of NMDAR-dependent burst firing by dopamine neurons provides selective assessment of phasic dopamine-dependent behavior. *Proceedings of the National Academy of Sciences of the United States of America,* 106**,** 7281-8.